


Doctoral Dissertation
Doctoral Program in Aerospace Engineering (30th Cycle)

Multidisciplinary modelling and simulation for assisting the space mission design process using Virtual Reality

Andrea Emanuele Maria Casini

* * * * * *

Supervisors
Prof. Paolo Maggiore
Prof. Nicole Viola

Doctoral Examination Committee:

Prof. A.B., Referee, University of….
Prof. C.D., Referee, University of…
Prof. E.F., Referee, University of….
Prof. G.H., Referee, University of…
Prof. I.J., Referee, University of….

Politecnico di Torino
Month dayth, 2018

I hereby declare that, the contents and organisation of this dissertation constitute my own original work and does not compromise in any way the rights of third parties, including those relating to the security of personal data.

Andrea Emanuele Maria Casini

Torino, Month dayth, 2018

Summary

Space mission design is a complex discipline. Several research studies are currently investigating how to ameliorate the process. Since the decision taken during the early phases of the project are those which affect the most the final solution of a system in terms of architecture, configuration, and cost, more efforts are sunk in these stages for not jeopardizing the entire product life-cycle stages. As the stakeholders and the other actors involved in the design process should face low levels of knowledge associated to the system in the conceptual stages, the decision-making process is intrinsically affected by uncertain results. Each choice made in this risky scenario affects the next design iterations, therefore a suitable design approach is needed. Several methodologies have been proposed by both academia and industry in the field of System Engineering (SE). The current trend is to adopt a Model Based System Engineering (MBSE) approach coupled with Concurrent Engineering (CE) paradigms.

The model-based methodology overcomes the weaknesses of a document-based one, aggregating all the relevant information and engineering data into a system model, which evolves as the real system throughout all the product life-cycle phases. The systematic CE approach is able to involve several experts in a multidisciplinary working context, where data, ideas, and solutions are shared at the same time using a common platform. Both the approaches help to shorten time and cost of the overall design process and prevent possible mistakes which could worsen the final solution if not identified earlier enough, thus maximizing the efficiency of each design session. However, negotiations still result to be as one of the most complicated and frustrating part of the whole design process. Moreover, the recent space exploration scenarios proposed by national agencies are characterized by multiple

actors of different extractions, but commonly participating into shaping future goals. The broader is the international cooperation framework, the more complex will be to design a space mission, especially considering the negotiation goals to be handled by the different experts involved.

The present Ph.D. thesis is aiming to cast some lights on the integration of Virtual Reality (VR) within the standard design tools to assist the space mission design process. The creation of a virtual model for simulating different features of a system allows to analyse aspects which may be overlooked, especially in the early design phases, such as ergonomics, operations, and training. The intuitive interaction with human senses and the immersion into a 3D Virtual Environment (VE) guarantee fundamental improvements and evaluation of different solutions that are updated in real-time, benefitting the entire design process, especially the early phases. The visualization of different system features at a single glance permits direct data and information exchange, enabling more direct communications among the design team. The possibility to use a distributed and shared architecture, implemented into a standard Concurrent Design Facility (CDF) setup, enhances in-depth analysis even in the product development phase. This unique VE can simulate functional and physical behaviours of the virtual replica, helping to optimize future space systems.

To test the VR-based methodology, a first proof of concept has been generated following the recent incremental and evolutionary architecture strategy of considering the Moon as the next step for the human exploration of Mars and the Solar System. According the exploration roadmaps, a permanent surface base is envisioned as an efficient test-bed for assessing critical technologies to be used for future deep-space endeavours. A preliminary mission scenario has been generated which targets to settle the outpost at the lunar south pole. The peculiar environment conditions make the area rich in volatiles to examine and exploit, especially considering the permanently shadowed regions that are supposed to contain icy water deposits, which are of paramount importance for human missions. A closed-loop power system, comprising solar panels, batteries, fuel cells, electrolysers, has been sized according the settlement power needs.

This research work presents an integrated simulation case study that has been run using a VE to arrive at a preliminary estimate of the performance of both the power system and the VR tool. Virtues and vices of the proposed VR-based methodology have been listed together with possible future improvements for this research field.

Acknowledgment

Lorem ipsum.

Ad inexplorata
Motto of the Air Force Test Center, Edwards Air Force Base, California (US)

To Infinity... and Beyond!
Buzz Lightyear, Toy Story, 1995

ATAF
Ufficio 28 aka “U.C.A.S.”

Alla mia famiglia, Chiara, Maria Pia e Armando
A chi mi guarda da lassù, Maria Grazia, Mauro, Margherita e Filippo

Contents

List of Figures

List of Tables

Acronyms

A

AIDA	Asteroid Impact and Deflection Assessment
AIT	Assembly, Integration and Test
AIV	Assembly, Integration and Verification
API	Application Programming Interface
AR	Augmented Reality
ARC	Ames Research Center
ASI	Agenzia Spaziale Italiana (Italian Space Agency)
ASTP	Apollo-Soyuz Test Project
ATV	Automated Transfer Vehicle

B

BEAM	Bigelow Expandable Activity Module
BFR	Big Falcon Rocket / Big Fucking Rocket
BGE	Blender Game Engine
BI	Blender Internal
BOL	Beginning Of Life

C

C&DH	Command and Data Handling
CAD	Computer-Aided Design
CAVE	Cave Automatic Virtual Environment
CCDev	Commercial Crew Development
CD	Concurrent Design
CDF	Concurrent Design Facility
CE	Concurrent Engineering
CFD	Computational Fluid Dynamics
CM	Crew Module
CNES	Centre National d'Études Spatiales (French Space Agency)

CNSA	China National Space Administration
ConCORDE	Concurrent Concepts, Options, Requirements and Design Editor
COSE	COllaborative System Engineering
COTS	Commercial Off-the-Shelf
CPS	Cyber-Physical Systems
CSA	Canadian Space Agency
CSIRO	Commonwealth Scientific and Industrial Research Organisation
CST	Crew Space Transportation

D

DEM	Digital Elevation Model
DG	Director General
DLR	Deutsches Zentrum für Luft- und Raumfahrt e.V. (German Aerospace Centre)
DMS	Data Management System
DoD	Department of Defense
DOD	Depth Of Discharge
DoF	Degree of Freedom
DSG	Deep Space Gateway

E

EAC	European Astronaut Centre
EdcAR	Engineering data in cross-platform AR
EM-1	Exploration Mission 1
EML1	Earth-Moon Lagrangian point 1
EML2	Earth-Moon Lagrangian point 2
EOL	End Of Life
EPS	Electrical Power System
ESM	European Service Module
ESTEC	European Research and Technology Centre
EVA	Extra Vehicular Activity

F

FDM	Fused Deposition Modelling
FEM	Finite Element Method

G

GCR	Galactic Cosmic Ray
GER	Global Exploration Roadmap
GLXP	Google Lunar X Prize
GMT	Greenwich Mean Time
GPS	Global Positioning System
GRAIL	Gravity Recovery and Interior Laboratory
GSP	Ground Support Personnel
GTO	Geostationary Transfer Orbit
GUI	Graphical User Interface

H

HDU	Habitat Demonstration Unit
HERACLES	Human-Enabled Robotic Architecture and Capability for Lunar Exploration and Science
HMD	Head Mounted Display
HST	Hubble Space Telescope

I

IAC	International Astronautical Congress
IMLEO	Initial Mass to Low Earth Orbit
INCOSE	International Council On Systems Engineering
IVA	Intra Vehicular Activity
IoT	Internet of Things
IP	International Partner
ISS	International Space Station
ISRO	Indian Space Research Organization
ISRU	In Situ Resource Utilization
IT	Information Technology

J

JAXA	Japan Aerospace eXploration Agency
JPL	Jet Propulsion Laboratory
JSC	Johnson Space Center

K

KARI	Korea Aerospace Research Institute

L

LADEE	Lunar Atmosphere and Dust Environment Explorer
LALT	Laser ALTimeter
LCROSS	Lunar Crater Observation and Sensing Satellite
LEM	Lunar Environment Model
LEO	Low Earth Orbit
LLO	Low Lunar Orbit
LOLA	Lunar Orbiter Laser Altimeter
LRO	Lunar Reconnaissance Orbiter

M

MBSE	Model Based Systems Engineering
MIT	Massachusetts Institute of Technology
mobiPV	mobile Procedure Viewer
MPCV	Multi-Purpose Crew Vehicle
MPPT	Maximum Power Point Tracker

N

NAC	Narrow Angle Camera
NAS	National Airspace System
NASA	National Aeronautics and Space Administration

O

OCDT	Open Concurrent Design Tool
OSB	OpenSG Binary

P

PDU	Power Distribution Unit
PESAI	Panel Effective Solar Albedo Irradiance
PESDI	Panel Effective Solar Direct Irradiance
PESI	Panel Effective Solar Irradiance
PPSB	Payload Power Switching Box

R

RMS	Remote Manipulator System
ROS	Russian Orbital Segment
RTG	Radioisotope Thermoelectric Generator

S

SAPS	Stand Alone Power System
SE	Systems Engineering
SELENE	SELenological and ENgineering Explorer
SEV	Space Exploration Vehicle
SLS	Space Launch System
SMART-1	Small Missions for Advanced Research in Technology-1
SNC	Sierra Nevada Corporation
SOI	System Of Interest
SoS	System of Systems
SPE	Solar Particle Events
SSAU	State Space Agency of Ukraine
STS	Space Transportation System

T

TAS-I	Thales Alenia Space Italia
TCS	Thermal Control System
TRL	Technology Readiness Level
TRO	Technology Research Office
TT&C	Telemetry, Tracking and Control

U

UAV	Unmanned Aerial Vehicle

UKSA	United Kingdom Space Agency
US	United States
USOS	US Operational Segment
USSR	Union of Soviet Socialist Republics

V

V&V	Validation And Verification
VE	Virtual Environment
V-ERAS	Virtual European maRs Analogue Station
VERITAS	Virtual Environment Research In Thales Alenia Space
VIEW	Virtual Interactive Environment Workstation project
VIVED	Virtual Visual Environment Display
VR	Virtual Reality
VR-Lab	Virtual Reality Laboratory
VRML	Virtual Reality Modelling Language

W

WAC	Wide Angle Camera
WPA	Water Pump Assembly

X

XML	eXtensible Markup Language

Chapter 1

Introduction

1.1 Background and context

Since the dawn of time, the night sky was always inspiring stories and dreams. Writers and artists were describing their great visions about space exploration as part of the human natural instinct to be drawn by the unknown. The breath-taking stories as well as the inspiring and the intriguing way how those genius depicted space travels through the centuries, sparkled the imagination and the intuition of a broad audience for out-of-the-world travels. In fact, thanks to these pioneering representations, some gifted people had spun the wheel of innovation far beyond fantasy to start the humankind journey towards modern day pursuing the final frontier of outer space.

Started in late 1950s, the space fever reached its maximum potential among the Union of Soviet Socialist Republics (USSR) and the United States (US): scientists and politicians were competing fiercely to leave an indelible mark in space, as launching the first satellite and sending the first human in orbit. The *space race* between these superpowers can be listed as one of the various aspects in which the *cold war* was declared. The 1957 launch of Sputnik I, the first man-made object to orbit the Earth, and the 1961 launch of cosmonauts Yuri Gagarin, the first human to fly beyond Earth's atmosphere, were the first milestones of an extraordinary timeline of consecutive one-upmanship that produced some of the history's greatest technology achievements. Even though Americans were the underdogs in the first phases due to some issues in rocket development, they soon bridged the gap with Soviet

Union's engineers. As the years were passing from Alan Shepard's space-flight, the first American astronauts to orbit our planet, the bets grew higher. John Fizgerald Kennedy claimed to raise expectations literally up to the Moon, setting to first step onto our natural satellite before the end of the 1960s decade as the final target of the American space program. After this golden era of breakthroughs, including the first spacewalk by Aleksei Leonov in 1965 and the first automatic landing on another celestial body by the space-craft Luna 9 on the Moon in 1966, culminated with the first human step on the lunar surface, the competition winds downs. The economical effort sank as well as failures and fatal disasters (e.g. Apollo 1 and Soyuz 1) led to belt-tightening budget cuts to space programs. If the interest for interplanetary ex-ploration of planets was still high enough, as testified by the unmanned probes flown by Venus, Mars, Jupiter, Mercury, Saturn, Uranus, and Neptune, the costly crewed missions suffered a setback.

The progressive declining political support to Apollo-style program in the US and the reaction to the loss of Moon race in the Soviet Union, shifted the efforts of both the national space agencies to orbital space stations in Low Earth Orbit (LEO). The first ever infrastructure successfully launched and operated was the Salyut 1 in 1971 by the USSR. This first breakout introduced the branch of orbiting laboratories, which are capable of supporting crew-members for an extended period of time and accessible to other spacecraft to dock. The US answer arrived in 1973 with the flying workstation Skylab 1. The dispute among the two countries resulted into an unexpected détente: US President Richard M. Nixon and Soviet Premier Leonid Brezhnev eased the *cold war* tension in 1972 via committing to launch the Apollo-Soyuz Test Project (ASTP). Soyuz 19 and the Apollo craft rendezvoused and docked in 1975, marking the symbolic subsiding of the *space race*, begun almost 20 years earlier, with joint scientific experiments and handshakes between three astronauts and two cosmonauts.

While the USSR was mainly focusing on the continuous development of the technology related to space stations, culminating with *Mir*, Americans were advocating reusable manned space vehicles to support extended opera-tions beyond the Apollo program, resulting in the Space Shuttle vehicle, later mimicked by the Orbiter K1 of the Buran program. With the Soviet Union dissolvement in 1991, the Buran program was shelved in 1993, and the Space Shuttle one 18 years later for cost saving and safety issues. The post-Soviet era of space plans mainly passed to Russia: the growing financial problems faced by both former leader governments led to negotiations. These resulted

in the Shuttle-*Mir* Program, founded on the successful heritage of ASPT, which set the basics for future cooperative space projects decades ago.

The latest result of the push for a broad international collaboration is the International Space Station (ISS): fifteen nations were involved in the project, which is still flying in LEO, acting as a scientific laboratory and a permanent inhabited outpost. Crew rotation, resupply missions, and continuous support operations are just few of the services guaranteed by partners. Mainly divided into two main sections, the US Operational Segment (USOS) and the Russian Orbital Segment (ROS), the ISS is the perfect example on how coordinated efforts can lead to exceptional achievements. The economic crisis and the spending review regime currently adopted by global politics have led to decreasing space activities. However, in recent years, the space sector has been experiencing a new renaissance: the rising interest of fresh actors, such as private enterprises and public institutions, is spinning the wheel of innovation, thus creating alternative and affordable solutions for space endeavours. Moreover, the incredible results of missions like Voyager (1 and 2) [1], Curiosity [2], Rosetta [3], Cassini-Huygens [4], New Horizons [5], and Juno [6] are inspiring the next generation of scientists, renewing the education and research fields. The legacy of these successful programs is feeding the fire of discovery to address the upcoming challenges in spaceflight. The innate human willing to explore the unknown is all but diminished, finally paving the way for a new era of space innovations.

1.2 Space exploration scenario

Despite the different visions for the strategic exploration of space, national agencies have agreed to sign, through the International Space Exploration Coordination Group (ISECG) [7][1], a statement of common intents. This document is the Global Exploration Roadmap (GER) which is intended to coordinate the mutual efforts and make use of synergies. The latest issue of GER [8] and [9, 10] outlined the future exploration targets: lunar vicinities

[1] ISECG is a voluntary and non-binding coordination forum of 14 space agencies. The members are: the Italian Space Agency (ASI), the French Space Agency (CNES), the China National Space Administration (CNSA), the Canadian Space Agency (CSA), the Commonwealth Scientific and Industrial Research Organisation (CSIRO), the German Aerospace Centre (DLR), the European Space Agency (ESA), Indian Space Research Organization (ISRO), the Japan Aerospace eXploration Agency (JAXA), the Korea Aerospace Research Institute (KARI), the National Aeronautics and Space Administration (NASA), the State Space Agency of Ukraine (SSAU), Roscosmos, and the United Kingdom Space Agency (UKSA).

and surface, near-Earth asteroids, and Mars. Those beyond-LEO objectives are especially suitable to pursue valuable scientific opportunities, which could be particularly enabled by coordinated human and robotic mission architectures.

While the National Aeronautics and Space Administration (NASA) and Roscomos were leading proponents of the previous phase of exploration, other agencies have joined the stage. As an example, more than 50% of the ISS habitable volume was built in Italy, both because of the direct agreements between the Italian Space Agency (ASI) and NASA, and of the European contribution to the ISS program by the European Space Agency (ESA), i.e. the *Columbus* laboratory and the Automated Transfer Vehicle (ATV) for cargo and resupply [11]. The autonomous logistical resupply vehicle HTV and the pressurized experiment module *Kibo* are the Japan Aerospace eXploration Agency (JAXA) contribution to the ISS program.

Furthermore, also private companies have foreseen business possibilities in the space sector. Alongside with historical contractor societies, which helped to design and build hardware and software solutions (e.g. TRW®, Boeing®, Lockheed Martin®, Thales®, etc.), new entities are participating since few years; they are offering a wide variety of services, ranging from space tourism (e.g. Space Adventure®, etc.) to services and technologies (e.g. Orbital ATK®, Sierra Nevada Corporation®, Bigelow Aerospace®, Blue Origin®, etc.), also including scientific operations (Virgin Galactic®, etc.). Under the push of those organizations, a novel approach to the space field has been born: apart from the futuristic and cutting-edge vision of SpaceX®, interplanetary journeys are currently debated by all the potential subjects actively involved in developing such concepts and technologies. This customer-driven approach, where science is not considered as the only purpose of the mission, breathes new life in the global space exploration scenario. The economic development guaranteed by the new business structure, where governments are supporting commercial space industries, will enable space agencies to off-load some of their activities (e.g. infrastructures development, etc.) to focus more on the ambitious challenges of science exploration [12]. The opportunities created can lead to stimulate economic growth of new stakeholders for spaceflight as well as for partner industries. Starting from the LEO commercialization, the establishing of a space market not achievable in the past will ensure cross-pollination of ideas, processes, and best practices, as a foundation for economic development [13]. Thus, the rising space economy can stimulate progress and accelerate scientific discovery, while inspiring the

young generations to pursue careers in the space sector and enhancing technical education (i.e. science, engineering, and math) [12].

The ambitious plans developed by single public entities, like Constellation by NASA or Aurora by ESA, as well as the Asteroid Impact and Deflection Assessment (AIDA) mission by NASA-ESA, were all shelved, never reaching full maturity, if not for promising technical alternatives and interesting concepts. The budget cuts and politics (minor factor) were the main reasons of the cancellation of those initiative: this fact partially demonstrate how this old monolithic-approach to space exploration is not anymore a fully viable alternative for the forthcoming exploration hurdles.

Focusing more on human missions, a progressive approach to pave the way for the crewed exploration of the Solar System envisages to start with Moon and Mars [8–10, 14]. Before starting lunar and Martian sorties, some technological gaps need to be filled: for this reason, robotic surveys are the best option to assess critical mission elements and possible resources to be exploited in situ. The expansion of the human presence beyond LEO should be based on the successful experience of the ISS: international collaboration is the main enabler for fulfilling this ambitious scope. A schematic view of these space exploration targets proposed by the ISECG is represented in Figure 1.1.

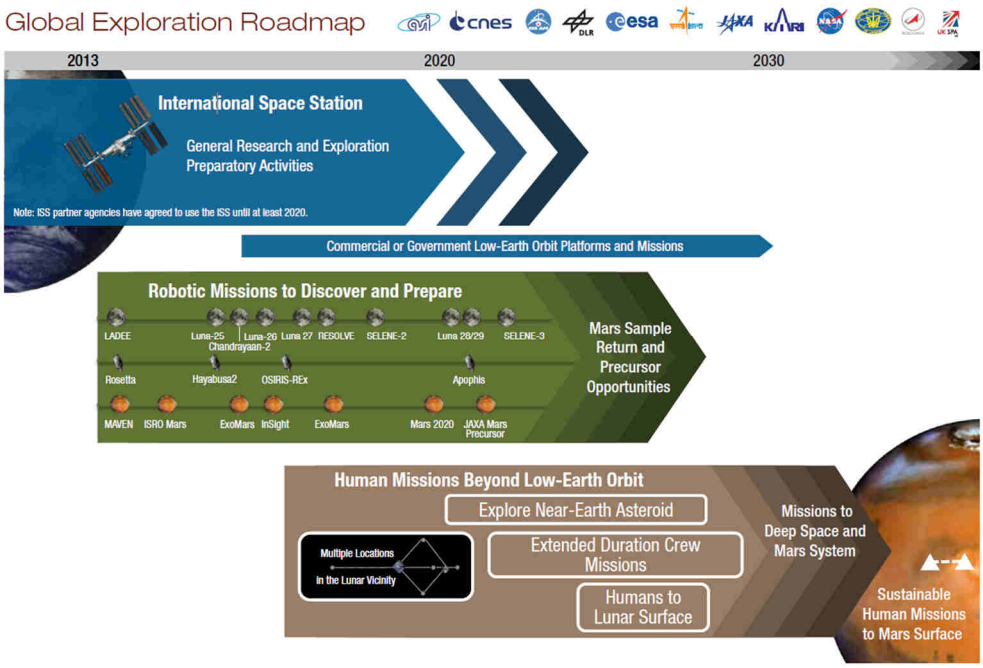

Figure 1.1: The 2013 Global Exploration Roadmap (GER) [8]

If some preparatory activities could be performed using the ISS infrastructure, there are others which require different environmental conditions. While past tendencies and the willingness of some entities were in favour of direct Red Planet journeys, the global vision is slowly converging in pointing back to the Earth natural satellite. Via directing efforts to the valuable cislunar environment and to the lunar surface, enabling technologies, different mission elements and architectures, and concept of operations could be progressively tested. The low gravity ambient conditions of the Moon surface are ideal to experiment and measure the short and long-term effects on the human physiology [15]: potential hazards, such as cosmic radiations, thermal gradients, medical diseases deriving from long stays in isolation and in extreme environments, could be better quantified and adequate countermeasures could be perfected to enable longer and even permanent stays on planetary surfaces. The cislunar operations are also helpful to improve the currently used communication paradigms (e.g. for the ISS in LEO) in view of future deep space missions, where communication delays with Earth will require a greater mission autonomy.

Scientific return could be eventually maximized by survey missions for resources assessment. Lunar extended operations are also interesting for harvesting mineral resources: In Situ Resource Utilization (ISRU) technologies are of paramount importance to reduce Earth-dependability and should be included in an overall design process. All those aspects come out in favour of lunar exploration to prepare the future Martian endeavours. The outcomes of this phase, can help to reduce cost and risk, if direct missions to Mars are considered for benchmarking [16]. The technical solutions produced in this campaign should be inevitably changed and adapted accordingly to the different Martian conditions, but very useful insights could be produced. Identifying, listing, quantifying, and rising the Technology Readiness Level (TRL) level of enabling technologies, which are part of the exploration roadmaps [17, 18], is another milestone to investigate.

All the previously listed consideration, which are related to an incremental evolutionary path for the upcoming space activities, are going to be addressed and better formalized in the upcoming new version of the GER, which is expected to be finalized in 2018[2]. A “Moon for Mars” approach is finally desirable, instead of “been there, done that” motto: Mars is still not a fully

[2] It has to be noticed that the present Ph.D. thesis was written starting from November 2017: all the updates in terms of documents, national agencies decisions, governments and private enterprises commitments subsequent to this date were not considered in this work.

viable destination for crewed exploration, especially with direct mission architecture as the NASA approach reported in Figure 1.2.

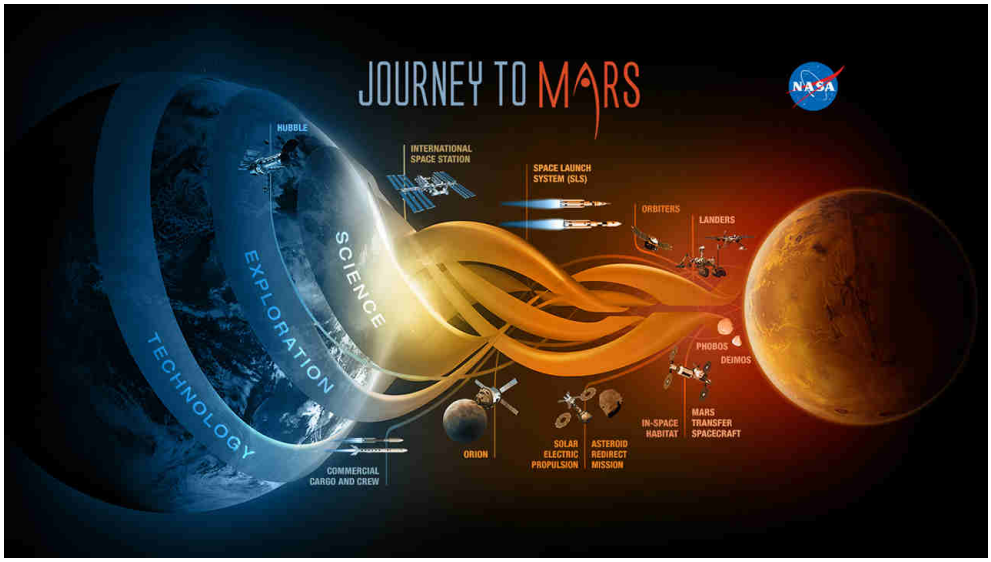

Figure 1.2: NASA journey to Mars (credit: NASA)

The attainment of even symbolic missions would require budgets, technologies, and risks far beyond the current situation [16]: as an example, the unsolved problem of attenuating dose rates for long interplanetary coast mission legs is still debated by the scientific community. Prior to attempt the next giant leap for mankind, i.e. stepping on Mars, it is important to gain more knowledge and experience, setting Moon as the first target for the upcoming space exploration scenarios as proposed by the ESA Aurora program, whose artistic impression is represented in Figure 1.3.

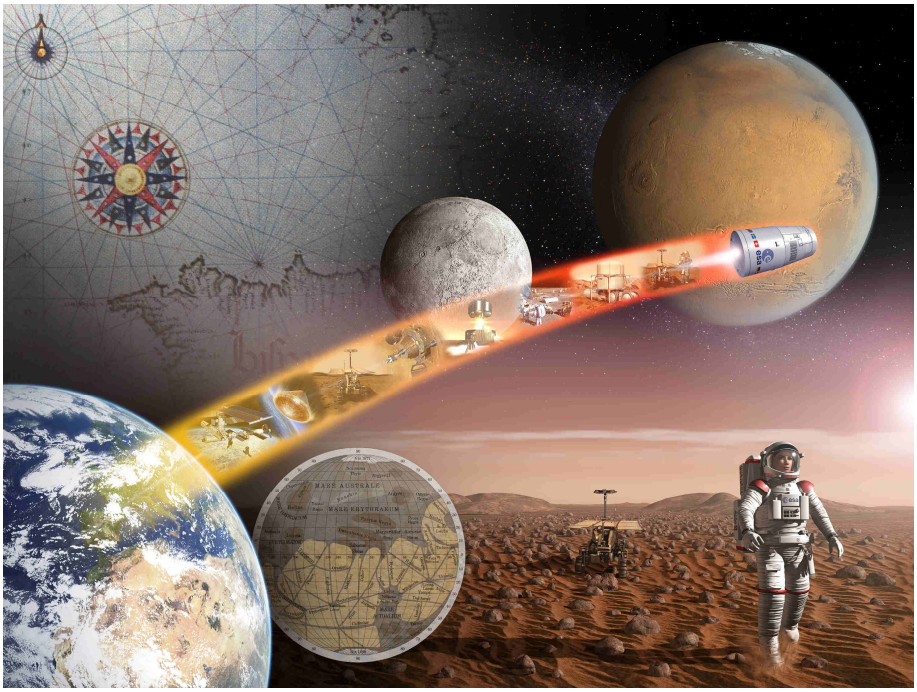

Figure 1.3 Aurora: en route to Mars and the Moon. Artistic impression of the ESA Aurora program, which aimed to prepare Europe to play a key role in the future human exploration of Mars and in the exploration of the Solar System [19] (credit: ESA)

1.2.1 Moon exploration

The Greek Lucian of Samosata was the first dreamer to think and postulate about lunar journeys in the 2nd century AD with his novel "A True Story" that could be considered as the first known science fiction text. After him, generations of enthusiastic explorers took actively part in shaping this fantasy. In 1865 the Jules Verne's captivating and futuristic book "De la Terre à la Lune" (From the Earth to the Moon) attempted to describe the technical feasibility of a Moon landing, eventually realized by the successful human first step onto our natural satellite during the Apollo program, alongside the Russian Luna initiative.

Despite the iconic accomplishment of landing men on another celestial body, Americans were the underdogs for quite a while in the lunar phase of the *space race*. Soviets were leading the competitions with a series of important firsts with its Moon missions. Luna 2 was the first man-made object to reach another celestial body: this unmanned probe hard landed on the lunar surface in 1959. In the same year, the subsequent mission, Luna 3, took the first ever picture of the far side of the Moon, a complete new and unexplored

space world. After few failures, Luna 9 finally succeeded into the difficult task of softly landing on our natural satellite in 1966, not sinking into lunar dust as feared by scientists and engineers. Later in that year, the Moon had its first artificial satellite orbiting around it, the Luna 10 spacecraft.

The strong commitment of NASA to achieve the goal of landing a man on the Moon and returning him safely back on Earth before the end of the 1960s decade, was slowly but continuously progressing. The human spaceflight program rolled out with the "Original Seven" astronauts of project Mercury in 1958, successfully achieved in launching the first US man into space. The natural continuation of those epic results was the project Gemini, started in 1961, which permitted to develop and master the necessary technologies and techniques for landing astronauts on the Moon, so for space exploration operations in general. In fact, the Apollo program benefited of the perfected Extra Vehicular Activities (EVAs) and of the pioneering rendezvous and docking manoeuvres, two major achievements tested during the extended space operations of the project Gemini. This intermediate step between flying a single man to orbit of project Mercury and flying a three-man spacecraft to the lunar surface and back of project Apollo was mandatory. Even if Apollo was conceptualized during Eisenhower's administration and ran from 1961 to 1972, some basics were missing in between the early stages of human spaceflight program and the futuristic dream to walk on our natural satellite. This gap was bridged by project Gemini outcomes.

The Apollo program is, without a doubt, the most iconic space initiative ever attempted and could still be considered as the strongest and solid ever foundation for the next generation of human spaceflight exploration concepts to Moon, Mars, and beyond. Despite two failures (the tragic Apollo 1 and safely-returned Apollo 13), one of the most expensive space program set several unprecedented milestones [20, 21], which are still unbeaten nowadays, like flying human beings beyond LEO and launching Saturn V, the biggest rocket ever built. Moreover, the crew of Apollo 8 became the first to enter lunar orbit, allowing Frank Borman, James Lovell, and William Anders to see the far side of the Moon in person. Only 8 years after the Gagarin's first flight and so the opening of the manned spaceflight era, humankind was able to step on the Moon. On July 21st, 1969, at 02:56:15 GMT, when the left foot of Neil Armstrong was set on the Sea of Tranquillity [22], commented with the famous quote «That's one small step for (a) man; one giant leap for mankind», the world is not anymore the same, also thanks to the incredible footages and pictures taken throughout the entire mission like Figure 1.4.

Figure 1.4 Aldrin's boot and bootprint in lunar soil. Apollo 11 photograph AS11-40-5877 (credit: NASA)

The outstanding completion of such a complicated task changed the history forever and was only possible thanks to the hard work, the strong dedication, and the commitment of thousands of people, brought together by a common intent.

Nevertheless, Soviets did not totally give up in this peculiar competition: even if the crewed lunar programs were jeopardized by several N-1 rocket failures, the super-heavy response to the American Saturn V, the unmanned spacecraft remained their strong point. Lunokhod 1 was the first lunar rover to land on the Moon in 1970, while the US rover landed just the following year, the so-called Lunar Roving Vehicle (LRV) used by the astronauts for surface mobility activities in the Apollo 15, 16, and 17 missions. To date, no cosmonauts made a step on the Moon and the last man to stand on it was the US astronauts Eugene Cernan, part of the last lunar mission Apollo 17, in

whose crew was part the geologist Harrison Schmitt, the first scientist non-military person to fly in space.

Budget restriction and the focus shift to other strategic plans, i.e. space stations and the exploration of other celestial bodies of the Solar System, almost suddenly stopped this golden era of Moon exploration, where Luna 24 was the last spacecraft to visit the lunar surface in 1976, with a sample return mission. The exploratory missions pause persisted until 1990, when Japan joined the stage of countries which successfully compete to put an object in the lunar orbit with the Hiten probe. This initiative contributed to spin again the wheel of lunar science, leading again US to launch a mission to the Moon, i.e. Clementine in 1994, which was able to create the first global topographic map of the Moon [23]. The Clementine data were complemented by the Lunar Prospector, launched in 1998, which mapped the surface composition of the Earth's natural satellite, especially founding the first direct evidence of water ice at the lunar polar regions [24]. Europe also contributed in the new renaissance with the Small Missions for Advanced Research in Technology-1 (SMART-1) probe, using this platform as a technology demonstrator [25]. Launched in 2003, the spacecraft was using solar electric propulsion for the spiral cruise between Geostationary Transfer Orbit (GTO) and lunar orbit, laying the groundwork for future interplanetary and deep space mission technology developments as well as for developing a real international program for lunar exploration, with common-shared scopes and purposes. Kaguya/SELenological and ENgineering Explorer (SELENE) by Japan and Chang'e 1 China (collaborating with ESA), launched both in 2007 just a few months away from each other, enriched the knowledge about the Moon with new measurements as part of an incremental exploration strategy of JAXA and CNSA, respectively. Another emerging country as India, pursued the same objective of lunar scientific exploration, with Chandrayaan-1 (2008), whose payloads were partially developed by the own ISRO and some others directly by European and US partners. More recently, NASA boosted again its strategic plans for returning to the Moon with the Lunar Reconnaissance Orbiter (LRO) and the Lunar Crater Observation and Sensing Satellite (LCROSS) impactor in 2009, especially investigating the presence of water reservoirs in the polar regions [26], an essential resource for manned missions.

Even if several missions studied different aspects of the Moon, some open questions remained unsolved [27], leaving enough room to justify additional investments in this field. The Chinese lunar exploration program, which consists in lunar orbiters, landers, rovers, and sample return spacecraft,

continued in 2010 with Chang'e 2, which prepared the soft landing of Chang'e 3 rover and lander of 2013. Also NASA continued the investigation of physical and geological phenomena with the Gravity Recovery and Interior Laboratory (GRAIL) mission in 2011 and the Lunar Atmosphere and Dust Environment Explorer (LADEE) mission in 2013. Since the early phases of space exploration, almost all the initiative had been sponsored by public entities, but more recently, the private sector had been investing time and resources since it was (and still is) attracted by the potential returns in terms of know-how and expertise. In this sense, the space competition organized in 2007 by the X Prize Foundation and sponsored by Google, the Google Lunar X Prize (GLXP), was one of the biggest pushes driven by non-governments investors. Nonetheless national space agencies had been supporting several initiatives to promote a world global vision for lunar exploration and Moon resources utilization, as testified by the public sponsored International Lunar Exploration Working Group (ILEWG) forum [28].

Due to the technological, political, socio-economic, and scientific rationales and pushed by a global civilizational imperative, exploring and exploiting the cislunar space and the lunar surface could be considered as the next big goal for humankind, by means of nations and stakeholders. Thanks to the lessons learnt from past experiences and relying on affordable and successful results of international cooperation as the ISS program, the space community is almost ready to for the next challenge, i.e. establishing and permanently inhabiting an outpost beyond LEO. The new tendency is based upon pre-existent concepts, taking advantage of the inheritance gained from shelved initiatives. NASA is in fact developing and testing the heavy-lift Space Launch System (SLS) rocket and the Orion Multi-Purpose Crew Vehicle (MPCV) spacecraft, derived from Constellation and ideally continuing the Apollo experience. The high costs related to design, produce, qualify, and eventually fly those advanced hardware have led NASA to jointly study and build them with commercial partners and other space agencies, as for the Orion European Service Module (ESM), which is the European contribution to the US exploration program signed with ESA [29][3]. Exploration Mission 1 (EM-1) will test both SLS and Orion MPCV in 2019 in a programmatic plan to have them finally flying for Mars from 2030s onwards. This milestone is not standalone: the actors involved in shaping the future exploration scenarios have been

[3] The Orion MPCV is composed by the Crew Module (CM) and ESM. ESM directly derived from the ATV and *Columbus* experience and it results from the agreement signed by ESA and NASA.

already discussing how to progress from the ISS collaborative experience to crewed Martian endeavours. Since lunar vicinities could offers assets, knowledge, a bench for enhancing technical and science skills, and resources for industries, and citizens at large, a cislunar station has been envisioned [14]. Officially known as the Deep Space Gateway (DSG), it will help to advance technologies to enable the crew to live and work in deep space, advancing technologies, discovery, and creating economic opportunities, where capabilities and systems will be used in conjunction with SLS and Orion. NASA and its International Partners (IPs) are nowadays developing a reference habitat architecture in preparation to deliver and assemble the first flight units, based upon conceptual studies and ground prototypes design by Bigelow Aerospace®, Lockheed Martin®, Boeing®, Orbital ATK®, Sierra Nevada Corporation® (SNC), and Nanoracks® [30]. The final purpose of DSG is to firstly verify the human crew health resilience in a deep space environment, then to assess the long duration systems and operations in the same harsh conditions [31]. The infrastructures and supplies transportation will be done by SLS, with MPCV assigned for crew travels to and from Earth. Additionally, logistical support could be guaranteed by a solar electric space tug [32, 33].

Before attempting a manned lunar landing again, more robotic probes are needed: using DSG as a radio bridge between our planet and the cislunar space, new concepts of operations could be tested, improving the human-robotic interaction and telerobotic. As the time progresses, according to the ESA Director General (DG), the natural evolution of this evolutionary exploration approach should aim to build a permanent inhabited surface outpost, described as the "Moon Village" concept [34]. Multi-lateral engagement and international cooperation are required: the human base should be self-sustainable and rely on work-sharing among industries, agencies, and any interested parties. ISRU techniques and other promising technologies could better prepare Martian voyages, helping to reduce risks and costs.

The history and the future perspectives of Moon exploration strongly suggest that, with the existing and near-term capabilities to be reached in the next decade, establishing a permanent human presence on the Moon is potentially feasible [35].

1.2.2 Future tendencies

The 3rd millennium brought civil society into a completely new world. With the birth and rise of social medias, the rapid expansion of the information-based business ventures, and the interconnection between smart

devices, digitalization and sharing has become imperative adjective for every kind of data. Newly born concepts, like the Internet of Things (IoT) and big data analytics, are starting to be familiar to everyone. The most evident example of this trend is the Industry 4.0 [36]: the 4th industrial revolution is projecting manufacturing into a cyber physical space, where globalization and networking are playing a major role [37]. Started in Germany [38], but rapidly expanded on a global scale, Industry 4.0 has changed a lot the company concept. The increasing utilization of information and communication technology allows digital engineering of products and production processes alike: in particular, virtualization of the process- and supply-chain ensures smooth inter-company operations providing real-time access to relevant product and production information for all participating entities [39]. Transparency and productivity have been enhanced by the machines connection to a collaborative community [40].

The wide spread of the newly born approach is also slowly affecting the space field, which historically has been always not so prone to great changes, mainly due to very high-demanding safety requirements to guarantee in the harsh environment of space. An attempt of formalizing those concepts has been proposed by ESA via Space 4.0 and its ESA-specific derivative Space 4.0i, which is represented by the logo in Figure 1.5.

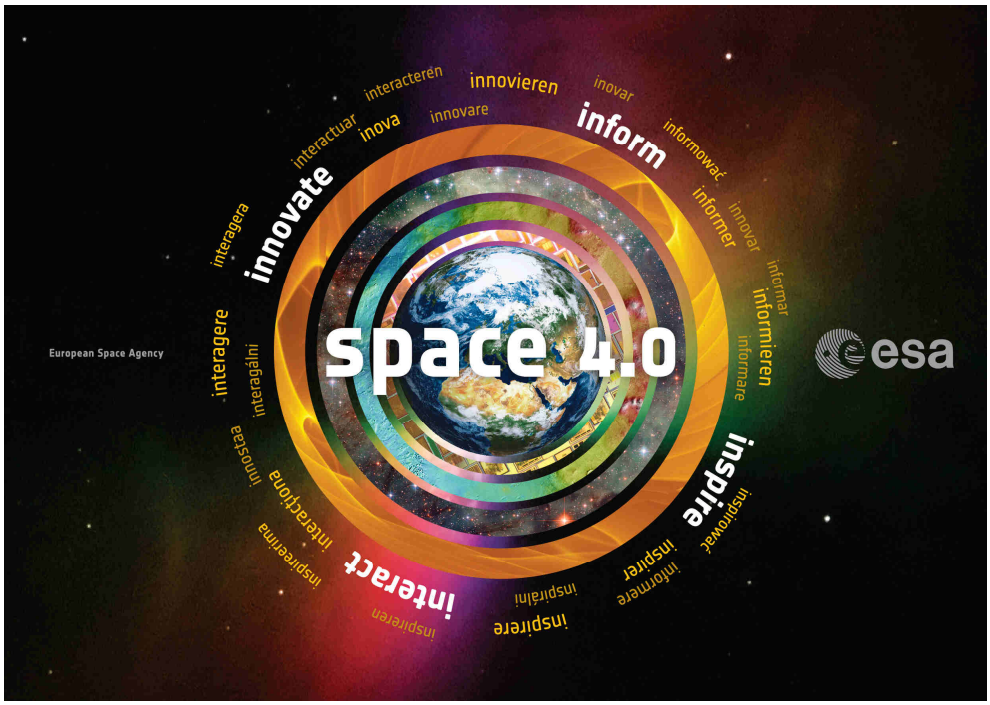

Figure 1.5 ESA Space 4.0i: Innovate, inform, interact and inspire (credit: ESA)

During the Ministerial Council 2016 it has been point out how the advent of a new era was taking place. If the first era (Space 1.0) was characterized by the early study of astronomy, the second (Space 2.0) by the competition among spacefaring nations that lead to Apollo missions, and the third (Space 3.0) by early international cooperation agreements that led to build the currently flying ISS, this last one (Space 4.0) is completely revolutionizing the classical approach to space endeavours in terms of participation [41]. In the past few spacefaring nations could access and actively shape the space field, but in this new era the situation is evolving in terms of numbers and role of the world actors. Diverse factors, including the emergence of private companies, participation with academia, industry and citizens, digitalisation and global interaction, are leading to an ever-closer cooperation between governments, private sector, society, and politics. Space is becoming globally competitive, offering essential services to society and economy (e.g. the Global Positioning System - GPS), in a safe, secure, and easily and readily accessible manner. The foundation of this wise vision should lay on the innovations brought by excellence in science and technology [41]. More specifically, the ESA role in Europe is targeting to implement the Space 4.0i concept [42], where the "i" stands for:

- Innovate, through more disruptive and risk-taking technologies;
- Inform, through the reinforcement of the link with large public and user communities;
- Inspire, through the launch of new initiatives and programmes, both current and future generations;
- Interact, through enhanced partnerships with Member States, European institutions, international players, and industrial partners.

The unfolding of this tendency is characterized by new challenges. The multiple stakeholders' involvement, like both national public space agencies and private enterprises, is a positive fact, giving the opportunity to shape together the next space exploration targets and unite face the hurdles which may appear, but at the same time turns the decision-making process much more complicated. However, sharing duties and efforts is without doubts a way more effective than facing them as a single entity. A good example in this sense are the ISS resupply missions: NASA, Roscosmos, and JAXA have been cooperating with SpaceX® (with Dragon capsule) and Orbital ATK® (with Cignus capsule). Some other partnerships are planned like the cargo unmanned version of Dream Chaser® of SNC®. Moreover, cooperation and

services endorsements have also been initiated with SNC® for the manned version of Dream Chaser® and Boeing® (in collaboration with Bigelow Aerospace®) for the Crew Space Transportation (CST) -100 Starliner® crew capsule, which are expected to transport crew to the ISS and to private space stations instead of the currently used Soyuz in a near future thanks NASA Commercial Crew Development (CCDev) program, and with Lockheed Martin® for the Orion capsule, which has been designed to bring humans to Moon and Mars. This sort of revolution is also happening for satellites launch business: alongside the agencies rockets (e.g. Atlas V by NASA, Ariane 5 and Vega by ESA), private companies changed the market and its equilibrium, offering cheaper and reliable solutions, especially (partially) reusing the rocket itself. SpaceX® Falcon 9 is one of the most used rocket and the first orbital class rocket capable of reflight, via recovering, reconditioning, and reusing its first stage which is able to land autonomously after separation [43]. New ideas are also flourishing for planetary exploration, willing to transform the access to space as truly economical, via exploiting resources. In 2007, Shackleton Energy Company® was established to extract water ice from the lunar pole, turn it into rocket fuel, and create fuel stations in Earth's orbit [44].

What is emerging from the outline of the current situation, considering also the non-prosperous global economic status, it is the urgent need of sharing efforts for a common goal. The Space Shuttle program was the most expensive space program run and paid by a single entity: the US billionaire budget allocation, as for the Apollo project, was one of the main causes of its end. With the predominant spending review actuated by all nations, resulting into a drastic reshaping for the space sector, a joint international effort to pursue the next exploration objective is mandatory. The driving concept is to have each entity bringing its own expertise at the service of the global community of space explorers. A substantial increase of the exploration budget by a single entity (if ever possible), such as NASA, Roscosmos or ESA, could not cover the necessary gap for human lunar and, especially, Martian

missions, unless if Elon Musk's will keep the promise of sending human to start colonizing Mars in 2024 with BFR [45][4].

The urgent need of use space for a sustainable future makes compulsory the sharing of scientific knowledge: it is desirable to create a common shared scientific database, easily accessible by a wide and heterogenous audience, ranging from kids up to scientists and engineering. The attainment of this enterprise could be the first step towards a real collaborative framework, devoted to design the future space exploration missions [46]. The already existing partnerships, such as NASA-Roscosmos to launch astronauts, operate and provide periodical maintenance for the ISS, CNSA-Roscosmos to develop the Chinese space program (rockets, vehicles, and space stations), and ESA-CNSA to train astronauts and taikonauts for future joint flights towards the Chinese space station, augur well. Besides those two-entities contracts, the upcoming decade 2020-2030 will further foster similar initiatives. A new era of coordinated human and robotic exploration is expected to begin, where the Moon is the principal subject to study. EM-1 is in fact offering a great opportunity as a test platform for secondary payload. Lunar IceCube [47], Lunar Flashlight [47], and LunaH-Map [48] are four of the 13 selected CubeSats to be flown on-board the maiden flight of SLS, scheduled for 2019, devoted to lunar scientific observations [49, 50]. Other missions are also envisioned as part of national programs, as SELENE-2 by JAXA [51–53], or joint plans, as Luna-Glob by Roscosmos and ESA [54]. Nevertheless, the interest in the Red Planet is undiminished, as testified by the extended operational period of the Curiosity rover and the upcoming 2020 ExoMars mission.

Alongside the already planned initiatives, several mission concepts have been already proposed. For instance, a conceptual end-to-end architecture, where growing plants on the lunar surface with partial gravity and high radiation doses and testing new technologies for autonomous tele-operations in cislunar space are the main mission goals, has been proposed by Lehner *et al.* [55]. Those type of feasible case studies are helping to identify other possible solutions for future endeavours. Being actively involved in communality of

[4] Announced on September 29th, 2017, at the 68th International Astronautical Congress (IAC), Adelaide (Australia) [347], it is the code name for the biggest rocket ever designed. It is yet unclear if BFR stands for Big Falcon Rocket, underlining its affinity to the SpaceX® Falcon rocket family, or for Big Fucking Rocket. According to Musk's speech, SpaceX® has already found a way to make it affordable with self-financing, also thank to its completely reusability. Anyway, it should be pointed out that no technical details regarding the unsolved problems, also faced by other Martian mission concepts proposers as NASA, of radiation shielding during the Earth-Mars transfer and the regenerative solutions for providing food, water, and consumables have been already disclosed.

intents will guarantee high innovation rates from each participating entity and will help to reduce the cost per mission. For example, one of the biggest design drive affecting cost is the mass to launch: the statistic referred to the launch vehicles market grossly estimate that the ratio between cost and kilogram per flight varies from 10000 to 25000 US$/kg for a LEO payload and is 15000 €/kg for an Ariane 5 GTO injection [56]. The dramatic decrease in space transportation costs is an inspiration that dates back to the Space Shuttle era: with reusable launchers, using SpaceX® Falcon 9 and Falcon Heavy as reference, it is expected to have a gross reduction of 30%, if comparing the same solution with an expandable version; using the SpaceX® Falcon 9 in a reusable configuration as reference would drop the customer price to 43.4 US$ million from the fully expandable version price of 62 US$ million[5] [43]. Also, SpaceX® believes rocket reusability is the key breakthrough needed to reduce the cost of access to space and enable people to live on other planets [57].

Innovative technologies, such as additive manufacturing, are revolutionizing the production methods: designers are now able to create structures impossible to realize in traditional ways, also combining a widespread of functions into a single-component object. New multifunctional and more performing components can be obtained, ranging from aeronautical Unmanned Aerial Vehicle (UAV) parts [58–61] to thermo-structural cold plates for space applications [62]. Even if 3D printing is still evolving research field, tangible improvements for space systems have been already observed. The challenges and the opportunities to be faced by engineers will affect the product development process eventually leading to innovative designs which will require different qualification procedures [63, 64]. The first satellite components are starting to be produced with metal 3D printers like the titanium brackets of Juno [65] and the aluminium antenna support bracket of Sentinel-1 [66]. Cost reduction and performance increasing are currently addressed by topology optimization, which together with production process optimization can lead to rapid end-to-end satellite production using additive manufacturing [67]. Furthermore, 3D printing might be considered as one of the key enabling technology for deep space long duration missions: production, repair, and modification of tools is an example of how this technology can modify the operations as currently investigated for Moon [68] and Mars [69].

[5] The fully expandable vehicle price includes to launch up to 5.5 tons into a GTO with 27° of inclination.

The other trend which can results into cost-saving is adopting more Commercial Off-the-Shelf (COTS) components: CubeSats and nanosatellites have extensively proven the technical feasibility and the full operative realization of this choice for space systems, making space access affordable also to low-budget sector like education (manly represented by universities, if specifically focusing on space projects). Originally conceptualized by NASA, inflatable habitation modules are currently studied to save volume and weight, as the Bigelow Expandable Activity Module (BEAM) demonstrator module attached to the ISS developed by Bigelow Aerospace® using a NASA patent [70, 71]. ISRU techniques, where its use is possible, can represent a huge turning point in the space domain, especially for deep space missions: reducing the Earth-dependability and lowering the Initial Mass to Low Earth Orbit (IMLEO) could allow more flexible mission architectures and longer stays.

To address the conflicting aspects which may rise in developing engineering solution in accordance with the upcoming exploration dictates, new methodologies are being proposed. A careful strategical planning is required, especially when dealing with a diverse stakeholders interaction: focusing on technologies to development, roadmaps play a key programmatic role and its assessment should be supported by effective tools, as the one proposed by Viscio *et al.* [72]. The model approach currently developed by ESA [17] seems to appropriate and it is supposed to help developing the framework for the next Moon exploration phase [18]. The contribution and creation of a real international lunar exploration strategy, where also academia and commercial services could be stimulated and actively participate, is the driver promoted by the ESA (and Europe in general) initiative in this field [73]: the return to the Moon for opportunistic science, technologies validation, and key challenges addressing (e.g. propulsion systems, logistic and life support, etc.) typical of beyond LEO missions, is starting to be actively advocating by many national agencies. The international partners coordination jointly with the human-robotic integrated mission scenarios are urgent, especially for the unprecedented futuristic opportunity to human mission towards Mars and beyond.

1.3 Research motivation

Space mission design is a complex and costly process, where stringent and contrasting requirements affects managerial and technical aspects. Extreme environment conditions offered by space are unique and pone major technological challenges to engineers [74–80]. Cosmic radiations, altered

gravity, vacuum, chemical contamination (e.g. atomic oxygen), micrometeoroids, and thermal cycling are the factors affecting space systems, which should be added to crew safety and security if human mission are considered. Complex systems, characterized by ambitious scientific and technological objectives, coupled with the most complicated machine ever, i.e. the human being, results in new challenges to overcome for space engineers. The cost effectiveness and environmental compatibility are also demanding aspects to consider for the new generation of space mission as well as their design process. If the scenario mentioned in section 1.2.2, where multiple actors' interactions and conflicting constrains, is the most probable path to be followed for the future space missions, regardless of the exploration targets, an impellent need of innovative techniques for space mission design is rising. Systematic strategies and solutions for space system design have to be accounted to improve and optimize classical paradigms, like proposed by Viscio [81]. New simulation paradigms should also be found: even if the computational capacity of the current processors is always improving, as predicted by the Moore's law [82], novel challenges are emerging, as the big data problem, whose implication are limiting the simulation tools.

The work here presented is intended to cast some light on the new disruptive space missions and systems design, which will help humankind in its transformation to become a multiplanetary specie. Technological and business hurdles still lie ahead, but sooner or later humankind will successful accomplish this future evolutionary challenge.

The founding idea of this research lays on the use of a relative new tool in a complete innovative way. Alongside the well-known approaches for space systems design, like the Systems Engineering (SE), its model-based explication named Model Based Systems Engineering (MBSE), and the Concurrent Engineering (CE), the integration of Virtual Reality (VR) since the very early design phases and its possible extension during the entire product life-cycle has been proposed in this Ph.D. thesis, analysing its associated benefits with respect to limitations and future tendencies in the space sector.

The classical paradigms were born to manage complexity that arise in dealing with systems and data organization, including the human component. SE focuses on how to organize the knowledge deriving from the different disciplines involved in systems design over their entire life-cycles. If in the past SE was document-based, the rising difficulties in managing large systems and the increasing computational power of computers led engineers to start adopting the MBSE methodology. Information can be exchanged by

means of models instead of documents, thus enhancing the integration with the simulation software used in the projects. To optimize the design process and to shorten the development time even more since the very early stages, CE is the other typical work methodology used for space systems and mission design, where all the domains and the relative functions are integrated.

The cutting-edge idea of the present work is to interface VR with the standard engineering tools, since it could offer a large suit of benefits, enhancing the decision-making process into collaborative design environments and the perception on how the is changing over time with respect to the design iterations and advancements, which are both typical of space missions and systems design. Thanks to the intuitive visualization techniques which can be offered to the end-users, VR is rapidly spreading out in many companies, both space and non-space related, not only as a plus or a nice-to-have for people's amusement, but as integrant part of the design process.

VR for space could be helpful and similar to what has already been achieved with Cyber-Physical Systems (CPS) in Industry 4.0. This transforming trend of the manufacturing industry is using advanced information analytics: in fact, CPS include and closely monitor information from all related perspective for achieving a full synchronization between the physical factory floor and the cyber computational space. The resulting networked machines will be able to perform more efficiently, collaboratively and resiliently [83].

Via spinning the wheels of innovation, Virtual Environments (VEs) can foster international space exploration initiatives and the development of new partnerships and governance schemes, facilitating the data sharing also to non-technical stakeholders, including a general public audience. The signature of new agreements among commercial space and non-space sectors for activities related to exploration of the Moon, Mars, and LEO. With this in mind, seeking to increase commercial and industrial utilisation of the ISS is one of the first strategies adopted by national space agencies, increasing even more the technological return for terrestrial applications. Engaging a wide variety of actors will providing lifeblood to the entire exploration field: in this sense, VR tools are particularly suited to address this purpose.

A survey about VR, its history in different research environments, and the applications chosen for this work are presented in chapter 2.

The integration of VR into the classical space missions and systems design has been analysed in chapter 3, where a novel approach is also proposed.

Chapter 4 is dedicated to define the reference mission scenario used as test case in this research study.

The simulation workflow, its initial settings, and final results are detailed in chapter 5.

Finally, conclusions are drawn in chapter 6, highlighting the innovative contribution of this work within the global space activities, also highlighting its limitation and possible future improvements.

Chapter 2

Virtual reality

2.1 State-of-the-art

In 1986 Jaron Lanier, founder of VPL Research®, defined the modern meaning of VR as "*a computer generated, interactive, three-dimensional environment in which a person is immersed*" [84]. The concept itself started to appear in the late 1960's and 1970's on several research fronts, laying the foundation for the first patented devices, that can be dated back to the mid-1980's, and the virtual applications as they appear today. The key ingredients of immersion in a simulated world and of complete sensory input and output, presented via head-mounted or computer-driven displays, were introduced by Sutherland [85]. Back in the days, the primary challenge was to offer presence simulation to users as an interface metaphor to a synthesized world [84]. The desktop metaphor, which transformed the modern Graphical User Interface (GUI), introduced at Xerox [86], offers the possibility to manipulate symbols on a computer screen within an illusive environment [87], i.e. simplifying the human-machine interaction. The enhancement of this 2D paradigm into a 3D form, where real physical objects can be palpable and concrete manipulated, results into synthetic simulated environments. Those VEs can be defined as "*interactive, virtual image displays enhanced by special processing and by non-visual display modalities, such as auditory and haptic, to convince users that they are immersed in a synthetic space*" [87, 88].

The novel information media, created through computer graphics, helps to overcome the main problems of GUIs and offers a unique possibility to

develop application using the presence simulation. VEs can be experienced either from egocentric or exocentric viewpoints: the users can actually be in the virtual world or they can see themselves represented by controllable symbols [87]. To return a more vivid and realistic sensorial experience, 3D simulations can be enriched by using several devices (haptic gloves, shutter glasses, omnidirectional treadmills, etc.) to finally convey the user's physical presence in the virtual space.

Virtualization, defined as "*the process by which a human viewer interprets a patterned sensory impression to be an extended object in an environment other than that in which it physically exists*" [87], can be distinguished in three main form: virtual space, virtual image, and VE. VR exploit those techniques to create the telepresence illusion where the operator can perform task on real, computer-generated, or both worlds. Since human beings' five senses allow a perfect interaction with real environments, the research focused on VR applications is targeting to make the end-users to interact with virtual worlds replica in the same natural manner as they do in the real ones, therefore helping to reduce the adjustment phase typical of the training periods. The potential of virtual reality systems as a more intuitive metaphor for human-machine interaction is thus enormous, since the user can exploit his existing cognitive and motor skills for interacting with the world in a range of sensory modalities [84]. The VR final goal is to create a real-time simulation loop, where the immersive world is both autonomous and responsive to external user actions: this is the main reason for which a special attention is given to study, analyse, and enhance input and output channels that create the virtual simulators. Information feedbacks derive from manipulation, locomotion, voice, gestures, and facial expressions [89], thus vision, touch and force perception, hearing, smell, and taste are the sensory data to replicate in VEs.

The predominant feature is without a doubt the vision: the higher is the quality of the synthetic world replica, the better is the visual representation presented to the user, so a more vivid immersion in the virtual world is possible. The evidence of this fact lies in a new branch of research named visual analytics: due to the human beings' nature of highly visual creatures, visual analytics has recently developed around the topic of assisting human-in-the-loop computerized analysis for both learning and decision-making [90]. To ensure a proper level of immersion, stereoscopic vision should be guaranteed as well as motion capture for at least head movements. Depending on the media used, ranging from Head Mounted Displays (HMDs) to passive VR

glasses, resolution, colours, brightness, and motion representation may vary on a wide scale, thus giving high- or low-quality rendering [84].

The secondary sense used for another type of communication, i.e. the verbal one, is hearing. In combination with vision, it can help to improve the overall situation awareness, so to give a better and more complete description of the ambient conditions where the user is located. The subjects involved in virtual simulations can extrapolate information from invisible parts of a certain virtual scene, as they do in the real world, especially when vision does not provide enough data. Audio feedbacks are more useful when sounds are replicated via 3D devices, which immerse even more in the simulated 3D space [91]. More sophisticated systems also foresee a verbal communication with computers using speech generators.

If vision and hearing can just sense the world where the user is projected, the haptic sense can return a more vivid feeling in terms of physical perception coupled with the possibility to act over the environment, thus actively influencing it. Force and displacements are the inputs and outputs of the haptic systems. Interactive means like sticks, pedals, and buttons are just few examples of typical haptic devices. However, accurate modelling is necessary to replicate complex 3D objects to be used in force-feedback devices. In fact, most of the applications requires non-linear representations. To ameliorate the overall performances of the haptic devices newly born methods are applying advanced numerical theories. An example in this sense is the usage of the Finite Element Method (FEM) to compute haptic force feedback and domain deformations of soft tissue models for use in VR simulators [92]. Those type of improvements are directly linked with the increased hardware computational capabilities as well as the algorithms efficiency and parallel programming: thanks to these technology advancements, more sophisticated models can be run in real-time, surpassing the simplified lumped parameter modelling techniques. Furthermore, additional requirements arise from the virtual variables introduced in such formulations: force magnitude and frequency of the force feedback [84].

The human's capability to sense motion and control posture (orientation and balance), i.e. proprioception linked to the vestibular system, requires spatiotemporal realism expressed in terms of timing constrains (e.g. visual feedback rate > 10 Hz, haptic feedback rate > 1 KHz) [84]. Violating those guidelines with lags for instance, can degrade human performance. Side effects can appear similarly as for disorientation and nausea. The synchronization is the crucial aspect to carefully monitor to avoid motion sickness, which is

generally considered to be caused by conflicts between the information received from two or more sensory systems [93].

The calibration of VR systems is peculiar due to the high sensitiveness of human beings. Even if the human body have adaptation capabilities, the conflicts that may rise from an incorrect setup of virtual simulations in terms of sensory cues have to be carefully addressed. The conflicts between the motion signals transmitted by the vestibular system, the eyes, and the non-vestibular proprioreceptors is what lead to motion sickness [93]. Quantifying the limits for lags and fine tuning the accuracy are essential features to measure and regulate for every application of VR: depending on the task to execute, the thresholds of spatiotemporal realism might vary. A standardization is desirable but a comprehensive review of theory and data on human performance characteristics from the viewpoint of synthetic environment systems is still an open research subject [84]. Moreover, further investigations are still necessary to explore the best trade-off solutions in terms of software and hardware to be used. The synthetic representation of reality and how the signals are delivered and used to communicate with the users are fundamental aspects which characterize virtual simulations: only a careful study of the specific fidelity level required by the final field of application of VR can really lead to define the most appropriate devices and trade-offs needed for satisfying the final application requirements at best.

For what concerns the hardware available on the market, at the present time, thanks to the wide spread of electronics devices, VR equipment are progressively becoming very popular crossing cultural thresholds, not only for research purposes but also for the recreational and entertaining sectors. Smartphones, game consoles, and cinemas are extensively using VR. Several devices are present on the market like Oculus Rift®, HTC Vive®, Sony PlayStation® VR, and Samsung Gear VR® represented in Figure 2.1. Each equipment is characterized by different strengths and weaknesses: opening the door of VEs to general public is pushing forward the entire sector since few years.

(a) (b)

(c) (d)

Figure 2.1 VR devices: Oculus Rift® (a) (credit: Oculus®), HTC Vive® (b) (credit: HTC®), Sony PlayStation® VR (c) (credit: Sony®), and Samsung Gear VR® (d) (credit: Samsung®)

The usefulness of VR has been demonstrated in several areas of technology-related applications, likewise in the amusement field. The new medium has in fact demonstrated its applicability and potentialities in medicine, chemistry, and scientific visualization in general, as shown in the example of Figure 2.2.

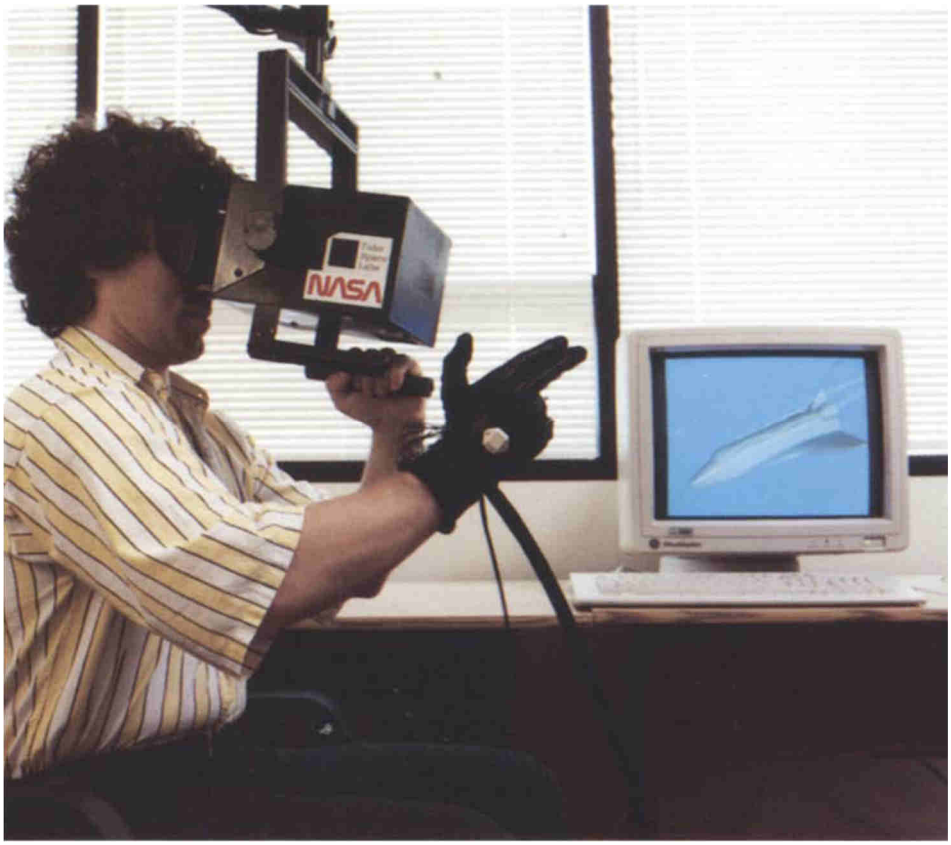

Figure 2.2 VE technology may assist visualization of the results of aerodynamic simulations. Here a DataGlove is used to control the position of a "virtual" source of smoke in a wind-tunnel simulation so the operator can visualize the local pattern of air flow [87] (credit: NASA)

The design phases, where virtual prototyping is used for testing different technical solutions, are also benefitting from using VR, actually opening new frontiers for architects and civil engineers, but also for car, aircraft, and space mock-ups manufacturers. The system design process is data-intensive, where the decision-making is driven by visualizations of that data: the better and diversely a tool can present the studied object, the more comprehensive and accurately will be the final result. The visual analytics insights can potentially increase stakeholder satisfaction to the final design outcome, tearing apart the occasionally “black box” nature of complex design. The benefits related to the visual analytics paradigm are: analyse first, show the important, zoom/filter and analyse further, and details on demand [94].

Those key elements can be detailed as:

- Analyse first – Reduce burden on human by performing some analysis in the background;
- Show the important – Direct attention to the most salient information;
- Zoom/filter and analyse further – Iterative learning with gradually increasing detail;
- Details on demand – Allow human to reveal the details originally hidden to reduce complexity when requested.

The complexity of system design can be reduced if an effective incorporation of the visual analytics guidelines is introduced into the process that support both decision-making and negotiation goals. Redirecting the attention to productive areas of the design alternatives belongs to the cognitive engineering domain, whose funding concepts are typical of a more descriptive research field. An example is given by largely normative and/or prescriptive area of decision-making such as utility theory and information processing [95]. As a result, foreseen the decisions that people make rather the rationale of the decision taken is the principal contribution of the cognitive engineering, which fits well with visual analytics, specifically in the methods with which new interfaces are tested and evaluated [96]. To understand how human begins make decision it is necessary to define when a rational decision can be taken; it requires a precise goal, enough information of the global scenario, and a strategy to optimize the final outcomes of the decision to take, i.e. the expected value. Ideally, in a perfect world, decision-makers have the perfect information to take decisions. However, reality is different since it is naturally affected by different uncertainties, but rational decisions should always be taken. An example of rational decision-making is a coin-flipping contest described by Bahill and Madni [97]: if heads is called and the coin comes up heads, the reward is 10 €; if tails are called and the coin comes up tails, the reward is 1 €. In all the remaining cases the reward is nothing. 5 € is the expected value of choosing heads, that is calculated by multiplying the probability of getting heads (0.5) and the value of the bet (10 €). For tails the expected value is 0.5 €. Rational individuals would choose heads because that would maximize the amount of money that they expect to get. Therefore, all the important information available about the system should be considered by the decision-makers since the effectiveness of the final mission design is uncertain.

Identifying the risk related to any uncertain decision to make will lead to:

- The complexity level raise for any evaluation to do;
- The optimal choice could change over time.

A good decision-making strategy should then not account for selecting the choice itself but rather to have a strategy of choice which makes the final decision to change with respect to external unforeseen events. Flexibility is then necessary to adapt for positive opportunities that may occur and to avoid adverse occasions. However, people are unable to make rational decisions: they tend to look for good enough alternatives that are alternatives that satisfice. For example, in the very early design phase of a space mission/system there are not enough information for taking rational decision because this is an innate human behaviour, even if experienced engineers participate to the design process: in fact, the confirmation bias affect humans that filter-out information that contradicts their preconceived notions and remember things that reinforce their beliefs [97]. This is why a robust aid is necessary to help the decision-making process such as VR.

Other researches demonstrated how the VR is enabling previously impossible applications via revolutionising the user interface. The main areas affected by the benefits introduced are simulation and training, where telepresence and teleoperation could be necessary [84]. The miscellaneous fields interested by this revolution ranges from sport to medicine: training athletes [98], flight and driving simulators, and surgical trainers have the peculiarity to represent scientific domain where the experience gained during virtual training can be directly used for real applications. The early medical purpose into using VR was for planning surgeries, but the current trend is to use VEs also for data fusion[6] [99]. As for designing objects and systems, also medical care with multiple professionals are starting to be provided in a shared VE that incorporates shared decision-making for an actual surgical intervention or a rehearsal [99]. The three major areas of virtual surgery applicability are: virtual humans for training, the fusion of virtual humans with real humans for performing surgery, and virtual telemedicine shared decision environments for training of multiple players, where the patient may be virtual or real, or a combination of both [99]. Those multi-user VEs are required by telesurgery and telemedicine, besides a set of functional, highly reliable

[6] Data fusion is the term used to address the capability of a system to integrate data from different sources.

network, and telecommunication facilities [99]. The surgical computer-based simulations realistic mimic the sense of touch with haptic devices: the reason behind the introduction of these tools is to permit a surgeon to practice a delicate surgical procedure on the patient's specific virtual anatomy before actually performing the procedure on the patient, providing to the surgeon the highest surgical care possible through the use of advanced technologies [100, 101]. Those biomedical applications employ advanced methods, like FEM, to create real vivid interactions [92].

Surgical simulations are just a branch of the emerging VR medical application: other disciplines have made progress in using this emerging technology, like rehabilitative medicine and psychiatry [100]. Virtual endoscopy is also a promising sector which aims to replace standard endoscopic procedures for diagnostic screening: virtual images may be displayed with HMDs or true suspended holograms [100]. The broadened VR applications of neuropsychological assessment enable the doctors to intervene on a specific psychological distress via programming a certain intervention procedure which help the patient to work on his/her disturbance through progressively managing the related problematic situation, as for [102]. Rehabilitation can also overcome the several typical limitations affecting it: the extreme time consuming (and then costly) standard procedures associated to labour and resource intense, dependent on patient adherence, the limited availability depending on geography, and the possible modest effects on subjects [103]. A tentative attempt has been discussed and studied for stroke rehabilitation [103, 104] which is confirming the goodness and the possible benefits which can be obtained.

Another important application of VEs is Augmented Reality (AR). Contrary to what happen with VR where the user can only see the synthetic world and not the real one, AR supplements reality with virtual objects superimposed upon or composited with the real world [105]. The combination of real and virtual in the 3D space with real-time features allows AR to supplement information that the user cannot directly detect with his own senses: virtual objects convey data to help the user performing a task in the real world [84, 105].

The most promising application of AR include military, medical, engineering, and robotics systems, both for training sessions and in real situations [84]. The scarcity and the still non-optimal ergonomic design of AR devices, almost limited to Google Glass® and Microsoft HoloLens® represented in Figure 2.3, is moderately limiting the application for general public, but the related research field is active. Improving hardware and software will

certainly project this interesting technology to a widespread of application for several technical domains.

(a) (b)

Figure 2.3 AR devices: Google Glass® (a) (credit: Google®) and Microsoft HoloLens® (b) (credit: Microsoft®)

For the medical domain, AR techniques are currently investigated to support surgery sessions in open surgery, endoscopy, and radiosurgery [106].

Finally, telepresence and teleoperations achieved using VR tools make possible the access hostile environments, otherwise impossible to reach: the possibility to supervise and control robots for executing tasks is appealing, especially for space applications. As the remote surgery is one of the most advanced application of telerobotic for the medical field, also the space sector uses it (e.g. the ISS robotic arm, named *Canardarm2*, for moving capsules and astronauts during in-flight activities of docking/undocking and repair operations). This particular feature is not the only one which nowadays attracts space engineers in using VR, as demonstrated by the almost pioneering usage of such technology for pre-flight training, but other potential applications exist.

2.2 Space field applications

The severe operative conditions imposed by space since the very early phases of its exploration, led engineers, borrowing from an aeronautical background, to adopt technological advanced solution, but not the latest technical discoveries in order to satisfy the stringent safety and reliability requirements. The sense of physical reality used in VEs was primarily required and developed for aircraft simulators: due to the high cost and risk related for training operators, VR immediately appeared to be appealing thanks to its ability to recreate, with a certain level of fidelity, a synthetic replica of contents, geometries, and dynamics of an aircraft. The intrinsic safety and the relative low-budget devices adopted, if compared with standard processes that use actual vehicles, made those type of application also well suited for testing new

training methodologies, procedures, and technologies. An example of a typical aircraft simulator is shown in Figure 2.4.

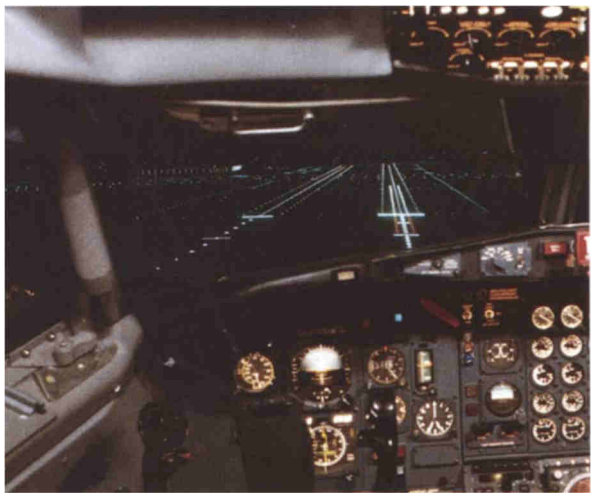

Figure 2.4 View through the cockpit of a 727 simulator at NASA Ames Research Center (ARC) which is used for human factors research. A simulated night flying environment is visible out the forward cockpit window [87] (credit: NASA)

As for other research fields, vehicle simulation may involve moving-base simulators for replicate its dynamics, thus programming the appropriate correlation between visual replica and human vestibular functions is crucial to create a vivid simulation environment. An example of these type of simulators is shown in Figure 2.5.

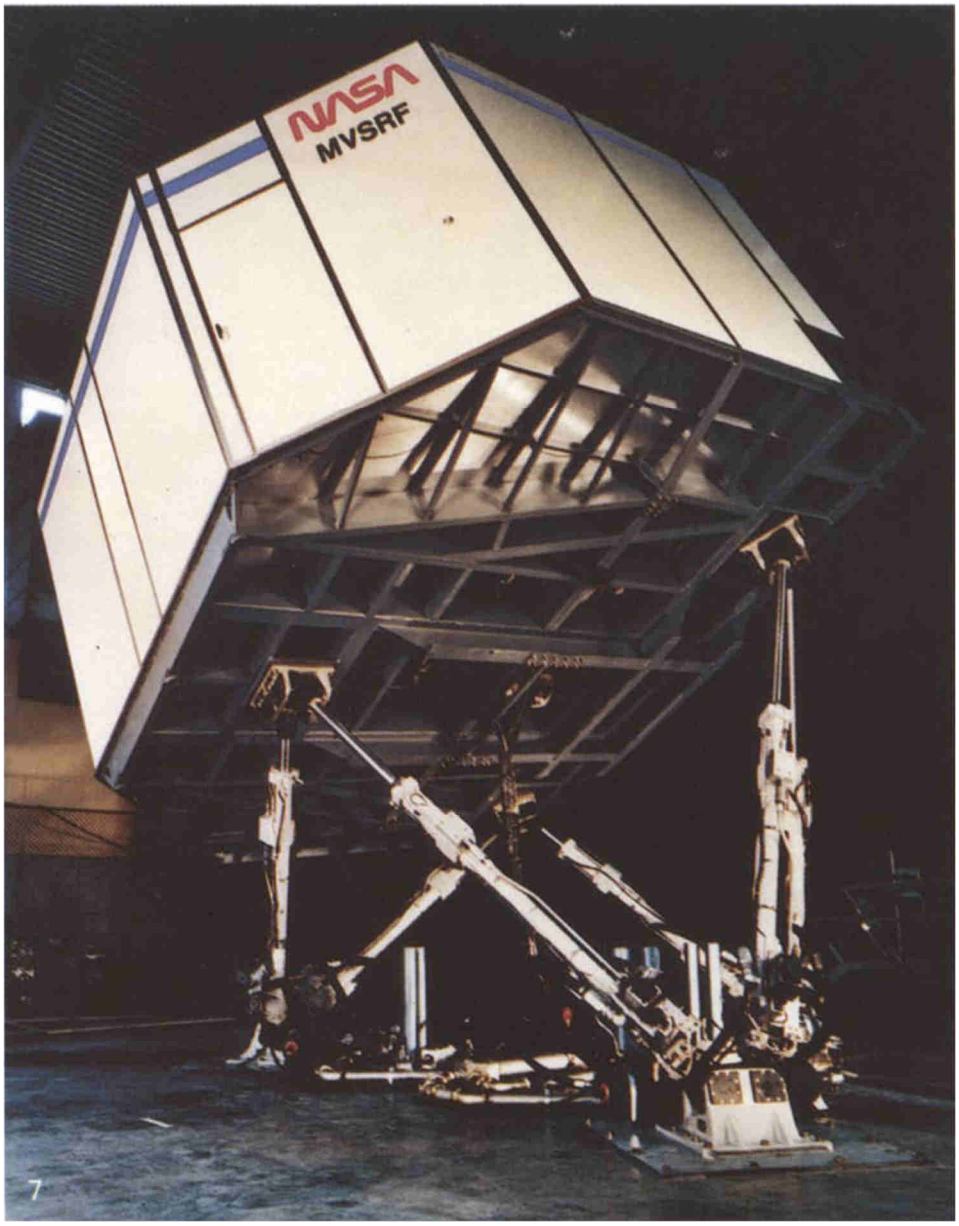

Figure 2.5 Moving base simulator at NASA ARC pitched so as to simulate an acceleration [87] (credit: NASA)

As was happening in other engineering domains, VR was progressively getting foothold also in the space field, despite its historical tradition of slow innovativeness. NASA, being both involved in the aeronautical and space research fields, was one of the first organization to start developing VR applications, following the first results obtained at the Massachusetts Institute of Technology (MIT) at the beginning of the 1980's with a limited three-dimensional virtual workspace in which the user interactively manipulates 3D

graphical objects spatially corresponding to hand position [107]. In fact, in 1984 at NASA Ames Research Center (ARC) the Virtual Visual Environment Display (VIVED) project and later the Virtual Interactive Environment Workstation project (VIEW) were started. The main purpose of the US space agency was to develop a multipurpose, multimodal operator interface to facilitate natural interaction with complex operational tasks and to augment operator awareness of large-scale autonomous integrated systems, whose specific activities were telepresence control, supervision and management of large-scaled information systems and human factors research [84].

The unexpected flourishing of VR was holding the promises shown to such an extent that NASA established a dedicated VR laboratory in the early 1990s at the Johnson Space Center (JSC) to support the human spaceflight division, especially during microgravity activities and EVAs familiarization for astronauts. The new trend introduced was also reflected in human factors and ergonomics studies: historical commercial partners like Boeing® successfully experimented and implemented VR tools inside the standard business areas [108]; the driving purpose was to enhance the current Computer-Aided Design (CAD) modelling properties with a more powerful and flexible design environment.

The first real success in using a VE was for crew training: more specifically, during the Space Transportation System (STS), i.e. the US Space Shuttle, Hubble Space Telescope (HST) repair and maintenance mission STS-61. The difficult task to perform stimulated the entire flight control team to use virtual techniques: the conclusion of the pilot study and the positive effects obtained, since the December 1993 mission was a complete success, suggested its use early in the flight planning activities [109]. Post-flight and post-training interviews to the subject evidenced an efficiency increase in delivering training tasks: the most impressive data which stood out was the compression of the EVA training. A 5-hours EVA took on average only 35 minutes to be completed in the virtual environment: this kind of statistic indicated a shifting from hours into minutes between using standard training procedures and using virtual devices [109]. The use of VR in the typical training sessions was not only involving different astronauts but also engineers as shown in Figure 2.6. Thanks to a more realistic rendering of the HST and Space Shuttle payload bay, VE were positive welcomed by flight team members as reported during the actual HST mission operations [109].

Figure 2.6 STS-61 crew utilizing VR in training for HST repair mission: Bowersox takes his turn manoeuvring the Space Shuttle Endeavour's Remote Manipulator System (RMS) while mission specialist Hoffman, wearing the VR helmet, follows his own progress on the end of the robot arm. Crewmembers participating during the training session are (from left to right) astronauts Akers, Hoffman, Bowersox, Nicollier, Covey, and Thornton. In the background, David Homan, an engineer in the JSC Engineering Directorate's Automation and Robotics Division, looks on. NASA photograph s93-36896 (credit: NASA)

Astronaut training for assembly operations in microgravity environments was using the successful heritage of the STS-61 experience, addressing the rarely covered aspects related to object handling in zero gravity. Overcoming the classical paradigms of classrooms training with VR hands-on experience, give to the trainees a better and concrete impression on how object behave in microgravity conditions instead of partly relegate this task to the imagination.

The current training trends are suggesting an increasing usage of new methods and tools. ESA, together with NASA astronauts, is trying to improve the classical paradigms of ground-based training: in fact, the enhancements targeted by the efforts of both European, acting as principal investigator, and American space agencies are to support procedure navigation, visualisation and hands-busy interaction support for astronauts on-board the ISS. The results obtained by this pilot-investigations lead to the development of a mobile Procedure Viewer (mobiPV): it enables distributed team work through a series of collaboration services between on-board crew members and ground experts, optimally distributing cognitive support for task execution [110]. The

entire research framework aims to create the path towards user-friendly and easily accessible systems, not only for LEO applications as the ISS, but extending the proposed communications infrastructure beyond LEO, i.e. Moon vicinities and Mars eventually, where spin-in technologies from the consumer market like VR and AR are included [110]. The device is currently tested with dedicated experiments on-board the ISS as shown in Figure 2.7.

Figure 2.7 ESA astronaut Paolo Nespoli while setting to use mobiPV to maintain the Water Pump Assembly (WPA) in Europe's *Columbus* space laboratory (credit: ESA)

3D-based applications can also represent the only media able to support crew activities which need to be performed without previous pre-flight training. Emergencies situations and non-nominal robotics tasks are impossible to

be taught by instructors before they actual happen during flight operations. Using such devices could indeed guarantee a successful crew on-orbit training for tasks that have not been previously trained on the ground, via helping to develop the necessary skills without necessarily covering them within preflight training [111]. ESA is one of the institutions that is actively exploring this possibility with a pilot research study carried out with NASA and ESA astronauts during two ISS missions in 2016 [111]. The 3D Visual Training (3DViT) tool developed by ESA was tested using a Columbus payload and a Columbus systems activity case studies: untrained crewmembers were the test subjects of the experiment. The assessment was successful, thus suggesting the possibility to partial substitute ground-based training with on-orbit training for specific activities [111]. In a near future, ground instructors will be provided with the necessary tools to build a 3D visualisation and animation of procedures that can be used for refresher training, which are particularly well-suited for short-notice tasks [111]. A similar project named "Sidekick" has been jointly run by NASA and Microsoft® to test Microsoft HoloLens® for potentially assisting astronauts during their daily scientific activities onboard the ISS [112]. Moreover, the future deep space missions (e.g. manned Martian missions) will specifically require to execute remote training and not only Earth-based training, making 3D animations and VR/AR tools the only viable alternative to classical training paradigms [111].

Other early NASA works were dealing with telepresence: in 1989, a NASA project was begun with the goal of developing a telesurgery system for use in the space program to perform surgery from Earth on an astronaut in an orbiting space station [99]. Apart from the medical field, the features of virtual applications are particularly appealing for teleoperations and telerobotic. Immersive VE systems have been employed and are still used, with several technical enhancements, to interactively visualize planetary terrains to be explore with immersive setups. The major limitation of this method is the models complexity: a realistic replica of a certain portion of a planetary surface is highly demanding in terms of rendering and polygonal discretization, due to the computational cost. Methods for user-based reduction has been proposed in the past by [113, 114] but, thanks to widespread of different devices, whose level of improvement considerably raised from the early stages of VR application, the related technology has made several steps forward, enabling always more realistic copies of the ground to be mimic. Actual photorealism is required to better address the typical duties of those type of VEs: they are mainly employed for robotic operations planning, i.e. where to

go and/or execute scientific measurements, and for site-selection strategies, i.e. landing site choosing and/or EVAs planning. The reconstruction and the consequent virtualization are done using real topographic data, mainly retrieved by remote-sensing probes [115]. 3D terrain representation have been successfully used to represent planetary soils, like the Moon and Mars [116]. Specifically focusing on application with humans-in-the-loop, controlled "boots on the ground" scenarios are effectively used to virtually place subjects onto another celestial body and to then measure situational awareness of a human standing on the terrain of interest. VR is able to create realistic simulations with presence where a test subject has the viewpoint of an astronaut on EVA: a first-person perspective with some level of head-tracking enabled is mandatory to be reproduced into the virtual scene. The future astronauts' training will always more enriched by innovative VR concepts, as also testified by Earth-based analogue campaigns. The AMADEE-15 Mars simulation [117] adopted the Virtual European maRs Analogue Station (V-ERAS) [118] as VR support to train analogue astronauts. The requirement of total immersivity, that was essential to provide an effective test bed platform for preparing the forthcoming crewed Martian expeditions, was fulfilled using gravity-load reducing devices, omnidirectional treadmills, Microsoft Kinect®, and Oculus Rift®. Field operation studies were executed and measured, where EVAs replica was combined with internal operation in a Martian virtual outpost, thus reducing the familiarization period if compared with standard approaches.

Virtual training benefits are amplified if the design stages are similarly treated, especially when human factors need to be taken into account in very early project phases. Reach, visibility, and accessibility are crucial for assembling or processing hardware: 3D replicated work environments with animation and avatars derived from motion-captured measurements can help to train and assess ergonomic risks, determinate negative interactions between technicians and their proposed workspaces, and to evaluate spaceflight systems prior to, and as part of, the design process to contain costs and reduce schedule delays [119]. The assessment of ergonomic risk through the use of software analysis tools in a safe, controlled environment without exposure to unknown risks and hazards was chosen to be tested into early stages of the Orion capsule by United Space Alliance (USA) [119]. An example setup adopted is shown in Figure 2.8.

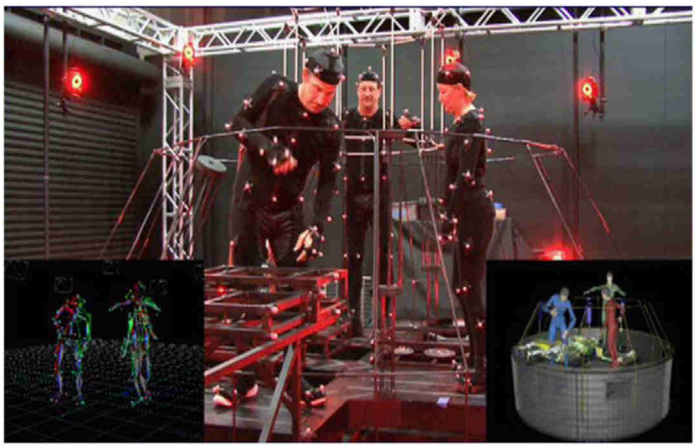

Figure 2.8 Actors provide human-in-the-loop simulated movement, VICONTM cameras capture the "stick figure" wire frames, and JACK Live™ generate the avatars [119] (credit: USA)

Considering a space system, the most intense part of its life-cycle are real operations: the more complex is the design, the more users are involved to operate it. The level of complexity rises even more when the engineers and operators involved come from different backgrounds. An example in this sense is the ISS, where different space-faring nations and agencies are working together using a common infrastructure to perform diverse scientific, logistics, and maintenance activities. One of the most time-consuming activity is tools retrieval and objects stowage. The Ground Support Personnel (GSP) in charge of assisting the delicate astronauts' tasks is sometimes mislead from the non-always up-to-date database with objects locations, whose spatial attributes are sometimes confused by the non-proper synchronization between ground data and actual flight configurations. To overcome and optimize those limiting aspects, VR and AR techniques have been tested with positive results. The tools developed by Thales Alenia Space Italia (TAS-I) for the ISS *Columbus* laboratory demonstrated how VEs can help in knowledge sharing among groups of different disciplines to optimize different aspects of the same module, especially supporting collaborative frameworks in which perform stage analysis verification such as stowage accommodation activities [120, 121]. One of the test case used for assessing the accessibility of the ISS *Columbus* module is shown in Figure 2.9.

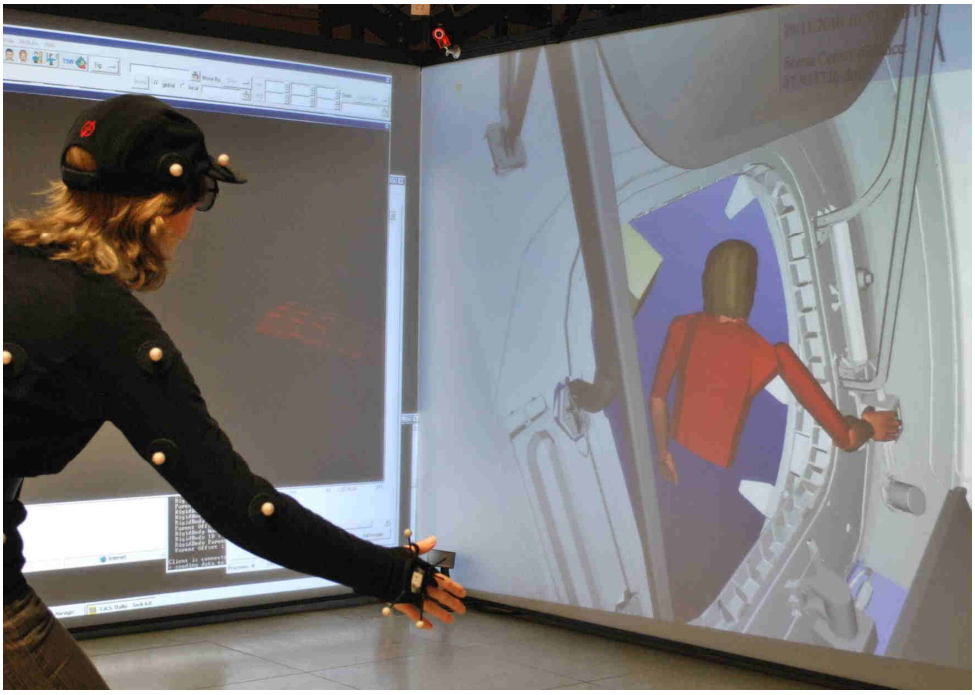

Figure 2.9 User with motion-capture sensors and the JACK Live™ mannequin virtual replica while assessing the ISS *Columbus* module hatch accessibility (credit: TAS-I)

Other examples also exist where VR was used to enhance the space mission design. DLR developed the "Virtual Satellite" tool to support the interdisciplinary data exchange required by CE, which is based on a MBSE approach [122–124]. The software has been integrated into a CE facility to transfer system model information among the different experts involved in the design process. Since interactive visualization is required when dealing with complex data and model, the "Virtual Satellite" was connected to a VR environment for helping the collaborative work and the cross-domain communication [122]. The feature of direct interactive manipulation in an immersive environment given by VR has demonstrated tangible improvement if compared to the classical desktop workstation (i.e. mouse and keyboard). The domain experts involved in the case study of satellite configuration experienced a more direct feedback when expressing their design ideas and discussing possible changes early in the design phases [122]. The collaborative environment and the intuitive access to the real-time immersive visualization, also coupled with the possibility to track the technical changes of the project, made the VR-based software an ideal platform for spacecraft design, especially when comparing different configurations of the system to be designed [123].

Additionally, VEs are also starting to be used in advanced project phases as verification and validation. AR devices can potentially improve Assembly, Integration and Test (AIT) and Assembly, Integration and Verification (AIV) as investigated by ESA. Together with other industrial partners, a prototype application named Engineering data in cross-platform AR (EdcAR) was developed and tested using different use cases: maintenance tasks and real-time equipment monitoring were performed using different devices, including the Microsoft HoloLens® used to replace the cabin filter of the ISS *Columbus* mock-up [125], as shown in Figure 2.10.

Figure 2.10 Operator using EdcAR with Microsoft HoloLens® at work on *Columbus* mock-up (credit: ESA)

The extension to these technologies in the normal product operational workflow has been also tested Lockheed Martin that applied VR and AR capabilities to the manufacturing process for the Orion MPCV [126]. A team of safety, manufacturing, and design engineers run simulations of spacecraft assembling using virtual counterparts as in the real production line to find possible mistakes in the components or in the build-up procedures [126]. Similar infrastructures have been used for satellite assemble troubleshooting: accessibility, ergonomics, wiring, and extent of damage are the aspects evaluated in the assessment of Geng *et al.* [127]. The successful implementation of virtual maintenance simulations helped to identify criticalities and to improve the satellite design in the early stages of the project, thus reducing risks and costs for the manufacturing company [127].

Finally, it is evident that VR is progressively innovating the space sector: several tools and software exist on the market, each characterized by virtues and vices.

Chapter 3

Methodology

3.1 General description

Starting from the classical SE approach, which is defined as "*a methodical, disciplined approach for the design, realization, technical management, operations, and retirement of a system*" by NASA [128], the found idea of the present work is to improve such methodology to better assist the space mission design process. Since a space mission can be assumed to be composed by several systems, it is important to improve the overall design procedure via focusing also system design. By definition, a system is "*a construct or collection of different elements that together produce results not obtainable by the elements alone, where the elements, or parts, can include people, hardware, software, facilities, policies, and documents*" [128]. For the space field is also not unusual to refer not only to single separated systems but rather, if those complex systems are design to be aggregated for absolving common functions, to the enlarged concept of System of Systems (SoS). [129] defined SoS as a System Of Interest (SOI)[7] whose elements are managerially and/or operationally independent systems: their interoperation and produce results unachievable by the individual systems alone.

[7] The SOI concept is related to the attributes of a systems, which are symbolically represented by variables. If a variable is measurable, its measurement is the outcome of a process in which SOI interacts with an observation system under specified conditions [129].

Finally, typical characteristics and relevant concepts of SoS include [130]:

- Operational and managerial independence;
- Geographical distribution;
- Emergent behaviour;
- Evolutionary development;
- Heterogeneity of constituent systems;
- Dependent and cascading failures;
- Copulas (non-linear correlations);
- Self-organizing properties (including criticality);
- Complex event processing;
- Chaotic behaviour;
- Scale-free phenomena;
- Weak coupling;
- Weak signals.

An example of SoS is the US National Airspace System (NAS) schematized in Figure 3.1: it involves several transportation systems that are operated independently but have to share the same space and somehow cooperate [131].

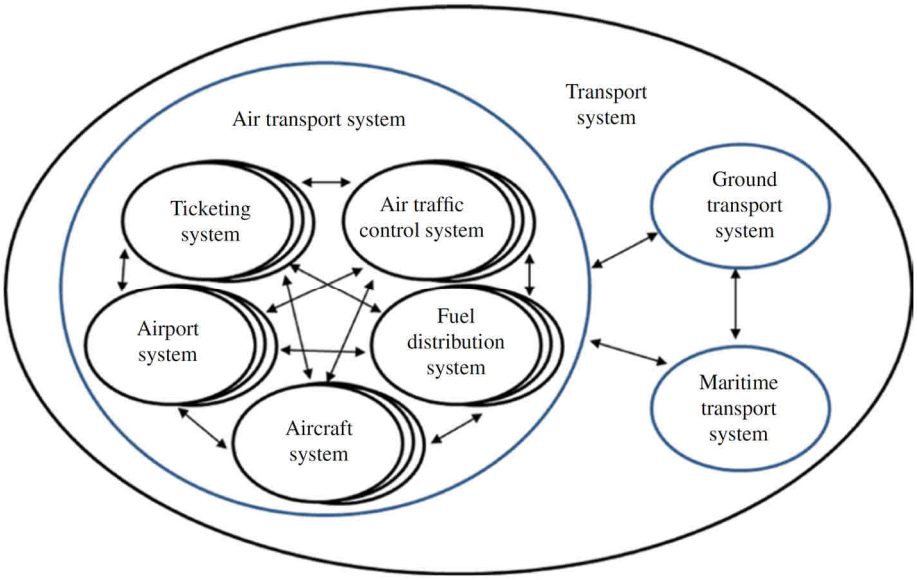

Figure 3.1 Example of the systems and SoS within a transport SoS [129] (credit: Judith Dahmann)

The air, ground, and maritime transport systems are operationally and managerially independent, also considering their geographical distribution on the US soil. Considering only the air transport system, its constituent systems are heterogeneous and characterized by non-linear correlations that can results into cascade failures (e.g. the failure of the fuel distribution system may result into a partial or complete failure of the aircraft system).

For the specific space exploration domain, SoS is generally dealing with extremely large, complex, and intertwined command and control and data distribution ground networks [132].

Because a SoS is itself a system, the systems engineer may choose whether to address it as either a system or as a SoS, depending on which perspective is better suited to a particular problem. The SoS main traits make it difficult to build and manage it with traditional engineering practices. In fact, a collection of systems can be analysed by summing the properties of each of them, but it is not the case of a SoS, which is indeed formed by different systems but is also characterized by an emergent behaviour. The emergent properties that appears in a SoS cannot be deduced by its constituent systems. This feature, together with the evolutionary nature of the internal structure of an SoS, is difficult to analyse using the classical design paradigms. Different design approaches have been proposed in literature. As an example, a "proto-method" has been proposed by DeLaurentis [130]: it is a tentative formalization method for dealing with the SoS complexity; it is divided into Definition, Abstraction, and Implementation phases. Those three major phases are dedicated to [130]:

- Definition Phase: classification of the SoS to be analysed and establishing categories and levels that will later be required to detect evolutionary and emergent properties;
- Abstraction Phase: the main actors, effectors, disturbances, and networks are identified and their real interrelations are used to organize them correspondingly, not in a hierarchical way, but rather unfolding the underneath complexity;
- Implementation Phase: the abstraction done in the previous phase is used to model and simulate the different part of a SoS.

Whether if referring to a single system or to a SoS, the overall space mission design process is complex and costly. Addressing the new challenges imposed by the global exploration scenario that is taking shape, as described

in section 1.2.2, requires novel techniques to assist and ameliorate the standard tools and approaches generally used.

The life-cycle of a space mission typically progresses through four phases [74]:

- Concept exploration: the initial study phase, which results in a broad definition of the space mission and its components;
- Detailed development: the formal design phase, which results in a detailed definition of the system components and, in larger programs, development of test hardware or software;
- Production and deployment: the construction of the ground and flight hardware and software and launch of the first full constellation of satellites;
- Operations and support: the day-to-day operation of the space system, its maintenance and support, and finally its deorbit or recovery at the end of the mission life.

A more formalized and systematic classification has been proposed by some aerospace entities, like NASA, ESA, and the US Department of Defense (DoD). The schematic division of the different phases specifically depends on the institution chosen as reference, but no substantial differences exist. According to NASA Procedural Requirements (NPR) [133], the life-cycle standard phases used for NASA programs and projects are six (Pre-Phase A and phases A through E), which are grouped into Formulation, Implementation, and Operations. A summary description of them is reported into Table 3.1.

Table 3.1 NASA project life-cycle phases [128]

	Phase	Purpose	Typical output
Formulation	Pre-Phase A Concept Studies	To produce a broad spectrum of ideas and alternatives for missions from which new programs/projects can be selected. Determine feasibility of desired system, develop mission concepts, draft system-level requirements, identify potential technology needs	Feasible system concepts in the form of simulations, analysis, study reports, models, and mockups
	Phase A Concept and Technology Development	To determine the feasibility and desirability of a suggested new major system and establish an initial baseline compatibility with NASA's strategic plans. Develop final mission concept, system-level requirements, and needed system structure technology developments	System concept definition in the form of simulations, analysis, engineering models, and mockups and trade study definition
	Phase B Preliminary Design and Technology Completion	To define the project in enough detail to establish an initial baseline capable of meeting mission needs. Develop system structure end product (and enabling product) requirements and generate a preliminary design for each system structure end product	End products in the form of mockups, trade study results, specification and interface documents, and prototypes
Implementation	Phase C Final Design and Fabrication	To complete the detailed design of the system (and its associated subsystems, including its operations systems), fabricate hardware, and code software. Generate final designs for each system structure end product	End product detailed designs, end product component fabrication, and software development
	Phase D System Assembly, Integration and Test, Launch	To assemble and integrate the products to create the system, meanwhile developing confidence that it will be able to meet the system requirements. Launch and prepare for operations. Perform system end product implementation, assembly, integration and test, and transition to use	Operations-ready system end product with supporting related enabling products
	Phase E Operations and Sustainment	To conduct the mission and meet the initially identified need and maintain support for that need. Implement the mission operations plan	Desired system
	Phase F Closeout	To implement the systems decommissioning/disposal plan developed in Phase E and perform analyses of the returned data and any returned samples	Product closeout

According to ESA and to the European Cooperation for Space Standardization (ECSS), the nomenclature slightly differs both for phases and for the interphases fixed reviews [134]. The main differences in terms of phases are [74]:

- Pre-Phase A is defined Phase 0 and is dedicated to Mission Analysis and Needs Identified;
- Phase A is dedicated to Feasibility;
- Phase B is dedicated to Preliminary Definition;
- Phase C is dedicated to Detailed Definition;
- Phase D is dedicated to Production and Ground Qualification and Testing;
- Phase E is dedicated to Utilization;
- Phase F is dedicated to Disposal.

A condensed visualization of the NASA standard is represented in Figure 3.2.

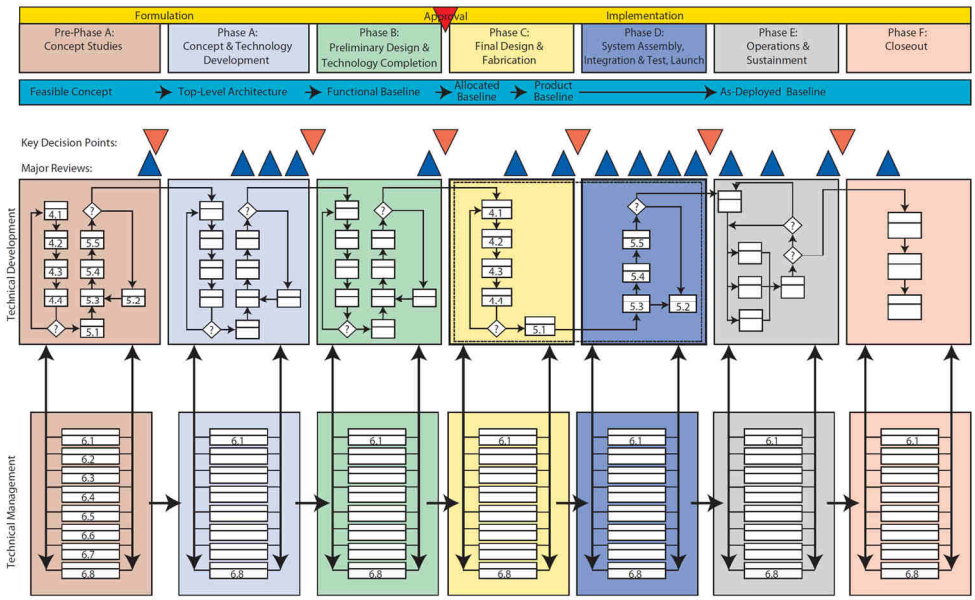

Figure 3.2 A miniaturized conceptualization of the poster-size NASA project life-cycle process flow for flight and ground systems [128] (credit: NASA)

The mandatory requirement to balance conflicting needs is the *leitmotiv* which designer must face throughout the entire product life-cycle. Furthermore, the design environment is not fully independent, but it is subject to external influencing factors which derives from socio-political, economical,

and technical implications. The heuristic part of the design process plays also a non-negligible role, where elegance and artistic beauty can influence the final result, even more than mere numerical optimization algorithms.

All the systems have a certain lifetime where they should meet the expected needs for what they have been design to. At each life-cycle stage, the performances of the systems may vary, but should anyhow fulfil the requirements imposed during the design phases.

The first project stages are characterized by a high level of uncertainty due to the non-total definition of goals. However, even if all the decisions taken at any project stage have a direct impact on costs, either immediate or delayed, best practices in systems design, which derived from experienced engineers and past projects, suggest how the most affected cost-related choices, especially of the advanced life-cycle phases (e.g. production and operations), are those taken during the early design phases (see Figure 3.3). The costs nature is a mix of financial, risk, environmental, technological, legal, and moral factors directly related to the stakeholders, whose fully realization may happen in the latter life-cycle phases.

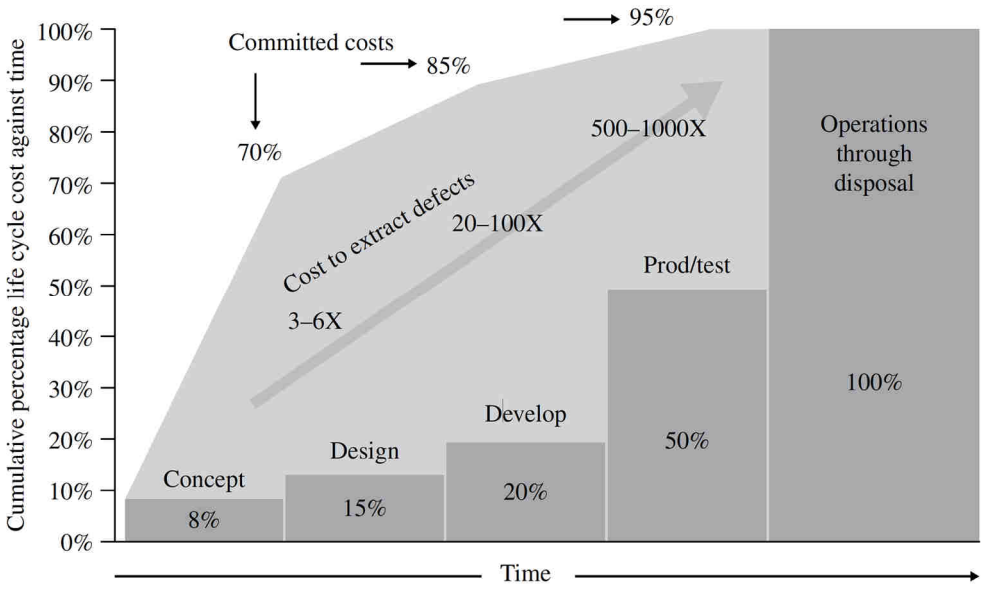

Figure 3.3 Committed life-cycle cost against time [129] (credit: Defense Acquisition University)

Therefore, because of what is emerging from the evidences observed since years within the system design domain, it is highly recommended to perform a careful needs analysis and to accurate develop conceptual designs in the early stages for not overlook any aspect of the project, which may

finally lead to a poor and costly system (final product). Additionally, some decision taken at the very beginning of the system development are irreversible, thus designers are not anymore free to assess other potential design solutions. In fact, a particular system concept and a detailed design, once fixed, intrinsically limit resources, such as time. Nevertheless, the knowledge associated to the system in the early stages is very limited, as represented in Figure 3.4: the importance of clarifying the problem to address (in terms of fulfilling customers' needs) with a high confidence level and a high quality description is a key aspect for better developing different solutions and to eventually choose the best one among them. In fact, a more efficient design approach will ensure to have a higher level of design knowledge since the very first design phases. The design freedom is consequently reduced because the higher knowledge about the product to design prevents to explore unfeasible and suboptimal design solutions already in the initial project phases, thus speeding up the entire design process.

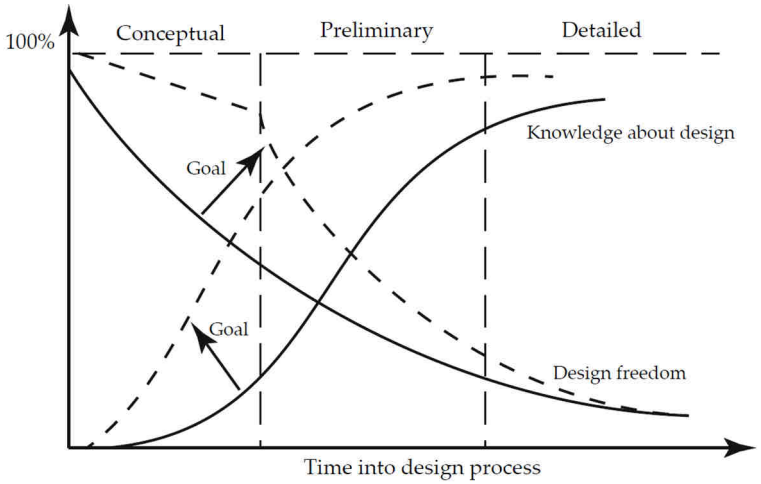

Figure 3.4 Comparison between the classical design process (continuous lines) and the target for a more efficient one (dashed lines) [135] (credit: Guido Ridolfi)

The classical design paradigms present some limitations with respect to the innovative ones, especially concerning the possibility to perform more detailed and faster assessment in the early design phases: those facts are very useful to discover and correct critical issues in the early design phases, so consequently lowering the risk of late changes; the later an engineering mistake is discovered in the design process, the higher are the costs associated to the change needed in the project.

During the past 60 years of space missions design, several approaches have been studied to deal with the early design problems, to save time, and to preserve the project integrity, not wasting all the efforts done in the previous design phases.

The sequential approach represents the most classical design method where all the phases and the related duties are executed “in series”. Each domain and its team of experts is separated from the others (sparse decentralized design team) and design convergence is reached by performing several design iterations: the non-real time updating of the design parameters and the associated variables make the convergence slow, since several changes can be necessary to reach the convergence. If this routine process has been very well consolidated throughout several past successful projects, on the other hand, the main disadvantage is related to the reduced possibility in finding compromises and multidisciplinary final solutions. An improvement to methodology is the centralized approach: subsystem design features are provided by each technical domain to the system engineer(s). Communication is enhanced and stimulated at each design level by the system engineer(s), helping to analyse and share information among experts. Thanks to the modern IT, a novel approach has been formulated to provide better performances: the Concurrent Design (CD). A schematic view of the main features and differences between the sequential and the concurrent design approaches is represented in Figure 3.5.

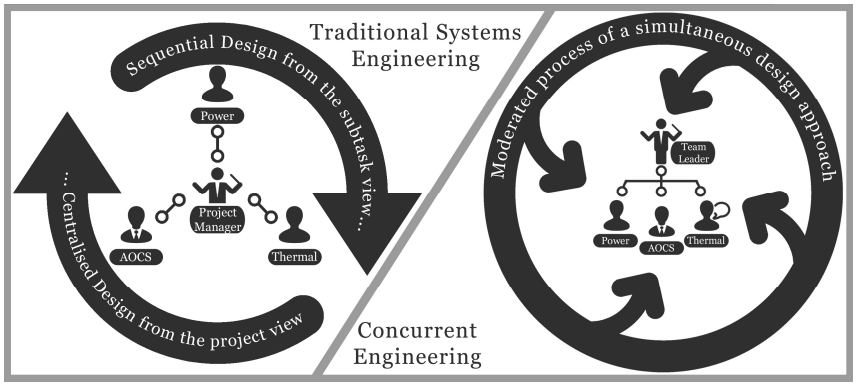

Figure 3.5 Comparison between traditional SE and CE (credit: DLR)

An enhancement of the currently used methodologies to support the complex space mission design process is proposed in this work. The main objective is to promote data and information sharing using a VR tool, added to the standard model-based technique into a CE: this is useful to support the decision-making process via fully exploiting the virtual models created, as

investigated by [136–140]. The mathematical and physical models used to explore the complex design space are enriched by a visual attribute, not limiting the assessments of the design iterations to be performed using only mere numbers but adding a more immediate feedback. The complete definition of how this novel methodology implements those paradigms is described in section 3.4. The standard approaches used for assisting the space mission design process are described in sections 3.2 and 3.3, respectively MBSE and CE.

3.2 Model Based System Engineering approach

The International Council On Systems Engineering (INCOSE) defines MBSE as "*the formalized application of modelling to support system requirements, design, analysis, verification and validation activities beginning in the conceptual design phase and continuing throughout development and later life-cycle phases*" [141]. The current trend for system engineers is to adopt this model-based approach instead of a document-based approach, performing in any case the required steps of the systems design. The activities to perform during the whole product life-cycle are driven by the items produced by the system engineers: for the document-based approach the entire process is manually generated. The concept of operations documents, requirements specifications, requirement traceability and verification matrices, interface definition documents, N2 charts (also known as N-squared charts, i.e. matrices of structural interfaces), architecture description documents, system design specifications, test case specifications, and specialty engineering analyses (e.g., analyses of reliability, availability, schedulability, throughput, and response time) results to be a disjoint set of text documents, spreadsheets, diagrams, and presentations, which are managed in a disjoint set of repositories configuration, using a document-based approach; the often inconsistencies and the fast obsolescence associated with this method makes it expensive, especially for maintenance costs, which are added on top of the total life-cycle cost [142]. Moreover, the sequential update operations are time consuming and defects can easily propagate within the workflow.

A famous fatal example of bad information management and update is the loss of the NASA Mars Orbiter for misunderstandings and inconsistencies of the units of measurement adopted, i.e. metric and imperial units. The discrepancy found between the ground and the on-board software led to wrong trajectory calculations that eventually resulted into a too close Martian orbit [143]. The lack of rigor in the application of the SE standard practices led to the mission failure [144]: the requirements imposed for the navigation were

not carefully verified. If a MBSE approach would had been used, also taking advantages of dedicated software, the accident could had been prevented. In fact, the standardization of the parameters used for designing a system with a model-based approach, including the units of measurement, cannot lead to mismatches as happened for the NASA spacecraft. Starting from the generations of the requirements, all the information and data of the system model are stored in a repository/database accessible from the various expert of the design team: keeping track of the anomalies and inconsistencies, and reporting them to the users are common features of the modern Information Technology (IT) as the DLR "Virtual Satellite" [145]. In this sense, MBSE is useful to overcome the main issues of a document-based approach.

The model-based technique does not differ from the document-based one in terms of deliverables to produce but rather on how they are considered in the product life-cycle. The central node of the entire methodology is the system model: it is a coherent, consistent, and integrated object created using a certain modelling tool [142]. The model represents a central repository from which gleans data to be used in the decision-making process at any design stage. Via conveniently querying the model, secondary derived artefacts can be obtained in an automated way: the diagrams and text documents produced exemplify different aspects of the model, but are not the system model itself, which is way more complex and complete [142]. The great advantage of using MBSE, and thus a system model, is the automatic propagation chain that is established whenever a change in the model happens. No inconsistencies and errors can ever occur with the affordable setup, lowering the maintenance costs and increasing the overall approach quality with respect to adopt a document-based methodology. The system model created can be translated into a software model with a modelling tool, which requires a modelling language and a modelling method [142].

The MBSE method started to be discussed in the academia in the 1990s and nowadays has been successfully implemented in industrial contexts, like space engineering. The intrinsic multidisciplinary nature of the space mission design process makes the system models particularly useful to tackle cross-domains challenges and optimizations within a common integrated workspace. The early design stages are the most affected by those engineering features whose systems engineers should deal with.

3.3 Concurrent Engineering approach

CE is a set of techniques in which the design, development, procurement and manufacturing of a product is carried out by near-real-time teamwork [79]. The fundamental concepts of CE started to appear in literature between the end of the 19th century and the 1960's, but proper definition were introduced in the 1980's [146]. Introduced by the aeronautical industry, the concept was borrowed, adapted, and improved by several entities from both academia and private enterprises. The manufacturing companies started pilot initiatives to shorten the developing time and the cost of products: team approached appeared in the US auto industry as response to the 1980's market decreasing and to the competitiveness of the Japanese enterprises, which were able to create a new automobile in roughly half the time taken by US counterparts [147]. The need to integrate design with other functions (marketing, maintenance, etc.) to optimize all the aspect of the final product and the inclusion of customers in the development phase led to the modern CE. The formalization of CD can be rooted back into the automatic assembly best practices suggested from the 1950's and 1960's in the industry but also in the research done in universities [146]. Tools and team management were the crucial aspects more affected by changes with respect to classical design methods: a high level of integration among all the different technical domains is required to better address all the needs of the stakeholders involved in the design process. With the advent of the modern digital era, the fast-evolving IT has been used to update physical facilities and design environments: product design time (and so product time to market) and development cost have been reduced while the global quality of the final product has been improved.

The principal aim why CE was born is to overcome the intrinsic difficulties of sequential design. The simultaneous development of project design functions with interactive communications among all the actors involved is what differentiate the concurrent approach from the "over-the-wall" approach, as sketched in Figure 3.6.

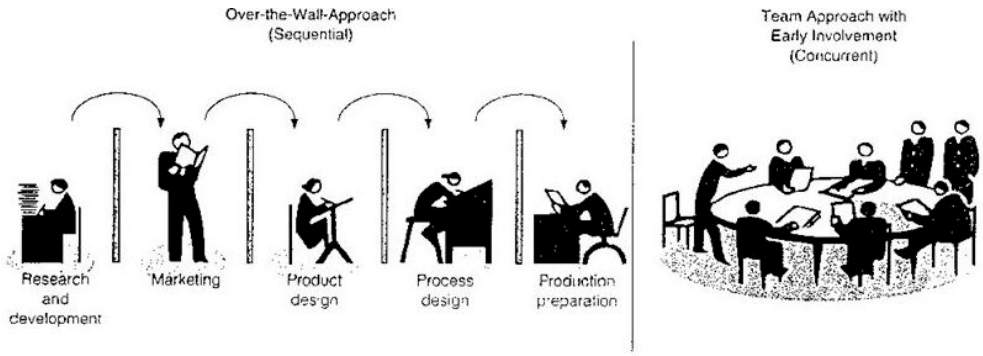

Figure 3.6 Comparison between over-the-wall and team approaches (credit: Wiley®)

The entire design team, which counts different selected technical domain specialists, if CE is adopted, starts to work immediately at the beginning of the design process on each different aspect to address in the project to develop: communications is enhanced thanks to barriers removal. However, contrary to what is expected, not all the experts are present in all the design sessions, but they are chosen depending on the mission part to analyse, its developing context, and its critical aspects. Process convergence is achieved by a (near-) real-time working context in which constant communications and data are interchange in a common environment. Moreover, advancements and progresses are obtained by an iterative process: each iteration can be compared to a trade-off session where proposals and results are presented by each expert; the scope is to spot eventual misalignments or disharmonic development process within the project. The minimization of those risks can only be accounted if a CD approach is used, otherwise a sequential methodology foresees meetings, interactions and data exchange only for brainstorming sessions and mandatory design reviews. A concurrent approach guarantees to stakeholders to always have an update project scenario, where their feedbacks can influence in real-time the design to meet last-minute changes and expectations, which is way faster if compared to sequential design. The continuous communication among team experts transform every decision in a collective shared decision: each design issues that might occurs can be faced and discussed by the entire team, ranging from the mission requirements decision to the tiniest detail (e.g. a screw diameter). The situation awareness is enriched by the constant data flow flanked to the design path: a sustainable and compatible approach is so adopted for systems design which helps to avoid mistakes, to save time, and to reduce workloads.

CE is principally effective for complex systems where several processes and various disciplines are involved and coupled by natural strong

interactions. Generally applied to the manufacturing industry [148, 149], other industrial fields have been using CE: its potentialities to less fragment the project, to reduce the project duration, to improve the project quality, to reduce the total project cost, and to increase the project competitiveness have been used for constructions [150], oil refineries [151], and large fire extinguishing systems [152]. The automotive and the aeronautical industries are other major areas where CE was firstly introduced, as well as for space mission design that embed the same level of complexity and coupling of the disciplines typically addressed by the CD methodology [153].

Several definitions of CE exist in literature but, according to ESA, it is "*a systematic approach to integrated product development that emphasises the response to customer expectations. It embodies team values of cooperation, trust and sharing in such a manner that decision making is by consensus, involving all perspectives in parallel, from the beginning of the product lifecycle*" within the space systems domain [154]. At the end of 1998, ESA applied this methodology to identify early mistakes that might influence the feasibility of a project or worsen its cost, thus maximizing design efficiency. An experimental design facility was developed at ESA - European Research and Technology Centre (ESTEC) to test those paradigms, i.e. a Concurrent Design Facility (CDF) [154]. The activities related to CD practices are various [155]:

- 180+ (potential) future mission studied and designed internally at pre-phase A, conceptual, system level;
- 3 SoS studies;
- 7 new launcher concept design;
- 11 complex payload instrument design;
- 28 reviews of industrial phase A studies (Internal + Industry) and phase B;
- Joint studies with other agencies, industry, academia;
- Education, training, promotion and standardisation activities.

A summary of the missions studied in the ESA CDF is reported in Figure 3.7.

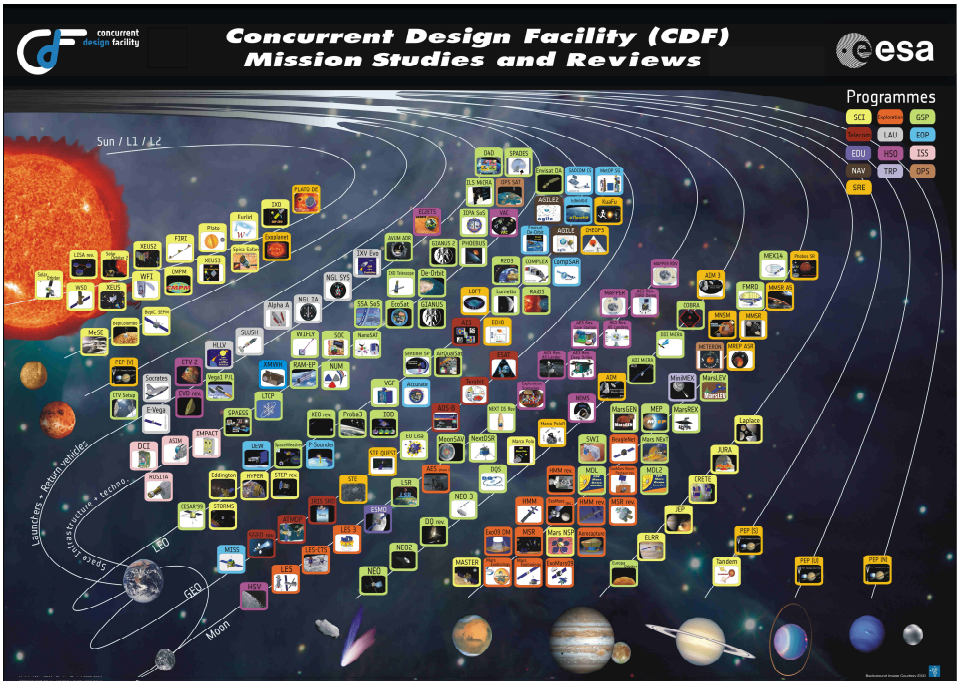

Figure 3.7 Mission studies and reviews done in the CDF of ESA-ESTEC (credit: ESA)

Thanks to the several missions studied and the number of experts within the CE sessions done in several years of activities since its creation, the ESA CDF database of knowledge accumulated throughout the decades is conspicuous. Furthermore, this more detailed and faster assessment for the new potential candidate missions allows to find and highlight well in advance the critical issues which may appear during the project life-cycle. Potential risks are reduced and mitigated, thus preventing mistakes and requiring less interventions in advanced phases. Those features persuaded several entities to adopt this methodology such as:

- ESA (CDF at ESTEC);
- NASA Jet Propulsion Laboratory (JPL) Team X/Team Xc;
- TAS-I;
- DLR;
- Aerospace companies with their own design centres.

Other concrete and quantifiable benefits can be obtained by CD, especially in Phase 0/pre-Phase A and Phase A [79]:

- The study duration has reduced from 6–9 months to 3–6 weeks;
- The corresponding cost has reduced by a factor of two;
- The number of studies that are performed per year has increased;
- The use of CD has resulted in an improvement in the quality of these technical assessments.

The results obtained from each CDF session and the good design practices of past missions are used as a knowledge database for the future missions/systems to be design. The lessons learned derived by previous projects are in fact accumulated in the organization/design team, i.e. the various experts of the different disciplines involved in the CE sessions. However, the specialists are not permanently and exclusively assigned to CDF activities, thus the knowledge can vary, especially because its human component tends to perish with time. In order to avoid any loss, the knowledge should be structured and managed properly: knowledge-based systems are offering a solution to this problem; using artificial intelligence algorithms, the knowledge can be permanently stored, easily replicated, evaluated, and is consistent during time [156].

Other benefits has been observed when CE was applied for later project phases as performing design consolidation, requirements engineering, and system performance optimisation [157].

3.4 VR-based proposed approach

The space mission design process takes advantage of using MBSE coupled with CE. The models created, ranging from a single system to an entire spacecraft and infrastructures (i.e. SoS), are useful to encapsulate all the technical and non-technical features of a product to be used by engineers for designing. The early adoption of the model-based concept since the very first design stages was tested by ESA to design the e.Deorbit mission, where the physical architecture was modelled using the ESA CDF [158]. Despite the great advantages achievable with MBSE, like the possibility to perform in real time on a personal computer all the analysis needed for the conceptual and preliminary design phases, and the wide spread of this methodology, which has been around for almost two decades, a non-fully industrial applicability has been reached yet, while it is pretty much an established and

consolidated concept in the academic world. The time and effort required from training, the deep level of understanding required by the modelling language, the complexity of the models adopted, and the limited flexibility of the tools makes the MBSE design approach still not widely adopt by the industry [159].

The extensive variety of software solutions available for each task to perform in the system modelling activity (CAD, simulations, storage and management of the requirements, etc.) often lead to a non-perfect data sharing, even if all the data are extracted from each software and are made available to the entire engineering team. Especially when large complex systems or SoS have to be design by a broad set of entities, since this is the current and future trend for space missions (as described in section 1.2.2), deliverables are exchanged in form of documents (e.g. Microsoft Word®, Microsoft Excel®, or PDF files) for being compliant to the standard (e.g. ECSS). The results are datasets not really interconnected, diminishing the appealing of the MBSE approach, that is somehow resulting into another form of document-based method. Back in 2009, Eisenmann *et al.* [160] stated that "*a fully operational MBSE process with a corresponding tool set has not yet been realized in space projects today*": the "*inability to sufficiently merge and integrate multiple engineering applications involved in the design, production, and inspection of products across the production network*" described by Lindblad *et al.* [159] is the main reason why "*MBSE needs significant evolution for interoperability*" [161]. One of the solution, proposed by Vanden Bussche *et al.* [162], is using web-based software tools: data are stored in the cloud and are accessible by each expert in a distribute architecture. Each design change is updated in real-time and tools are already available on the market. The principal drawback is the data safety related to cloud computing, but some commercial solutions already exists.

Despite the benefits related to the MBSE approach and its adoption for CD, one of the major problem appears to be robust decisions. The web-based solution partially solves the issue with a distributed access to data, but still using the same paradigms which weaken the model-based methodology. The approach proposed in this research work deals with the integration of VR, thus the creation of a virtual model, to enhance the standard model-based approach. The currently used design tools can perform quantitative physical analysis on the different aspects and components whose space missions are composed. Data resulting from simulations may result to be incomplete and meaningless for some of the actors involved in the design process, depending

on the specific discipline under analysis. VR can offer to the different experts a better understanding of the product, where all the system features are evident at a single glance thanks to the immersion and the interaction that VR can grant. This fact makes VR tools particularly suitable for multidisciplinary, collaborative, and shared work environment into which there are many information and data to exchange. Space system design is one of the engineering branch that can benefit more if VEs will be introduced: the harsh environment conditions to withstand for space products make their design difficult, especially when dealing with crewed applications, where security and safety are the most stringent and demanding requirements. A virtual tool can then facilitate the design process for space engineers.

The proof of concept proposed in this Ph.D. thesis aims to adopt a VR setup for a preliminary performances analysis of the power system that supply the crewed outpost at the lunar south pole described in chapter 4. The purpose is to demonstrate the feasibility of integrating VR since the early design phases instead of using classical design tools. The main scope is to overcome the limitations imposed by the MBSE methodology via transforming the product to design into a computer-based virtual replica. As an example, the standard CAD modelers used present some limitations, especially for concurrent and interoperability operations typical of broad consortiums, as it is common for space missions design. Even if the 3D desktop visualization of the modern CAD software has enhanced the design process with respect to the past 2D drafting, VEs can offer huge advantages for engineers and designers. The intrinsic constraint of the standard CAD tools is the usage of 2D screens to display 3D objects: this inaccurate depiction of the real world can partially reduce the users' perception of some aspects of the project. Mouse and keyboard can likewise limit the direct interaction with the object which results simpler by using human machine interfaces, such as tracked interaction devices [122]. VR helps to improve inter-domain communication via offering a common developing platform where to implement and test various engineering solutions.

The outcome of this VR-based design approach is the virtual model of the product: it should represents a semantic and systemic aggregation of data, simulations, and processes of a system; humans, product, and their interaction are also included to complete the overall picture about the product [163]. An example of virtual model has been schematically presented by Krassi *et al.* [163], as portrayed in Figure 3.8.

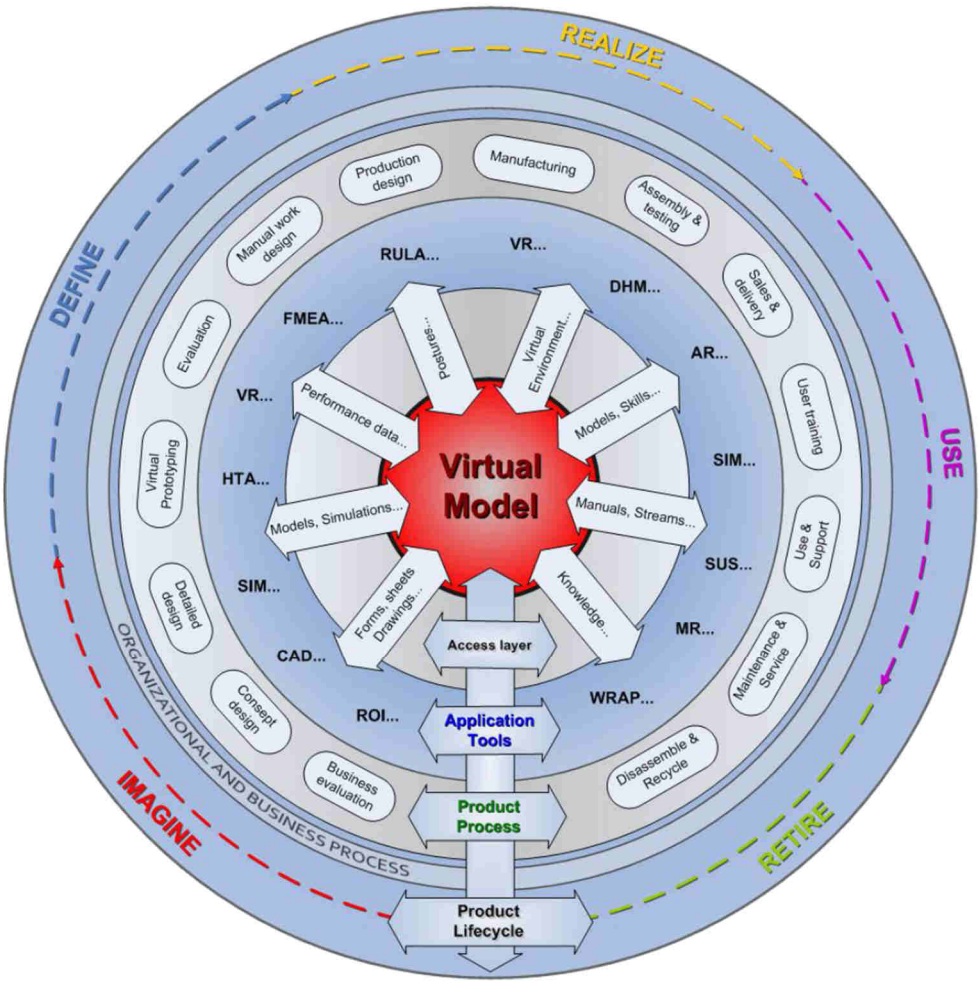

Figure 3.8 Virtual model schematic view [164] (credit: ManuVAR)

The so defined virtual model should be accessible at any stage of the space missions/systems design process by all the actors involved. The intuitive data visualization and the possibility to real-time modify the virtual objects since the very early design phases enables the collaborative design and the evaluation of different design alternatives by multiple domain experts [122, 123]. For example, the evaluation of human factors is one of the paramount aspects that can be assessed: non-standard experts can participate in the design sessions for addressing the entire set of features that the final system will face during the real operative life. Astronauts and flight controllers, which have a first-person experience of real operations and microgravity environment conditions, are the best candidates to avoid poor design mistakes that may not work once in orbit. By creating a common platform of data access and sharing for all the experts involved in the design process, i.e. the

virtual model of the product to design, the creation of user-centric/user-oriented product will be enabled and more “user-friendly” and “easy to use” interfaces will be developed. An attempt for transforming the classical design paradigms via a user-centric prospective for space systems was done by [165, 166]: starting from the operational experience gained on board the ISS by astronauts, the *Columbus* module toolbox has been redesign. End-users (i.e. astronauts) and GSP (i.e. engineers, designers, and flight controllers) were sharing feedbacks that resulted into an optimized and effective solution which is still currently used on-board. Novel technologies were used for production: the toolbox has been 3D printed using Fused Deposition Modelling (FDM) technology for processing the thermoplastic polymer ULTEM 9085 and is currently part of the standard equipment of the ISS *Columbus* laboratory as reported in Figure 3.9.

Figure 3.9 ESA astronaut Luca Parmitano while showing the new *Columbus* toolbox (credit: ESA)

The feasible applicability of this new type of design approach has been demonstrated jointly with its being prone to innovations. The process, which led to finally realized the toolbox, underlines how important is to involve each actor that can analyse all the final system features under a different prospective, thus using his/her personal point of view. A schematic representation of the workflow followed during the design phases is depicted in Figure 3.10.

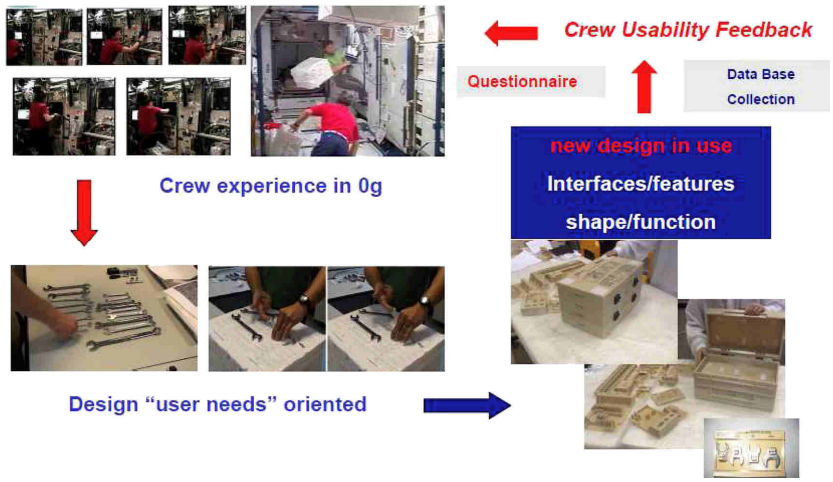

Figure 3.10 Columbus toolbox crew usability feedback [166] (credit: TAS-I)

While in the classical design-implement-test cycle the final users test physical prototypes and subsequent modifications are implemented using their feedbacks with a multiple iterations scheme [84], the introduction of VR is a cost-effective alternative which could upgrade the current trends: motion capture technologies and digital human interfaces are improving human factors analysis since the early project stages in a more efficient and flexible way if compared with the physical prototyping associated to a complex launch vehicle or spacecraft [119]. In fact, a VE is a more responsive ambient where to assess design changes, including the virtual test of operations and training procedures.

By starting from the preliminary design, as proposed in this work, the virtual model should replicate the evolution in time of the product under development during all its life-cycle phases. Pilot initiatives have already investigated the incorporation of virtual attributes in different phases of the design process. A common platform based on a VE to prevent misalignments and incorrect data flow was used for the ISS *Columbus* analysis [167]. TAS-I is actively working in this direction with its internal COSE facility [168–170], but other projects have been studying the integration of VR in the classical design paradigms of space systems [163, 171–175]. As already discussed in section 2.2, positive examples already exist, and the research is active for the verification and validation phases, like AIT and AIV procedures for equipment integration. Virtual assembly schemes, ergonomics, and maintenance has been respectively investigated for the Orion MPCV spacecraft [126], for satellite assemble troubleshooting [127], and for replacing the cabin filter of the ISS *Columbus* laboratory [125]. Training and operational procedures were

also interested by improvements obtained with VR. A first successful example was implemented by NASA for training the Hubble space telescope flight team [109], where the time required for the EVAs familiarization phases was shorter thanks to the adoption of a VR tool. Additionally, encouraging results have been obtained for the ISS *Columbus* laboratory stowage operations [120, 121].

As it is evident from those first results obtained in different project phases, the extension of the virtual model alongside the entire product life-cycle can help all the actors involved in the space missions and systems design process. The successful tests are suggesting that the possibility to account verification and validation aspects earlier in the project stages using VR and AR tools can help to anticipate possible problems, also lowering risks and costs of the entire manufacturing processes [127]. Similarly, instead of using standard processes, as for the ISS training and operations scheme [176–179], the progressive VR (and also AR) tools integration will bring furtherance in terms of time and cost for training procedures. Considering the EVA training, composed by neutral buoyancy, parabolic flights, and field analogue tests, the hardware interaction aspects can be easier addressed within a VE, apart from microgravity mimic[8]. Moreover, hardware reconfigurability and trouble-shooting for on-board failures will be surely take advantage of the potentialities offered by VR. Inexpensive (preliminary) tests can be performed on ground to elaborate a procedure to be used in case of unexpected problems during nominal operations. The GSP can unlimited test, in a controlled and truly vivid VE, the list of actions to perform in order to solve the criticalities identified during flight activities, so always giving the best solution possible to the operators in space.

The general founding concept related to the VR-based methodology applied to space missions and systems design described in this research work is that to migrate all the product life-cycle activities in a VE. In fact, the earlier in the product life-cycle a VR-based tool is adopted and the more experts are involved in the design phases, including end-users, the less errors will be done and the more optimized and customized is the final product, especially when dealing with complex machines and extensive space exploration programs. Even if the possibility to make design mistakes are almost limitless, using this

[8] It should be promoted however that partial gravity levels, as for the Moon and Mars, can be simulated with gravity-reduction devices such as alter-g and vertical treadmills, and gravity-load reducing systems (using both weights and springs). An example of this technology has been tested by [118].

approach will at least help to save time and costs within both advanced life-cycle phases and initial ones, because the majority of total product costs are determined with early design decisions (as represented in Figure 3.3).

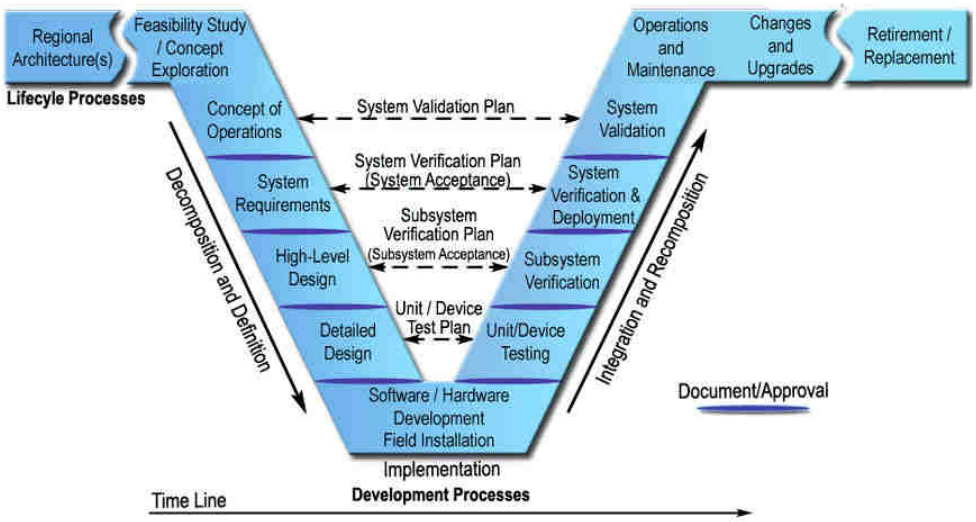

Figure 3.11 SE "V" model [129] (credit: INCOSE)

With respect to the classic "V" model project development represented in Figure 3.11, where all the Validation And Verification (V&V) procedures and the integration tests are performed in the deductive branch, early stages evaluations can be performed in the inductive branch of the product development process using VR. This entails lower efforts and stress level for the engineering team, preventing over costs and project delays. In fact, if a design change (e.g. at the system level) should be implemented during the integration phases, the process should be stopped: from the deductive branch, designers should return to the inductive branch of the "V" model at the same level (e.g. system level), covering all the already done steps backwards. The modified "V" model conceptualized in this work is presented in Figure 3.12.

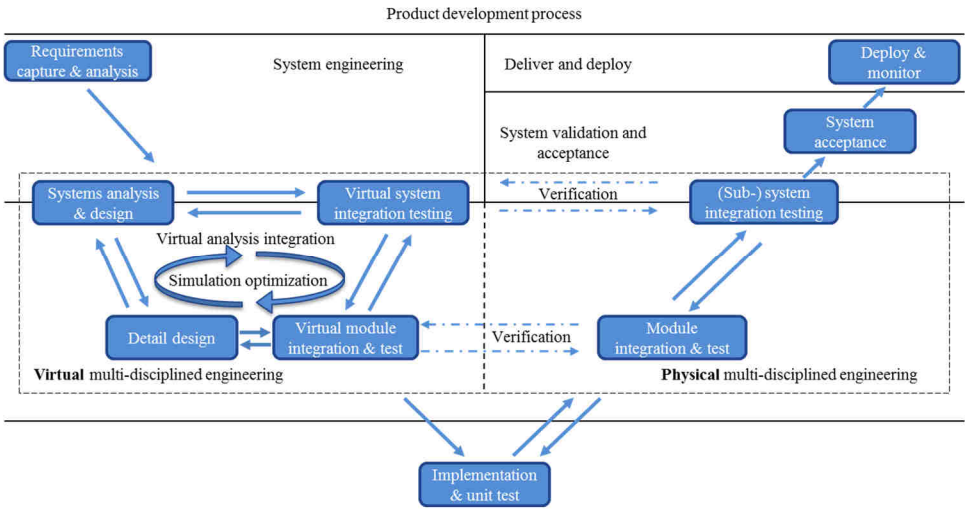

Figure 3.12 Modified version of the "V" model with VR integration

The same VR-based approach can also be extended to the operational phases, which are part of the second "V" branch of the "W" model typically used for software engineering (see Figure 3.13).

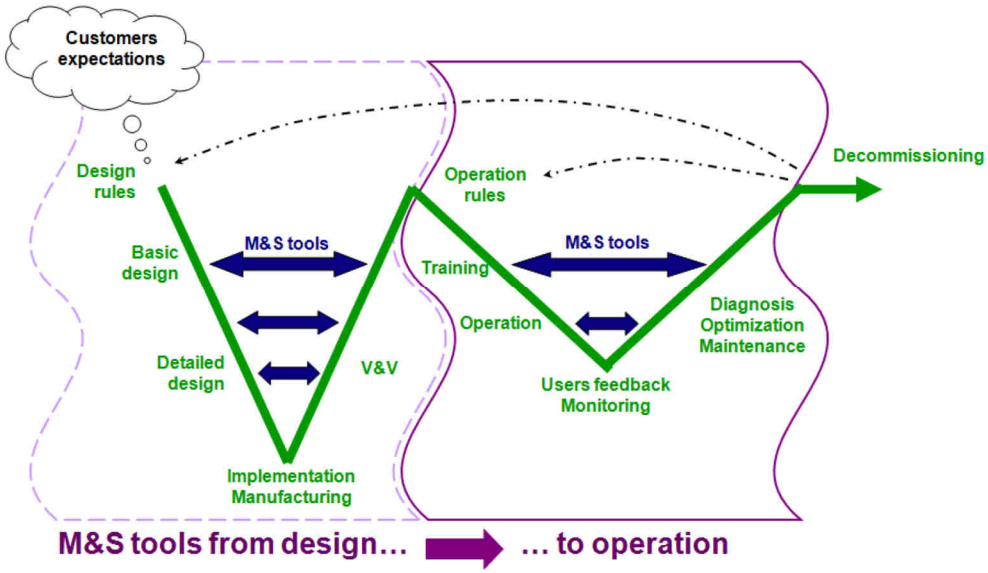

Figure 3.13 "W" model [180]

Chapter 4

Case study

4.1 Mission scenario

National space agencies and industries are actively advocating to explore lunar vicinities as described in section 1.2.2. The Moon is starting to be again considered as the focal point towards the human exploration of the Solar System after the Apollo era, especially for the upcoming Martian sorties. According to the GER [8, 181, 182], to ESA technology roadmaps [17, 54, 72], and to other international institutions [183], the proposed long-term future exploration scenarios define the cislunar space and the lunar surface very appropriate for testing critical mission elements and partial gravity operations. Those milestones assessments aim to reduce risks and costs related to future exploratory endeavours. A broad international cooperation framework is required to develop this incremental strategy to validating enabling technologies. Earth-based initiative are currently simulating and training future astronauts, with both Moon [184] and Mars [117] campaigns, while other researches are investigating how the reliable ISS-concept (orbiting space station and laboratory) can evolve, taking all the useful insights from past operational experiences.

In the 2020-2030 timeframe precursor robotic probes will continue to study, expanding the already existing scientific knowledge, the problems related to waste management, power generation and storage, water processing, automation and robotics, paving the way for the forthcoming crewed campaigns, also addressing human factors analyses. A deeper understanding of

the lunar environment is necessary for complementing the Apollo [20] and the remote sensing data archive: gravity field, temperature variations, cosmic and Sun radiations level, and Earth visibility needs experimental on-site precise measurements. Abundant mineral resources are widely present on the lunar soil: their potential exploitation could be used to pursue the establishment of a permanently inhabited lunar surface outpost. This base can be considered as the natural stepping stone while progressing to attempt the first Red Planet crewed sorties and the its latter colonization [31, 185–187]. Self-sustainability is a mandatory requirement for deep-space exploration: reducing the Earth-dependability will enable to reach farther destination, even beyond the Solar System (e.g. near-Earth asteroids, Jupiter's Moon Europa or Saturn's Titan and Enceladus), and longer stays. Communications delays also pone major challenges for mission autonomy and telerobotic operations: that is why preparatory unmanned missions are of paramount importance.

The ESA visionary concept called "Moon Village" [34, 35] is actively proposing a novel concept to incorporate, under a common framework, all the lunar exploration efforts sunk by multiple actors. Contrary to what happen in the past with the *space race*, ESA DG called together private companies and public institutions (space agencies, universities, and research centres) to globally work as a single-entity scientific community as progressing towards lunar exploration. The return to the Moon with a permanent surface outpost, which can be similar to the one represented in Figure 4.1, should not be intended as a technology-driven project, but it rather have to gather resources, ideas, and plans from the participating entities.

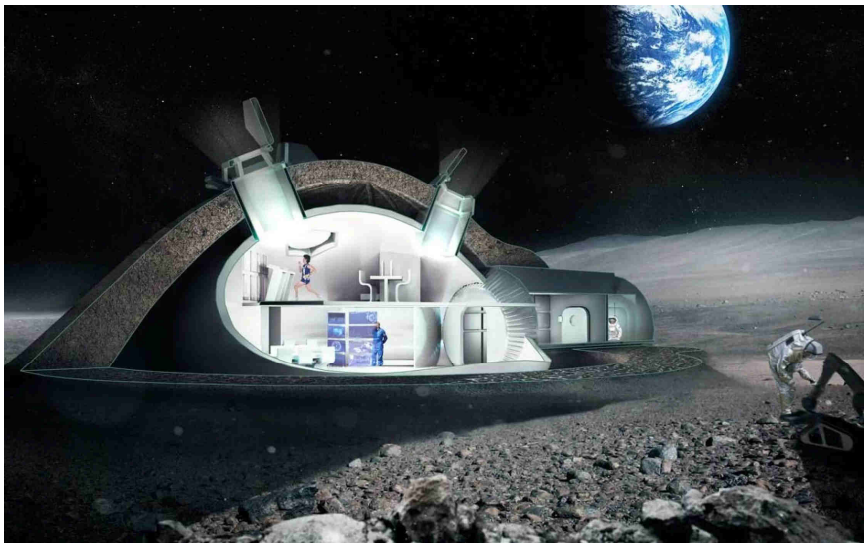

Figure 4.1 Artistic concept of lunar base (credit: ESA – Foster + Partners)

The purposed self-sustainable outpost is intended to be modular, thus upgradable and scalable in terms of crew and equipment. The commonality of intents of the potential international stakeholders makes the base as the perfect platform for scientific activities, also accounting for potential commercial partnerships that may flourish with a lunar economy. Extending the human presence beyond LEO is the principal goal for the upcoming exploration phase: precursor missions, as the already planned ones (Luna-Glob program, Chinese lunar program, SELENE-2 by JAXA, etc.), will enhance the preparation process, also with sample return campaigns. The knowledge shared database which should be created, will highlight the missing key elements to account for enabling permanent human stays in the harsh environment conditions of planetary surfaces; learning how to cope with the Moon peculiarities will also help to scale other future exploratory missions. Once the fully operational capability of the permanent station will be reached, useful insights can be derived to actively support Martian missions. A general mission statement to summarize all the listed features of the proposed permanent lunar base can be written as: "*To enable human exploration of the Moon and to support the utilization of lunar potential mineral resources as an incremental step towards Mars; to account for the creation of a permanent base for scientific activities and technology development and validation*" [188]. The Moon is indeed considered as the focal starting point for the next giant leap for mankind, i.e. stepping on the Red Planet.

ISRU techniques could be integrated, after pilot studies, into the mission architecture, because they can enable longer and even permanent stays while reducing the Earth-dependability. In fact, the more resources are manufacture in-situ, the lower the IMLEO. The most abundant raw material presents on the Moon, to be used and processed with ISRU techniques, is regolith: it is mixture of fine dust and rocky debris produced by ancient meteor impacts. Its thickness varies depending on the area: on lunar maria is around 5 m while on highlands is around 10 m. The lunar regolith composition also varies across the lunar surface: plagioclase, pyroxene, olivine, ilmenite ($FeTiO_3$), and spinel ($MgAl_2O_4$) are its primary constituents. The regolith is a fine grey soil similar to dust in terms of texture, with a roughly bulk density of 1.9 g/cm^3, but it also contains rock fragments, breccia from the local bed rock and even boulders. The lunar regolith appears as porous at the surface and becomes denser as the surface depth increases. The median size of submillimetre lunar soils is 70 μm on average, ranging from 40 to 130 μm, and the size distribution can be approximated with an almost straight line on a log-normal

graph [189]. Cosmic radiations shielding, power generation (e.g. with He-3 [190]), structure and equipment construction, site preparation, in-situ repair and use, and ECLSS consumables are the technical domains which can take advantage of lunar soil resources processing [191]. However, instruments and humans should be protected: its strong adhesive and abrasive behaviour is dangerous for hardware but can also have side effects on human health as a consequence to long exposition periods. Lunges alveoli can accumulate small portions of the finest size regolith grains, eventually leading to silicosis. Apollo astronauts reported that regolith tends to strong clung on everything so there was no way to remove it: after EVAs, spacesuits (especially gloves and boots) were full of dust and, once tracked inside the Lunar Module, some of it easily became airborne, irritating lungs and eyes. An opportunely filtration system should be designed with multistage levels of increasing filtration efficiency. Pre-screening and pre-stage bulk filters should be place prior to high-efficiency devices to remove big particles, like cyclonic separators [192, 193].

Oxygen and water, and so hydrogen, are vital for supporting human life: those resources can be produced with regolith excavation, mining, and conveniently processing [194]. A complete closure of ECLSS is achievable with oxygen produced in-situ, but this element is also very useful for rocket science: together with hydrogen, oxygen can be used for propellant production [194–198], not only for Earth-LEO-Low Lunar Orbit (LLO), but also for Martian journeys with non-nuclear-based propulsion systems. Among all the possible solutions for propellants storage, an interesting concept is to adopt on-orbit space depots for reducing to mass to be launch from our planet. The Earth-Moon Lagrangian point 1 (EML1) and/or 2 (EML2) are ideal candidates to host a space depot infrastructure: low ΔVs are required for station-keeping, thus refuelling operations and tanks assembly results easier, also considering to depart from there towards other destinations [199–201].

Effective mitigation methods to preserve the integrity of equipment and humans need to be addressed due to the lack of atmosphere, that is the principal responsible of screening cosmic radiations. Protection capabilities are essential for extending the overall mission duration and to reduce launch mass from Earth. The life-threatening hazard for crewed long-stay missions are related to chronic exposure to highly ionizing ions in the Galactic Cosmic Rays (GCRs) and sporadic acute exposures to Solar Particle Events (SPEs). On the Moon, the radiation quantities to account for sizing a radiation protection system are approximately half that of deep space thanks to the presence of the

soil. These are not negligible at all because of for the presence of secondary radiations, which comes from radiated neutrons which interacts with the ground. The easiest shielding technique is using lunar regolith [202] that can also provide protection against micrometeoroids and diurnal cycle temperature buffering [203]. Layers of regolith can be clumped to bury (totally or partially) the outpost modules, using the regolith removed to accommodate them [204]. An evolution of this concept is using 3D-printed regolith layers as shown in Figure 4.2: robot-operated 3D printers should build up over the modules a protective shell, also resistant to debris impacts [35, 205]. This in-situ approach can be adapted also for Martian solutions, as investigated by [206].

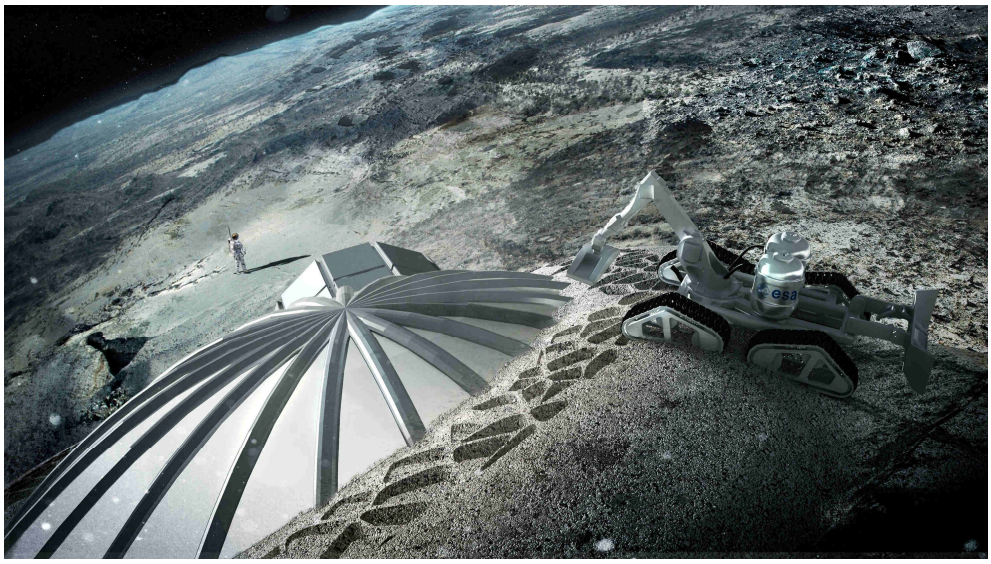

Figure 4.2 Multi-dome lunar base being constructed, based on the 3D printing concept (credit: ESA – Foster + Partners)

Dose reduction can also be done using a multiple strategy, i.e. different shielding layers. Polyethylene and water are materials with interesting properties in reducing radiations absorption. For example, experimental tests onboard the ISS proved how foldable and flexible bags, normally used for cargo stowage, can be modified and adapted to host a passive membrane for water treatment, thus helping for both recycling operations and additional radiation shielding (e.g. in case of a SPE) [207, 208]. In addition, water can be taken directly from the ECLSS utilization loop [209], reducing system complexity. Another possibility to explore for radiations shelters is exploiting lava tubes. The existence of those peculiar geological formations have been postulated and observed by survey spacecraft (e.g. Kaguya/SELENE [210]): they can be

potentially used as astronauts' habitats, offering an unprecedented opportunity for geological on-site measurements as well as radiations protection [211–214]. Despite the advantages offered, the debate among the scientific community on exploring lava tubes and lunar holes is still open, mainly for sample contamination reasons (i.e. the human presence can alter data measurements and lead to wrong assumptions like the precise geological formation era and the relative mineralogy composition). The study of geology, geochemistry, and geophysics will help to understand the Moon formation history. For example, the actual soil conformation and composition is may due to the ancient lunar volcanic activities [215].

Since there is no lunar atmosphere and the lunar radio environment has particular features, some areas of the Moon results well suited for radio telescopes, which should have opportunely shielded from Earth radio noise. Telescope operations for stars and galaxies observation is then enhanced, also with infrared telescopes, to be placed in low-temperature areas (e.g. craters floors).

Depending on the base power consumption and the power system adopted in the conceptual design phase, ISRU can also be useful in this field. Oxygen and hydrogen can be extracted from regolith and used as fuel cell consumables, potentially leading to an integrated power system highly coupled with ECLSS. Futuristic ideas foresee to manufacture in-situ solar cells [216] to further reduce mass to be launched.

Food provision is another problem to face for deep-space exploratory missions. Food stocks can be launched from Earth but, to enable longer journeys and permanent stays, harvesting vegetables directly on-board is a promising research field. Pilot studies of space crop systems and greenhouses have been (and currently are) running, opening new possibilities for mission concepts that incorporate this technology, as the ones proposed by [55, 188].

Astronauts should live and work together in a staffed-crew rotation scheme, as is nowadays done by the ISS increment campaigns: physiology and phycological assessment can be performed in the valuable lunar environment. Low-gravity environment studies to monitor the human body adaptation and eventual side effects can be performed, also accounting the Earth-based research in this field [15], to better address countermeasure procedures. The long-term effects of cosmic radiations can also be measured. Confinement, isolations, tasks and duties division, and personal space (habitable volume) are aspects to deal with for designing the final base configuration.

Another useful feature would be to have a lunar positioning system (e.g. satellites or CubeSats constellation), as the satellites of the Earth-based GPS, to assist navigation of astronauts and rovers as proposed by Levrino *et al.* [217].

The present work is intended to provide a plausible draft mission scenario for the upcoming lunar exploration campaign. Depending on future developments to be outlined by national space agencies, private enterprises, and international institutions, the assumption made in this research may result outdated and the choices made may be questionable, as for example whether to incorporate or not ISRU techniques since the very early development phases of the lunar base such as proposed by Gatto *et al.* [218]. Preliminary calculations have been done in order to provide the necessary simulation input, but the flexibility of the proposed VR-based simulation methodology guarantees the rapid update and reconfiguration of the solution found. This feature is essential when dealing with early design concepts exploration and it is the main reason of this research. The potential integration of a VR tool among the standard design tool in the design phase of a lunar permanent outpost have been tested and simulation results have been obtained for the mission architecture proposed in section 4.1.1.

4.1.1 Mission architecture

The final goal set by the proposed mission scenario, i.e. to establish a permanent human lunar surface outpost, requires a set of technologies and properly-scheduled preparatory campaign. Precursor missions have to be planned and should be intended to be part of an evolutionary approach towards the ultimate scope to land humans on Mars, and not only limited to explore the lunar vicinities. Machines, robots, rovers, transportation vehicles, logistic systems, and habitation modules have to be design, manufactured, and tested. Useful insights can be derived for developing the future concept of operations needed for deep space missions, where communication delays major affect data uplink and downlink.

Focusing on the Moon and its vicinities, a valuable environment where to test and validate the technologies required by the future exploration endeavours, some strategies have been already proposed by [35, 54, 55, 73, 181, 182, 188, 200, 203, 218–225]. The new era of coordinated human and robotic exploration will be ideally initiated by EM-1: apart from testing SLS and Orion MPCV, it will also contribute to launch survey spacecraft for collecting useful scientific data, therefore trying to answer the open questions about

lunar science [27]. The decade 2020-2030 is expecting to have the flourishing of new ideas and concepts, widening the horizon of the international partners involved and potentially offering partnership opportunities for business of private industries [10, 14]. Autonomous and teleoperated robotic demonstrator missions will start in 2020s [220]. Alongside the unmanned campaign, human elements should be also developed: an evolvable cis-lunar station will be assembled and operated in the mid-2020s. The DSG will act as a hub for missions to the lunar surface, eventually Mars, and other deep space destinations. The staging of payloads and crewmembers are the main DSG features around which the DSG will be designed and developed: docking ports, airlocks for EVAs, propulsion and power systems are the other envisioned components of the lunar gateway. NASA, Roscosmos, ESA, JAXA, and CSA partners currently discussing and defining its final configuration, taking advantage of ISS experience. Due to the different environment between LEO and the cis-lunar space, the DSG will have a more efficient ECLSS with higher regenerative features, a more durable food supplies system (also investigating and enhancing the current capabilities of on-orbit production), a higher radiations screening, and will also be able to withstand the longer communication delays [226]. Conceptual habitation modules and ground prototypes have been developed under NASA commercial agreements that involve Bigelow Aerospace®, Boeing®, Lockheed Martin®, and Orbital ATK®. The necessary logistic support between LEO, lunar orbit, and the lunar surface can be guaranteed by a solar electric space tug [32, 33]. An artistic impression of the DSG during operations with the Orion MPCV is represented in Figure 4.3.

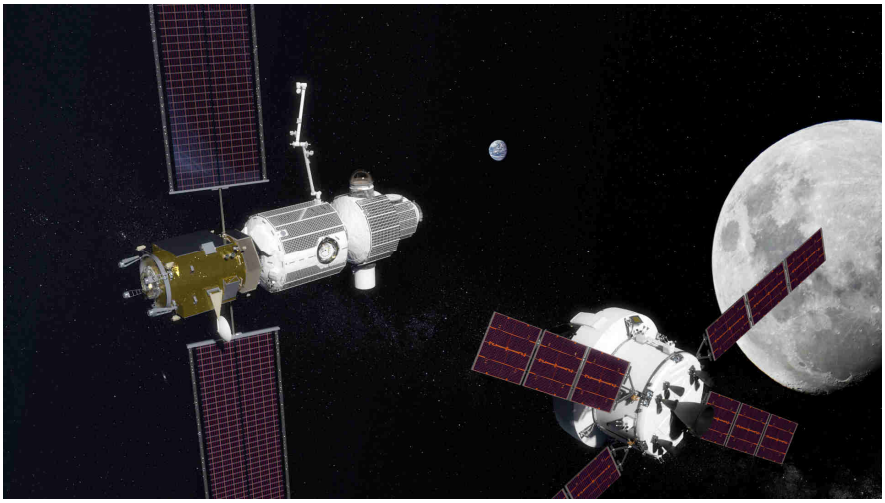

Figure 4.3 DSG and Orion MPCV artistic concept (credit: NASA)

At the end of 2020s, a first crewed mission is expected to come on-board a deep-space transportation system, assessing its transport capabilities for distant human missions which aims to be Earth-independent.

Surface operations will be progressively integrated into the standard scientific activities, including sample return missions, where soil samples can be directly analysed on-board the DSG: this is the current purpose that the Human-Enabled Robotic Architecture and Capability for Lunar Exploration and Science (HERACLES) initiative will address. Robot and rovers will be launched towards the DSG and finally assembled on the lunar surface. The station modules and the other elements will be launched using SLS[9], while Orion MPCV will be used for crew (and cargo) transportations. A surface lander is also envisioned as ascent/descent vehicle [225, 227].

ESA is one of the most active institution in proposing mission concepts, especially to support and enforce the "Moon Village" concept [35, 54, 181, 182]. Starting from the GER [8] and using the Mars-forward assets in cislunar space, human missions for returning to the lunar surface are under discussion: the campaign will be composed of five missions to explore the five locations showed in Figure 4.4 and is designed to carry out valuable lunar science, also providing the necessary experience in planetary surface operations, especially to reduce risks associate to human missions to Mars [182]. A crew of 4 astronauts will spend up to 42 days on the Moon using a mobile surface habitation, i.e. two pressurized rovers, exploring different locations and volatile components for future ISRU. A human lunar lander is required, and it will be composed by an expandable descent module for landing on the lunar surface (one per mission) and a reusable ascent module for returning to the DSG.

[9] The SpaceX® Falcon Heavy and BFR are plausible commercial alternatives, but they are still under development and not flight-qualified yet.

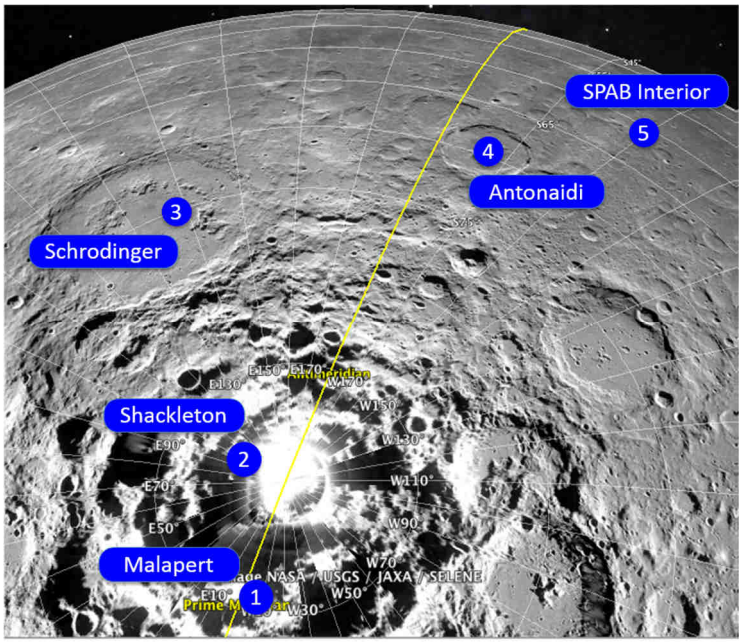

Figure 4.4 Notional landing site for the human lunar surface missions campaign [182] (credit: ISECG)

The proposed timeline is to have the first human surface mission in 2029. Using this timeframe as reference and assuming to have one mission per year, with an additional "bonus" year for eventual failures and mission about, led to assume 2035 as the starting year for the scenario studied in this dissertation. Accordingly, the permanent base construction should begin in 2035, thanks to the knowledge acquired throughout the preparatory phases. Supporting human life, continuous operations, and scientific activities are the outpost primary goals. The daily routine activities should also account for maintenance and unscheduled upgrades (of eventual technologies, modules, and crew).

The recent trends for site selection strategy are suggesting to explore the polar regions instead of the already visited (with the Apollo missions) equatorial areas. In fact, the mission scenario outlined by Whitley *et al.* [182] plans to visits south polar locations, moving towards the far side of the Moon to study geological formation processes and assess the potential usage of ISRU techniques. Additionally, a complete characterization of the lunar soil is not available yet: the Apollo and Luna campaigns collected a total amount of 382 kg of lunar samples, but most of them come from equatorial regions, hence exploring polar regions will enrich the knowledge on our natural satellite.

The lunar exploration history and missions planning report how different criteria should be adopted with respect to the final purpose to achieve [228]. Indeed, for establishing a lunar surface base, the criteria to adopt shall

consider not only science operations but shall also address human factor needs and the relative implications of supporting human life on a planetary surface. Temperature gradients, radiations, illumination conditions, crew security and safety, easy access to resources and consumables are just few example of the several aspects to account when selecting the outpost location [228–231]. Engineers and scientists have been discussing the possibility to explore the lunar polar regions due to the peculiar environment conditions. Since the lunar spin axis is tilted of about 1.54° with respect to the ecliptic, the illumination, insolation, and temperature rates of the lunar poles are pretty unique (in the Solar System in general) and not comparable with any terrestrial locations. The combined effects of the 6.68° Moon's spin axis obliquity relative to the Moon's orbital plane and the 5.14° Moon's orbital plane obliquity relative to the ecliptic, and their seasonal variation, are the causes of the distinct ambient conditions variations at high lunar latitudes [232]. Therefore, the subsolar latitude experience a variation of approximately ±1.54° [233]: the distinct seasonal changes are due to the ~18.6 years-cyclic precession of the lunar orbital plane. The 18.13-days difference between the 346.62-days draconic year (i.e. lunar seasonal cycle) and the 365.25-days sidereal year (i.e. orbit of the Earth-Moon system around the Sun) is the responsible for the non-exact repetition of diurnal and seasonal insolation: the lunar rotation period is a non-negligible fraction of its annual period, thus the longitude of the maximum insolation point (noon at summer solstice) changes from one year to another [232]. The resulting scarce direct solar illumination is due to the seasonal variations and the resulting illumination levels are strongly influenced by the local orography [233]: as a consequence, highly illuminated and permanently shadowed regions coexists. The particular geometry in combination with low angles of the incident light (with respect to the surface, i.e. the local horizon) do not allow Sun rays to reach the areas of permanent darkness, which are either terrain depressions or crater floors. A schematic view of those regions is reported in Figure 4.5.

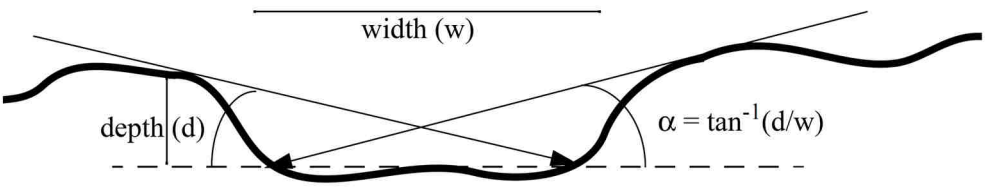

Figure 4.5 Geometry of permanently shadowed regions [234]

The most interesting feature of permanently shaded (examined also by Apollo 16 and 17, but at different latitudes) areas is that some of them are supposed to be cold traps. These low-temperature geological formations were firstly observed by terrestrial radar interferometry [235] and remote sensing satellites, like Cassini [236], Clementine [237] and LRO [26, 233], and they are prime candidates for housing water ice deposits [235–237]. The extremely low temperatures, i.e. below 40 K, allows the presence of stable icy-water reservoirs [26, 233]: at the lunar south pole, for example at Shackleton and Cabeus craters [235, 238, 239] and at the Aitken Basin [234], water ice grains of 10 cm or less can be found mixed with regolith or possibly appears as a thin coating of ice on rocks. It is yet unclear their origin and their certain existence. The most accredited hypotheses are: solar wind reduction of Fe in the regolith, meteoroids containing traces of water, cometary impact, and (the least certain) degassing of the interior [240]. Hydrogen atoms excess has been measured in some cold traps [241] (e.g. Shackleton crater) but their presence might not be related water but to trapped solar wind protons from our planet magnetotail plasma [24, 242, 243]. Interesting data have also been gathered by LRO mission: LCROSS, launched the on-board Atlas V rocket with the LRO spacecraft, was designed to provide direct evidence of water ice deposits at lunar poles. On October 9th, 2009, it was crashed within the Cabeus crater and the resulting ejected plume was observed and analysed by radiometers and spectrometers, revealing an estimated water ice content of 5.6 ± 2.9% by mass [244].

Other recent data measured from the Chandrayaan-1 orbiter have been also suggesting water presence in the Apollo landing sites (at equatorial latitudes) of indigenous origin, i.e. pyroclastic materials sourced from the Moon deep interior have a widespread occurrence of water content [245].

Nevertheless, lunar poles are more attractive in terms of scientific exploration of undiscovered sites and of potential mineral resources to exploit. It is actually a huge turning point for ISRU techniques if water ice deposits in the polar could traps can be accessed: H_2O, hydrogen (H_2), and oxygen (O_2) can be produced in-situ for the habitat needs (e.g. drinkable water, ECLSS consumables, and propellant production), thus reducing the supplies to launch from Earth. Among all the chemical processes to extract water from lunar regolith, ilmenite reduction is the more technologically mature in terms of TRL. The reaction starts via heating up the titanium-rich regolith at 1050°C and obtaining water as primary product, which can be further electrolyzed to produce oxygen and hydrogen. The produced hydrogen can be used for

further reduction processes. The chemical processes of ilmenite reduction and water electrolysis are respectively reported in Equations (4.1) and (4.2).

$$FeTiO_3 + H_2 \overset{\text{heat}}{\longrightarrow} Fe + TiO_2 + H_2O \tag{4.1}$$

$$H_2O \rightarrow H_2 + \frac{1}{2}O_2 \tag{4.2}$$

Other techniques as sulphuric acid reduction, methane reduction, solid lunar regolith electrolysis, molten oxide electrolysis, and vapour phase pyrolysis are currently studied but they have lower TRL. If the presence of water reservoirs will be confirmed, the extraction from the cold traps will be a very promising technique: the ice-soil mixture has to be dried out and heated up to 50°C to separate regolith and water [76]. The water vapour produced is then liquefied to be either directly stored or electrolyzed to produce hydrogen and oxygen as for Equation (4.2). Since there are heat losses in the ilmenite reduction process, which are related to the high temperature required (1050°C), they can be used to melt regolith grains with icy water that require only 50°C. If production plants will be designed, these heat losses of the main reaction chambers of the ilmenite reduction process could be used to estimate the additional plant elements and masses required (e.g. tanks, loaders, filters, and heat-melting chambers) to possibly couple it with the cold trap plants.

The result of the survey on ISRU techniques highlighted how the verification of water presence in the cold traps is compulsory to develop an exploration strategy as well as a long-term plan to sustain the permanent human outpost. Rover exploration mission concepts have been already proposed for in-situ data collection and resources assessment: soil samples shall be drilled from the crater to be then analysed and classified in terms of chemical composition [242, 246].

Even if the lunar north pole has been also proposed as a potential location for possible future exploration scenario [247], the Moon south polar regions have been strongly suggested as the most probable site for establishing a permanent human presence, also accounting the novel discoveries and strong proofs about south pole surface water ice [26, 248].

A more detailed analysis of the selected location for settling the permanent human lunar village has been described in section 5.2, where simulations data have been obtained using VR software.

The overall scenario considered in the research here presented is composed by the following building blocks:

- A cis-lunar station, i.e. the DSG;
- A telecommunication system with Earth, i.e. radio network to ensure continuous link with Earth-based ground stations;
- Transportation systems to/from DSG and Earth, i.e. SLS, SpaceX® Falcon Heavy and BFR, and/or an electric space tug;
- A crewed base on the lunar surface (specifically located at south pole of the Moon) permanently inhabited.

The surface outpost is the main building block of the mission and some of its functionalities directly depend on the other building blocks. The cis-lunar station shall host the crewmembers while waiting for surface sorties or for return trips to Earth: thus, the DSG and the Moon base housing capacity are mutually influenced by one another. The transportation systems are devoted to transport crew and supplies to the DSG, which act as cis-lunar handling centre in between Earth and Moon. Moreover, the orbiting station shall support the telecommunications between Earth and Moon as a radio bridge when the outpost in not in line of sight for our planet.

The main outpost elements to deploy for building the permanent outpost studied in this research are the habitation modules. A bi-modular structure has been considered with an inflatable module, to save space and mass at launch and to have a larger habitable volume, and a rigid one. This choice has been made following the recent guidelines and concepts proposed by terrestrial analogues [249] and preliminary designs [35]. Moreover, the overall scenario shall also include transportation systems such surface mobility elements, i.e. rovers, and ascent/descent vehicles (for crew and cargo). An artistic impression of the future surface outpost is represented in Figure 4.6.

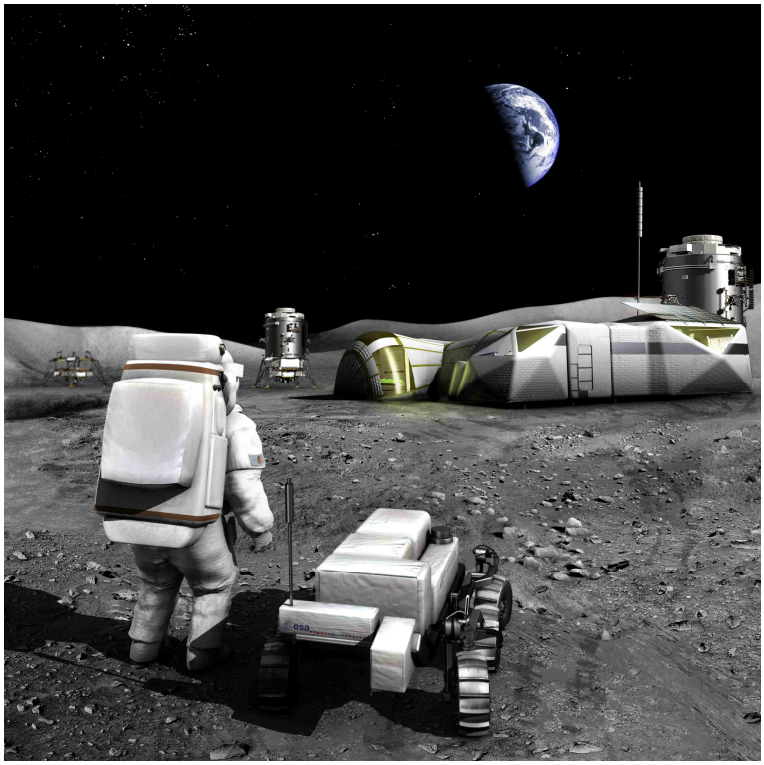

Figure 4.6 ESA Aurora program Moon base artistic impression (credit: ESA)

4.2 Mission budgets

According to the mission scenario outlined in section 4.1.1, the mission budgets of the permanent settlement have been estimated. The calculations have been made by firstly estimating the crew size. The main activities to be carried out during the mission by crew are both Intra Vehicular Activities (IVAs) and EVAs (with or without rovers assistance): communicate, teleoperate rovers, navigation, systems supervision, science, medical backup, and maintenance are the principal common duties to be performed by every crew component. Other activities require indeed a specific training and depend on personal background and skills: piloting, medical qualifications, and geology samples collection are just few examples. Since EVAs play a central role in the scientific activities for Moon exploration, major issues could be easily managed and safe handled with two crewmembers outside and other two supporting the activities from inside the base: thus, the smallest number of crewmembers required is 4. More crewmembers could be part of the expedition, but their total number shall consider the return vehicle capacity (e.g. for an Orion capsule is 6). Other constrains are referred to the psychological areas

[250], like the volume available for each astronaut (social density), crew size/expected mission duration (confinement), freedom of movement, subjective perception of habitable volume, atmosphere, time outside the outpost, workload, rest and leisure time, tasks relevance and variations (motivation and morale), reduced communication with ground, need for leadership, connectedness with family and friends, time lag, confidentiality, interpretation and clarity of ground instructions, illness or injuries, and high demand situations due to dangers and contingencies. Moreover, the mission duration is another key driver to consider: based on the ISS experience, a 180-days mission per crew is envisioned, with a possibility to extend this period to 240-360 days at maximum. The lower physical impact guaranteed by the reduced-gravity Moon conditions is one of the positive feature that could allow an extension of the mission, but studies are still on-going in this field (e.g. the ISS One-Year Mission of 2015 investigated the effects on the human body of a long-term spaceflights [251][10]). All those aspects lead to finally establish 6 crewmembers as the number of permanent inhabitants of the lunar surface settlement: the assumptions and calculations done in this research work for systems configurations and mission budgets are based on this number. By following the ISS-proven scheme of tasks to perform and habitability, two 6-members crews with shift rotation every six months is the operative plan adopted (the increment rotations of 3-members per round-trip flight can be also adopted).

The scientific activities to be carried out on the lunar surface shall include long-range EVAs with pressurized rovers and unmanned rovers for telerobotic exploration activities and/or to assist the crew during EVAs. To enhance the overall effectiveness of the coordinated human and robotic exploration, several concepts and their relative robotic operations plans have been already proposed such as [234, 242, 246, 252]: locating, excavation/mining, and studying of in-situ resources (especially water ice deposits) is of paramount importance to establish a permanent human presence on the lunar surface. An example of those mission concepts has been developed by NASA-JPL and is shown in Figure 4.7.

[10] The American astronaut Scott Kelly and the Russian cosmonaut Mikhail Korniyenko spent 342 days on-board the ISS as part of a collaborative investigation on functional tasks, behavioural health, visual impairment, metabolic processes, physical performances, crewmembers' microbiome, and human factors.

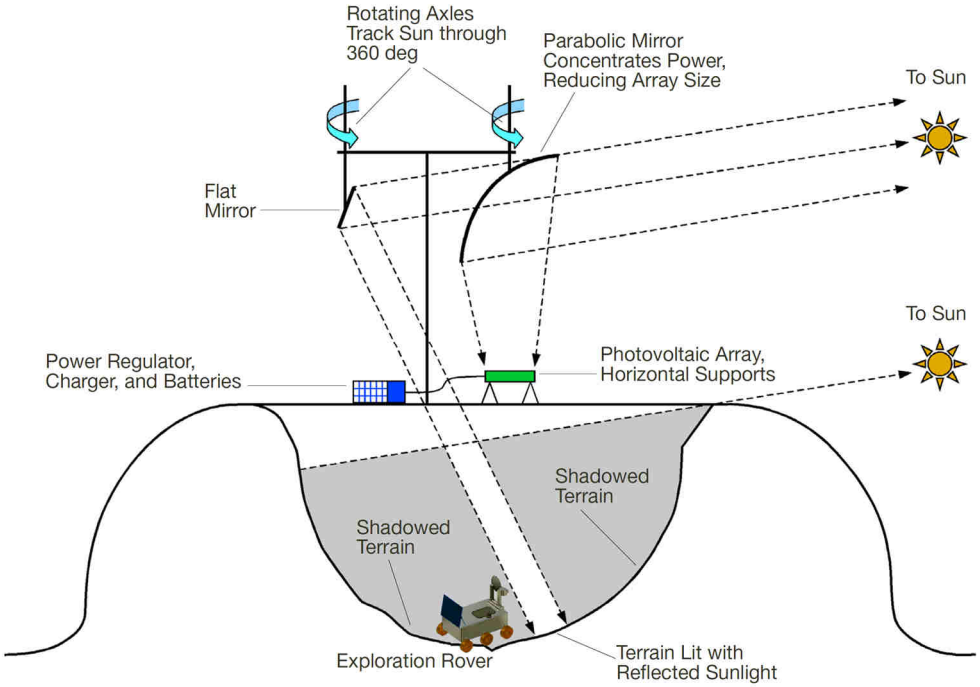

Figure 4.7 Periscope mirror design to eliminate cable wrap for the robotic exploration of permanently shaded regions [252] (credit: NASA-JPL)

Collecting samples with novel geotechnical tools to measure the soil properties, such as the one proposed by Zacny *et al.* [253], and precisely assess the resources available in-situ are the main tasks to execute. However, a detailed concept of operations, a complete list of ISRU requirements and infrastructure, and the relative mission budgets of those exploration tasks were not considered in this research work. In fact, the difficult a priori quantification of the lunar resources available and the relative extraction methods may jeopardize the entire mission [182]. It has been considered rather safer to include the in-situ resources analysis as one of the mission requirements (e.g. studies on volatile components for future ISRU) instead of considering futuristic (and eventually not applicable, depending on which raw materials are present and the relative extraction and utilization processes) production plants as the ones proposed by Gatto *et al.* [218]. Other elements may exist such as a greenhouse for the food loop closure: pilot studies have been investigating the possibility to build a crop system or a lunar greenhouse for harvesting vegetables and to help the crew self-sustaining like [55, 188]; even if human metabolic and ECLSS needs can be derived from Anderson *et al.* [254], greenhouse technologies for planetary surfaces are not enough mature yet, hence were not included in the scenario here described.

The elements considered for sizing and estimating mass and power budgets are therefore the habitation modules (inflatable and rigid structures), two pressurized rovers for long-range EVAs, and two ascent/descent modules. The number of required infrastructures and the amount of materials to be launched from Earth for building the different outpost elements can be drastically reduced by using additive manufacturing techniques. Different methods and different type of materials (e.g. metals and polymers) have been tested for both large structures [35, 205] (e.g. habitat parts for radiation shielding, micrometeoroids protection, and temperature insulation) and small equipment [68, 69] (e.g. tools and recyclable spare parts). The TRL is still low for some of the solutions under study (as the ISS-based 3D printer for space manufacturing), especially for those using lunar material, thus 3D printing technologies were not considered as integrant part of the scenario selected in this work for budget calculations.

The sizing criteria adopted for estimating masses and power consumptions, respectively in sections 4.2.1 and 0, of the permanent lunar base encompass common engineering guidelines defined by [74–78, 80, 185, 221, 222, 255–259].

4.2.1 Mass budget

The bi-modular configuration of the habitation modules, which should host 6 crewmembers, consists of an inflatable module and a pressurized rigid structure.

Two airlocks and a scientific laboratory have been assumed as part of the inflatable module, which should host 6 crewmembers for more than 180 days: the overall volume required is 380 m^2, that has been calculated according to [76]. The ISS inflatable module BEAM of Bigelow Aerospace® [70] is the most advanced flight-proven concept and the most technology-scalable solution to the actual outpost inflatable structure. Other examples, with lower mass to volume ratio, have been found in [255], but their features are not comparable at all with state-of-the-art technologies under study nowadays. A summary of the inflatable solutions available is reported in Table 4.1.

Table 4.1 Mass and volume budget for different inflatable modules

Type	Mass [kg]	Volume [m^3]	Mass/volume [kg/m^3]
BEAM [70]	1400	16	87.5
Sphere [255]	16300	2145	7.6
Box [255]	256	90.8	2.8
Cylinder [255]	17000	2145	7.9

If a technology improvement is assumed for the future applications, lighter inflatable structure will be produced, therefore the mass to volume ratio can be lowered to 50 kg/m^3 [260][11]. Finally, the total mass of the inflatable module of the permanent base is 19000 kg and is calculated using the Equation (4.3).

$$M_{inflatable} = V_{inflatable} \cdot \left(\frac{M}{V}\right)_{inflatable} = 380\ \mathrm{m}^3 \cdot 50\ \frac{\mathrm{kg}}{\mathrm{m}^3} = 19 \cdot 10^3\ \mathrm{kg} \qquad (4.3)$$

To size the pressurized rigid module, the ISS *Columbus* laboratory has been used as reference since this module is designed to be used as a scientific laboratory. A re-scaling factor of 2 has been assumed to calculate mass and volume, as reported in Table 4.2.

Table 4.2 Mass and volume budget for the ISS *Columbus* module and the pressurized rigid module of the permanent human lunar outpost

Type		Mass [kg]	Volume [m^3]
Columbus [261]	Structure	10275	50
	Payloads	2500	25
	Total	12775	75
Rigid module		25550	150

The surface mobility device for exploring the Moon and support EVAs has been identified starting from the lessons learned of the Apollo missions. Instead of adopting unpressurized open rovers, that might contribute to the contamination of the samples collected and may lead to life-threatening situation for the crew [262] (especially for regolith and it relative debris as rock fragments and breccia), pressurized rovers have been selected for the present mission scenario.

[11] The value assumed has been derived from Seedhouse [260] using the NASA TransHab concept (~35 kg/m^3), the Bigelow Aerospace® *Skywalker* concept (~67 kg/m^3), the cancelled Bigelow Aerospace® *Sundancer* module (~46 kg/m^3), and the upcoming Bigelow Aerospace® BA-330 module (~67 kg/m^3) as references to estimate the final value adopted.

The surface rovers have been sized using the NASA Space Exploration Vehicle (SEV) concept [263]. Two rovers, each hosting 3 crewmembers, have been used for the mission scenario considered. Since long-range mobility operations are foreseen in the mission plans for scientific exploration campaigns, 240 km is the maximum potential range design requirement, achievable via an electric propulsion system composed by batteries and fuel cells. The extensive exploration range allows to have longer rover operations: life support systems have been included to sustain the crew during those phases, which can continuously operate for 28 (terrestrial) days. The rover can be assumed as a small mobile habitation system that incorporates the necessary scientific equipment for analysis (in-situ samples collection and study). An airlock is present to allow EVAs operations for the crew. The overall rovers features are reported in Table 4.3.

Table 4.3 Human long-range exploration rovers data

Crewmembers	3
Mass [kg]	2993.7
Volume [m^3]	15.57
Operative time [days]	28
Range [km]	240
Average speed [km/h]	10
Maximum speed [km/h]	20

The ascent/descent vehicles have been sized to accommodate 3 crewmembers and, for safety reason (redundancy and emergency escape situations), two vehicles have been considered. Using [76] as refence for the design procedure, a first estimation of mass and volume has been carried out as reported in Table 4.4.

Table 4.4 Mass and volume budget for the ascent/descent vehicle

Type	Crewmembers	Mass [kg]	Volume [m^3]
Ascent/descent vehicle	3	1777.8	8

4.2.2 Power budget

In order to opportunely size the power system of the crewed lunar settlement, a first estimation of the power loads of each base element has been done.

The inflatable module total power consumption is 170 kW, calculated using [70, 255] as reference.

The rigid module power consumption has been rescaled of a factor of two using the ISS *Columbus* laboratory(in the nominal mode) as reference [261], also for what concerns the power loads division in terms of subsystems. The subsystems considered are:

- Electrical Power System (EPS) that also include the Power Distribution Unit (PDU) and the Payload Power Switching Box (PPSB);
- Thermal Control System (TCS);
- ECLSS;
- Data Management System (DMS) that is part Command and Data Handling (C&DH) system;
- Telemetry, Tracking and Control (TT&C) system.

Other ISS common equipment has been considered as reported in Table 4.5. The total power consumption of the rigid module of the lunar outpost is 36 kW.

Table 4.5 Power consumption of the ISS *Columbus* module in the nominal mode [261]

Subsystem	**Component**	**Power percentage [%]**	**Power consumption [W]**
EPS	Lighting	5.22	235
	Harness	7.31	329
	PDU/PPSB	9.73	438
TCS	-	30	1350
ECLSS	-	10.93	492
C&DH	DMS	11.78	530
TT&C	Video	4.67	210
	Audio	1.51	68
Other	ISS common equipment	1.56	70
	Power to subsystems (average)	82.71	3722
	Power to subsystems (maximum)	25	4500
	Power margin (maximum-average)	17.29	778
	Power to payloads	75	13500
	Total power	100	18000

The pressurized exploration rovers require ~12 kW per rover: this value has been calculated using [76], where the power consumption of each subsystem has been estimated as reported in Table 4.6.

Table 4.6 Power consumption of the pressurized rover subsystems

Subsystem	Required Power [kW]
Airlock	1
Hygiene	1
Kitchen	1
Internal science equipment	1
External science equipment	1
Thermal control	1
Internal lights	0.2
External lights	1
Drive power	3
Security factor	1.6
Total	11.8

The ascent/descent modules average power consumption is 2.5 kW and the peak power is 4.37 kW: those values has been estimated using [76].

4.3 System architecture

The permanent surface outpost of the mission scenario described in section 4.1 shall support the human life, scientific activities and operations. However, the environmental conditions and the needs to fulfil are quite different for orbiting laboratories (e.g. ISS and the future DSG) and surface habitats, thus the system architecture varies. On the other hand, since both the orbiting stations and the surface outpost share the same goal of support human operations and scientific activities, the subsystems composing the systems and their functionalities are similar.

Fractional gravity, thermal gradients, and regolith adhesion are just few of the ambient factors to which the equipment have to withstand. Structure, ECLSS, TCS, C&DH, TT&C, and EPS are the main subsystems considered to be part of the outpost. The propulsive and the tracking subsystems are not present because of the intrinsic static attribute of the Moon base. As introduced in section 4.1.1, the structure shall be composed by an inflatable module and a pressurized rigid structure, also considering two airlocks for EVAs. The TCS shall have a double architecture, i.e. incorporating passive and active solutions: since the inflatable and the rigid modules can possibly be

buried into layers of 3D printed regolith, also contributing to the structural integrity, hazardous working fluids (e.g. ammonia) for thermal heat rejection could be unnecessary due to a better passive insulation than the LEO-orbiting ISS (i.e. exposed to open-space conditions). In order to support humans, the ECLSS shall be present and shall potentially adopt an ISS-like closed loop regenerative architecture that is schematized in Figure 4.8: oxygen, water, and other consumables might be produced in-situ via exploiting the lunar resources potentially available. The possible incorporation of ISRU techniques to actively sustain the outpost and future deep-space endeavours is an unexplored domain for space missions, which can be firstly studied and applied in the present mission scenario.

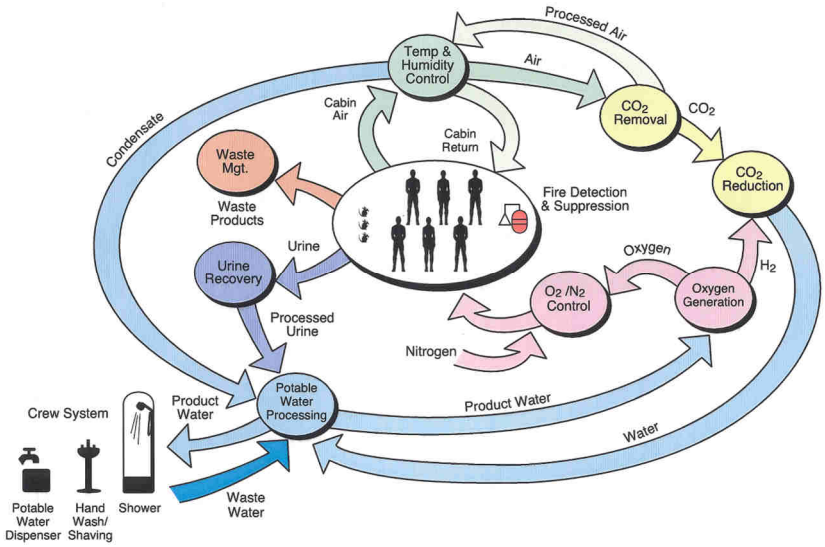

Figure 4.8 ISS regenerative ECLSS flow diagram (credit: NASA)

The C&DH and the TT&C shall provide the communication and data management capabilities to allow the proper telemetry and command interface with both orbiting and surface elements, and to handle remote and outpost-local live commands. Those subsystems shall indeed deal with delays, but a constant radio connection between the surface outpost and the DSG (for telerobotic and emergency operations) shall be guaranteed for safety reasons as well as certain level of independence for the outpost surface operations. Furthermore, the DGS shall be used as a communication relay to guarantee the continuous communication link with Earth when the lunar base is out of view of terrestrial ground stations.

Finally, a detailed analysis of the EPS has been done in section 4.3.1 to test the innovative VR-based approach proposed in this research work.

4.3.1 Power system specifications

Different types of space power systems exist in relation on the power source to adopt: chemical, nuclear, and solar are the available solutions. As reported by Hyder *et al.* [264], the general trade-off studies for designing and sizing the power system take in consideration the power level required and the mission duration, whose trends are shown in Figure 4.9.

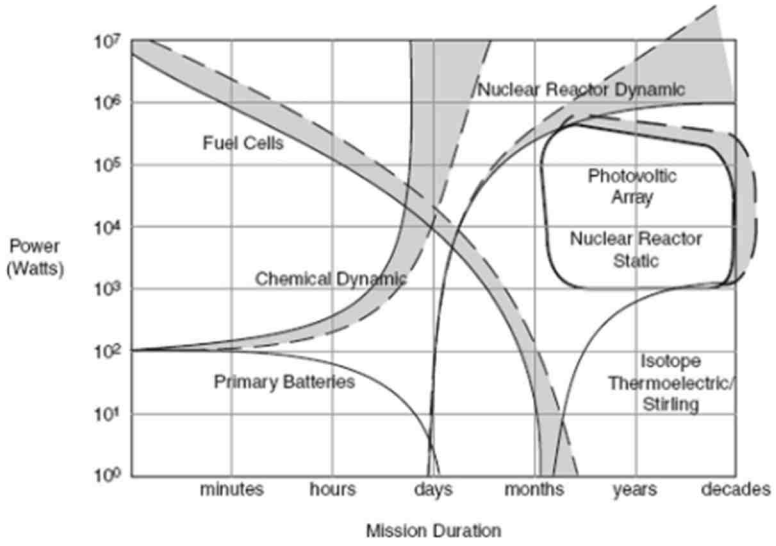

Figure 4.9 Different options of space power systems as a function of mission power needs and duration. The grey areas are potential growth beyond the solid line for future applications [264] (credit: Anthony K. Hyder)

Since the envisioned outpost shall be permanently inhabited, the power system choice is restricted to nuclear (Radioisotope Thermoelectric Generators, RTGs, or reactors) or to photovoltaic arrays (coupled with batteries and/or fuel cells) solutions. The stringent safety requirements of manned missions exclude a priori the utilization of this power source, especially for European initiatives [265, 266]. However, the promising results in past and present unmanned missions (e.g. planetary rovers and interplanetary probes), and the future trends suggested by space agencies and international entities pone this technology as the principal alternative for EPSs of deep-space and long-duration missions. Pilot experimental campaigns have been already envisioned by future mission scenarios to test the critical issues of nuclear plants [182, 188, 218]. If those preparatory studies will be successful in assessing the feasibility and the critical issues (mainly safety and risk factors analysis since the technology itself has been Earth-proven since years) of nuclear energy-based systems, they can be incorporated into the future human mission

architectures. Even if waste-free solution with the in-situ usage of lunar materials have been proposed [190], enforcing the promising results that could possibly be obtained using nuclear sources, in this research work another encouraging concept has been adopted to supply power to the Moon base. A hybrid closed-loop system, i.e. a Stand Alone Power System (SAPS), has been adopted. Developed for terrestrial applications [267], this class of systems is able to supply power without being connected to an electric grid. The "Spaceship EAC" initiative [268, 269], run by the ESA European Astronaut Centre (EAC), is investigating the possibility to use a carbon-free SAPS to meet the energy request of the terrestrial analogue facilities LUNA and Flex-Hab currently under development in Cologne (Germany): this power system shall partially represent a first implementation of the potential lunar power-supply scenario [249].

By using the ESA-EAC first studies in the energy field [268, 269] as reference, the future lunar permanent base power system adopted in this research work is a photovoltaic-hydrogen SAPS. It is composed by a photovoltaic plant (i.e. solar panels), batteries, fuel cells, tanks, and electrolyser. The working principle is based upon using different devices to supply the required power with respect to the ambient conditions: the photovoltaic plant will be used for suppling power to all the base elements and to electrolyze water during sunlit periods, while fuel cells will be active to power all the settlement elements during shadowed periods. Batteries will be used to absorb peak loads and for energy storage. They will be recharged by the photovoltaic arrays that should be opportunely sized to supply this additional load. A common electric bus is required to connect all the equipment to a standard common interface (as done by the ISS EPS architecture), where dedicated electric converters will adjust the tension and current levels required by each device. A schematic view of the SAPS is represented in Figure 4.10.

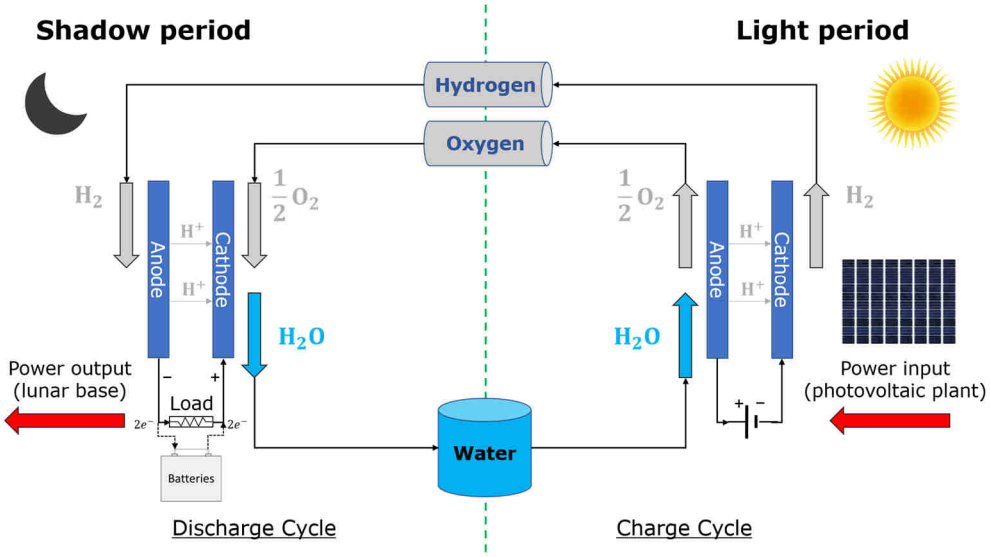

Figure 4.10 Photovoltaic-hydrogen SAPS block scheme

The necessary O_2 and H_2, produced by water electrolysis, should be compressed and stored in tanks: if the low-temperature permanently shadowed areas will be used, oxygen and hydrogen can be stored in a cryogenic state, not requiring a liquefier [270]. If water ice deposits will be confirmed to be present in the cold traps, in-situ water extraction can be performed instead of launching the required supplies from Earth. This type of water-including SAPS allows higher integration level with the ECLSS and eventually the TCS. Among all the different power systems used in space shown in Figure 4.11, the coupling of high power density devices as fuel cells, the low risk for crew operations (e.g. accessing the components for maintenance) related to batteries and photovoltaic arrays, and the high energy efficiency of water electrolysis to produce hydrogen (non-fossil fuel-based solution), make the proposed SAPS as the best solution for a permanent human settlement on the Moon.

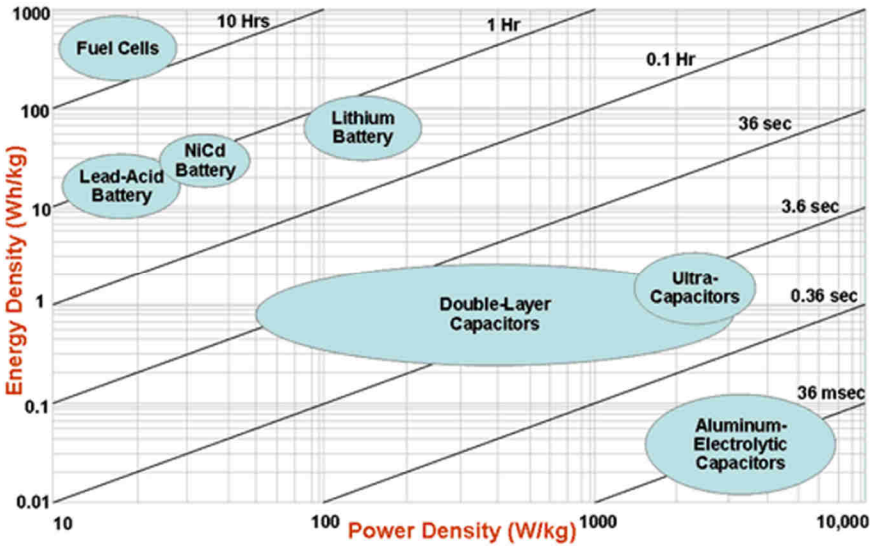

Figure 4.11 Comparison between different power systems in terms of energy density, power density, and utilization time (source: US Defence Logistic Agency)

The power budgets estimated in section 0 have been used as input data to size the SAPS elements. Typically, the power demand of a space system can be divided into housekeeping/baseline, nominal, and peak power. Housekeeping is defined as the minimum power level required to operate the only the vital functions of a system: only the necessary equipment to withstand the harsh environment conditions are active. The nominal power is the average power request by a system to operate and fulfil the tasks for what it has been design to. The peak power is the maximum power level that a system may request and is usually needed for short-time periods.

As a first estimation, the permanent lunar base SAPS has been designed using the housekeeping and the peak power as the two extreme working design conditions. The lower power level, i.e. housekeeping, is assumed to be requested during shadowed periods, while the peak power during the sunlit periods: as it will be discussed in section 5.2, the peculiar illumination conditions at the lunar south pole have been driving the SAPS design. In fact, it has been assumed that the fuel cells should supply the housekeeping power during shadow time and the photovoltaic plant the peak power during light time.

To firstly estimate the housekeeping power of the surface outpost, ISS has been used as scaling reference[12]: 84 kW are the power supplied by the

[12] Even if the environmental conditions between LEO and lunar surface are different, the ISS has been used as a "conservative" reference (e.g. open space is very different from a planetary surface from the thermal point of view) because it is the most similar space-qualified human outpost in terms of activities performed on-board. The permanent lunar

ISS EPS for nominal operations and 42.8% of it represent the housekeeping power percentage [271–273]. The same value has been assumed for the proposed human settlement, using 206 kW (170 kW for the inflatable module and 36 kW for the rigid module as reported in section 0) as the nominal power level to be rescaled accordingly. Moreover, an engineering margin of 13% [274] has been used to further increase the nominal base power. As reported by Equation (4.4), the housekeeping power is around 100 kW: this value is in line with the Mars surface habitat baseline power estimated by NASA in [76].

$$P_{housekeeping} = 0.428 \cdot (170 + 36)\cdot(1 + 0.13) = 103.71 \text{ kW} \cong 100 \text{ kW} \quad (4.4)$$

The housekeeping power request shall be supplied by regenerative fuel cells in accordance with the guidelines of the "Spaceship EAC" initiative [249]. In particular, two Proton Exchange Membrane (PEM) fuel cells, each able to provide 100 kW, are used in the SAPS. For safety and redundancy reasons, the fuel cells are arranged in parallel, thus providing 50 kW each, i.e. every stack works at half power: this architecture is able to guarantee continuous power (housekeeping level) because is one-time fault tolerant. In addition, once having fixed the fuel cells working point at half of their maximum power, it results to have a positive effect on their efficiency. Lower working current and tension, i.e. power, corresponds to higher efficiency because of the intrinsic limitations of the fuel cell technology[13] (due to ohmic and mass transfer/concentration losses). The high-power level required led to consider non-space-qualified fuel cells, even if Apollo and Space Shuttle missions successfully proven their suitability for human spaceflights. The model selected is the Ballard FCveloCity®-HD100 whose main characteristic are reported in Table 4.7.

settlement described in this work is in fact dedicated to support human life and scientific experiments as the ISS and the future DSG.

[13] The typical polarization curve of a fuel cell stack reports how too low current corresponds to high voltage values: these activation losses can damage the fuel cell and it is not recommended to operate the stack in this point also because of the related low efficiency values. In order to preserve the stack from damages and to have high efficiency rates, it is common use to operate the fuel cell within the flat part of the polarization curve, close, but not too much, to the knee that represents the voltage drop for to high current (mass transfer/concentration losses).

Table 4.7 Ballard FCveloCity®-HD100 main data [275]

Power [kW]	100
Idle power [kW]	6
Mass [kg]	285
Supply pressure [bar]	8
Efficiency [%]	60

Using the formulas reported in [276], it was possible to estimate the oxygen and hydrogen masses required by the fuel cells. The final calculation led to consider 1893.7 kg of H_2 and 15029.1 kg of O_2. Those data have been finally used to estimate the mass of water and the power required by the electrolyser to produce the calculated mass of fuel cells. The total mass of water required is 16923 kg has been estimated using [255]. Finally, the electrolyser total power required has been calculated using the Equation (4.5), taken from [255].

$$P_{ez} = \frac{m_{H_2O} \cdot E_{ez}}{t_{cycle} \cdot RF} = \frac{16922.76 \cdot \frac{4900}{0.95}}{(29.5 \cdot 0.76) \cdot 0.9} = 180 \text{ kW} \tag{4.5}$$

The electrolyser specific energy, i.e. the energy necessary to electrolyse 1 kg of H_2O, is 4.9 kWh (typical value of the products currently available on the market), and once assumed a process efficiency of 95%, the total energy density of the electrolyser can be estimated and is equal to 51571 kWh/kg. A 10% margin on the electrolyser operations has been assumed, that results into a risk factor estimation of 90%. Using a generic lunar day as the reference time period, which is equal to ~29.5 (Earth) days, and assuming that the electrolyser working time is 76% of this reference time span (due to the peculiar illumination conditions at the lunar south pole), the total power required by the electrolyser is 180 kW.

The batteries present in the SAPS are devoted to absorb power peaks and to supply power in case failure of other SAPS components (emergency/off-nominal condition). They will be recharged during sunlit periods by the photovoltaic plant, because of the long light periods of the Moon south polar areas. Their sizing should account for the maximum power requested in output: since two fuel cells are present, 50 kW (half of the housekeeping power) has been assumed as the batteries power peak. Another important design parameter is the voltage: as it will be discussed for the outpost main bus architecture, the photovoltaic plant is regulated to 900 V; DC-DC and DC-AC converters will be present along the distribution line to adjust voltage and current for

each connected utility, as it happens for the ISS EPS. Then, 160 V is the voltage chosen for designing the batteries. Finally, even if the surface base is permanent, the mean time between maintenance and/or substitution of the SAPS batteries has been set to 15 years, which is their expected life period. Different types of batteries are available: Nickel-Cadmium (Ni-Cd), Sodium-Sulfur (Na-S), Nickel-Hydrogen (Ni-H_2), and Litium-ions (Li-ions) are the most used for space applications [74]. A performance comparison, in terms of efficiency (η), energy density (ρ_{batt}), and mass, has been done in order to select the most adequate battery technology. A Depth Of Discharge (DOD) of 80% and a discharge period of 169.92 h (i.e. 5.92 days, equal to the longest shadowed period experienced in the most illuminated point at the Moon south pole, as studied in section 5.2.2, where an engineering safety margin of 20% is applied thus having in total 7.08 days) are the other data used for calculating the total energy capacity and mass of the different batteries types using Equations (4.6) and (4.7) [74].

$$C_{batt} = \frac{P_{req} \cdot t_{dis}}{DOD \cdot \eta} = \frac{50\ \text{kW} \cdot 169.92\ \text{h}}{0.8 \cdot \eta} \tag{4.6}$$

$$M_{batt} = \frac{\rho_{batt}}{C_{batt}} \tag{4.7}$$

The overall performances of the four different types of batteries are reported in Table 4.8.

Table 4.8 Principal features of space batteries

Type	Ni-Cd	Na-S	Ni-H_2	Li-ions
Energy density [Wh/kg]	35	132	70	100 - 180
Efficiency [%]	80	80	70	70
Operative temperature range [°C]	-40/+70	115	-5/+20	-40/+70
Energy capacity [kWh]	13275	13275	15171.43	15171.43 ÷ 15174
Mass [t]	379.3	100.6	216.7	151.7 - 84.3

Since the required energy will be the same regardless of the technology chosen, Li-ions batteries have been selected as the best solution due to their higher energy density, which helps to save mass so launch cost, and for their successful application for space missions as the Mars exploration rovers

[277]. Even if this technology is relatively new for space applications, a state-of-the-art terrestrial solution has been selected for the lunar outpost: in fact, the research for improving the performance of Li-ions batteries is active, especially for testing large capacity prototype cells for future planetary orbiters, rovers, and landers [278]. The Tesla Powerpack 2® [279] is the batteries plant used as reference to estimate the performance of the batteries required by the Moon base. This Li-ions system already embeds thermal management, electronics, and regulation controls, resulting into a more integrated and cost-efficient turnkey solution [279]. The overall properties of batteries plant to be used on the Moon are reported in Table 4.9, whose data are in line with those reported in Table 4.8.

Table 4.9 Data of the batteries plant final configuration

Capacity [kWh]	210
Mass [kg]	1622
Operating temperature range [°C]	-30/+50
Efficiency [%]	89
Discharge margin [%]	20
Total required capacity [kWh]	11455
Required batteries	55
Batteries total mass [kg]	89210

The sizing of the photovoltaic plant requires to consider the Moon environment in terms of solar radiation, temperature ranges, and solar incidence, as well as the power to supply to the base elements. To estimate the total area required by the solar panels, a design lifetime of 15 years has been assumed, as already done for the batteries. Due to degradation phenomena, the power at the Beginning Of Life (BOL) and at the End Of Life (EOL) of the solar arrays is different: the necessary oversizing in the solar production plant is needed to guarantee the power suppling to the human outpost throughout the entire design lifetime. The procedure adopted to size the photovoltaic arrays is the one described by Larson and Wertz [74] that has been adapted from being spacecraft-specific to lunar base-tailored: once fixed the operative lifetime and the total power required for both shadow and light periods, it is possible to calculate the total power to be produced by the solar arrays. After selecting the specific type of solar cells needed and computing the Sun irradiance and incidence, the BOL and EOL power levels can be calculated, finally leading to estimate the required total area of the solar panels for producing the power needed by the surface settlement (based on the EOL power request).

The parameters to calculate the total power of the solar arrays (P_{sa}) are:

- The maximum outpost power request during sunlit periods (P_{light});
- The average light hours in a lunar day, that equal to almost one terrestrial month (T_{light});
- The transmission efficiency from the solar arrays to the loads during sunlit periods (ε_{light});
- The maximum outpost power request during shadowed periods (P_{shadow});
- The average shadow hours in a lunar day, that equal to almost one terrestrial month (T_{shadow});
- The transmission efficiency from the solar arrays to the loads during shadowed periods (ε_{shadow}).

Those parameters have been reported in Table 4.10 using the lunar outpost data. In particular, the light and shadow time have been derived from the simulations run in section 5.2.2.

Table 4.10 Lunar outpost data to estimate the total power of the solar arrays

P_{light} [kW]	T_{light} [h]	538.08
	ε_{light}	0.6
	Habitat (inflatable and rigid modules)	414.86
	Rovers	72.8
	Ascent/descent vehicles	18.23
	Electrolyser	180.24
	Batteries	17.74
	Total energy (sunlit) [kWh]	348104
P_{shadow} [kW]	T_{shadow} [h]	169.92
	ε_{shadow}	0.8
	Fuel cells	169.92
	Batteries	50
	Total energy (shadow) [kWh]	25488

Lastly, using Equation (4.8), the total power of the solar arrays has been calculated.

$$P_{sa} = \frac{\left(\frac{P_{light} \cdot T_{light}}{\varepsilon_{light}} + \frac{P_{shadow} \cdot T_{shadow}}{\varepsilon_{shadow}}\right)}{T_{shadow}} = 887.6 \text{ kW} \tag{4.8}$$

The computed value is pretty conservative, but it is the result of a first design iteration where great engineering margins have been adopted due to uncertainties related to system design (e.g. estimation of the base elements power demand and environment conditions). As the project evolve during time and phases of the product life-cycle change, further refinements are possible that will lead to the final value to establish before the production phase begins.

To calculate the solar arrays area necessary to produce the estimated power, a selection among different cell technologies and solutions have to be carry out. The most advance type of solar cells for space application are the multi-junction ones: their efficiency ranges between 30% and 40% in the latest laboratory tests [280]. The Spectrolab $GaInP_2$/GaAs/Ge XTJ Prime® solar cells have been selected among the space-qualified solar cells currently available on the market because of their high BOL efficiency of 30.7%: specifically, the SuperCell class of 73 cm^2 has been selected [281]. The modularity guaranteed by this particular model type is another important feature considered for benchmarking: in fact, bypass diodes (to protect cells from over currents) and space-qualified coverglasses (to protect cells from cosmic radiations) are already mounted for an easier integration into modular structures [281].

The main external factors which influence the more the photovoltaic plant performances are the solar cells working temperature (T_{cells}), the solar irradiance (I_{solar}) and the Sun incidence angle on the solar cells (ϑ). To optimize the solar arrays sizing and positioning, three conditions have been considered: maximum temperature, the minimum of the average direct irradiance (excluding the component related to the Moon albedo), and the highest incidence angle (due to orbital mechanics, this value is equal to maximum inclination experienced by the Moon spin axis). For each condition (worst value of the variable considered) the other two physical parameters have been calculated at the same instant of time. As already assumed in section 4.1.1 and how will be describe later for the simulations in section 5.1, 2035 is the reference year used for calculations. A summary of the values obtained is reported in Table 4.11.

Table 4.11 Worst design values of the external influencing factors for the solar cells

	Maximum temperature	Minimum average direct irradiance	Maximum incidence
I_{solar} [W/m^2]	1545	1378	1390
ϑ [°]	0.5	0.33	-1.54
T_{cells} [°C]	140	127.5	129.5

Ideally, the amount of power per unit of area to be possibly produced by a solar cell is equal to the normal incident solar radiation multiplied by the conversion efficiency. For example, this value at BOL can be calculated using the Equation (4.9).

$$P_{ideal} = I_{solar} \cdot \eta_{BOL} \tag{4.9}$$

Other losses should be accounted to correctly estimate the overall performances of the photovoltaic plant. Inherent degradation takes into account for shadowed areas, temperature, and design limitations, which result into three different efficiency factors as reported by Equation (4.10).

$$I_d = \eta_{shadows} \cdot \eta_{temperature} \cdot \eta_{packing} \tag{4.10}$$

The efficiency related to the shadows possibly present on the solar arrays has been assumed equal to 1 because a detailed illumination analysis of the photovoltaic plant has been studied using a VR tool, as described in section 5.3.

The temperature increase is directly affecting the solar cells performances: the higher is the temperature, the lower is the output power. Depending on the cell type, the working temperature, and the radiations level, different temperature efficiencies have been estimated for each design condition directly using the solar cells datasheet [281].

The packing efficiency is a value referred to the solar cells area density with respect to the total area actually covered by the cells themselves. The geometry of the cells and their positioning one another are the influencing factor of this type of efficiency. Using values of typical triple-junction cells derived from [74], the packing efficiency is 90%, i.e. 10% of the total occupied area is lost for both design and assembly of the solar cells. Once the total area of the photovoltaic plant is known (calculated later in this sizing estimation process), a more precise estimation of this efficiency has been calculated by using the Equation (4.11). An iterative procedure has been used to finally

estimate this value, since the overall dimension of the final plant are a priori unknown.

$$\eta_{packing} = \frac{N_{cells} \cdot A_{cell}}{A_{panel}} \cdot 100 = 77.68\% \tag{4.11}$$

All the efficiencies values, and therefore the related inherent degradation, have been calculated for each condition associated to the external influencing factors for the solar cells. Additionally, cable losses have been considered with a dedicated efficiency set to 97% [74]. The inherent degradation and its values multiplicated by the cable losses efficiency are reported in Table 4.12 for each of the three worst design conditions. Those values are in line with the typical data reported by Larson and Wertz [74].

Table 4.12 Worst design values of the external influencing factors for the solar cells

	Maximum temperature	**Minimum average direct irradiance**	**Maximum incidence**
I_d	0.5798	0.5837	0.5594
$I_d \cdot \eta_{cables}$	0.5624	0.5662	0.5426

The actual BOL power per unit of area to be possibly produced by all the solar arrays can be calculated using Equation (4.12), where ϑ is the angle between the Sun incident rays and the vector normal to the solar cell.

$$P_{BOL} = P_{ideal} \cdot I_d \cdot \eta_{cables} \cdot cos\vartheta \tag{4.12}$$

The EOL power per unit of area to be possibly produced by all the solar arrays can be calculated using Equation (4.13), where L_d is the corrective coefficient related to the performances degradation caused by cosmic radiations. The lack of lunar magnetosphere and atmosphere is responsible of secondary radiations that originates from the interaction of particles (galactic or solar origin) with the Moon surface. Even if the Apollo surface data and the more recent cislunar data measured by Chandrayaan-1 and LRO missions [27] have contributed to cast some lights on the complex lunar radiation environment, which is composed by a mixture of primary and secondary energy particles with different energy levels, the knowledge in this field is still limited and needs to be complemented by additional surface measurements [282]. However, models and simulations suggested that emission from the Moon surface is less than 1% of that resulting from cosmic rays [282]. For this reason,

secondary radiations have been neglected in this research study, thus assuming the lunar surface radiation environment as similar to interplanetary space, and in particular to a geostationary orbit. To calculate the degradation coefficients related to the expected lifetime of 15 years, assumed as the EOL for the photovoltaic plant (before a complete refurbishing), the ECSS-E-ST-20-08C standard [283] has been used: the related fluence has been estimated to be $1 \cdot 10^{15}$ MeV [283]. According to the selected solar cells datasheet [281], the EOL efficiency of the solar cells is equal to 26.71%, the annual degradation is 0.92%, and the total degradation for 15 years is 87%.

$$P_{EOL} = P_{BOL} \cdot L_d \tag{4.13}$$

The BOL and EOL power per unit of area for each of the three worst design conditions have been reported in Table 4.13.

Table 4.13 Worst design values of the BOL and EOL power per unit of area

	Maximum temperature	**Minimum average direct irradiance**	**Maximum incidence**
P_{BOL} **[W/m²]**	257.4	239.5	239.9
P_{EOL} **[W/m²]**	223.9	208.4	208.7

Finally, the area required by the entire photovoltaic plant can be calculated using Equation (4.14).

$$A_{sa} = \frac{P_{sa}}{P_{EOL}} \tag{4.14}$$

This value has been computed for each of the three worst design conditions and reported in Table 4.14.

Table 4.14 Worst design values of the total area of the photovoltaic plant

	Maximum temperature	**Minimum average direct irradiance**	**Maximum incidence**
A_{sa} **[m²]**	3964	4260	4253

By following a worst-case approach, the selected solution for the photovoltaic plant positioning among the three design conditions is the one characterized by the minimum P_{EOL}, i.e. the largest area as reported in Table 4.14. Consequently, the temperature and the incidence have been calculated in the same conditions, i.e. 127.5°C and +0.33°, which correspond to the minimum of average direct irradiance.

The final architecture of the photovoltaic plant can be different but total area have to be the calculated one. Among the several solutions to possibly arrange the plant and satisfy the requirement related to the total area, three design alternatives have been considered:

- Horizontal (so parallel to the terrain surface) solar arrays with vertical-standing solar concentrators which redirect the sunlight from the Sun to the panels (similar to Earth-based solar farms);
- Distributed vertical solar towers;
- Single modularly-mounted panel.

Although the first two solution could appear as the more suitable and technologically feasible, they are characterised by problems with non-trivial solutions. The relative positioning of the concentrators and/or the solar towers is not simple. At the lunar south pole, the Sun is almost in the same position regardless of the time period considered, with very low elevation angles (i.e ±1.54°). The relative casted shadows result to be very long, consequently an optimization for the secondary shadows have to done in order to avoid shaded areas, which are casted among elements (on each other), in the distributed architecture. Cabling the entire plant, so each single element of the distributed architecture, can result to be challenging and expensive. The more spread are the elements of the architecture chosen, the more cables are needed. Insulating and screening kilometres (or even more) of cables in the harsh Moon environment is not simple and could led to excessive additional costs.

The last solution is thought the preferred one, also accounting for structural advantages deriving from the lunar fractional gravity: structural loads for both mounting and sustaining the entire modular structure are less than a terrestrial analogue, that indeed result disadvantageous. The base of the single modularly-mounted panel should be Sun-tracking to follow the annual Sun motion. Since the solar rays inclination is almost constant, just 1 rotational Degree of Freedom (DoF) is needed (i.e. the panel inclination respect to the terrain local vertical remains fixed): a simple gears mechanism or a gimbal is required, similar to those used for the big antennas of the radio telescopes; this solution also reduces the global mechanical complexity of the entire plant. The solar panel inclination has been set equal to the “optimal” incidence defined during the solar panel sizing, i.e. +0.33°. Furthermore, the base of the single modularly-mounted panel is 2 m high above the local surface: this implies a raising of the Sun visibility percentage, i.e. the local horizon as seen from the panel [284]. Additionally, this mounting solution can prevent

potential performances degradation of the solar panel due to mechanical (assembly phases) and electrostatically (magnetic causes) dust levitation phenomena, as described by experimental data and analytical models [285–288], in combination with surface adhesion (due to van der Waals forces) [225].

Using the ISS EPS as reference, the internal architecture of the solar panel has been mimicked. A total of 8 modular power channels have been selected: each channel should be able to produce 117 kW at EOL, with a voltage of almost 900 V and a current of 130.74 A, and is composed by 10 solar arrays, connected in parallel to increase the current output. Each solar array has the same tension of the channel into which is mounted in and is able to produce maximum 11.7 kW. The solar array is made by 3 strings connected in parallel: each string is composed by 15 modules, each capable to produce 256 W at 60 V (maximum value) and composed by 3 parallel-connected strings with 42 serial-connected cells per strings. The detailed data of every component (cell, module, array, channel, and panel) are reported in Table 4.15.

Table 4.15 Final dimensions and mass of the photovoltaic plant

Element	Cell	Module	Array	Channel	Panel
Length [m]	0.13	1.37	11.97	12.2	97.5
Height [m]	0.063	0.78	4.15	43.7	43.7
Space [cm]	0.2	2	20	100	-
Area [m^2]	0.0073	1.06	49.7	532.8	4263
Mass [kg]	0.0049	2.18	112.5	1207.4	9659
Elements	453600	3600	80	8	1
Packing factor	-	1.15	1.04	1.07	1.28

Each of the 8 channel is hold up by two lateral telescopic pillars/bars (9 in total), which have not been accounted in the total structure area: ideally, all the channels have been assumed adjacent one another. The resulting total area is then slightly greater than the one calculated using Equation (4.14), i.e. the required for satisfying the power demand of the lunar outpost. As a consequence, the next maximum power at EOL can be recalculated using Equation (4.15), where cable losses are already included.

$$(P_{max})_{EOL} = P_{EOL} \cdot A_{panel} = 208.4 \cdot 4263 = 888 \text{ kW} \tag{4.15}$$

In order to allow astronauts (during EVAs) to mount this massive structure in compliance with their limited working area reachable with a pressurized EVA suit, each telescopic pillar/bar shall be designed to incorporate a guiding movable mechanism as guide rails. For each channel, several

rectangular frames are present: the shortest sides of these components slide into the vertical pillar through the rails, while the longest ones provide the structural support to the solar panel elements. Once each row of elementary modules is completed, astronauts pull up it and, considering a horizontal "inverse shutter/portcullis" mounting scheme, the next empty frame is available for assembling the following row. Those actions should be repeated until the solar panel is completed.

4.4 VR simulation tools

In order to analyse the power system (in particular the solar panel) performances and the base elements optimal positioning, VR-based simulations have been run. In fact, the site selection strategy further described in 5.2 has been used as the case study in this thesis to test the VR-based methodology proposed in section 3.4. The simulations are intended to be used for studying the system is regulation that is one of the most important aspects not to be overlooked. The control logic to develop shall effectively manage transitions between light and shadow periods for maximizing the overall SAPS performances and, also including the conversion efficiency.

Among several virtual modelling options, the research work presented in this thesis takes advantage of two different VR software. The result of a survey among all the products available on the market led to decide which to use for the purposes to be addressed. The main distinction between all the possible solutions is open-source codes or proprietary licensed: in the former case, these are generally developed for multipurpose uses, where customers and their community are the principal developers which can tailor varied applications, solution in the latter category are *ad hoc* written by suppliers for meeting specific needs and standards. The benchmarking of pros and cons of each solution is important to choose the most appropriate tool, also accounting the expertise level required by the potential end-users.

The current context of this Ph.D. dissertation led to choose one product of each category, i.e. Blender® as the open-source software and the Virtual Environment Research in Thales Alenia Space (VERITAS) as the *ad hoc* one.

4.4.1 Open-source solution

Blender™, whose logo is represented in Figure 4.12, is a free open-source modelling and graphics computer software, which is able to run on Linux, macOS®, and Microsoft® Windows® machines. This cross-platform

application is also compatible with most of the current VR systems, including the HMD Oculus Rift® and stereoscopic screen-type systems. Its features range from video editing and composing, motion graphics, rendering, camera tracking, match moving, animating, sculpting, texturing, raster graphics editing, rigging and skinning, UV unwrapping, 3D modelling, soft body simulation, particle simulation, and fluid and smoke simulation [289]. Thus, it can generally be used for creating images, video, and videogames.

Each Blender™ file contains a database that incorporates all scenes, objects, meshes, textures, etc. created by the user. A file can contain multiple scenes and each scene can contain multiple objects. Objects can contain multiple materials which can contain many textures. It is also possible to create links between different objects.

Figure 4.12 Blender™ logo (credit: Blender™)

Blender™ can create 3D VR scene using its two embedded engines, named Blender Render Engine and Cycles Render Engine: the first one, known also as Blender Internal (BI), is the original core render engine able to glossy reflections, ray-tracing, and subsurface scattering, but substantially lacks photo-realisms; the second engine helps to overcome the realistic rendering limitations of the first one using full-fledged global illumination and physically accurate calculations [290].

To create real-time visualizations and interactive 3D simulations/applications the Blender Game Engine (BGE) have to be used. This embedded game engine is different from the other built-in Blender™ features because the rendering process is in real-time, also allowing user interaction (e.g. videogames), while the other two Blender™ engines can only be used to create off-line scenes (i.e. once rendered cannot be modified). However, BGE is currently not very supported and that there are plans for its retargeting and refactoring that, in the very least, will break compatibility [289].

The typical Blender™ user interface is represented in Figure 4.13: this editor provides a way to view and modify the work under development by using specific panels with buttons, tabs, controls and widgets. Moreover, this interface is enriched with a Python-language scripting add-on where it is

possible to import/export files with formats, to automatize tasks, and to create custom tools for prototyping [289].

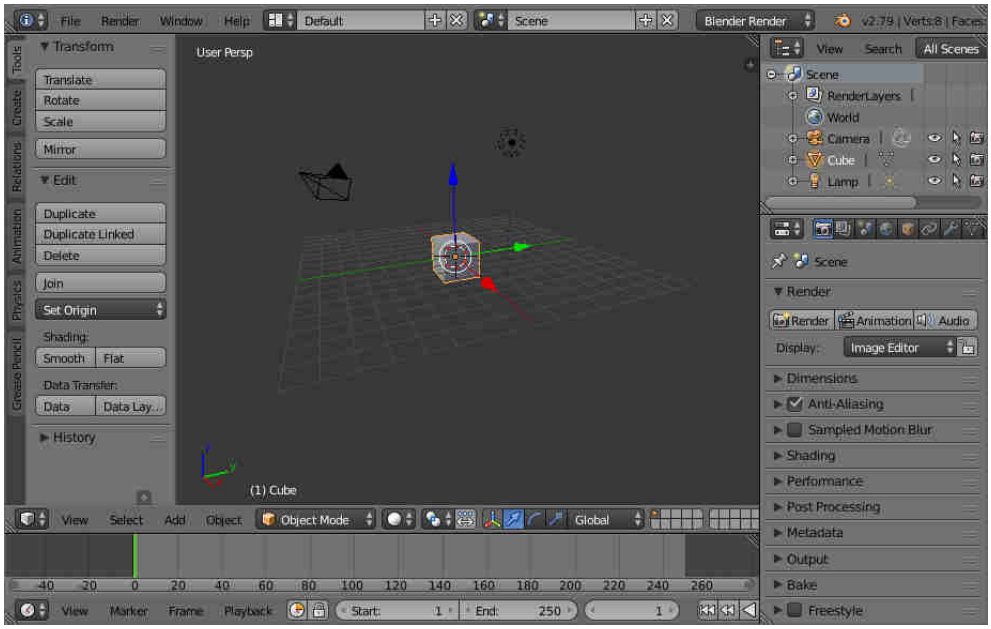

Figure 4.13 Blender™ user interface (credit: Blender™)

All the listed features make Blender™ as an ideal developing environment where to create and test VR scenes. Its flexibility and adaptability with several hardware enhance the collaborative aspect among different users, which is essential for the purpose of this research work, as described in sections 1.2.2 and 1.3. Specifically, the Blender™ release adopted in the simulations described in chapter 5 is the version 2.75a.

4.4.2 Proprietary *ad hoc* solution

Developed at TAS-I, specifically by the COllaborative System Engineering (COSE) centre, composed by the Technology Research Office (TRO), Virtual Reality Laboratory (VR-Lab) and a Collaborative Room [168, 169], VERITAS is an in-house developed and multi-software VE whose logo is represented in Figure 4.14. It is not strictly a software but rather a framework in which several applications can be developed. Based on open-source components platform, VERITAS allows virtual immersive and stereoscopic simulations in the 4D format: VR scenes can be displayed into a setup with 1 to 6 screens, using the Cave Automatic Virtual Environment (CAVE) [291] as an example, or into a single computer (desktop application). 4D, 3D and

2D user-interactions, using the immersive-wise or the desktop application, enable to concurrently design a system while having multidisciplinary (functional and physical) representations of the system itself [169]. The development phases of system design are user-centric, thus interactive devices (e.g. haptic pointers) can be used to improve the immersive level, where web-based collaboration are possible [169].

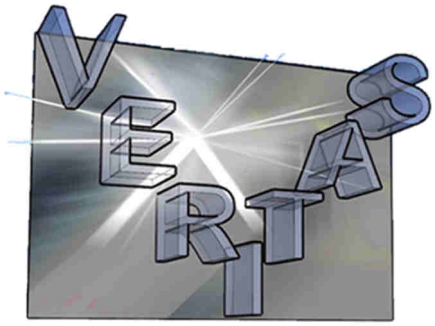

Figure 4.14 VERITAS logo (credit: TAS-I)

The creation of virtual scene is done loading file eXtensible Markup Language (XML) coded configuration files. Objects are imported into the scene via stand-alone 3D models (e.g. CAD models) that are loaded and extracted in Virtual Reality Modelling Language (VRML) or in OpenSG® Binary (OSB) file format: these could be anything that the user would like the option to manipulate, from a component of a vehicle to a planetary terrain. Data resulting from other simulation domains (e.g. aerodynamic, structural, thermal, etc.) can be displayed using Tecplot© 3D models.

VERITAS functionalities can be summarized by the following main usage scenarios [292]:

- Spacecraft trajectories analysis in the Solar System using ephemeris for the orbiting celestial bodies;
- Virtual interactive mock-ups analysis;
- Inverse kinematic scenario with motion capture and virtual mannequin replica;
- Radiations analysis depending on the positions of a specific path in space;
- Stowage support simulations;
- Lander and rover analysis for operations planning;
- AR scenarios;
- Distributed collaborative virtual sessions.

Moreover, virtual scenes can be displayed in a first-person perspective with some level of head-tracking enabled as represented in Figure 4.15. Head-tracking allows the scene to move in response to the subject's own motion such that, ideally, their view of the scene changes in the same way it would if they were standing in a real location and moving their head. VERITAS VR scene can be set to respond to translational movements, or to translation and rotation coupled movements. Including rotation is useful for microgravity scenarios, such as the ISS interior model: this allows the scene to freely change orientation to match position and orientation of the user, such that there is no fixed virtual floor or ceiling. However, when this kind of adaptation is used in a planetary setting, where there is a ground and gravity, the effect can be extremely disorienting. When the subject turns his/her head with rotation enabled, the ground and the scene before him/her turn as well with a sensitive and high-precision response, whose side effects could potentially induce motion sickness.

Figure 4.15 User in the Mechdyne CAVE™ while interacting with a virtual scene created using VERITAS (credit: TAS-I)

The features listed so far make VERITAS particularly suitable for developing VR simulations, in which its data representation is essential thanks to the applicability and transferability to space mission design, as required by the framework described in sections 1.2.2 and 1.3. Specifically, the VERITAS release adopted in the simulations described in chapter 5 is the version 8.

4.4.3 Tools integration

The VR-based methodology described in section 3.4 has been applied for the site selection strategy to locate the lunar human base on the Moon south pole. Specifically, to assist the early stage design phases of the power system,

virtual simulations were used for performances prediction. The procedure adopted to fulfil the scope of creating a virtual shared environment that is accessible by all the experts involved since the early design stages is schematically reported in Figure 4.16

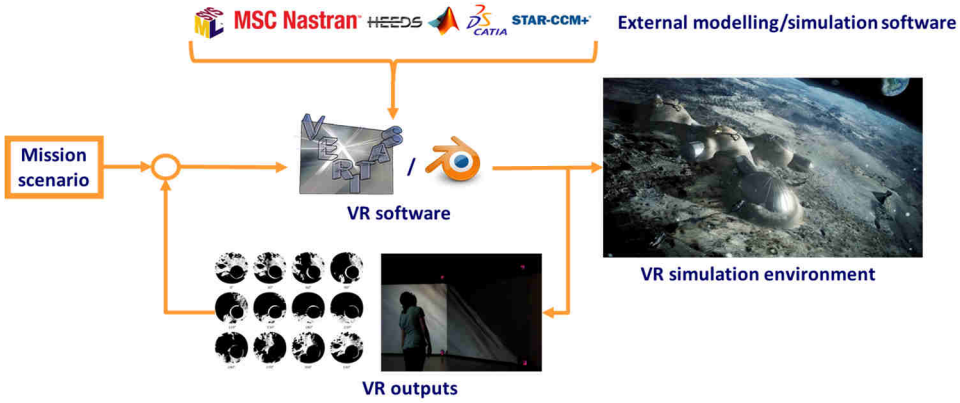

Figure 4.16 Block diagram of the VR-based setup used for simulations

Once defined the mission scenario or the systems to be designed, its virtual model is created using a VR software: this is not meant to be a mere visualization but is intended to serve as a real engineering tool for simulation and data analysis. Not only the graphical appearances are rendered in the virtual world, but also the physical properties and functional behaviours of the product under development: to do so, information and data from external software are gather together using the virtual model as a common repository. Structural, thermal, radiations and fluid dynamics analysis data, and 3D CAD models can be imported and integrated. The final result is a complete virtual replica of the system and/or the SoS: output information can be extracted from VR simulations and these data can be used for trade-off analysis. Depending on the results obtained, some modifications might be necessary, thus requiring updates to the virtual models. A loop architecture can be then defined to be used for subsequent design iterations typical of the early life-cycle phases. The automatic update of the model can help to speed up the decision-making process into which visual attributes and the possibility to virtually interact with objects play a significant role.

Both Blender® (described in section 4.4.1) and VERITAS (described in section 4.4.2) can be used as virtual modelling software for creating the virtual model to be used in the simulation approach described in this work.

Blender® is in fact a valuable 3D modelling tool for the purpose to address because it is a well-known open-source software under constant

improvement, whose frequent updates are always well documented by the developers' community. The integrated Python Application Programming Interface (API) enable a full control over the Blender® features for personal customization, including the GUI components (e.g. screens, panels, and menus).

VERITAS has been specifically tailored for VR space application by TAS-I and it is already part of the COSE centre, which is dedicated to the design and development activities of complex systems, including training tasks, integration, verification, and testing. The TAS-I VR-Lab started to use VERITAS also for the engineering assessments using CD processes [168, 169]. Moreover, VERITAS is able to import and manipulate Blender® file objects: the flexibility guaranteed by this possibility opens the doors to the potential integration with other compatible VR systems; virtual scenes and models created by other software can be opened using VERITAS and vice versa.

Both software were tested using the illumination analysis of the terrain as benchmark: final rendering, virtual scene development, and software-specific features were evaluated to select the best VR tool, as detailed described in section 5.2.2. Moreover, as part of future improvement for testing the VR-based methodology proposed, both software were integrated and tested in a CDF architecture to examine how the integration of VR tools will enable faster, better, and cheaper design evaluations, additionally assisting the actors involved in the design sessions. The software architecture adopted and the fist results are described in section 5.6.

Chapter 5

Integrated simulations

5.1 Initial set up and boundary conditions

In order to test the VR-based design methodology described in section 3.4 and to create a first simulation workflow that integrates VR tools and standard software as described in section 4.4.3, the permanent lunar outpost has been selected as the case study to analyse. The use-case demonstration proposed has been chosen as the first proof of concept for integrating VR technologies into the classical design paradigms and methods. VR is intended to serve not only as a powerful graphical media which can realistically render the optical properties of an object but should serve as a real engineering tool for modelling and simulating its physical properties. The results obtained by the creation of a virtual model that is part of a VE results to be more complete than using the standard MBSE approach: the simulation of different disciplines in the same common environment greatly helps all the actors involved in the design process to better understand the peculiarities and the coupling relationships of different elements. Specifically, the data obtained with virtual simulations were used as inputs for lumped parameters models.

The mission scenario described in section 4.1 has been analysed using a VE, after selecting the better VR software to use with comparisons against data from similar literature. In particular, an illumination analysis of the Moon south pole has been carried out to precise locate the permanent base and the SAPS elements. Detailed simulations of the modularly-mounted solar panel have been run to estimate the performances variation due to transient

shadows, which have been real-time rendered by the graphical engine of the VR software adopted. Lumped parameters models have been used for the SAPS components, then also for the solar panel: Microsoft Excel® was used for preliminary data estimation and MATLAB®/Simulink® was used to precise model the functional behaviours of each element. The selected timeframe for the analysis is the year 2035, which was assumed as the starting year for establishing the human surface outpost. The results obtained are preliminary and referred to a single selected location at the lunar south pole, but the flexibility of the tools and the method used guarantees immediate updates if data inputs are changed. The terrain illumination analysis is described in section 5.2, while the specific solar panel simulations are reported in section 5.3. The entire SAPS model and some preliminary assessments are presented in section 5.4. A first tentative implementation of a virtual lunar base is addressed in section 5.5.

5.2 Illumination analysis

Surveys of potential landing sites at the Moon south pole have been already studied by several entities [227–231]: depending of the criteria/figures of merit adopted, the site selections strategies change as a function of the final purpose to fulfil. Whether it is an unmanned rover or a human base, the preferred locations can be completely different and very distant from one another. The thermal and the radiative environment are major drivers for deciding where to place the surface outpost, but, since scientific experiments and volatiles assessments for future ISRU activities are the principal objectives of the permanent settlement, also the easy accessibility to potential resources is of paramount importance.

The peculiar topography and the extremely low inclination of solar rays make the south polar areas a pretty unique place in the Solar System. An accurate estimation of the illumination rates for precisely locate the outpost elements is necessary: sunlit and plane areas are the preferred places where to land and settle the base, always accounting for the cold traps exploration for possible water ice extraction. The analysis has been run using the VR software VERITAS, after a benchmark with the open-source software Blender®. In order to limit the high computational cost, the real-time simulation of the shadowing conditions has been restricted to the entire year 2035, but few tests were run also for the 2020-2030 decade to account the small variations of the ~18.6 years-cyclic precession of the lunar orbital plane that are responsible for seasonal changes.

5.2.1 Terrain topography generation

The illumination analysis of whatever planetary surface requires a terrain topography. The computer-based version of any real site is the Digital Elevation Model (DEM), i.e. the finite discretization of the real orography. The datasets used to create a mesh are derived by measuring of the actual terrains features. Remote sensing spacecraft and telescopes have been used to characterize the lunar terrain: the pictures taken by (high resolution) cameras and/or the data samples measured by altimeters are processed and assembled to create the digital replica of the terrain under study.

The lunar polar areas and their soil conformation have been studied by different missions such as: the NASA Clementine [23] and LRO [293, 294], the ESA SMART-1 [238, 295], the JAXA Kaguya/SELENE [284, 296–298], and the CSA Chang'e-3 [299]. Radar interferometry has been instead used by NASA JPL to create a lunar topographic map [252][14]. Moreover, the data measured can be used to generate and display maps with dedicated software like the one proposed by Wessel and Smith [300].

For the purpose of this work, different datasets have been used to generate lunar south pole DEMs for comparing the two VR software performances in terms of data handling capabilities and final surface rendering. The selected DEMs have been retrieved from:

- Kaguya/SELENE database, measured by the Laser ALTimeter (LALT) [301][15];
- LRO database, measured by the Lunar Orbiter Laser Altimeter (LOLA) [302][16].

[14] The NASA JPL Goldstone Solar System Radar (GSSR) group used the NASA Deep Space Network (DSN) to create radar image and models of the Solar System objects, as the Moon south pole DEM.

[15] The LALT_GT_SP_NUM file has been specifically used: it is a grid topographic data set around the lunar south pole. Altitude values were rounded off to the third decimal place. Data are ordered from -79.00390625°N to -89.99609375°N in latitude and from +0.015625° to +359.984375° in longitude. Raw altimetric range data were converted to the local topographic altitude with respect to the sphere of 1737.4 km radius based on the gravity centre of the Moon, by using the satellite orbit data.

[16] The LDEM_128 file has been specifically used: this data product is a shape map of the Moon, based on altimetry data acquired through mission phase LRO_ES_09 by the LOLA instrument. LOLA data used are geolocated using precision orbits based on a revised lunar gravity field.

Raw native data have been processed and transformed using a Cartesian coordinate system. The respective cloud points obtained (i.e. x, y, z) have been interpolated and quadrangular meshes have been generated. For comparison, also Delaunay triangular meshes have been created, but no rendering and computational cost improvements have been noticed, so they were discarded for the analysis.

Since the major area of interest are the rims of the Shackleton crater, the selected DEMs are centred in the Moon south pole. The entire Kaguya/SELENE database has been used (i.e. 79° – 90°S), but also a restricted version has been considered whose area extends from 88° to 90°S. Indeed, the LRO-LOLA dataset convers an even smaller area, i.e. from 89° to 90°S.

The topographic map of the widest Kaguya/SELENE dataset with a 2.36 km/pixel resolution is represented in Figure 5.1, where longitude values are defined east-wise and the 0° meridian is pointing to the Moon near side.

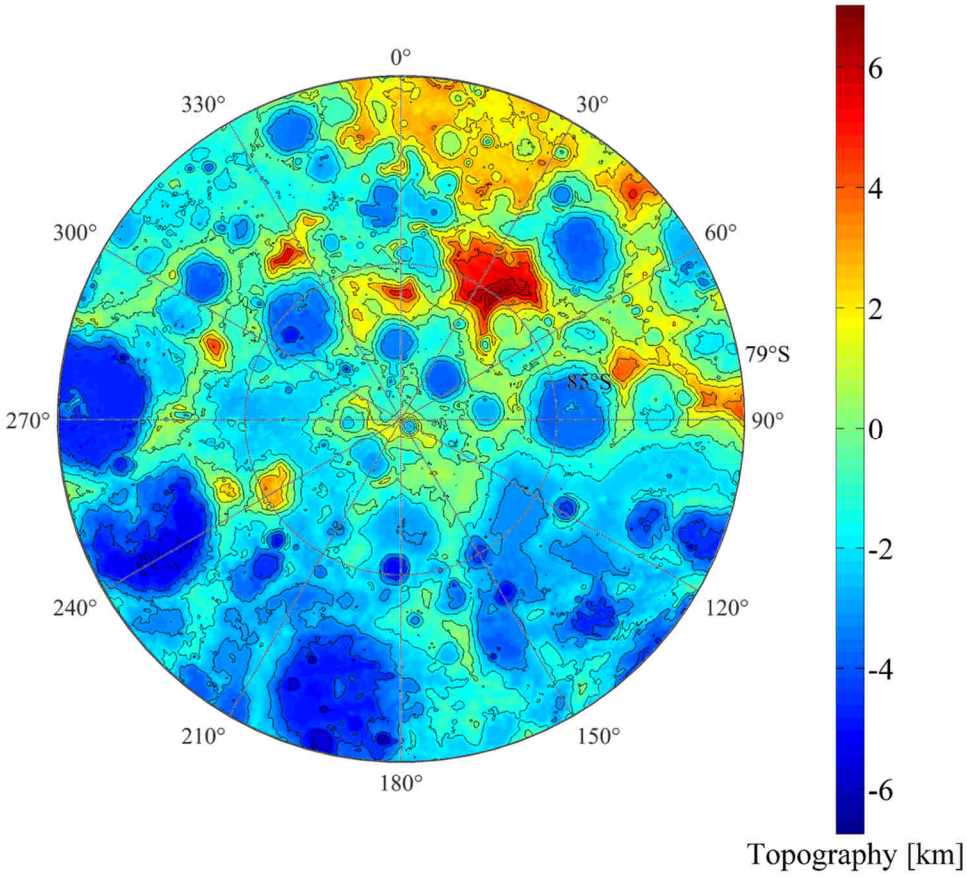

Figure 5.1 Kaguya/SELENE lunar south pole topographic map (79° – 90°S)

The topographic map of the reduced Kaguya/SELENE dataset with a 430 m/pixel resolution is represented in Figure 5.2, where longitude values are defined east-wise.

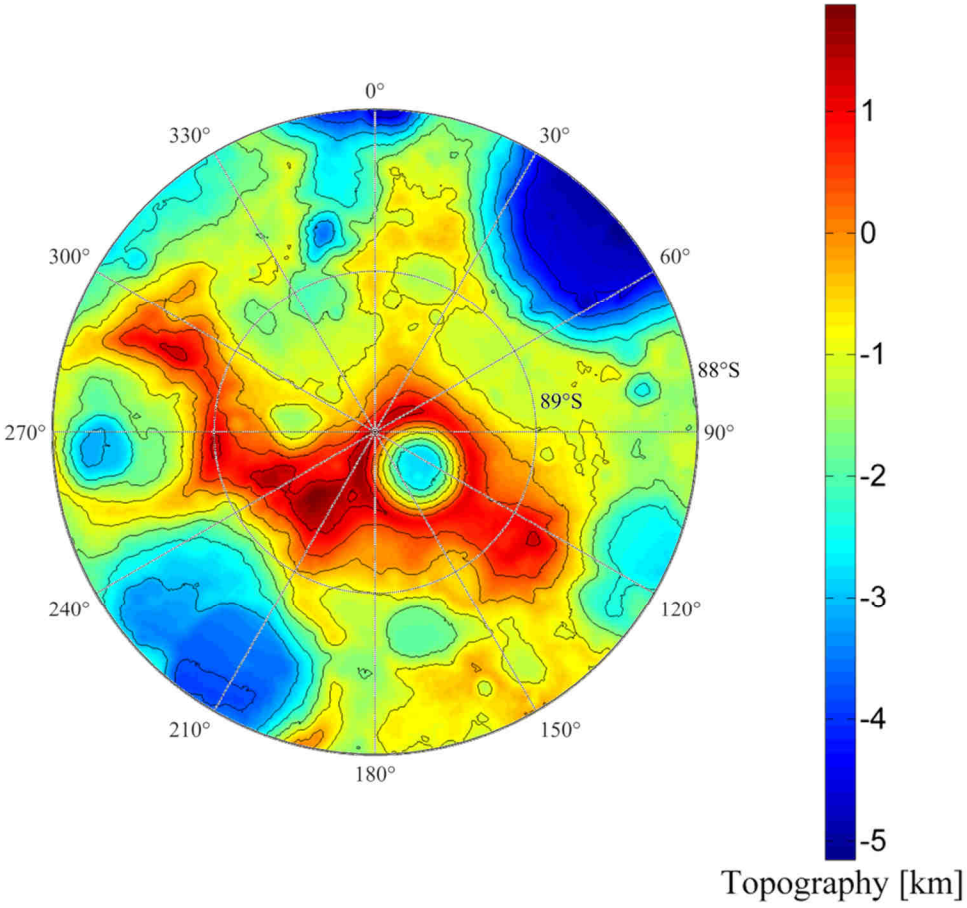

Figure 5.2 Kaguya/SELENE lunar south pole topographic map (88° – 90°S)

The topographic map of the reduced LRO-LOLA dataset with a 230 m/pixel resolution is represented in Figure 5.3, where longitude values are defined east-wise.

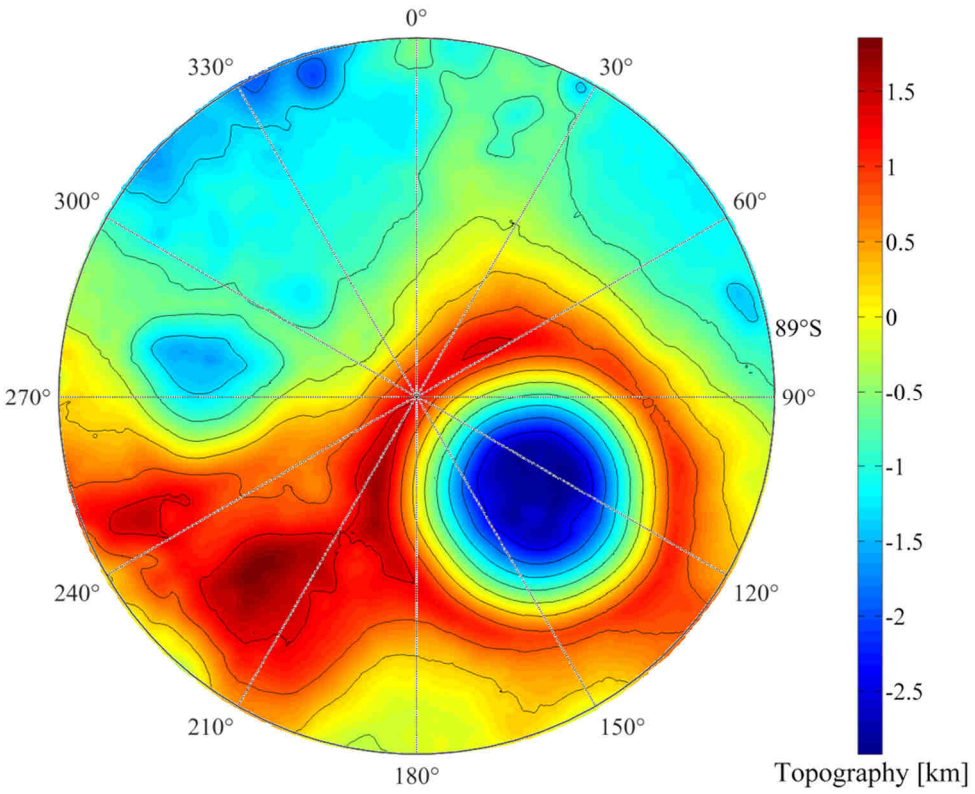

Figure 5.3 LRO-LOLA lunar south pole topographic map (89° – 90°S)

The different resolutions chosen are the result of a compromise for a high-quality terrain rendering and the computational cost to produce it. Moreover, the higher is the mesh resolution, the slower is the shadows rendering in the virtual scene. A summary of the properties of the DEMs used is reported in Table 5.1.

Table 5.1 DEMs topographic data

DEM	Latitude range	Mesh resolution
Kaguya/SELENE	79° – 90°S	2.36 km/pixel
Kaguya/SELENE	88° – 90°S	430 m/pixel
LRO-LOLA	89° – 90°S	230 m/pixel

Additionally, since the morphology of the terrain is important for landing and placing the outpost elements, a slopes map has been also considered and is represented in Figure 5.4.

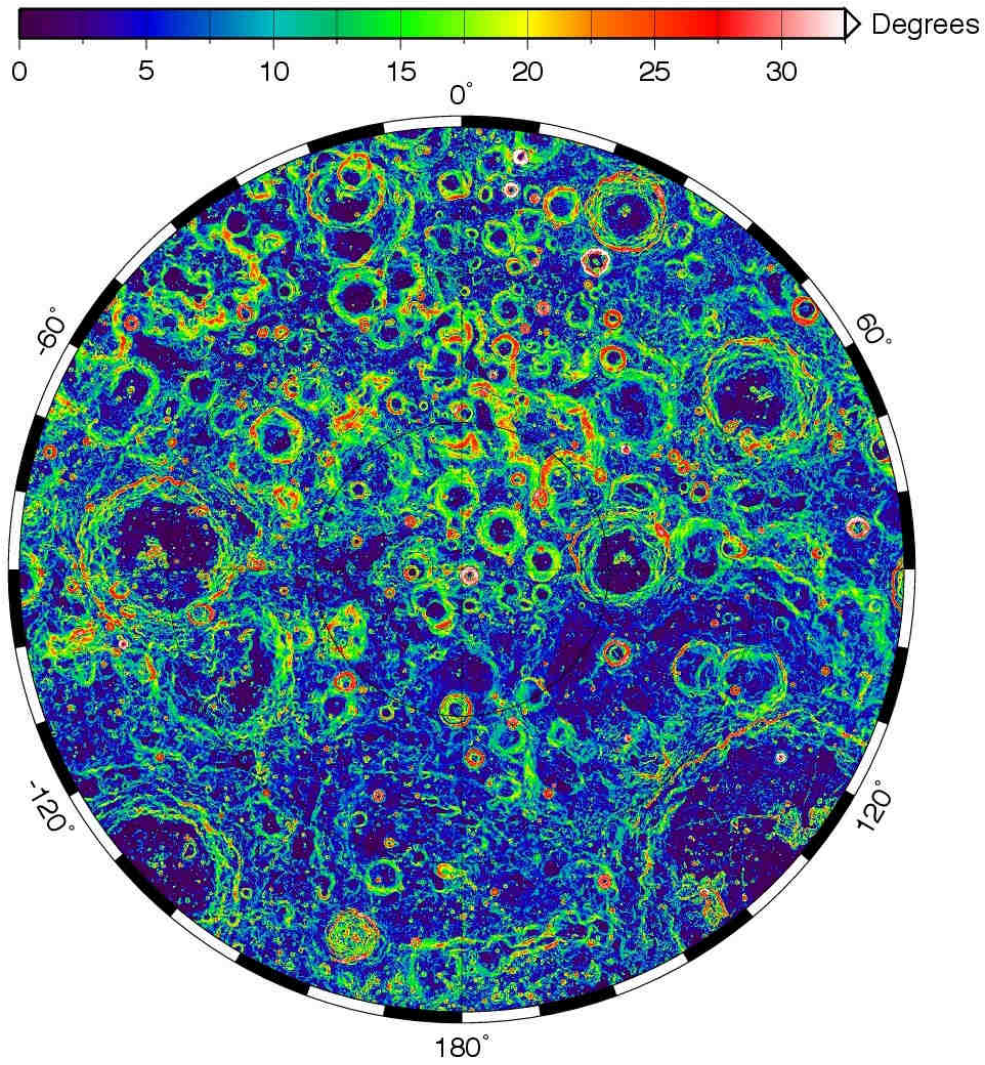

Figure 5.4 Slopes map of the Moon south pole (75° - 90°S) degrees South. The bright red to white areas have the highest slopes (25 degrees or more) while the dark blue to purple areas have the lowest slopes (5 degrees or less). The steepest slopes are found in impact crater rims, which appear as brightly coloured circular features throughout the image [303, 304] (credit: NASA)

5.2.2 Terrain illumination conditions

Once having generated the lunar south pole DEMs, illumination analyses have been run to simulate the light conditions: identifying highly illuminated spot and permanent shadowed regions is paramount to asset placement, solar energy availability, and cold traps accessibility. The preferred points on the lunar surface where to set the permanent human base and its power system shall have high illumination percentage over the year, have low surface roughness (in terms of slopes), be in direct communication with Earth, and near permanently shadowed regions for volatiles study and extraction.

Among several location alternatives offered by the Moon south polar region, five sites have been identified as the best candidates:

- Mount Malapert: it is an old and highly illuminated mountain with high slopes. Hydrogen and helium enclosed with thick regolith layer. The site is permanently in line-of-sight with Earth;
- Shackleton crater: it is a permanently shadowed crater close to the south pole. Temperatures inside the crater are extremely low thus water ice deposits are supposed to be present. Its rims are highly illuminated.;
- Cabeus crater: it is a large crater similar to the Shackleton crater in terms of environmental conditions;
- Faustini crater: it is the crater where the lowest temperature of all the Solar System has been ever measured;
- Shoemaker/Nobile region: it is a highly illuminated area located between the rims of the two namesake craters.

The main features of the selected sites are reported in Table 5.2.

Table 5.2 Coordinates location of the selected potential outpost sites

	Latitude	Longitude	Diameter/elevation [km]
Malapert	86.04°S	1.71°E	4.21
Shakleton	89.6°S	137.83°E	19
Cabeus	84.9°S	324.5°E	98
Faustini	87.3°S	77°E	39
Shoemaker	88.1°S	44.9°E	50.9

The geographical position of each selected sites is indicated in the map of Figure 5.5.

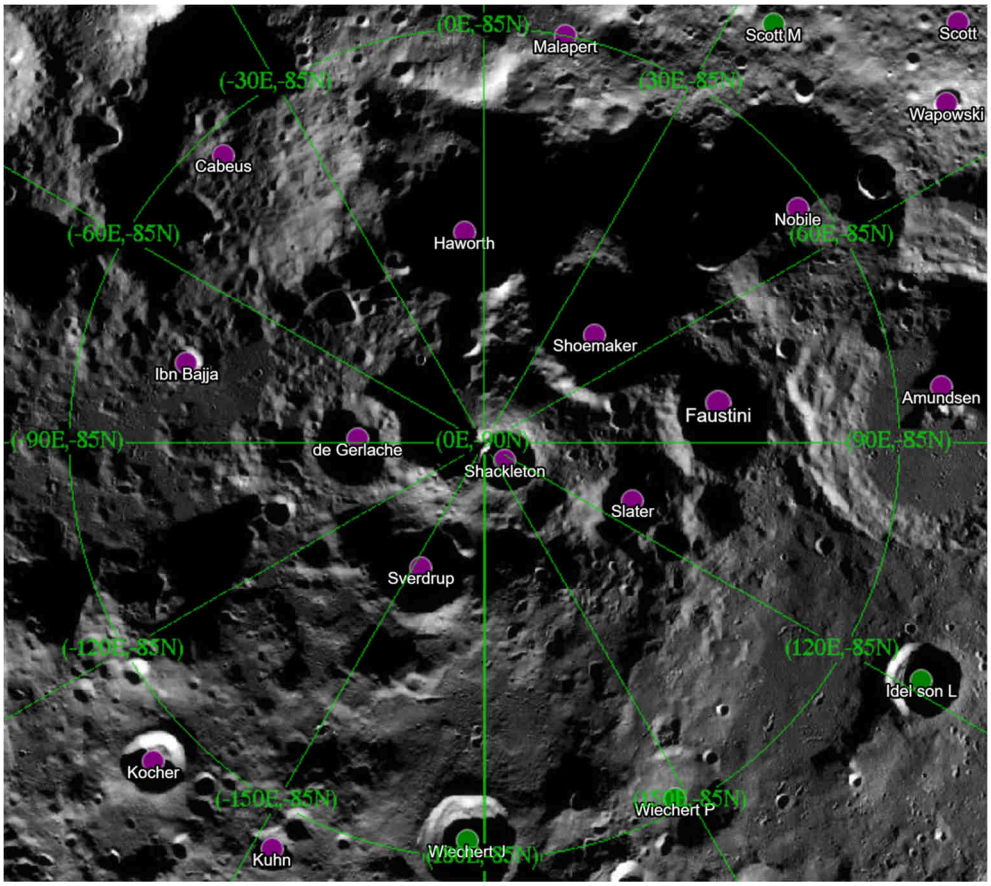

Figure 5.5 LROC Narrow Angle Camera (NAC) high resolution images (0.5 m/pixel) laid over the Wide Angle Camera (WAC) Global Morphologic basemap (100 m/pixel) with the principal names of the topographic sites [305] (credit: NASA)

Despite the suitable properties of all the listed locations, the Shackleton crater area has been selected for settling the human base. However, a constant direct communication with Earth is not always possible because of the librations of the Moon rotational axis [252]. Since the Malapert massif is permanently in line-of-site with the Shackleton crater and with Earth, it can be used as a radio relay for ensure permanent direct communication to and from Earth [188].

Before proceeding with in-depth and computational-heavy simulations, the performance of Blender® and VERITAS were benchmarked. The VR tools used offer the possibility to project shadows over a terrain model via computing the Sun position and tracking the shadows location. The virtual

scenes created with both software incorporate a terrain model (i.e. DEM) and a light source (i.e. Sun). The same generic lunar day has been chosen as the reference timeframe for the analysis. The mimic of the lunar soil graphical properties has been scaled using a real picture of the Shackleton crater taken by SMART-1. The fidelity of the results can be noticed in Figure 5.6.

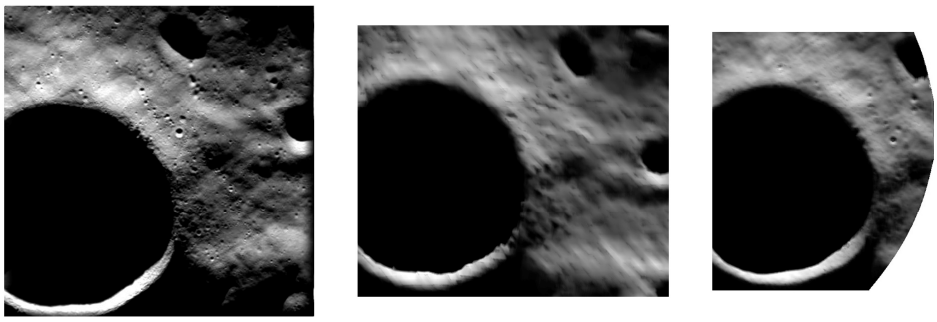

(a) (b) (c)

Figure 5.6 Shackleton crater area as seen by SMART-1 (a) (credit: ESA) and its virtual rendering using the DEMs derived from Kaguya/SELENE (b) and LRO-LOLA (c)

The LRO-LOLA DEM described in section 5.2.1 has been used as reference for comparing Blender® and VERITAS features.

Blender® calculates the shadow map using ray-tracing: the method consists in tracing a line between each point of the terrain and the Sun. The point (i.e. pixel) is shaded if the line intersects the terrain, otherwise it is illuminated. The finite angular size of the Sun, i.e. its light cone, is difficult to render with the current hardware available on the market, also considering the great distance from the DEM (i.e. 1 AU). To limit the graphical computational cost, parallel light rays have been used to illuminate the terrain virtual scene. The Sun positions have been specified by means of azimuth and elevation. The azimuth angle has been referenced to the zero-longitude meridian because the usual definition referred to north direction is meaningless at the Moon south pole. The elevation angle has been set to +1.54°. Static images have been generated and one image per 10° of Sun motion has been extracted starting from an azimuth angle of 0°: for each of the 36 images considered for the illumination analysis, pixels have been set to 0 (i.e. black) if they were not reached by any light ray while they were set to 1 (i.e. white) in the opposite condition.

All the images have been then stacked together to create an overall illumination map and measure the average illumination rate for each single picture as shown in Figure 5.7.

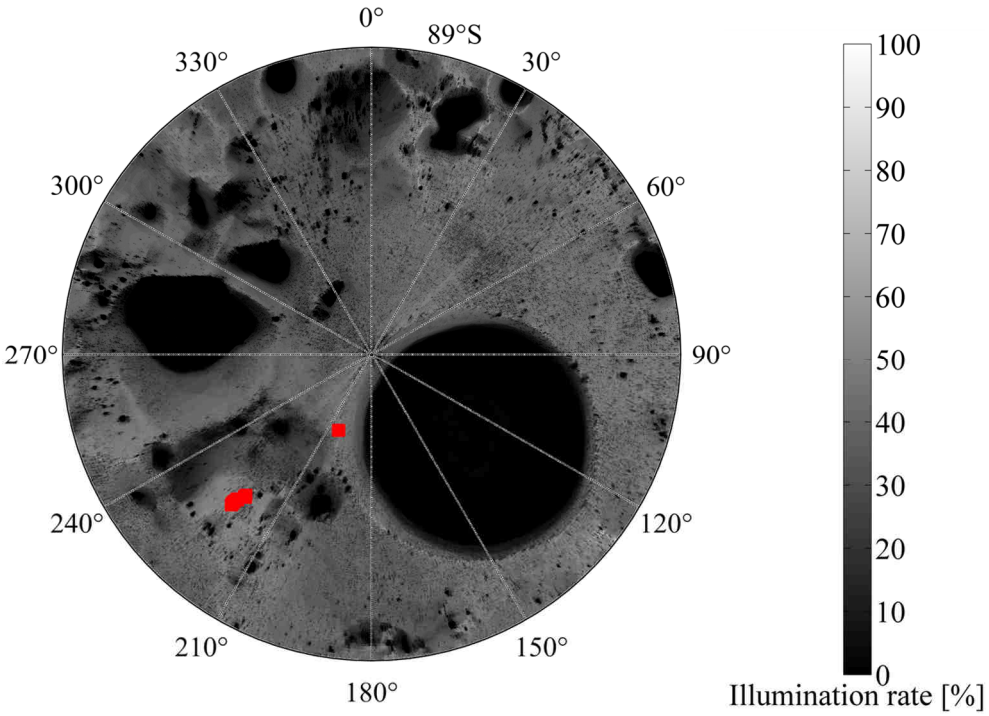

Figure 5.7 Blender® illumination map computed for a generic lunar day using the LRO-LOLA DEM (89° – 90°S) with a resolution of 230 m/pixel. The red squares represent the maximum illuminated points

The red squares in Figure 5.7 indicate the maximum illuminated points: in this case, those are peaks of eternal light because they are always illuminated in the simulated period (i.e. 100% of illumination rate); specifically, those points are located at the "Connecting Ridge", the ridge connecting the Shackleton and de Gerlache crater, and at the Shackleton craters rim, more precisely at 89.79°S – 204.75°E.

The same setup of Blender® has been used for VERITAS: 36 Sun position of the same generic lunar day and with the same elevation angle have been used for the illumination analysis of the LRO-LOLA DEM. Real-time shadows have been generated using the VERITAS internal graphical engine. The greyscale images obtained for each of the 36 time-steps chosen as the simulation timeframe have been converted into binary images by setting a convenient threshold for distinguishing sunlit and shadowed areas, and for not

underestimating illumination rates: if the pixel was illuminated, it was set to 1 (i.e. white) while it was set to 0 (i.e. black) if shadowed.

The illumination map has been created by stacking all the extracted images and the average illumination rate for each single pixel has been computed as shown in Figure 5.8, where this procedure is the same adopted by Speyerer and Robinson [306].

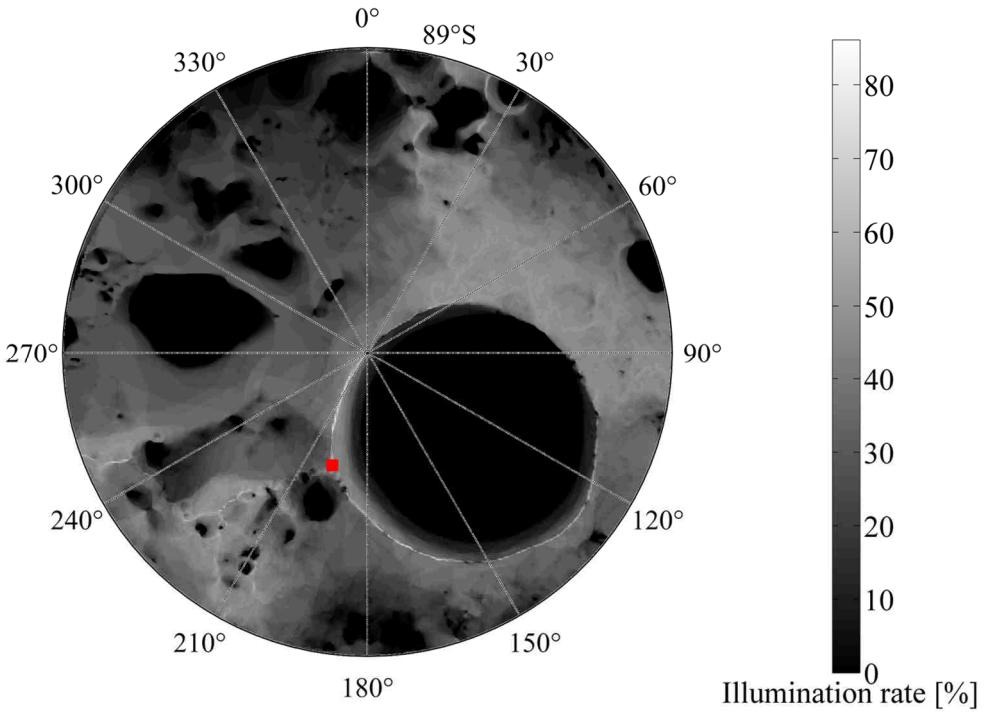

Figure 5.8 VERITAS illumination map computed for a generic lunar day using the LRO-LOLA DEM (89° – 90°S) with a resolution of 230 m/pixel. The red square represents the maximum illuminated point

The most illuminated point with a total illumination rate of 86.11% is marked with a red square in Figure 5.8: it is located at 89.69°S – 197.91°E.

The two illumination maps produced are qualitatively coherent one another but only the VERITAS one showed consistency with state-of-the-art studies [227, 284, 293, 294, 306–311]. The peaks of eternal light calculated by Blender® do not exist as confirmed by [26, 252, 284]: the more the local horizon level is risen above the local terrain topography, the more illuminated will be the point/area, but perpetual light conditions can be found only above several kilometres over the lunar surface.

The comparison between the results obtained by the two different VR software highlighted the differences of the simulation methods used by

Blender® and VERITAS to render the peculiar light conditions of the lunar south pole. While the Blender® graphical engine uses the ray-tracing function to off-line calculate and statically render the shadows and how they cast over the lunar terrain, the VERITAS one is capable to real-time render and dynamically simulate the light conditions and their change over time. The Blender® technique require an average of ~10 min to render each illumination state which results into ~6 h-long simulation, while VERITAS is able to real-time render every illumination step once the virtual scene is created, thus the simulation time is only equal to the time require to extract each image and create the illumination map that is equal to ~5 min (i.e. 8 s per image). Moreover, the total size of the images produced by Blender® is ~22 MB (i.e. ~626 KB per image on average), while is ~6 MB (i.e. ~171 KB per image on average) for VERITAS, even if the DEM grid resolution used is the same. Other illumination studies such as [293, 310] used the horizon method to calculate the light/shadow state of each terrain mesh element: the horizon elevation is computed along a defined number of directions (azimuths) for each point of the DEM and the resulting data are stored in a series of matrices (one for each direction); those fixed-direction horizon elevation data are then used to interpolate a given Sun location and calculate the visible Sun disc ratio. If compared to ray-tracing, both methods require heavy off-line calculations, but the horizon method is faster when the first step of the process (i.e. horizon calculation for each grid point) is preprocessed, in fact the illumination state can be calculated very fast for any given set of Sun temporal and spatial coordinates. However, the principal drawbacks of the method are the high computational cost associated with the preprocessing step and the need to save big data files[17]. Even if VR software generally do not use this method, it was anyway used as reference to compare the results obtained and the principal features of Blender® and VERITAS because of its wide use in literature.

Despite the scene creation is simpler thanks to the intuitive GUI, the inaccuracies observed in correctly estimate the illumination rates of the lunar south pole, the high computational cost related to the ray-tracing function and the possibility to render and simulate only static/discrete virtual scenes/states finally led to discard Blender® as VR software to be used in this research work. Instead VERITAS has been chosen as the preferred VR software for the analyses to carry out in this thesis. Even if there is just a command editor

[17] Typically, for a DEM with a mesh of 512 x 512 elements with a horizon resolution of 0.5°, the size of the file would be in the order 512 x 512 x 720 x 2 Bytes (around 330 MB) if the data are mapped to 16 bits integers.

and not an intuitive GUI for creating the virtual scenes, the real-time attribute guaranteed by the VERITAS graphical engine is a key feature for trade-off evaluations that are typical of the early space mission design phases. Specifically, for the illumination studies described, the user can actively interact with the virtual scene created while the rendering and the shadows calculation are running.

Once established VERITAS as the only VR software to be used for the illumination analysis, more precise simulations have been run. Thanks to the VERITAS embedded feature, real ephemeris data have been used to correctly simulate the relative positioning of the Sun-Moon system. Since precise measurements are necessary to account the small variations of the Sun elevation angle over the lunar terrain, the SPICE DE 421 ephemeris have been selected. Developed by NASA JPL, they have been specifically tailored for accounting the Moon libration phenomena that major affects the illumination rates and their seasonality of lunar polar areas [312].

Further test simulations have been run for the 2020-2030 decade. All the three DEMs, two from Kaguya/SELENE and one from LRO-LOLA (see Table 5.1 for resolution details), have been used for the illumination analysis. The Sun positions have been directly calculated by VERITAS using real ephemeris data: the real-time shadows on the DEM are casted accordingly to the light rays rendered by the VERITAS graphical engine. Starting from midnight of January 1st, 2020, and finishing at midnight of January 1st, 2031, one image every 24 h has been extracted and converted into a binary format using the same procedure already described. All the images (4019 in total) has been then stacked together for creating global illumination maps. All the three simulations lasted for ~9 h that is the time required for extract each of the 4019 images (i.e. 8 s per image) and calculate the relative illumination maps.

The illumination map obtained for the widest Kaguya/SELENE DEM is represented in Figure 5.9.

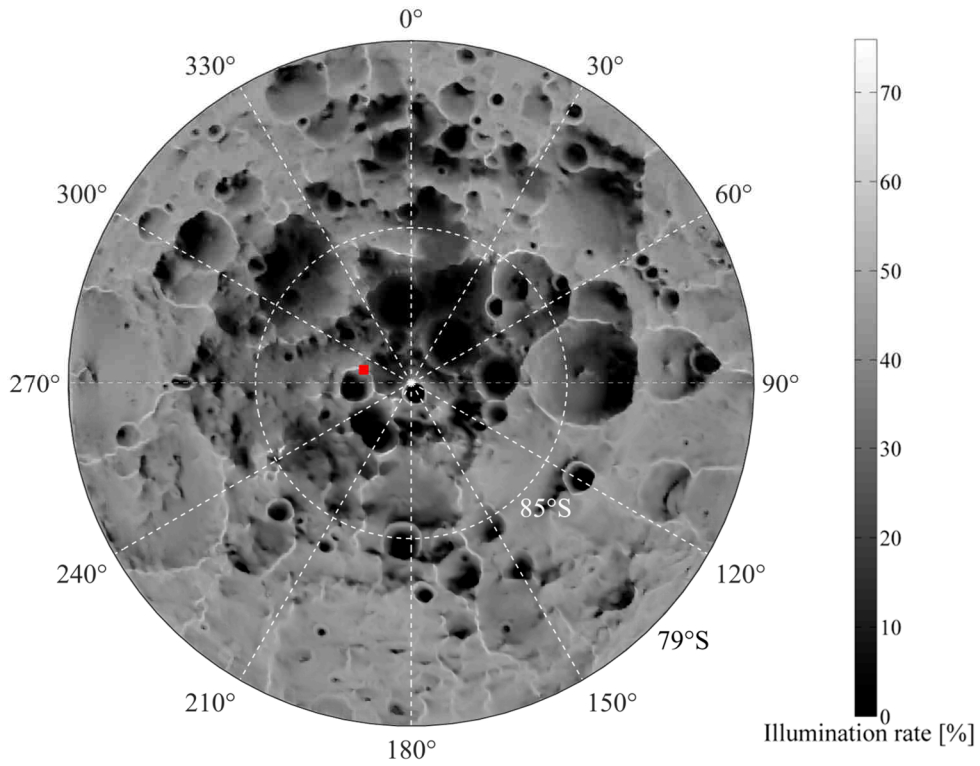

Figure 5.9 Kaguya/SELENE illumination map computed for the timeframe 2020-2030 using the Kaguya/SELENE DEM (79° - 90°S) with a resolution of 2.36 km/pixel. The red square represents the maximum illuminated point

The most illuminated point with a total illumination rate of 76.08% is marked with a red square in Figure 5.9: it is located at 88.65°S – 292.98°E. There is a mismatch in the proximity to the boundary: in fact, the DEM spans only from 79°S to 90°S, i.e. the surrounding topography was not included in the model, which causes wrong illumination conditions.

The total size of all the 4019 images produced to create the illumination map is ~1.4 GB (i.e. ~365 KB per image on average).

The illumination map obtained for the reduced Kaguya/SELENE DEM is represented in Figure 5.10.

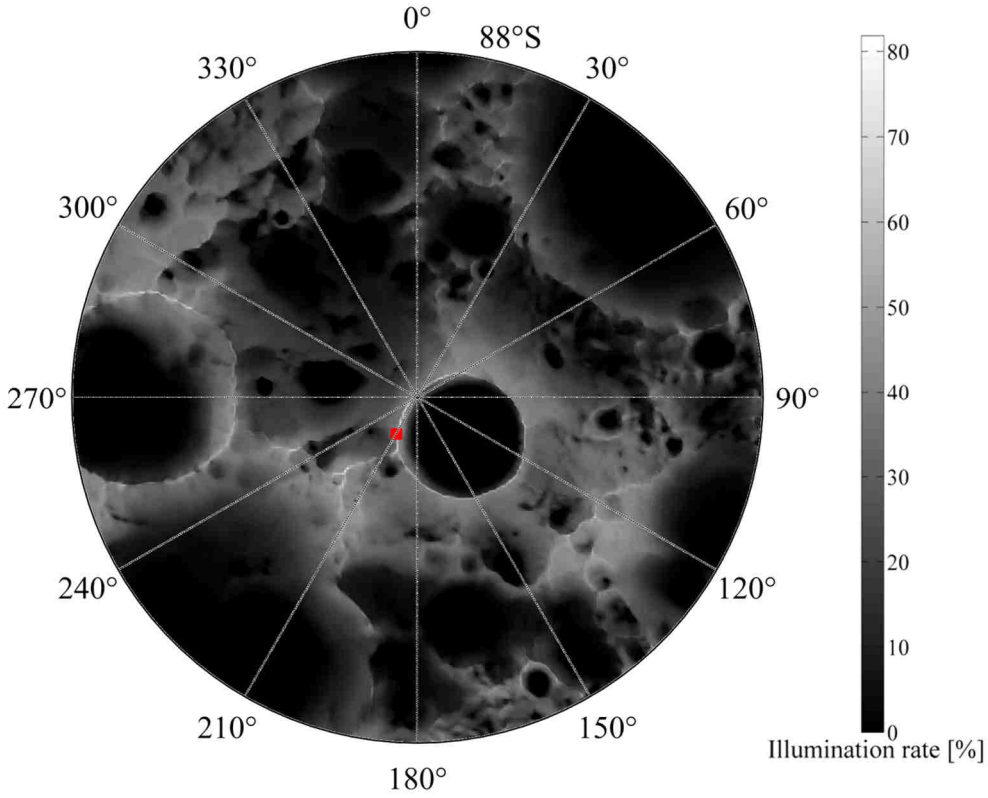

Figure 5.10 Kaguya/SELENE illumination map computed for the timeframe 2020-2030 using the Kaguya/SELENE DEM (88° - 90°S) with a resolution of 430 m/pixel. The red square represents the maximum illuminated point

The most illuminated point with a total illumination rate of 81.89% is marked with a red square in Figure 5.10: it is located at 88.65°S – 292.98°E. The map show consistency with the one obtained with the ESA Coverage Tool that calculated the accumulated illumination percentage in the time period ranging from March 31st, 2010, to September 24th, 2010 with a time-step of 1 h [227], and with the one produced by using the LRO WAC images taken from February 15th, 2010, to February 5th, 2011 [306]. Both those maps are represented in Figure 5.11.

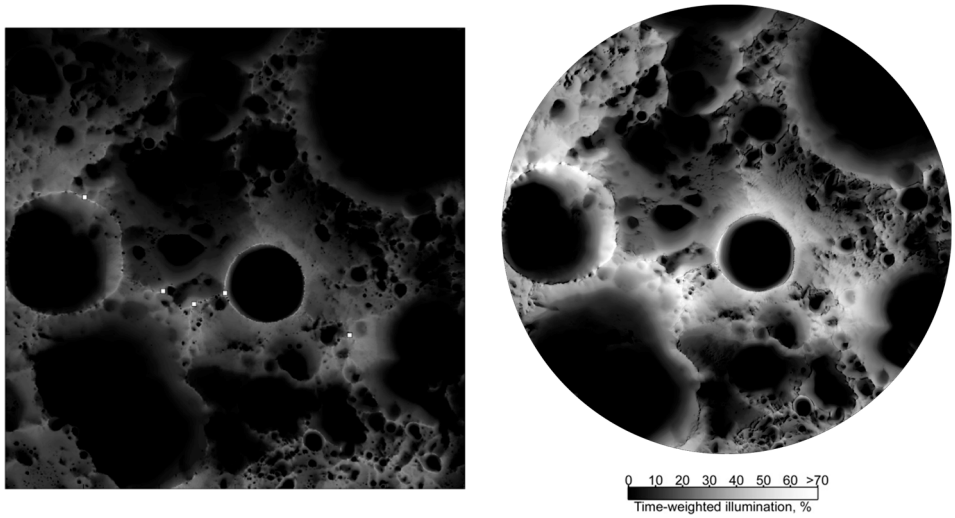

(a) (b)

Figure 5.11 Multi-temporal illumination maps of the lunar south pole obtained by De Rosa *et al.* (a) [227] and by Speyerer and Robinson (b) [306]

The total size of all the 4019 images produced to create the illumination map is ~800 MB (i.e. ~204 KB per image on average).

The entire simulation process that led to obtain the final illumination map using the Kaguya/SELENE DEMs is schematically represented in Figure 5.12.

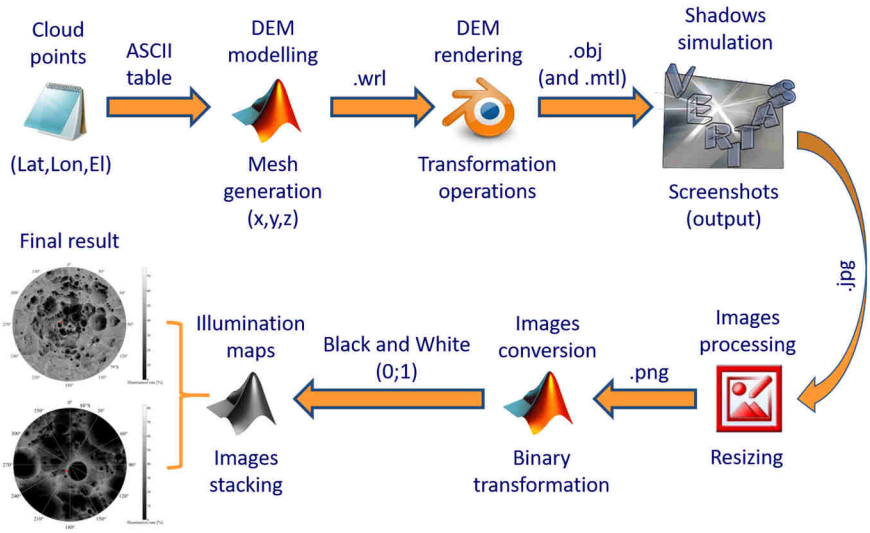

Figure 5.12 Simulation scheme adopted for generating the illumination maps using the Kaguya/SELENE DEMs

The illumination map obtained for the LRO-LOLA DEM is represented in Figure 5.13.

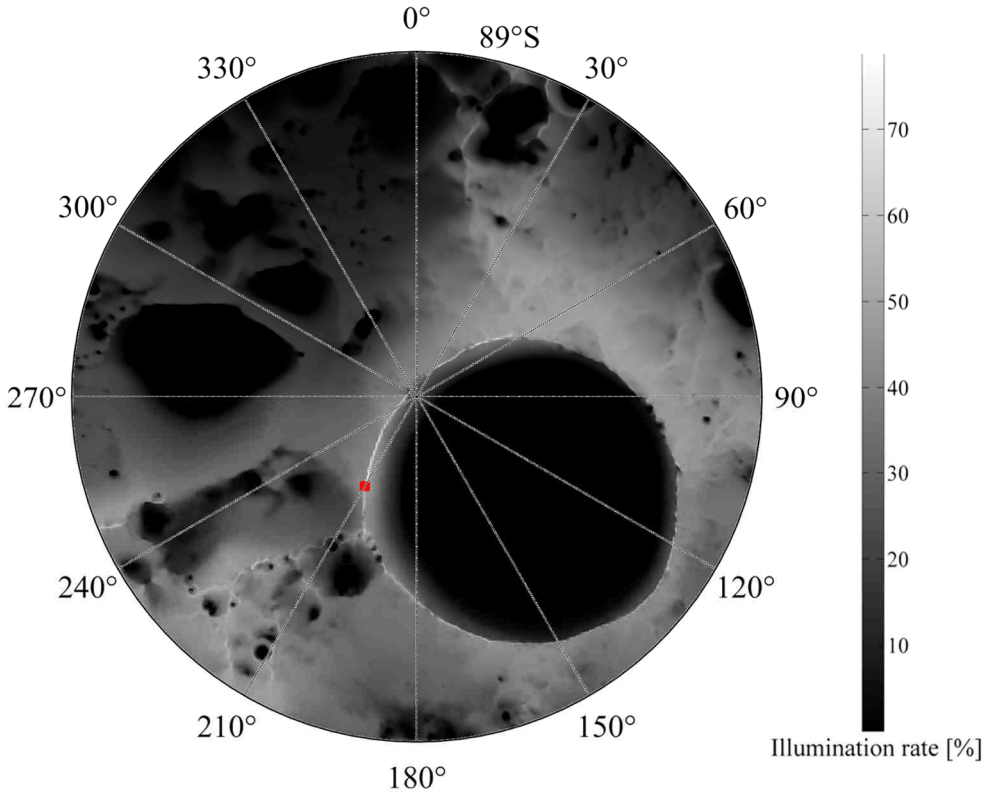

Figure 5.13 LRO-LOLA illumination map computed for the timeframe 2020-2030 using the LRO-LOLA DEM (89° - 90°S) with a resolution of 230 m/pixel. The red square represents the maximum illuminated point

The most illuminated point with a total illumination rate of 78.84% is marked with a red square in Figure 5.13: it is located at 89.78°S – 203.74°E.

The total size of all the 4019 images produced to create the illumination map is ~740 MB (i.e. ~189 KB per image on average).

The entire simulation process that led to obtain the final illumination map using the LRO-LOLA DEM is schematically represented in Figure 5.14.

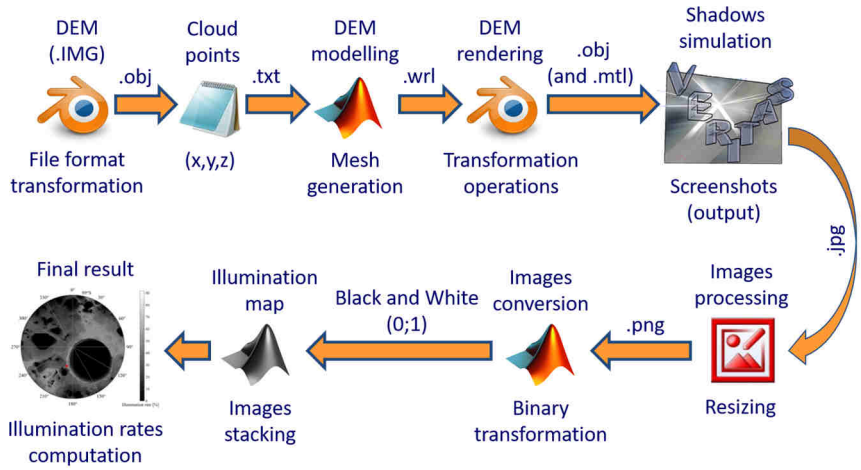

Figure 5.14 Simulation scheme adopted for generating the illumination map using the LRO-LOLA DEM

A summary of the illumination analysis of each DEM is reported in Table 5.3.

Table 5.3 DEMs illumination data

DEM	Maximum illumination rate	Coordinates
Kaguya/SELENE	76.08%	88.65°S – 292.98°E
Kaguya/SELENE	81.86%	89.76°S – 201.06°E
LRO-LOLA	78.84%	89.78°S – 203.74°E

The result of this assessment survey of the VR-based illumination analysis using different DEMs with different spatial resolution is consistency with state-of-the-art results which uses different methods (e.g. horizon method, remote sensing data, etc.). The results obtained for both the Kaguya/SELENE DEMs are coherent with [284, 307] but also with [293], apart from the errors found for the widest DEM: its lower resolution also led to locate the most illuminated spot not in the usual area around the actual Moon south pole, but on the de Gerlache crater rims. The illumination map obtained for the LRO-LOLA DEM is in line with the results of [26, 293, 294].

The absence of a lunar atmosphere coupled with the peculiar sun-lit/shadow conditions results into extreme temperature. For equatorial regions the day/night cycle is 14.5 (terrestrial) days long and stable, daylight temperatures can reach 400 K and go below 100 K during the nights. Polar areas are

colder for the low direct illumination annually received. To better estimate the temperature ranges experienced by a specific point, mathematical models have been developed. The regolith is the media through which the heat is transferred: solid particles conduction and radiation are the two different transmission modes; thus, the thermal conductivity can be expressed as a function of these two components. [313] developed a 1D numerical model with a perfect spherical Moon to estimate temperatures at sunrise, noon and sunset. For a simulation of 400 (terrestrial) days, the equatorial surface temperatures have a 250 K-total variation, while the same data is around 100 K for polar regions. The maximum estimated polar temperature is 170 K. The minimum estimated polar temperature is 60 K. The global trend is represented in Figure 5.15.

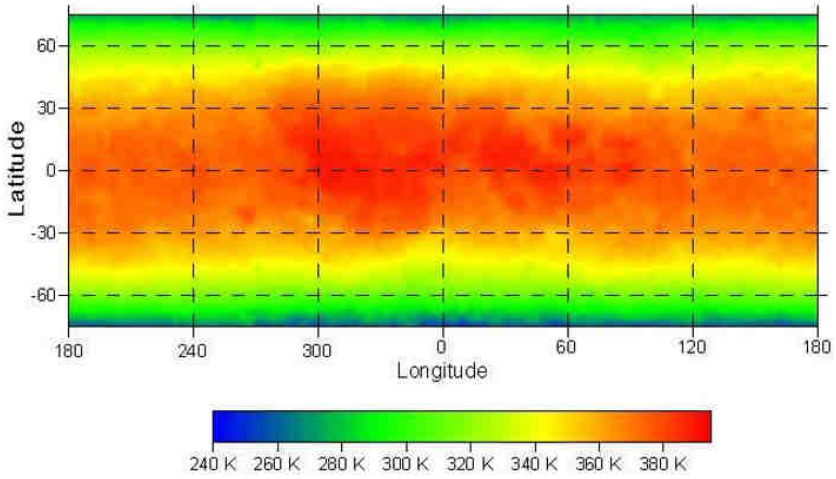

Figure 5.15 Global map of maximum surface temperatures with a resolution of 0.4° [313]

The results obtained for the Moon polar region by Bauch *et al.* [313] are in line with other models. Specifically, Vasavada *et al.* [314] calculated a temperature variation that ranges from 128 K to 180 K during the summer solstice, i.e. with a continuous illumination, and 38 K during the winter solstice, i.e. with a shaded polar night. Those results have been obtained using horizontal surface placed at 89°S. Both the models are consistent with the data measured by the Diviner instrument on-board LRO. The complete radiometric data acquired since 2009 have been showing how average maximum temperature of the lunar south pole is ~200 K, with average minimum temperature of ~50 K [232, 233, 315, 316]. The global map of the measured average temperature is depicted in Figure 5.16.

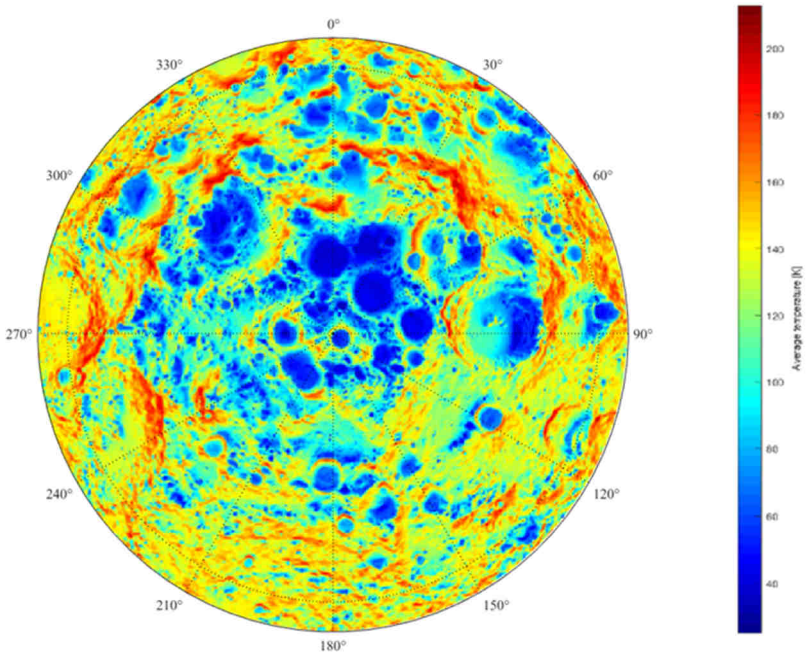

Figure 5.16 Map of the average lunar south pole temperature derived from the LRO-Diviner measurements [233]

The global map of the measured maximum temperature is depicted in Figure 5.17.

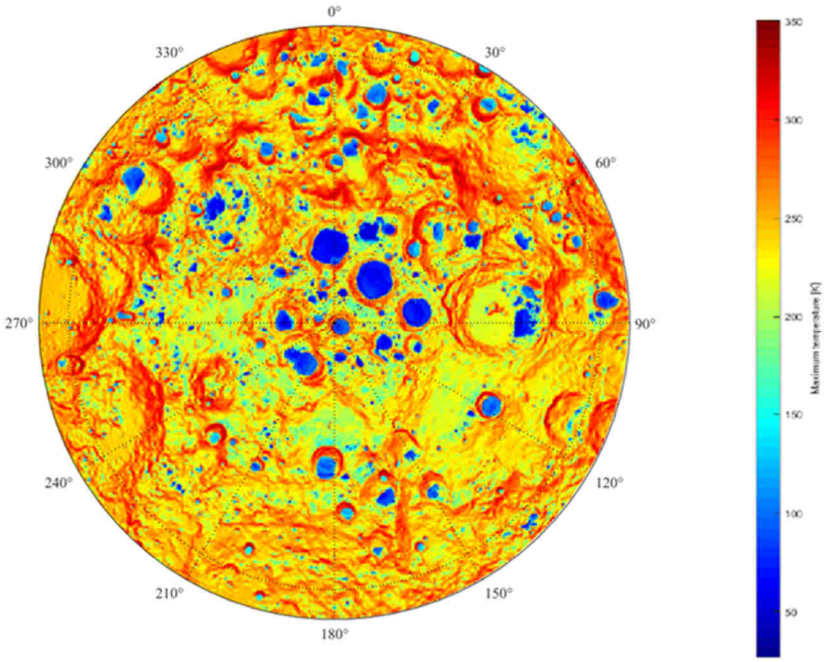

Figure 5.17 Map of the maximum lunar south pole temperature from the LRO-Diviner measurements [233]

The steady light conditions of some areas make the temperature almost constant: thermal control results easier. Those spots are potential favourable spot where to possibly locate some outpost elements. Additionally, a precise estimation of the temperature variation over time is crucial to plan EVAs and robotic exploration activities [317, 318].

To better estimate the specific illumination conditions and the temperature time evolution, and to identify the area to locate the base modules, a dedicated simulation has been run for the entire year 2035 using VERITAS and the setup already validated with the previous set of analyses. The LRO-LOLA DEM has been used to model the lunar terrain, but with an increased resolution of 178 m/pixel. The simulation starts at midnight of January 1st, 2035. A time step of 1 h has been set for the illumination studies over time because, during this period, the Moon rotates of ~0.5°, which corresponds to the angular diameter of the Sun: no azimuth gaps happen where the Sun could be completely blocked or fully visible [294]; an example of the Sun visibility conditions is sketched in Figure 5.18.

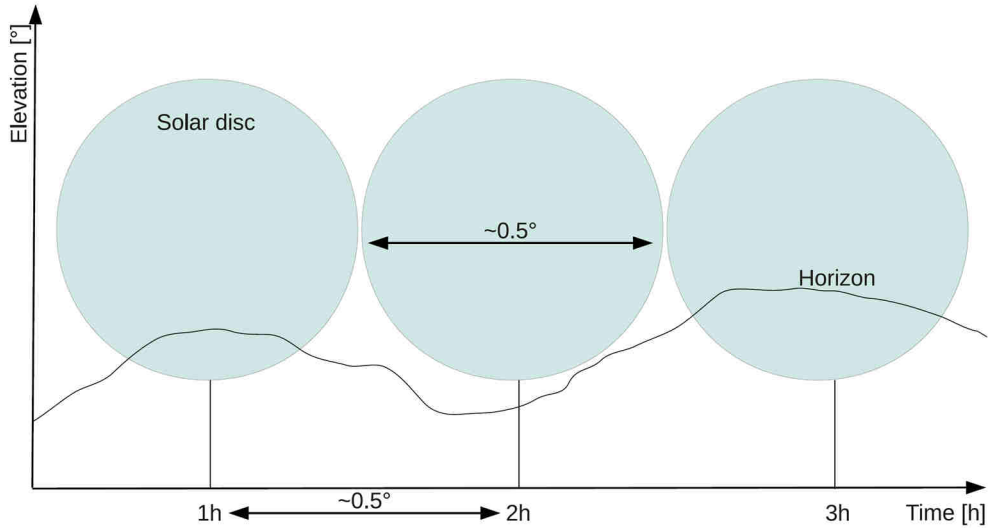

Figure 5.18 Example of Sun visibility: the solar disk is completely visible at t = 2 h whereas it was partly blocked 1 h before and after (t = 1 h and t = 3 h) [294].

The timestep imposed resulted into generating 8761 images in total: to complete this one-year simulation, ~19 h were necessary (i.e. 8 s per image). The same conversion method has been applied to create binary images. By stacking the entire database, a global illumination map has been obtained as shown in Figure 5.19.

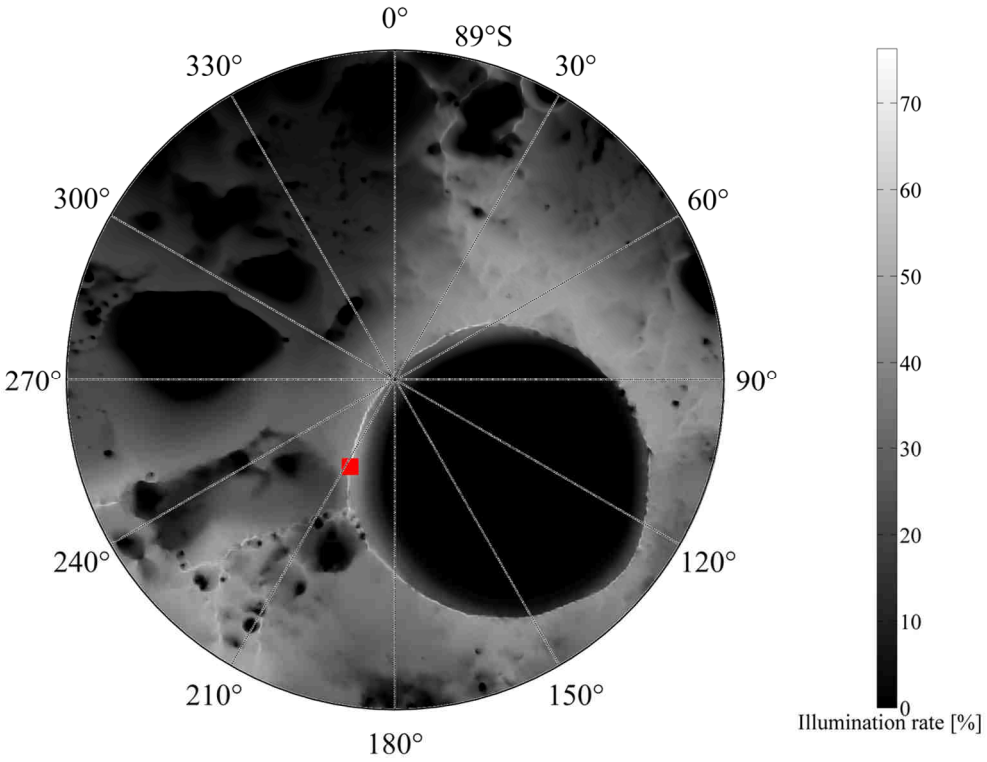

Figure 5.19 LRO-LOLA illumination map computed for the year 2035 using the LRO-LOLA DEM (89° - 90°S) with a resolution of 178 m/pixel

The most illuminated point with a total illumination rate of 76.29% is marked with a red square in Figure 5.19: it is located at 89.78°S – 204.93°E. The results is perfectly in line with the latest results obtained by [294, 310, 311] and with other state-of-the-art studies as reported in Table 5.4.

Table 5.4 Illumination studies comparison

Study	DEM resolution [m/pixel]	Maximum illumination rate [%]	Coordinates
Noda *et al.* [307]	474	87	89.8°S – 207.5°E
Bussey *et al.* [308]	474	82	89.44°S – 218.2°E
Mazarico *et al.* [293]	240	89.01	89.45°S – 222.69°E
De Rosa *et al.* [227]	40	84.13	89.69°S – 196.14°E
Speyerer and Robison [306]	100	71.7	89.74°S – 201.2°E
Gläser *et al.* (2014) [294]	20	73.84	89.78°S – 203.94°E
Speyerer *et al.* [310]	20	75.04[18]	89.69°S – 196.7°E
Gläser *et al.* (2017) [311]	20	81	89.78°S – 203.97°E
This study	178	76.29	89.78°S – 204.93°E

The total size of all the 8761 images produced to create the illumination map is ~2.15 GB (i.e. ~257 KB per image on average).

The time history of the light conditions of the most illuminated point is reported in Figure 5.20 where 0 represent the shadowed hours and 1 the illuminated ones.

[18] Calculated at 2 m above the surface

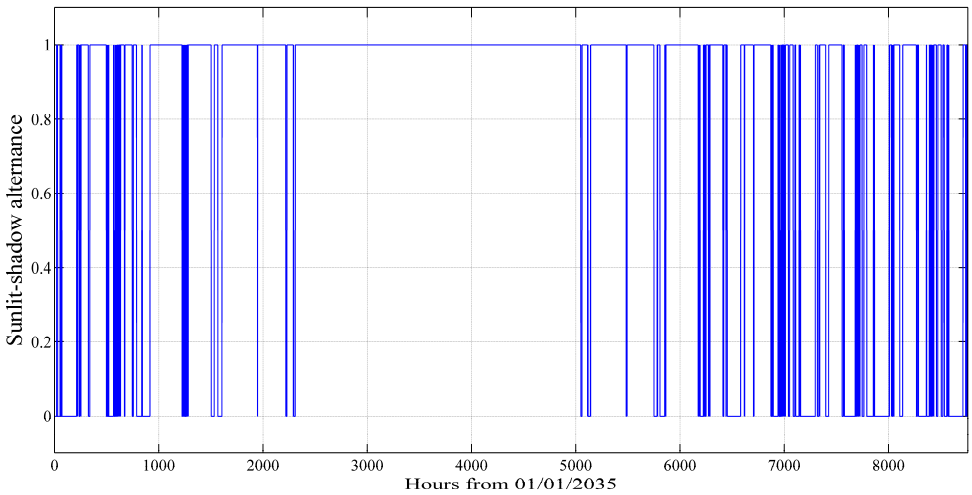

Figure 5.20 Time history of the illumination conditions of the most illuminated point

The longest continuous shadowed period is 5.92 days and the longest sunlit period is 114.13 days. The result obtained is similar to [309]: winter and autumn periods are characterized by more pronounced light variations, while during summer there is a more stable and continuous illumination. Those data confirm the goodness of having chosen a hydrogen-photovoltaic SAPS. The solar panel sized in section 4.3.1 appears to be as the most active SAPS component: an in-dept analysis has been carried out in section 5.3 using VR to estimate its performances and the relative variations due to the changes in the environment conditions.

The local Sun elevation angle, as seen from the most illuminated point, has been also computed using VERITAS: it has been directly calculated by the VR software as the angle between the plane tangent to an ideal sphere, whose radius is equal to the Moon one, and the light vector, which connects the centre of the south pole DEM and the Sun (light source in the VR scene). The local horizon is influenced by the terrain topography: using a rotation matrix (for a coordinates changes, i.e. latitude and longitude) and the local terrain conformation, both relative to the most illuminated point, the final elevation angle has been computed for each time step of the simulation (for the illumination analysis). The points obtained (one per hour) have been interpolated to generate the final curve, as reported by Figure 5.21.

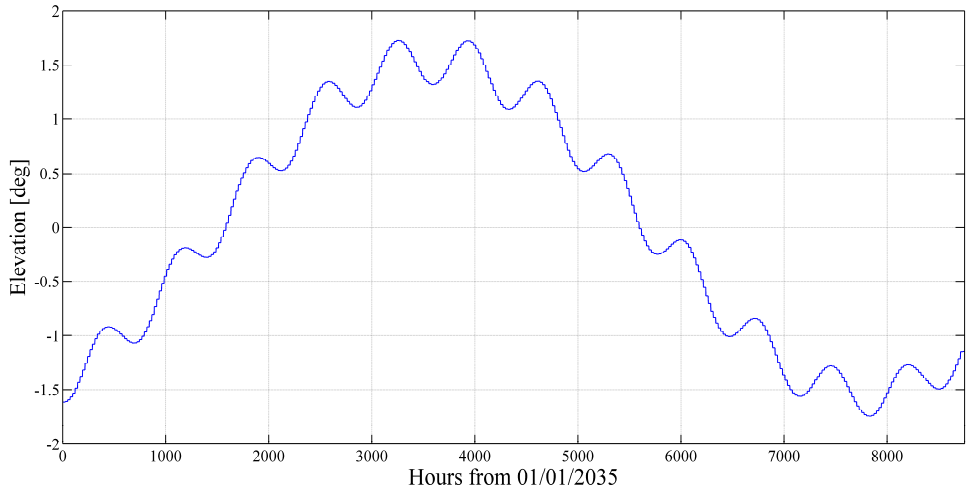

Figure 5.21 Solar elevation angle computed for the most illuminated point

Two periodical oscillations of the Sun elevation angle result evident from Figure 5.21. The smaller one is relative to short-period variations: the Moon rotation cycle around its rotational axis lasts for a synodic month, which an average duration of 29.53 days (~708 h); when the Moon is at its perigee the period is shorter, while it is longer when is at its apogee. The maximum local value of the Sun elevation angle is almost always reached in the middle of the month. The other variation happens in a long-period: the global oscillation of about ±1.5° has an average duration of 8496 h (~12 synodic months). The maximum value of the Sun elevation angle is reached during the spring/summer months, which results into longer sunlit periods.

The same trend is evident by plotting the distance between the Sun and the most illuminated point. Figure 5.22 shows the same periodical oscillations: during the winter period the Sun is closer to the Moon, so its rays are more inclined, while it is the opposite in summer.

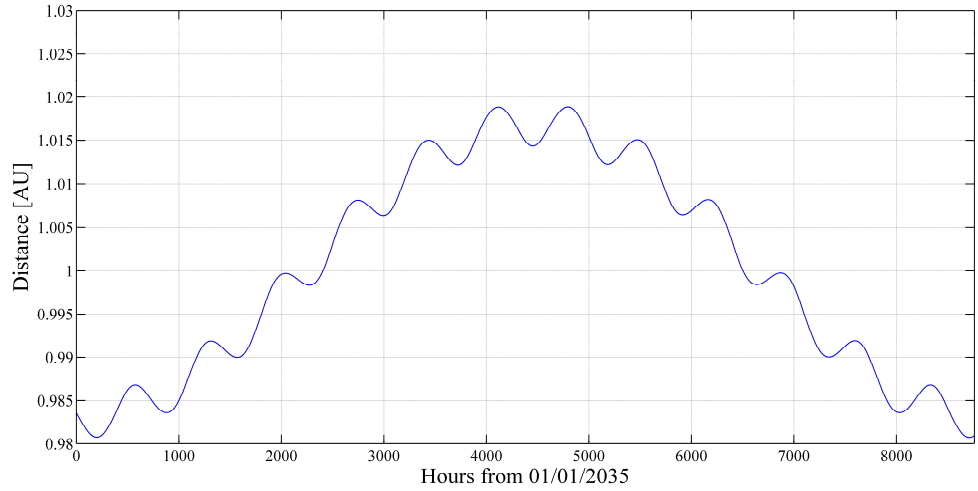

Figure 5.22 Distance between the most illuminated point and the Sun

5.3 VR integration

The specific analysis of the illumination conditions of the Shackleton crater area led to identify the most illuminated point. Using this point and its relative features as reference, other simulations have been done. Specifically, VERITAS has been coupled with a lumped parameter model of the solar panel to simulate the performance variations during the selected timeframe. The integration obtained among the two different tools (VERITAS and MATLAB®/Simulink®) is the first applicative demonstration of the methodology proposed in this research work.

5.3.1 Solar panel analysis using VR

Starting from the virtual scene used for the terrain illumination analysis, the solar panel designed in section 4.3.1 has been modelled. The same simulation period and time step have been used to compute the performance variations due to transient shadows, casted by the surrounding topography, and to the environment conditions changes (solar irradiance and temperature).

A simple CAD model has been used to represent the solar panel in the VERITAS VE: it is a white slim parallelepiped 43.7 m high and 97.5 m long, where the 8 power channels have been considered adjacent one another, i.e. not accounting for the space occupied by the telescopic bars to sustain the panel itself. The model has been placed at the maximum illuminated point, tiled of +0.33° (with respect to the terrain normal plane), and it has been raised of 2 m above the local DEM surface, as justified in section 4.3.1. An

animation has been created to mimic the 1 DoF-Sun tracking movement of the panel base. The same method used for the surface illumination analysis has been adopted: one image per hour has been extracted for the year 2035. An Ultra-High-Definition (UHD) resolution (i.e. 3840 x 2160 pixel) has been used for extracting the images: 8761 solar panel states have been saved, each having a 38 m/pixel resolution that result from the actual 3717 x 1653-pixel relative size of the panel. All the images have been converted into a binary format and stacked together to create an overall illumination map of the solar panel, similar to what has been done for the LRO-LOLA DEM. The simulation was run for ~1 day (i.e. 10 s for each image to be extracted) and the images database size is ~37 MB (i.e. ~4.3 KB per image on average).

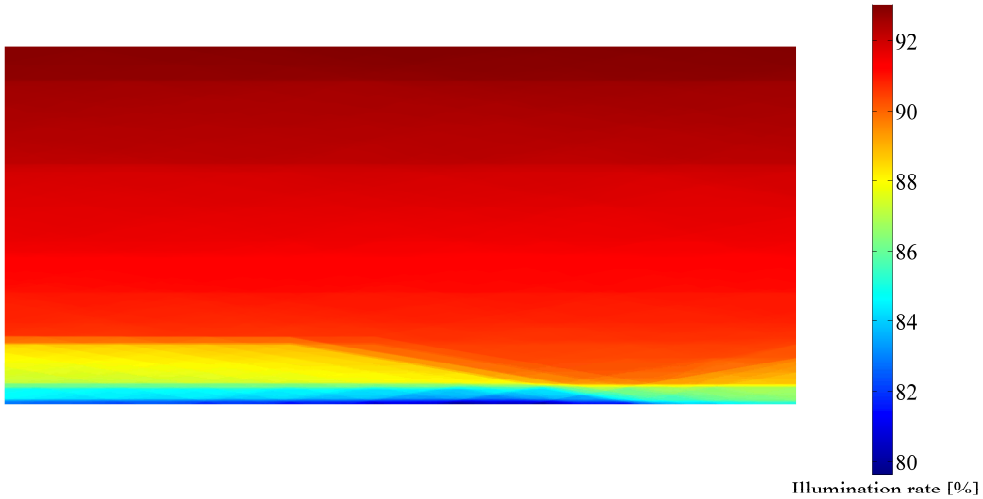

Figure 5.23 Solar panel illumination map computed for the year 2035 with a resolution of 38 m/pixel

Figure 5.23 shows how the solar panel experiences a global illumination rate ranging from 79.60 % (in the lower part closer to the terrain) to 93.02 % (in the upper part). The trend which indicates the more a point is raised above the ground, the more lights it gets in the south polar regions, is confirmed by the result computed. In addition, no peaks of eternal lights have been discovered even though the panel is ~44 m high (~46 m high if the base rising is also considered): those point are located several kilometres away from the Moon surface [294].

A comparison between the DEM and the solar panel illumination analyses is reported in Table 5.5.

Table 5.5 Illumination data relative to the LRO-LOLA DEM (with a resolution of 178 m/pixel) and the solar panel

	DEM	Bottom pixel	Central pixel	Solar panel
Longest shadowed period [days]	5.92	7.17	2.79	2.63
Longest sunlit period [days]	114.13	117.54	146.75	159.54
Total eclipse rate [%]	23.71	19.31	8.36	6.73
Total illumination rate [%]	76.29	80.69	91.64	75.83
Transition rate [%]	-	-	-	17.44

The three first columns (DEM, bottom, and central pixel) are referred to single points, while the data reported for the solar panel are referred to its entire surface. The longest shadowed and sunlit period confirms the trend of having a major Sun visibility (direct illumination) the higher is the point above the surface. An exception is represented by the bottom pixel of the solar panel (2 m high) that experience a longer shadowed period that the most illuminated point on the lunar surface: interpolation errors in converting the images into a binary format and the shadows rendering (by the VERITAS graphical engine) are the main causes of this mismatch. The central pixel (~23 m high) experiences more days of consecutive shadow that the entire panel, but this is in line with the expected trend and is the result of comparing punctual to global data.

When referring to entire panel, not only fully illuminated or shadowed images have been computed, but also partial transient shadows have been found: the transition rate row in Table 5.5 accounts the amount of time into which the panel is in this condition.

As already done for the most illuminated point, the local Sun elevation angle, as seen from the solar panel (its central point), has been also computed using VERITAS: it has been directly calculated by the VR software as the angle between the solar panel surface (i.e. panel orthogonal plane) and the light vector, which connects the centre of the solar panel model and the Sun (light source in the VR scene). Figure 5.24 represents the light vector of the solar panel used by using the VR software to compute this effective solar elevation angle.

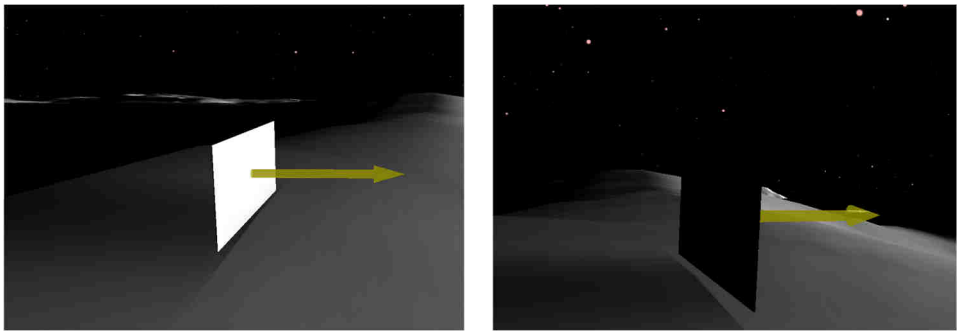

(a) (b)

Figure 5.24 Front (a) and rear (b) view of the solar panel model and its light vector as rendered by VERITAS

The final elevation angle has been computed for each time step of the simulation (for the illumination analysis). The points obtained (one per hour) have been interpolated to generate the final curve, as reported by Figure 5.25.

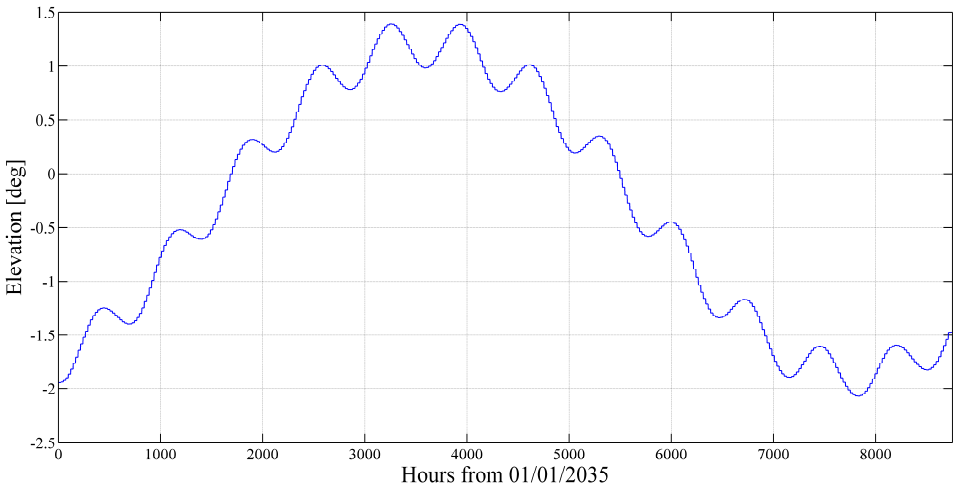

Figure 5.25 Solar elevation angle computed for the solar panel

The two periodical oscillations (short- and long-period variations) observed in Figure 5.25 are the same computed for the most illuminated point (see Figure 5.21). Since the solar panel is tilted of +0.33° and is placed at 2 m above the lunar surface, the solar elevation angle computed for the solar panel is slightly different from the one computed for the DEM most illuminated point.

5.3.2 Lumped parameters model

To estimate the performance of the solar panel for the same timeframe of the VR simulations (i.e. 2035), a lumped parameters models have been developed using MATLAB®/Simulink®. Different approaches exist in literature for modelling multi-junction cells like [319–325], but in order to reduce the computational time, to lower the model complexity, and to better integrate VR with a standard design tool as the MATLAB®/Simulink® environment, a simpler approach has been adopted. The single solar cells were not modelled with the typical electrical equivalent circuit (i.e. semiconductor diodes) but, as it will be described in section 5.3.3, the model adopts as the fundamental scaling unit the string of modules to match the data obtained from the VR simulations. Several sub-blocks have been used to create the entire solar panel model, but they can be grouped into three main blocks that are:

- The "Lunar Environment Model (LEM)" block that calculates the variables related to the Moon ambient which influences the solar panel performances;
- The "shadows" block that accounts the solar panel performances drop related to the shadows, which have been simulated using VERITAS;
- The "power system" block that includes the actual solar panel, the Maximum Power Point Tracker (MPPT), and the DC-DC converter models.

The LEM block incorporates sub-blocks and functions which calculates data and values of the lunar environment. By setting in input the selenocentric coordinates of interest, the LEM block is able to calculate the Panel Effective Solar Irradiance (PESI) and the solar panel temperature. Specifically, the coordinates of the most illuminated point, obtained by the VR analysis of section 5.2.2, have been set as reported in Figure 5.26.

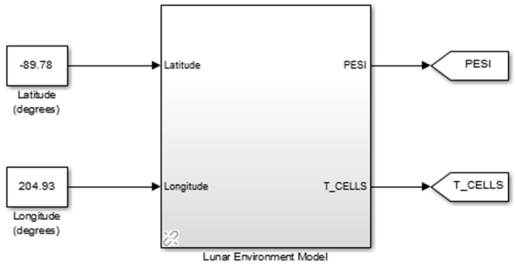

Figure 5.26 LEM block

Dedicated functions have been created to compute the values of irradiance and the temperature, as shown by the overall internal structure of the LEM block of Figure 5.27.

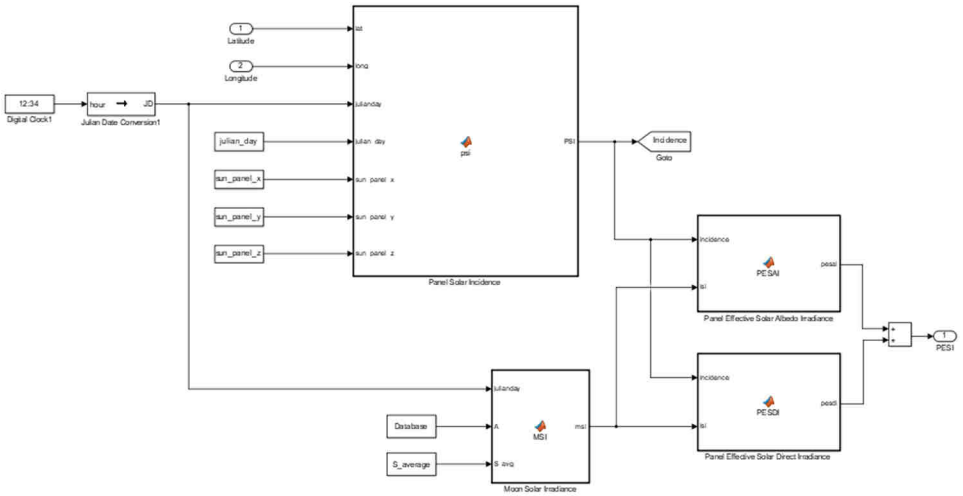

Figure 5.27 LEM block internal structure

The data obtained by the VR analysis were used to calculate the PESI. At each timestep of the simulation (i.e. 1 h, set by using a digital clock), the value of the elevation angle as seen from the panel is calculated: starting from the elevation angle extracted from VERITAS using the terrain analysis (see Figure 5.21), a rotation matrix is computed to transform the value relative to the maximum illuminated point and refer it to the solar panel.

PESI is the sum of two distinct contributions: the Panel Effective Solar Direct Irradiance (PESDI) and the Panel Effective Solar Albedo Irradiance (PESAI). PESDI is the normal component of the solar irradiance that directly hits the panel. By defining α as the Sun elevation angle relative to the Moon surface (maximum illuminated point), β as the panel inclination angle calculated with respect to the terrain local vertical, and I_{solar} as the solar irradiance, PESDI can be calculated using Equation (5.1).

$$PESDI = I_{solar} \cdot \cos(\alpha - \beta) \tag{5.1}$$

A schematic view of both the angles and how there are geometrically calculated is represented in Figure 5.28.

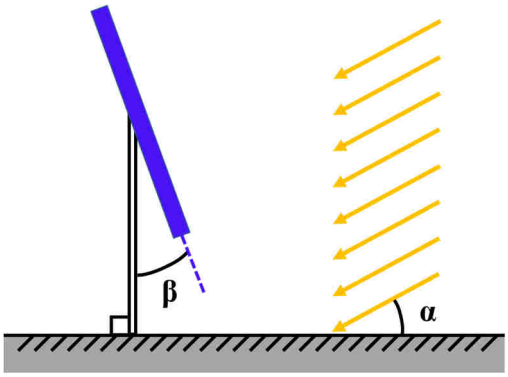

Figure 5.28 Angular parameters definition: α is the Sun elevation angle relative to the Moon surface (maximum illuminated point), β is the panel inclination angle calculated with respect to the terrain local vertical

The net effect of the two angles has already computed from VERITAS as the solar elevation relative to the solar panel, reported in Figure 5.25.

PESAI is the normal component of the solar irradiance that is reflected by the lunar surface and hits the panel. By defining α and β as the same angles used for Equation (5.1), I_{solar} as the solar irradiance, and a as the albedo coefficient (assumed equal to 0.12), PESAI can be calculated using Equation (5.2).

$$PESAI = I_{solar} \cdot a \cdot \cos(\alpha + \beta) \tag{5.2}$$

The effective solar irradiance has been estimated using the NASA Solar Radiation and Climate Experiment (SORCE) mission database [326]. Since there is no atmosphere on the Moon, the solar irradiance that hits the lunar surface has been assumed equal to the one measured by the SORCE spacecraft[19], due to the small variations among these two values. The average solar irradiance value of a specific timeframe has been calculated as the average (over the years 2003–2017) of the values computed for the same timeframe: the extrapolation method adopted to predict the specific 2035 trend is represented in Figure 5.29.

[19] The SORCE spacecraft was launched in 2003 into a 40° Earth orbit with an altitude of 645 km. Its purpose is to study the solar radiation with accurate measuring instruments.

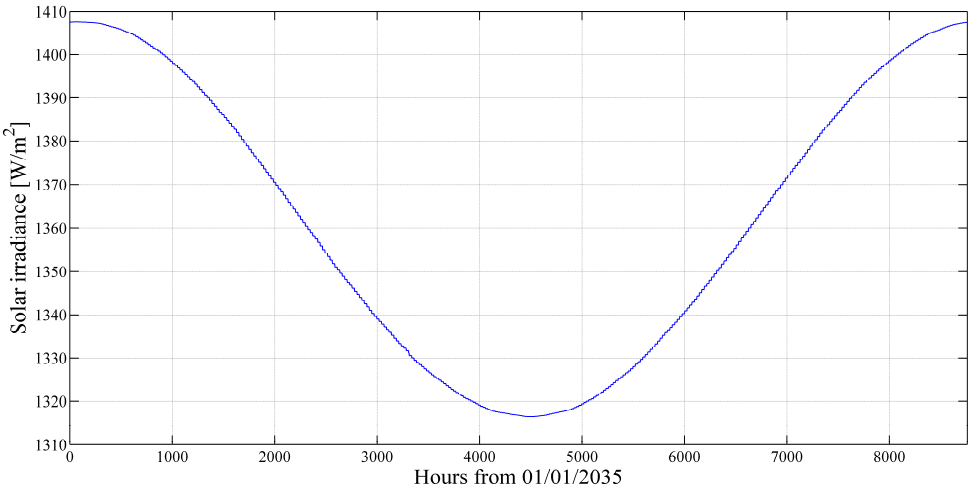

Figure 5.29 Solar irradiance variation as seen from the from the most illuminated point

The seasonal variation of the solar irradiance is due to variation of the Sun-Moon distance: in winter is lower than in summer, as represented by Figure 5.22.

The total value of PESI, calculated as the sum of PESDI and PESAI, is represented in Figure 5.30.

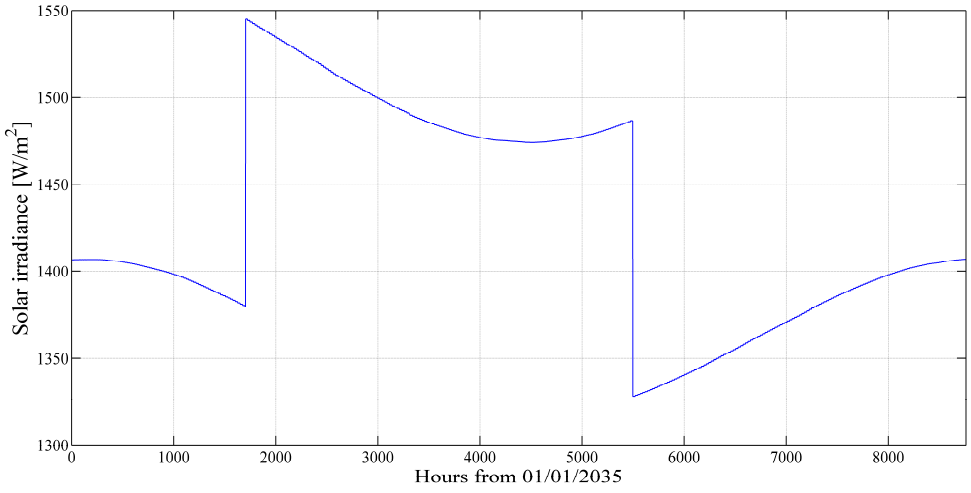

Figure 5.30 PESI variation

The discrete step present during the summer period is the consequence of the assumptions made: the lunar albedo (and so the PESAI) is only considered when the Sun elevation angle as seen from the DEM is > 0. The effects of the local topography have been neglected and the Moon has been assumed as a

perfect sphere: the resulting irradiance is calculated with respect to the terrain parallel surface, which is tangent to the lunar sphere at the maximum illuminated point. If the local terrain slope is positive (i.e. the effective local terrain elevation is > 0), the albedo contribute to PESI is not considered (PESAI = 0), which means to underestimate the real value of the PESI.

Finally, the solar panel temperature is calculated using the "grey body" radiation equation. Since there is no lunar atmosphere, the thermal equilibrium does only account heat conduction and radiation. Moreover, the conduction contribute has not been considered due to its low value[20]. The solar panel temperature is calculated using Equation (5.3) as a function of PESI, the Boltzmann's constant σ, the solar cells absorptivity ρ, and the solar cells emittance ε[21].

$$T_{cells} = \left(\frac{PESI}{\sigma} \cdot \frac{\rho}{\varepsilon}\right)^{0.25} \tag{5.3}$$

Since it is a function of PESI, the solar panel temperature experiences the same seasonal abrupt change due to the lunar albedo as shown in Figure 5.31.

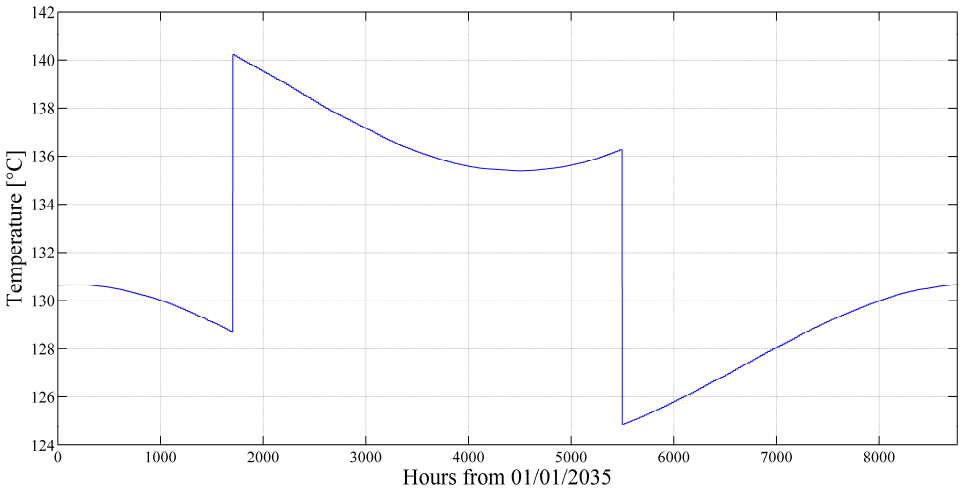

Figure 5.31 Solar panel temperature variation

The "shadow" block represents the interconnection block among VERITAS, i.e. the VE used to simulate the shadows, and MATLAB®/Simulink®, i.e. the design environment used to create a solar panel lumped parameters model. The models integration is achieved using this block: a first tentative

[20] It only occurs between solar cells and the substrate over which they are placed. The joining process is usually done in vacuum.

[21] ρ = 0.9 and ε = 0.849. Data derived from [281].

creation of a complete virtual model has been fully realized; VR and other software data are linked to create a complete description of the system under study.

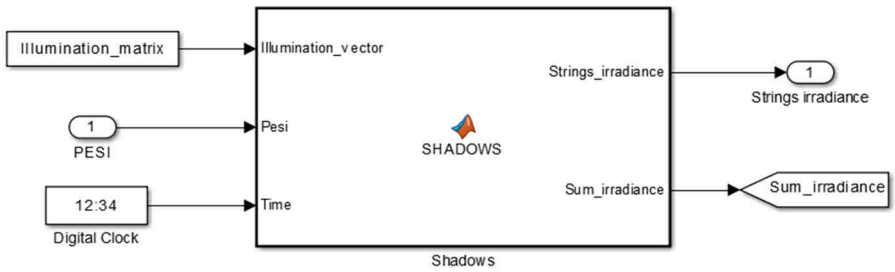

Figure 5.32 Schematic view of the “shadows” block

The “shadows” block represented in Figure 5.32 has been created to modulate the PESI with respect to the transient shadows that reduce the solar panel performance. For each timestep (simulated using a digital clock with a frequency of 1 h as the timestep used for the virtual simulations) the effective solar irradiance, experienced by each string of the whole solar panel, is computed. As it will be detailed described in section 5.3.3, each irradiance value is multiplied by an illumination matrix that has been extracted from VERITAS. This matrix represents the binary illumination state (either 0 if shadowed, or 1 if sunlit) of each solar string which composes the 8 power channels of the solar panel at a given timestep. Every matrix has been previously saved into a tensor with 30 x 8 x 8761 dimensions, as it will be discussed in section 5.3.3. To monitor when the channel is completely shadowed, and so its tension value is null, a sum of the irradiance value of all the strings in a channel is computed.

The “power system” block has been modelled to mimic the power production of the solar panel depending on the environmental conditions computed by the LEM and “shadows” blocks. It is composed by three different macro sub-blocks: the “photovoltaic plant”, the MPPT, and the “DC-DC converter” blocks as schematized in Figure 5.33.

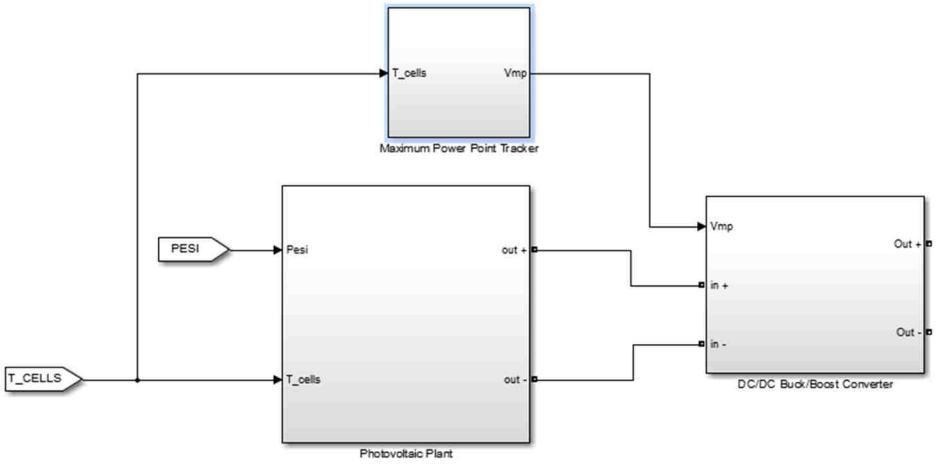

Figure 5.33 Internal structure of the “power system” block

The “photovoltaic plant” block has been modelled to mimic the internal structure of the solar panel: 8 power channels, each with 10 arrays, have been created; for each array, 3 strings of 15 series-connected modules are present. This massively-populated model is partially represented in Figure 5.34.

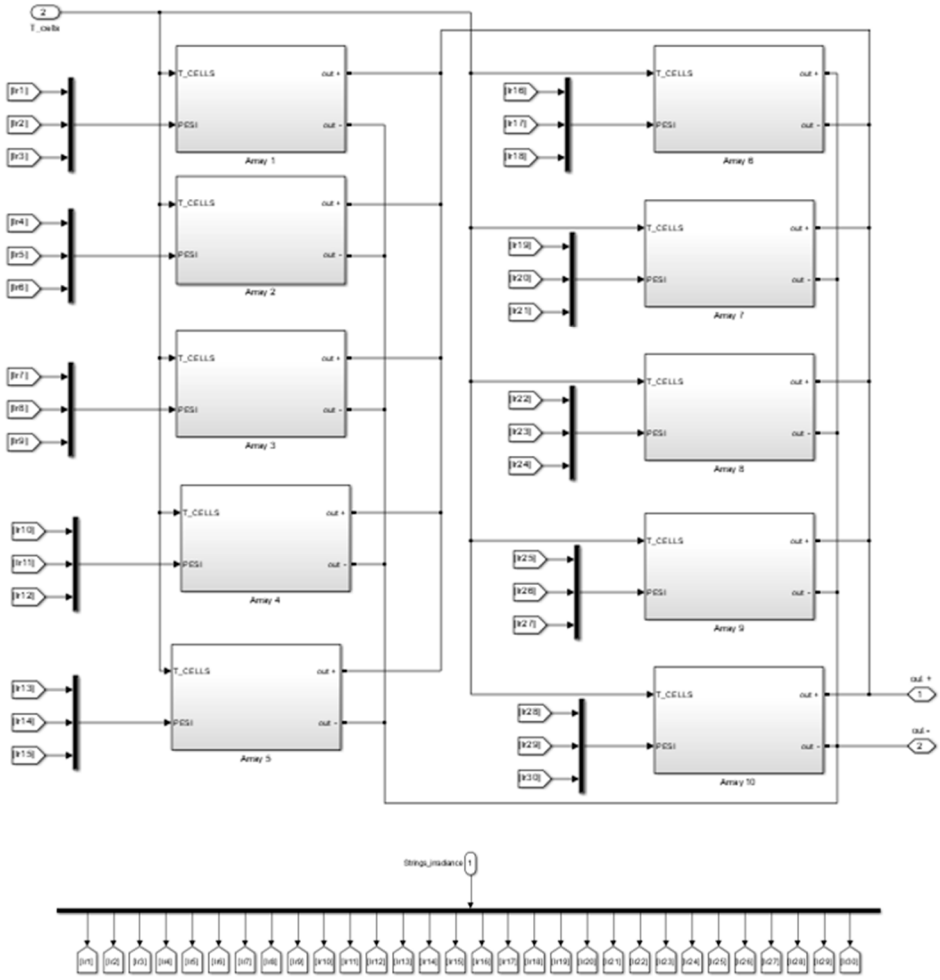

Figure 5.34 Internal structure of the power channel. A total of 8 channels are present in the “photovoltaic plant” block

For each of the 8 power channels, 10 arrays have been modelled, each with a separate block as represented in Figure 5.34. Every block computes the tension and current relative to one array using the temperature of the solar panel (to compute the thermal efficiency) and the PESI calculated by the LEM block, both affecting the performances of the array, and so those relative to the entire solar panel. Furthermore, PESI is divided into the three components computed from the “shadows” block: for each of the three strings that compose the array, PESI is modulated with respect to the actual illumination experienced (done for each timestep with an illumination matrix).

Each array has been precisely modelled by stopping at the string level: in fact, for every array, its internal structure is represented by three strings as shown in Figure 5.35.

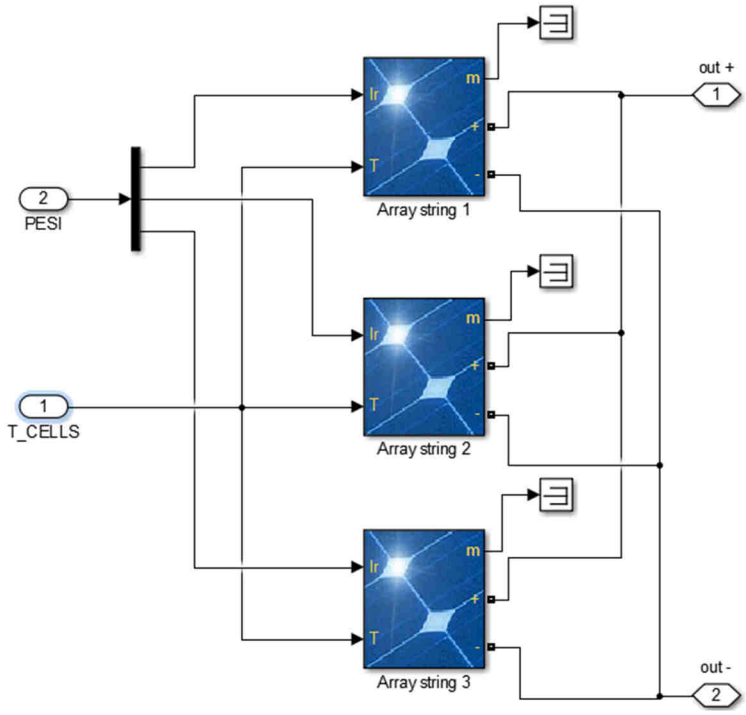

Figure 5.35 Internal structure of the array. 10 arrays are present for each of the 8 solar panel power channels

The three strings that compose one array are connected in parallel scheme. To limit the computational cost, this is the last level of detail considered for the analysis, also considering the data extracted from the VR analyses. The representation mode chosen led to consider only fully illuminated o fully shadowed strings to proportionally reduce the power produced (using the illumination matrices). The strings are modelled using the "PV array" block of the Simulink® SimScape toolbox, whose internal values have been set using the solar cell datasheet [281].

The complex "photovoltaic plant" block described is coupled with the MPPT to replicate the real system configuration of the solar panel. This device regulates the working mode of the photovoltaic plant: the maximum power at which the system can work is fully defined by a unique value of tension and current. This point can change during time if the temperature and/or the solar irradiance vary: the MPPT impose to the solar panel to operate at voltage that corresponds to the maximum output power, once the boundary environmental conditions are given. Specifically, an indirect method has been adopted for calculating the maximum power tension (V_{MP}):

it is expressed as a function of the temperature-dependent open circuit tension (V_{op}) as reported by Equation (5.4).

$$V_{MP}(T) = k \cdot V_{oc}(T) \tag{5.4}$$

Moreover, a life degradation factor (L_d) is accounted to quantify the maximum power voltage reduction throughout the solar panel operative life (EOL of 15 years by design).

$$V_{MP}(T, t) = L_d(t) \cdot V_{MP}(T) \tag{5.5}$$

Therefore, the resulting maximum power voltage is reduced by a factor of 0.87 at EOL, with a linear decrement during the 15 years, as reported by Equation (5.5).

A schematic view of the MPPT block is represented in Figure 5.36.

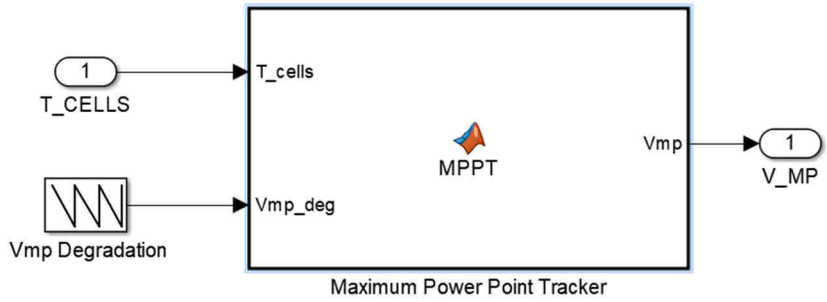

Figure 5.36 MPPT block

The other real component modelled is the DC-DC converter. This device is needed to regulate the power level between the production plant (i.e. the solar panel) and the loads connected to the bus. Specifically, it has been decided to model a buck-boost converter which converts a source of direct current both increasing or decreasing its voltage level. A schematic view of this component is represented in Figure 5.37.

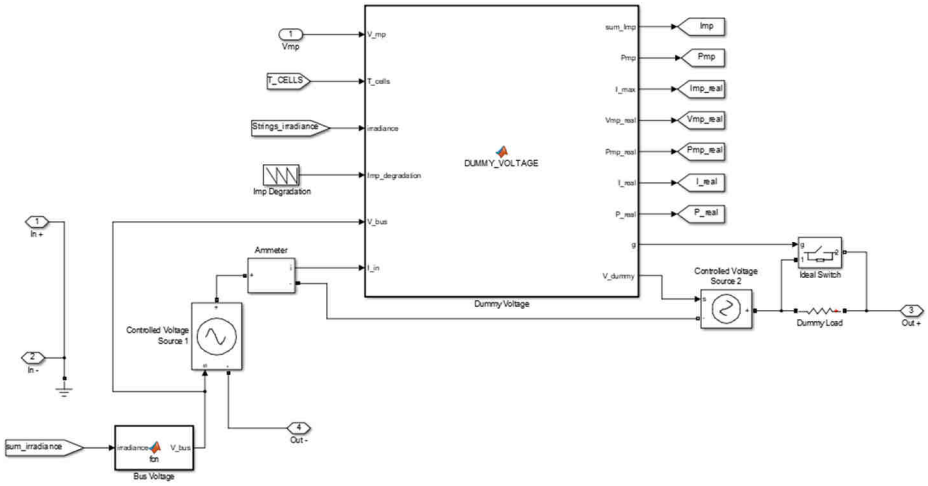

Figure 5.37 Internal structure of the "DC-DC converter" block

The DC-DC converter model created mimic the control logic of the real system, but not all its components have been modelled to reduce the complexity of the overall solar panel model and its computational cost. This block calculates the power level output that an external load connected to the bus can absorb. The MPPT block computes the maximum power level (i.e. tension and current) that each channel of the solar panel is producing at a given timestep: the value depends on the illumination conditions and the temperature of the channel. This power level is used to compute the output current absorbed by the external load: since the output voltage has been set to 900 V (bus tension), the output current is the only unknown variable in the power equation to be calculated. This equation equals the maximum power produced by a channel to the load power output. If the channel is partially shadowed, i.e. some of its arrays are shadowed, the output power is reduced proportionally: the parallel-connected arrays guarantee to have the same tension (i.e. 900 V), but a varying channel current level depending on the channel illumination state. The output power drops to a null value only when the channel is completely shadowed.

5.3.3 Models integration

Via integrating the data obtained from the VR-based simulations into the lumped parameters model of the solar panel, an overall estimation of the photovoltaic plant performances has been carried out. The information exchanged by VERITAS and MATLAB®/Simulink® are related to the illumination rates of both the DEM most illuminated point and the solar panel. As described in

section 5.3.2, the data obtained from the illumination analysis have been used to calculate the temperature and the actual illumination state of the solar panel during the selected timeframe (i.e. 2035). An image of the solar panel has been extracted and converted into a binary format for each timestep (i.e. 1 h). The resolution of every image (i.e. 1653 x 3717) has been set to model every component of the solar panel, up to the cell element: despite this initial choice has been made to accurate simulate even the smallest component, the images resolution has been reduced to limit the computational cost of the simulations. A good compromise has been found by selecting the string of modules as the fundamental scaling unit. Each image has been proportionally downsized from 1653 x 3717 pixel to 30 x 8 pixel: this merging operation led represent each string (of modules) with one pixel, where the space between the elements have not being considered. The conversion procedure of the 8761 solar panel images is represent in Figure 5.38.

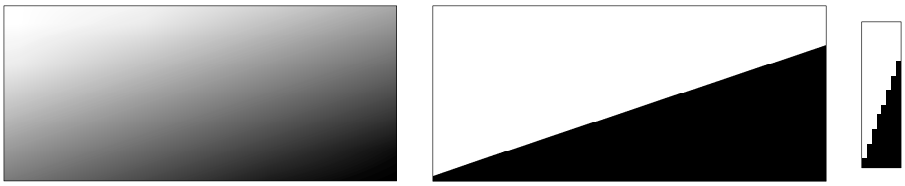

(a) (b) (c)

Figure 5.38 Original (a), binary (b), and reduced (c) images of the solar panel[22]

The original image has been directly extracted from the virtual simulation using VERITAS. The original and the reduced images have the same resolution, i.e. 1653 x 3717 pixel, while the reduced one has a resolution of 30 x 8 pixel. The conversion procedure applied is coherent with the technique adopted by Speyerer and Robinson [306]. The resulting shadows and sunlit areas are sharp since there is no lunar atmosphere, thus no light diffusion apart from the portion reflected by the terrain. The grey areas of the original images are related to rendering problem which has been solved using a conversion threshold (i.e. grey level of 0.5) for the binary transformation. The reduced images have been saved into a tensor that serve as input for the "shadows" block of the MATLAB®/Simulink® to calculate the effective illumination state of each string of modules: this process is done for every channel into which the solar panel is divided. The tensor is 30 x 8 x 8761 elements, i.e. one reduced image of 30 x 8 elements per timestep (i.e. 1h; 8761 h in total for the year 2035).

[22] All the images are referred to the same date, i.e. 3:00 GTM of January 4th, 2035.

Using the data obtained from VERITAS, a first complete simulation for testing the MATLAB®/Simulink® was run. The maximum power output has been computed for one power channel as reported in Figure 5.39.

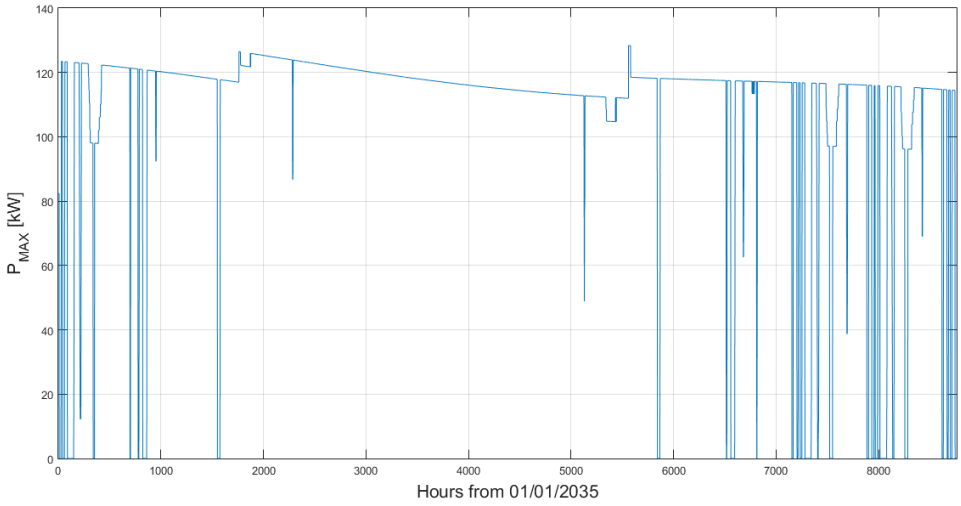

Figure 5.39 Maximum power production of one channel of the solar panel

The long-period variation of the channel maximum power is due to its life degradation, which has been set to 0.92% per year (EOL is 15 years). The short-period variations are due to the lunar topography: in fact, these variations are similar to those experienced by the maximum illumination point that is the point where the solar panel is located (see Figure 5.20 for the corresponding diagram). When the maximum power is null, the entire channel is shadowed: this happens 6.73% of the total simulated time (i.e. the year 2035) as reported in Table 5.5. However, fuel cells and batteries are active in these periods to provide the housekeeping power request by the base systems (design constrain). When the maximum power decrease but does not reach 0 kW, transient and partial shadows are present on the channel: they reduce the maximum current producible by the channel, but not the maximum tension because of the channel structure (made by parallel-connected arrays). The other variations are due to PESI and temperature variations, which is PESI-dependent.

Once tested the maximum power production of the photovoltaic plant, variable loads have been connected to the bus for simulating the response of the solar panel to different output power levels. The electrical loads have been modelled according to the channel performances (i.e. maximum power) and the bus voltage. Simple resistors have been used: 120 kW is the maximum power level modelled per channel, that implies having variable resistors from

6.7 to 162 Ω. The resistors have been connected in parallel: each of them is a constant and fixed-value resistor that is controlled by a switch. Variable resistors have not been used to reduce the computational cost of the entire lumped parameters model. A schematic representation of the externa loads blocks is reported in Figure 5.40.

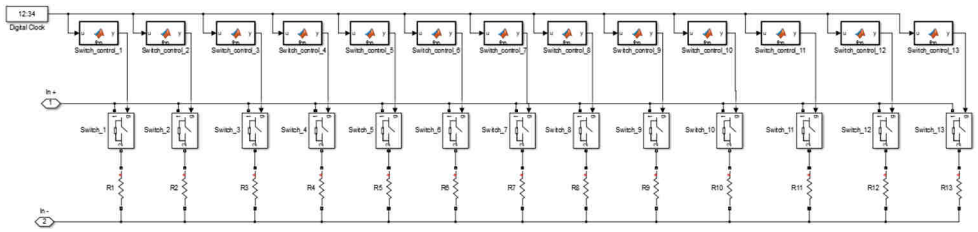

Figure 5.40 External loads model of one of the power channels

The switches are controlled by a digital clock with the frequency of the timestep adopted in the other parts of the model (i.e. 1 h). When a channel is totally shadowed, the external loads are disconnected from the channel causing a dropping to a null value for the channel voltage (otherwise is constantly fixed to 900 V). A generic load profile has been assumed as a test case for each of the eight power channels: an example is reported in Figure 5.41.

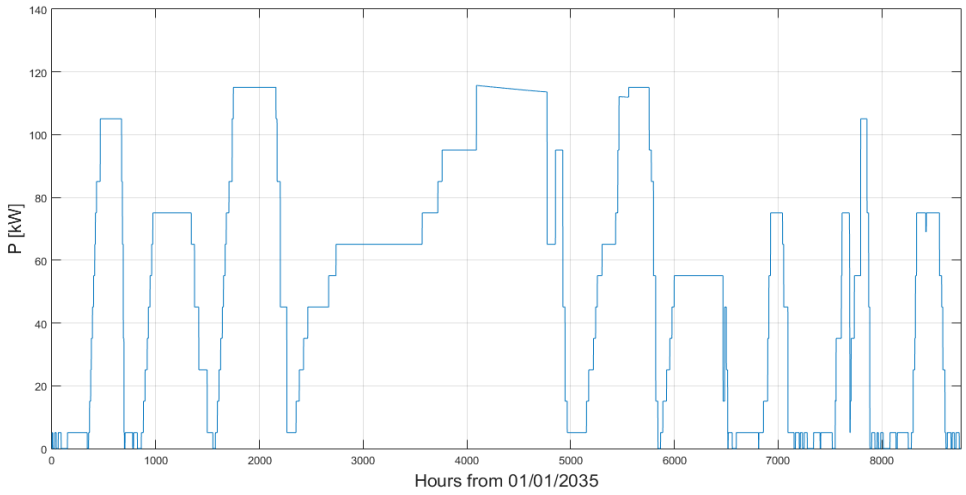

Figure 5.41 Output power of one of the eight power channels

Eight different load profiles have been generated for each of the power channel by using the ISS *Columbus* laboratory power request as reference [261], where the same power lever cannot be simultaneous request by every channel. The complete power output has been computed for the entire solar panel as reported in Figure 5.42.

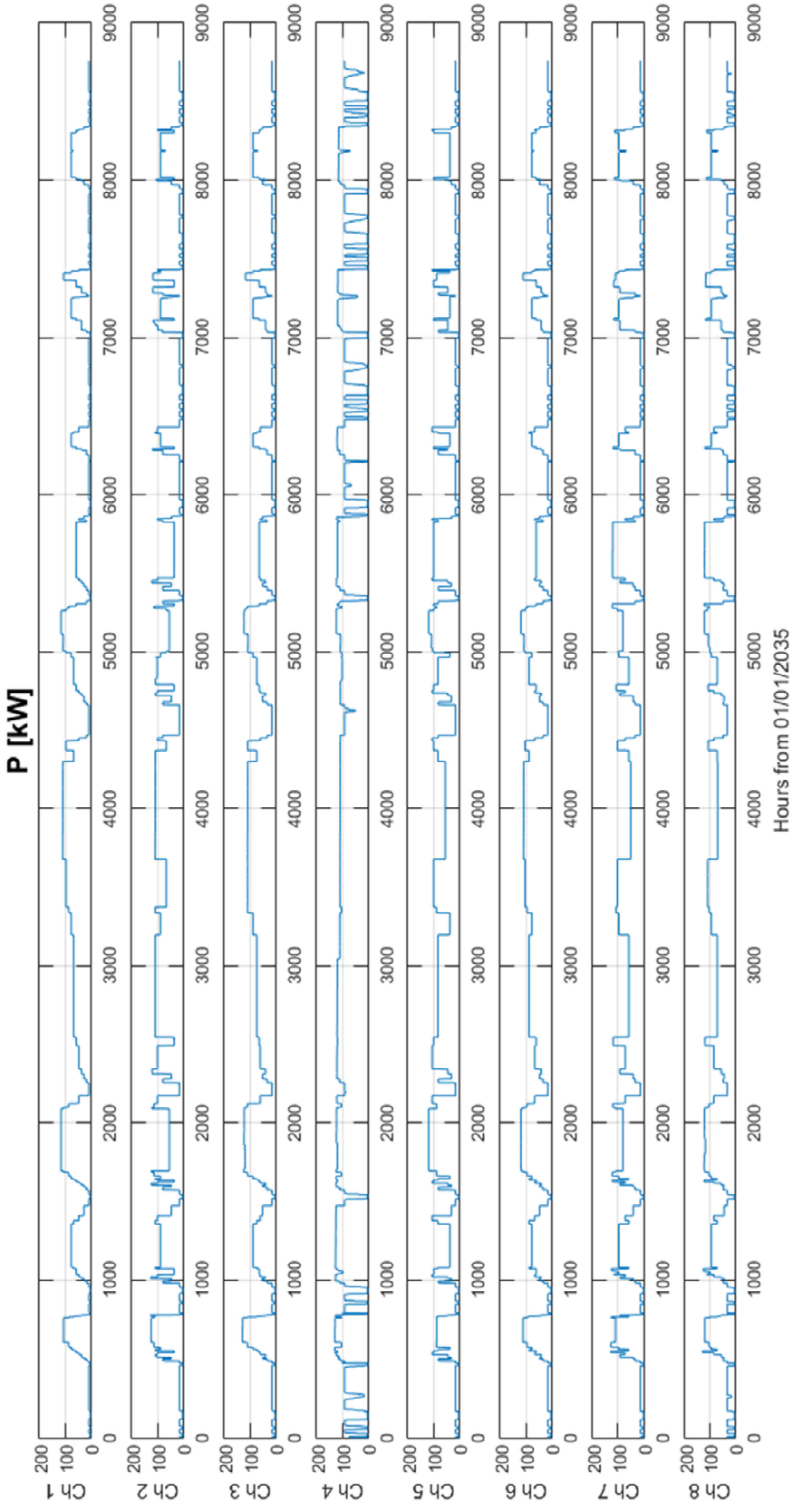

Figure 5.42 Power output of the eight power channels

5.4 SAPS modelling

Since the solar panel is just one of the SAPS components, also the other subsystems have to be modelled for totally simulating the power system of the permanent lunar outpost. A first tentative in this sense has been made in collaboration with EAC: in fact, the ESA centre is directly involved into research activities that address the upcoming challenges for the future human exploration campaigns. The "Spaceship EAC" project is the framework within the different activities are developed [268, 269]. Since the "Moon Village" concept has been indeed introduced by the ESA DG, the research areas covered by EAC are targeting the investigation of some of the technologies needed to fill the knowledge gap for enabling the human life support onto a planetary surface. One of the most important field of study is the energy provision. Using the analogue facility currently under development in Cologne (EAC site), a terrestrial carbon-free SAPS will power the LUNA dome and FlexHab [249]. This system incorporates fuel cells, hydrogen electrolysers, batteries, and solar panels to partially represents a potential lunar energy-supply scenario, but predominantly using non-space-qualified solutions [249]: it could be a great advantage for spinning the wheels of innovation for terrestrial applications, but also great steps forward for the next generation of lunar space exploration missions can be achieved (e.g. more-COTS system architecture can help to reduce the mission costs).

To perform trade-off analysis and to evaluate the performances of this SAPS, a lumped parameters model has been developed. Even if the SAPS shall be tailored for a terrestrial use, the ultimate scope is to provide useful insights for the future Moon exploration activities. Therefore, the SAPS model has been developed considering a lunar base as the use-case scenario for the simulations. To limit numerical problems which may rise from coupling all the different sub-systems of the SAPS, a reduced Moon outpost has been developed. All the necessary input data for the lumped parameters model have been calculated using the mission budgets of an equatorial unmanned surface settlement. The cyclic illumination conditions between nigh time and diurnal light periods, each ~14.75 days long[23], have net and stable variations as on Earth (with different time spans): the transitory phases result to be smoother, thus allowing easier control and switching of the power system elements.

[23] The lunar day lasts ~29.5 days, i.e. about one terrestrial month. At the Moon equator, nights and days have the same duration of ~14.5 days.

The outpost should be intended as a precursor unmanned base to assess ISRU techniques and the potential exploitation of lunar volatiles. Propellant and consumables production are the main activities considered. The nominal power required by the ISRU plant is 2000 W, while is reduced to 500 W for night operations, when only the fuel cells are active [327]. A growth chamber system has been also accounted for food and oxygen production [55]. Sensors, artificial lighting systems, and water pumps are the necessary equipment to be considered. 11 chambers, where 20 plants per chamber have been considered, require 5500 W (500 W per chamber) for 16 h (light cycle time). After each cycle, the lamps are switched off, thus the total power request drops to 2750 W (250 per chamber) [55]. Additionally, a small unmanned rover has been considered: its required power is 1000 W for internal batteries recharging; the charge process is 3 h long, while 16 h of continuous operations have been assumed. Finally, the peak power required by this lunar base has been calculated as the sum of the peak power to supply to each outpost element and it is equal to 7800 W (both for night and day time). This value has been used to calculate the volume of consumables required by the fuel cells, to be then opportunely size the tanks. Since fuel cells only work during the night (~14.75 days/375 h long), 28.3 m^3 of oxygen and 21.6 m^3 of hydrogen are needed to feed them. 6 m^3 of water are produced: for electrolyzing all the water, 85 kW is the power required by the electrolyser. Batteries shall be used only for 7% of the night, which led to calculate a total required energy of 252 kWh and total (recharge) power of 25 kW by using the procedure of [74]. The same design method adopted in section 4.3.1 has been used to estimate the photovoltaic plant power to supply the base (i.e. ISRU plant, growth chamber, and rover), the electrolyser, and the batteries (recharge cycle). 297 kW is total power that has to be produced by the solar panel.

The overall structure of the SAPS lumped parameters model, including the load profile of the outpost required power, has been implemented in the MATLAB®/Simulink® developing environment by following the guidelines provided by ESA experts, as part of the collaboration with the “Spaceship EAC” initiative [249]. The final arrangement of each block is reported in Figure 5.43.

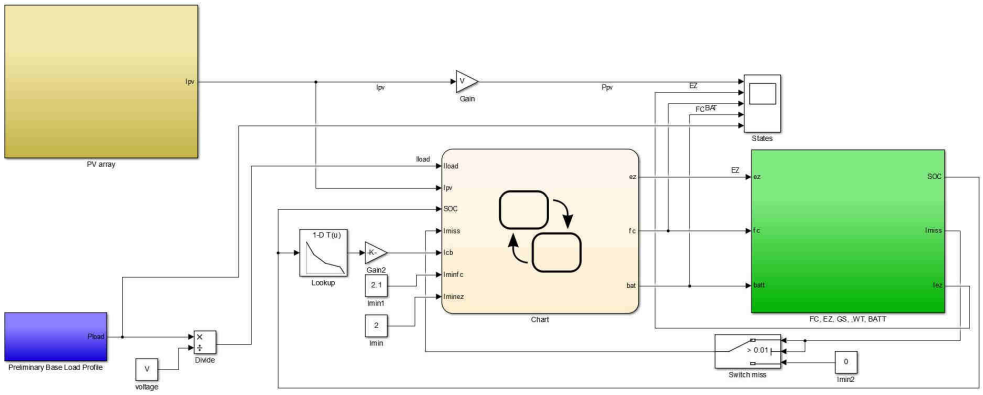

Figure 5.43 SAPS internal block structure

Apart from the solar panel, the batteries, the fuel cell, the tanks, and the electrolyser models, a control logic block has been modelled to regulate and switch from one component to another accordingly to the simulated time phase (night or day). All the main components of the SAPS have been modelled with separate blocks. The equations used in the different blocks have been selected to describe in detail the main components of each element: the level of precision adopted took into consideration the typical time constant of each physical process. In fact, the overall SAPS model has been developed to be used for preliminary trad-off analysis, thus a fast run time is required for simulations (i.e. tens of minutes). Too precise models that eventually results into computational heavy calculations have been excluded.

Not only the electrical connections but also the fluidic interfaces have been modelled: H_2, O_2, and H_2O flow rates are their tanks are present to simulate the empty/refill process, also based on the different lunar diurnal phases. The control logic has been developed to monitor and manage those values, which are related to the different SAPS elements, via regulating the transitions by using flow diagrams.

A LEM block has been incorporated into the "photovoltaic array" block for estimating the values related to the Moon environment that influence the solar panel performances. Similarly to what has been done in section 5.3.2, the photovoltaic plant temperature and PESI has been computed. Despite using data calculated using VR-based analyses, the illumination conditions have been estimated using the analytical model developed by Li *et al.* [328]: the results obtained only depend on the time set and the local lunar coordinates. Instead of using a complex solar panel model, as the one described in section 5.3.2, the Simulink® embedded "solar array" block has been used, where the required input data has been set using the information derived from the

mission budgets. This choice has been made for reducing the overall computational cost.

A more detailed description of the other SAPS components is reported in sections 5.4.1 (fuel cells) 5.4.2 (batteries), 5.4.3 (electrolyser). The results obtained for a six lunar days complete simulation are reported in section 5.4.5. A complete description of the control logic is presented in section 5.4.4.

5.4.1 Fuel cells model

The fuel cells model has been derived from [329]: this very complete and comprehensive model of a PEM fuel cell incorporates specific chemical details and precise data derived from Computational Fluid Dynamics (CFD) simulations [330]. Its level of detail, required to have accurate and precise estimation of the fuel cell performances, exceeds and goes beyond the scope of the research here presented. The model has been reduced in terms of resolution and values to compute for saving computational time. The result is a faster but still reliable model that is able to coexist with the other SAPS elements blocks of the lumped parameter model described in this dissertation.

The total peak power required to be supplied by the fuel cells during the nigh period is 7800 W. Instead of using a single fuel cell which is able to satisfy the power request, it has been decided to use 8 PEM fuel cell stacks, each able to produce 1.2 kW (maximum unregulated power). The modular arrangement has been chosen to ensure a fault-tolerant architecture (if one of the stacks fails, the power requested can be supplied by the other active stacks) and to validate this model. In fact, a fuel cell test rig is currently under development at EAC: it shall be used for hardware-in-the-loop testing and for validation purposes. Specifically, the fuel cell stack chosen is the BZ100-13 produced by ZSW® and all the data used have been derived by its datasheet [331]. Moreover, using the polarization curve of the datasheet, the fuel cell lumped parameters model has been statically validated.

The result obtained by the model reduction, i.e. the one used in this thesis, is represented in Figure 5.44.

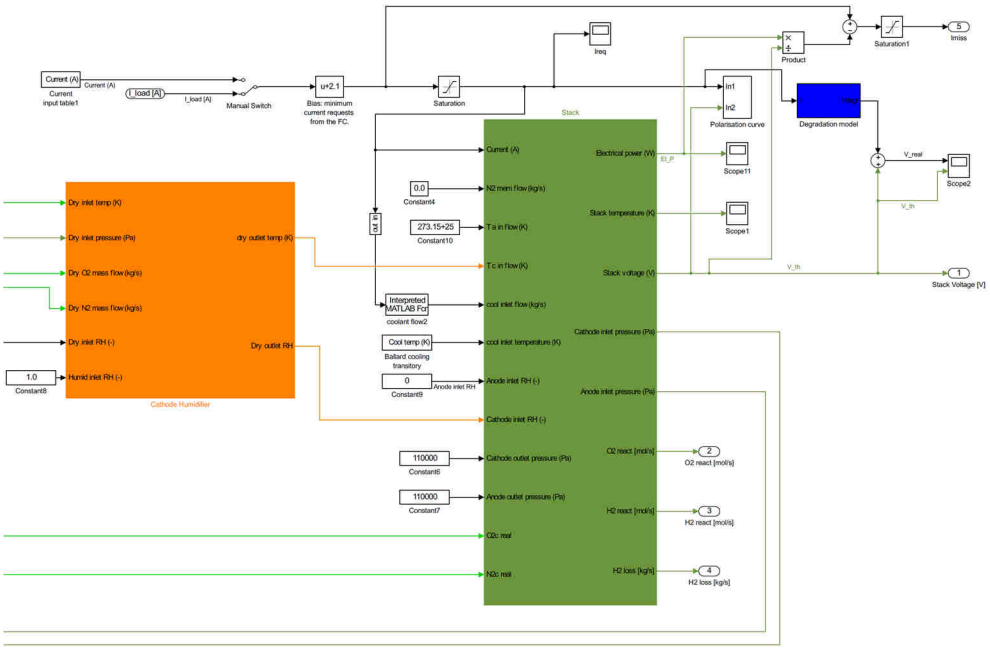

Figure 5.44 Fuel cell model

The model is composed by the “cathode humidifier” block (orange), the “stack” block (green), and the “degradation” block (blue).

The “cathode humidifier” block computes the reactants relative humidity level for the passive humidification process of the fuel cell (internal) membranes.

The “stack” block computes the pressure, temperature, and mass flow values of oxygen and hydrogen for both anode and cathode. The overall fuel cell stack voltage is also computed: the ideal voltage, influenced by the working temperature and the kinetics of the electrochemical reaction, is reduced by the intrinsic losses (activation, ohmic, double layer effects, concentration voltage, and crossover current)[24] of the fuel cell itself [329].

The “degradation” block computes the voltage drop related to the plate failures and the relative degradation rate: when the fuel cell is active, 0.03 V/100 h is the average loss assumed, while 0 V/h has been assumed when the fuel cell is not active [332].

[24] Activation losses are due to slow reactions that take place on the electrode surface. Ohmic losses are due to ions and electrons flow resistance when respectively passing through the electrolyte and the cell hardware. Double layer effects account the voltage slow reaction in reaching a new steady-state value when the current changes. Concentration voltage losses are due to the reactants finite diffusivity at the catalyst surface. Crossover current losses are due to electrolyte secondary currents.

5.4.2 Batteries model

Instead of using Lithium batteries, Nickel-Hydrogen batteries have been selected in accordance with the "Spaceship EAC" guidelines for reducing the cost: in fact, the project aim is to supply energy to terrestrial analogue facilities with a SAPS, where a more-COTS architecture is desirable for testing cheaper components also considering the future lunar missions. A schematic view of the Ni-H_2 batteries model is represented in Figure 5.45.

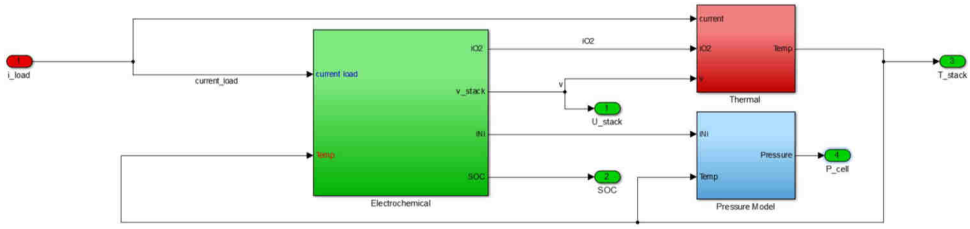

Figure 5.45 Batteries model

The model is composed by the "electrochemical" block (green), the "thermal" block (red), and the "pressure model" block (light blue), and is able to computes the output voltage, the batteries stack temperature, and its state of charge. The only input required is the load current: negative values are assigned for the discharge phases, while positive for the charging ones.

The "electrochemical" block computes the batteries stack voltage and its state of charge using the stack temperature and the load current. The chemical reactions of reduction and oxidation are simulated.

The "thermal" block computes the stack temperature variations using the stack the voltage and the load current.

The "pressure model" block computes the hydrogen pressure in the stack which is another parameter that indicates the stack state of charge.

5.4.3 Electrolyser model

The electrolyser has been designed to electrolyze the water produced by the fuel cell during the night periods. It will be powered by the photovoltaic plant during daytime. A schematic view of the electrolyser model is represented in Figure 5.46.

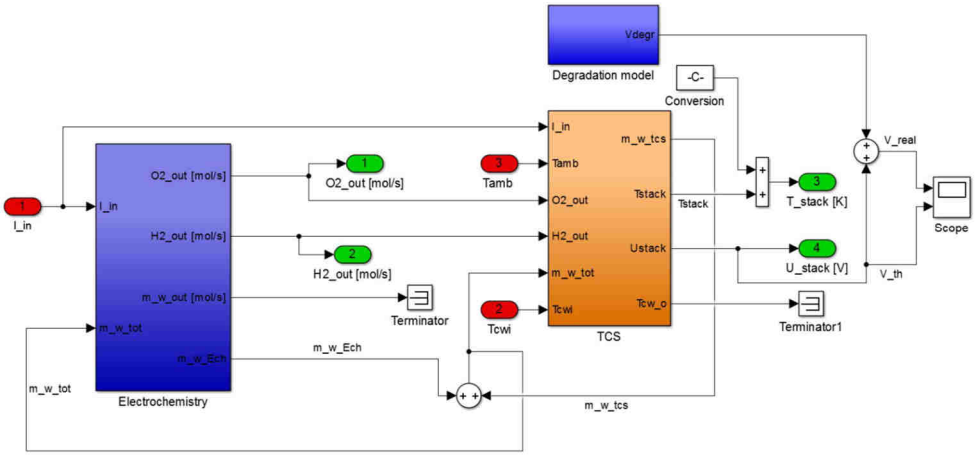

Figure 5.46 Electrolyser model

The model is composed by the "electrochemistry" block (dark blue on the left), the "thermal" block (orange), and the "degradation" block (blue on the upper right).

The "electrochemistry" block computes the total oxygen and hydrogen rates produced by the electrolyser using the water stored in the tank and the output current of the solar panel. The Faraday's efficiency has been also considered to compute the losses in the electrochemical transformation process.

The "thermal" block computes the water molar flow required for regulating the electrolyser temperature, the output temperature of the cooling fluid (i.e. water), and the electrolyser voltage and working temperature, using the oxygen and hydrogen flows calculated by the "electrochemistry" block.

The "degradation" block computes the voltage drop related the elapsed time (of the simulation). It is similar to the fuel cell "degradation" block.

5.4.4 Control logic

To regulate a complex and multi-component system as the SAPS, a dedicated control logic has been created. Each SAPS element is managed depending on the simulated phase (night or diurnal cycle): the power produced shall always satisfy the power required by the outpost (i.e. ISRU plant, growth chamber, and rover). Basically, the primary power source used to supply the base load during the light hours is the photovoltaic plant. If the current (and so power) produced by the solar panel is greater than the required one, its surplus is used to feed the electrolyze. If also the current request for water electrolysis is saturated, the photovoltaic plant recharges the batteries. Vice versa, the fuel cells are active during the shadowed periods to supply the

power request of the base: if the current (and so power) produced is not enough or abrupt power peaks are request to the SAPS, batteries are used to support the fuel cell stack power production.

For preventing too fast transients and activation procedures, which may result in severe damages for the fuel cells (also for the high losses and the consequent efficiency drop), the fuel cells are active also during daytime: the stationary low-level power production will ensure stable and continuous operations that help to preserve the stacks integrity for longer periods (with respect to an on/off switching method).

The changes of illumination levels due to the Sun setting or rising results into delicate transition phases to handle. Apart from managing the switch between the photovoltaic plant and the fuel cells, the control logic has been also designed to turn on the batteries in case both the solar panel and the fuel cell stacks (joint use) cannot supply the power request at a certain timeframe.

The entire control logic has been modelled using the MATLAB®/Simulink®-embedded Stateflow® environment, where state machine diagrams and flow charts can be developed. The equations used for the fuel cells are schematized in Figure 5.47.

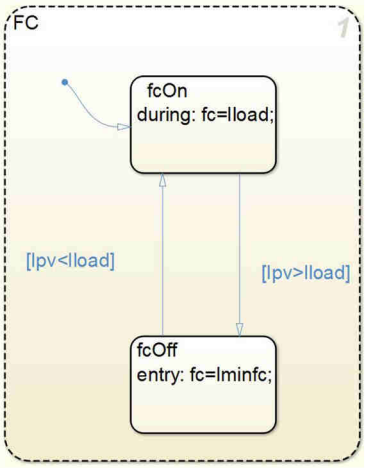

Figure 5.47 Fuel cells control logic scheme

When the fuel cells are active during the night periods, the current required by the outpost is equal to the current produced by the stacks, while it is set to a minimum constant value when the fuel cells are not active (i.e. daytime). To avoid excessive complications for fine-tuning the control logic, when the current produced by the solar panel is not sufficient to supply the outpost request, the fuel cells provide the entire base power, thus neglecting the residual power produced by the photovoltaic plant.

The equations used for the electrolyser are schematized in Figure 5.48.

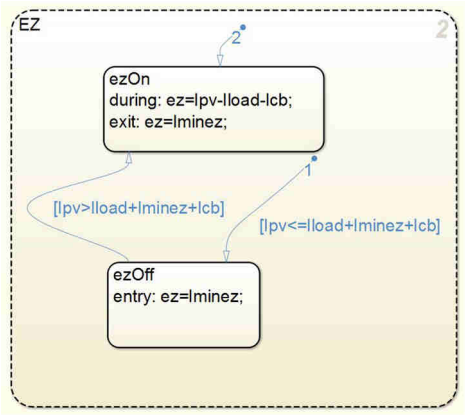

Figure 5.48 Electrolyser control logic scheme

The electrolyser is active only when the solar panel is producing more current that the one requested by the lunar base, otherwise is turned off. The maximum current level required for water electrolysis has a threshold limit to ensure the batteries recharge when needed.

The equations used for the electrolyser are schematized in Figure 5.49.

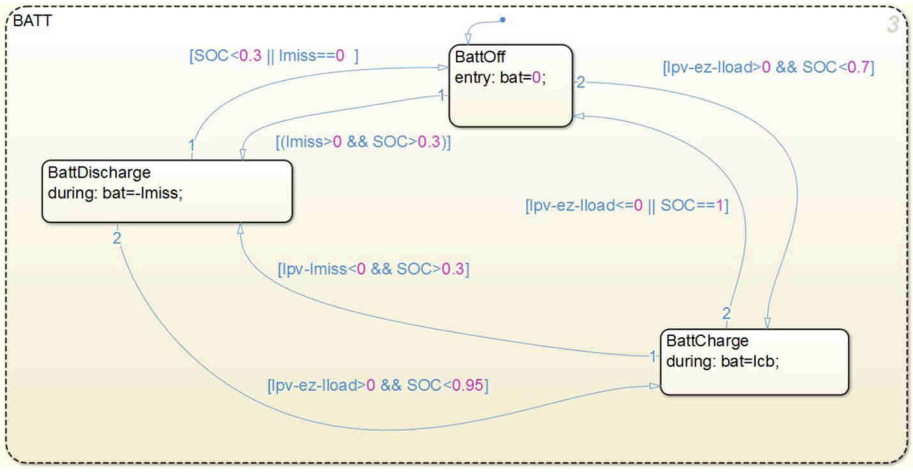

Figure 5.49 Batteries control logic scheme

Since the batteries can both require and produce power, depending on the outpost load and the working status of the other SAPS elements, their behaviour in the transient phases should not be overlooked. It has been assumed that the batteries shall work only during the night time or transients, while they are recharged by the solar panel during daytime. The state of charge is the variable monitored to command the mode change: if it is greater that a set

value and the fuel cells cannot supply the power request, the battery stacks start to provide the missing power (discharge state); this condition is true until the charge status is high enough (to prevent fully discharges), otherwise the batteries are turned off (this condition is true also when the base load drops under a certain threshold or to a null value). The recharge procedure is enabled only if the state of charge is lower that a fixed value (also considering self-discharge phenomena) and when the photovoltaic plant is able to supply the power for both the lunar settlement and the electrolyser. In all the other cases, the batteries are not active.

5.4.5 Model testing

The overall SAPS model has been tested using the input data estimated in section 5.4 (i.e. power levels of the Moon base). A complete simulation has been run for six lunar days to analyse the cyclic variations of the Moon environment and its effect of the regulation of each SAPS component.

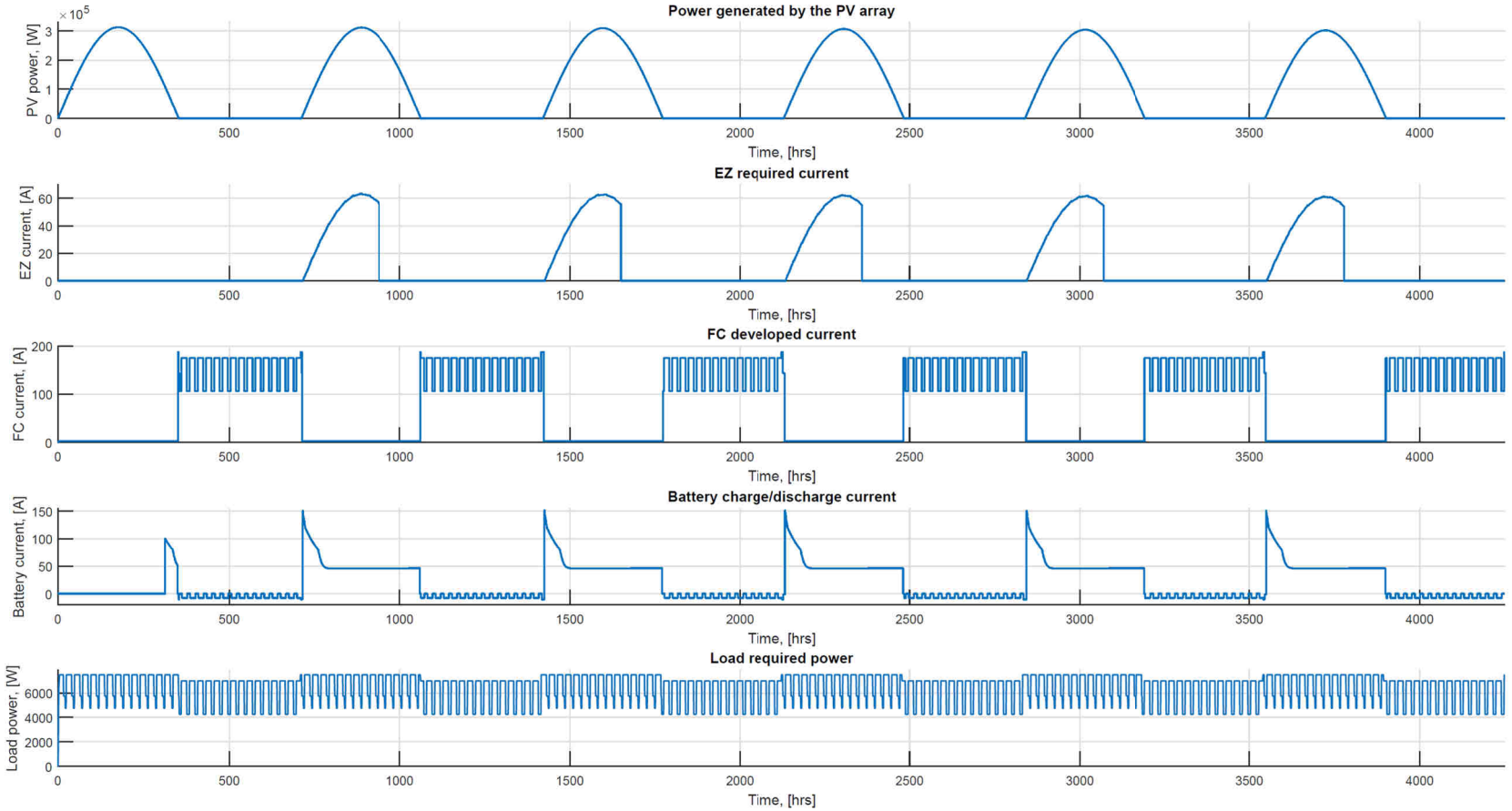

Figure 5.50 SAPS model testing during six lunar days

The SAPS elements functional time history is reported in Figure 5.50: specifically, the photovoltaic plant produced power (first row from top), the electrolyser absorbed current (second row from top), the fuel cells produced current (third row from top), the batteries current (forth row from top), and the lunar base requested power (fifth row from top) have been represented.

The time evolution of the photovoltaic plant produced power follows the PESI variation, due to the solar elevation angle variation), typical of equatorial areas, with peaks at the middle of the diurnal periods.

Apart from the first cycle (during the first lunar day) where the oxygen and hydrogen tanks are already fully filled, the electrolyser starts to produce the fuel cells consumables during daytime, when the solar panel is able to supply its power request. When the electrolyzed water has completely refilled the oxygen and hydrogen tanks, the electrolyser is turned off.

The fuel cells power profile mimics the lunar base one: the stacks are actively used to produce the power required by the lunar outpost only during the night periods, otherwise they are switched to an idle mode (i.e. set a minimum power production level to avoid start-up and turn-off procedures at each cycle).

Apart from the first lunar day cycle where the state of charge is too low (due to self-discharge), the batteries are charged (positive current values) by the solar panel during daytime and they are jointly used with the fuel cell during the night periods (discharge cycle, i.e. negative current values).

As reported in section 5.4, the base power experiences short-period variations due to the rover cyclic operations and the growth chamber light cycle, while the difference between day and night time is due to the power level reduction of the ISRU plant during the night periods.

This “reduced” SAPS model has positively demonstrated the possibility to couple all the different SAPS components one another in a MATLAB®/Simulink® environment, also allowing to test a control logic scheme for managing the entire power system. This robust model can be used to explore different SAPS architecture for lunar applications, which is one of the goal of the “Spaceship EAC” initiative. In addition, this model can be modified and adapted to estimate the performances of the terrestrial SAPS that will power the analogue facilities to be built by ESA-EAC, where an experimental validation campaign is envisioned for each SAPS component. Moreover, since the SAPS model has been developed using MATLAB®/Simulink®, the integration with the VR-based models presented in sections 5.3.2 and 5.3.3 will result easier. In fact, as described in section 6.2, the final

purpose of the entire research is to create a fully functional virtual model of the permanent human outpost used as case study in this thesis.

5.5 Outpost modelling

The entire virtual modelling activity aims at creating an accurate digital twin of the permanent human base located at the Moon south pole. By choosing the most illuminated point and its surrounding area as the preferred location where to locate the base modules and the SAPS elements, it is important to consider the local terrain topography with respect to the requirements imposed by each element (e.g. casted shadows, direct Sun visibility, thermal gradients, etc.). Since the surface settlement shall be located in the Shackleton crater rims area, the final outpost configuration may be similar to the one proposed by the NASA shelved Constellation program [333], whose schematic view is represented in Figure 5.51.

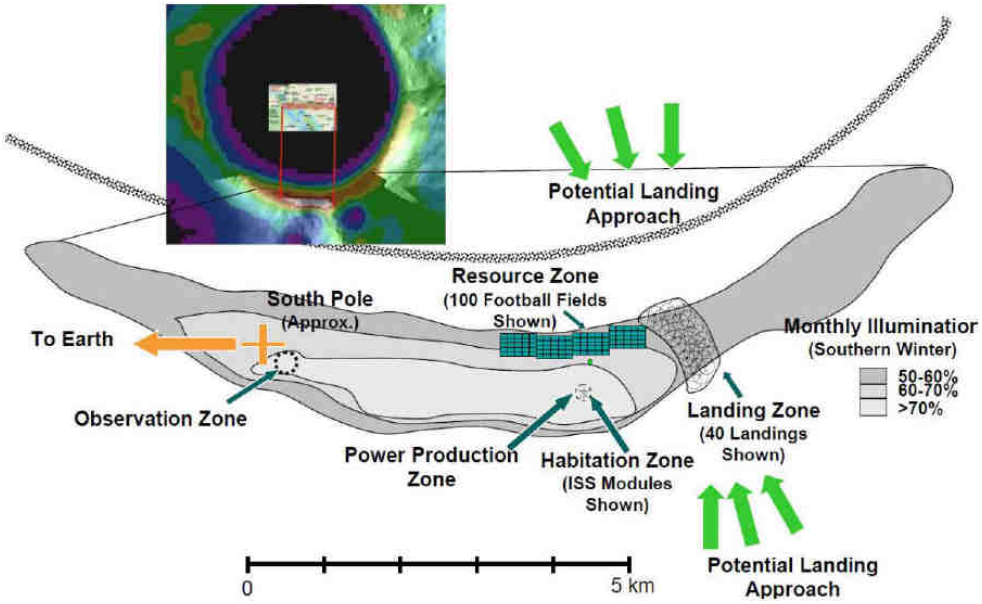

Figure 5.51 Shackleton crater rim with notional activity zones of a potential human surface outpost [333] (credit: NASA)

Despite the paramount importance of the task, the final positioning has not been made yet since refined analyses are still necessary for the mission architecture and the incremental exploration strategy adopted. However, a first-person immersive virtual scene has been created using VERITAS, which simulates the viewpoint of a crewmember at the lunar south pole. Using the LRO-LOLA DEM as the terrain replica and adopting motion-capture sensors

to enable head-tracking, a first EVA virtual replica has been generated. The navigation into an active-responding VE allows the user to have a direct feedback of the future lunar working environment: the immersivity is guaranteed using head-tracking functions that make the scene to move in response to the subject's own motion; ideally, his/her view of the virtual scene changes in the same way it would if the user was standing in a real location and moving his/her head. This solution was tested by using the TAS-I CAVE, as represented in Figure 5.52.

Figure 5.52 User in the TAS-I CAVE while interacting with a Moon south pole landscape (credit: TAS-I)

Rotational and translational movements have been modelled and enabled by VERITAS. Even if rotational attributes are very useful for create a more vivid immersion into the simulated world, i.e. the scene freely changes its orientation to match position and orientation of the user as there is no fixed virtual floor/ceiling, a too high-precision response could eventually induce motion sickness. The extremely disorientation is the result of a non-realistic behavior of the virtual scene since the terrain tends to completely rotate according to the head movements of the subject. The lack of a virtual floor is another source of annoyance: when the user is surveying the virtual surroundings into which he/she is immersed (in this case the lunar south pole), he/she cannot look down at the ground near his/her feet.

Additionally, a first tentative implementation of a fictitious lunar base into a VE has been carried out to complete a first fully functional virtual prototype of a permanent human lunar base. Due to graphical limitations (too different resolutions between the terrain and the other 3D models), it was not possible to adopt the same LRO-LOLA DEM already used for the other analyses (illumination and first-person immersion). The Linné crater surroundings have been instead rendered and different 3D models have been putted in the same virtual scene to test the integration of heterogeneous elements into

the same common VE. The simulated lunar base scene has been created incorporating two crewmembers with EVA suits, the TAS-I pressurized lunar rover, the NASA Habitat Demonstration Unit (HDU), and the NASA Apollo lander, where both the NASA models have been retrieved from [334]. Moreover, the ESA stars catalogue derived from the Hipparcos mission has been used to create realistic background appearances, where specific Moon-frame ephemeris data have been used to correctly orient the virtual scene sky. The virtual scene created is represented in Figure 5.53 as it is visualized using the VERITAS desktop application (suitable for local customization or for large audience).

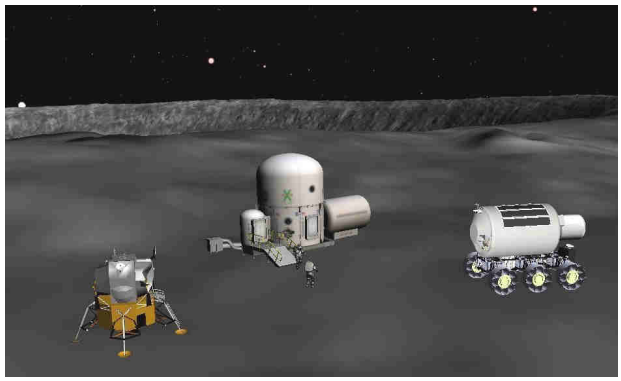

Figure 5.53 Virtual lunar base visualization test using the VERITAS desktop application

The same virtual scene can be visualized with a different setup for a more immersive simulation, i.e. using 3D (passive) glasses with stereoscopic screen, as it is reported in Figure 5.54.

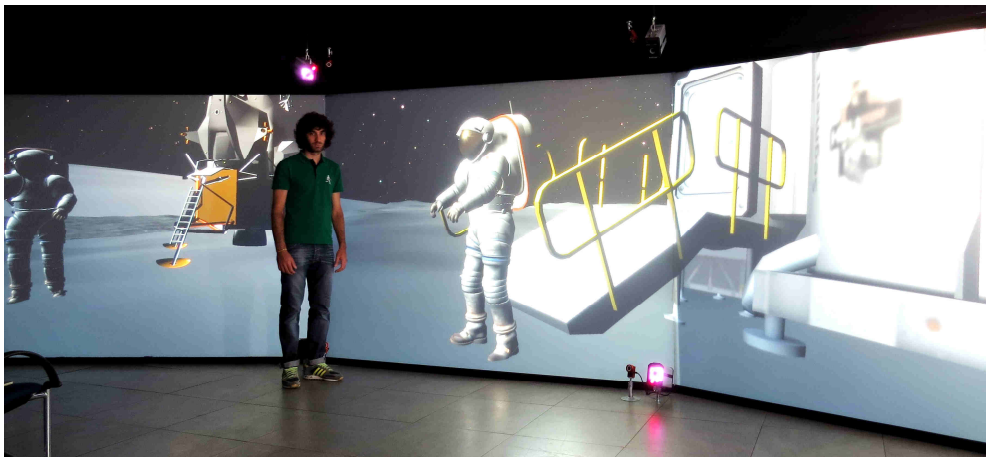

Figure 5.54 Virtual lunar base visualization test using the TAS-I CAVE

In order to test the flexibility of the VR software, a similar virtual scene has been created. Instead of using a lunar setting, it has been selected a Martian one: in fact, the ultimate exploration goal set as the next target for human mission is Mars. Considering an incremental approach where the cis-lunar environment is the ideal environment where to test new technologies, mission architectures, and platforms for the upcoming Red Planet sorties, it is natural to consider also this scenario for virtual simulations. A first tentative implementation of a fictitious virtual-based Martian outpost has been implemented using VERITAS. The base has been rendered near the Victoria crater via integrating a crewmembers with EVA suit, the NASA Curiosity rover, and the NASA HDU, where both the NASA models have been retrieved from [334]. The same Hipparcos stars catalogue have been used and oriented using ephemeris data. The desktop visualization of the Martian outpost is reported in Figure 5.55.

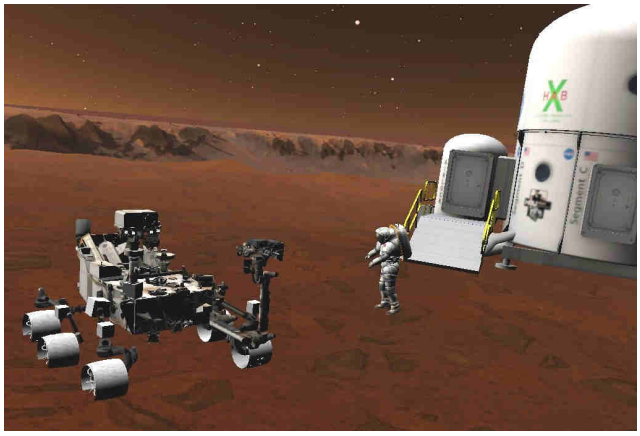

Figure 5.55 Virtual Martian base visualization test using the VERITAS desktop application

Using the same 3D-immersive setup, the virtual scene has been visualized into the TAS-I CAVE as represented in Figure 5.56.

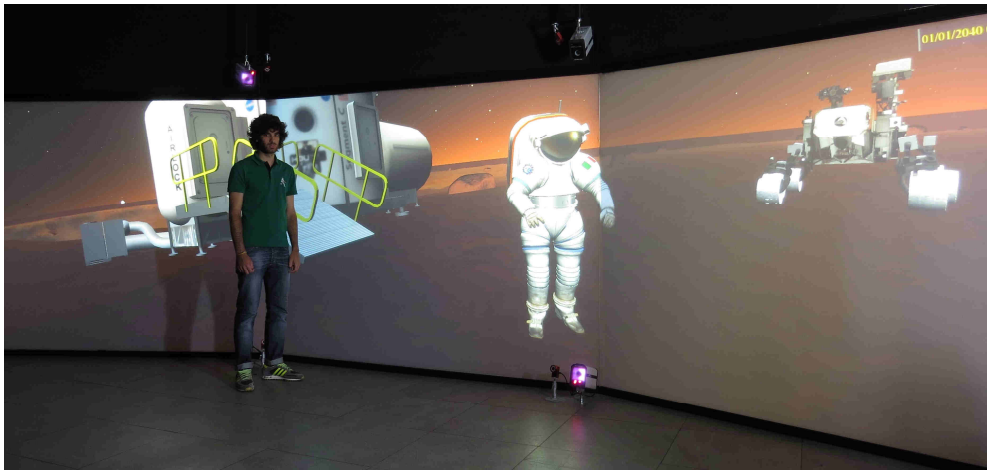

Figure 5.56 Virtual Martian base visualization test using the TAS-I CAVE

5.6 Concurrent Design Facility integration

In order to fully test the methodology proposed in this research work, the coupling of VR tools within a CD environment has been analysed. The main scope is to assist the decision-making process and to support real-time feedback from the experts involved in the systems design. The four principal phases that characterized the systems design decision process are [335]:

- Problem definition: the most important task in any systems decision process is to identify and understand the problem which is informed by understanding the concerns, objectives, and constraints of the decision makers and stakeholders;
- Solution design: having developed a clear understanding of the problem during the problem definition phase of the decision process, it is possible to proceed with the finding a system solution to the problem;
- Decision-making: thanks to the information gathered previously is now possible to make a decision. clients must give their approval of a system solution;
- Solution implementation: once a decision is accepted by the client, is possible to implement the system solution.

Thanks to human senses, the interaction with 3D (or even 4D) environments is a natural and innate feature: VEs take full advantage of this fact. Those kinds of visualizations permit a more direct communication of different ideas and information, thus permitting an easier negotiation between the different experts in the design process.

As reported in sections 2.1 and 2.2, VR systems can tangibly help the product design optimization, especially in the early iterations of CE sessions. Several solutions can be discussed by the expert present in a certain design session, always accounting for all the different aspects involved in the product life-cycle: in fact, the mission/system to be designed must effective fulfil each stakeholder and decision-makers' needs since they are the core of the entire design process. Each discipline and its relative compliance with the imposed requirements, which can be verified almost in real-time, are transformed from the classical "static" vision into more dynamic features: novel designs can be discussed by all the expert of the different disciplines, also considering aspects which may be overlooked like ergonomic analysis and user operations. The productivity and the communication effectiveness between the different actors involved in the design can benefit from the creation of a virtual model: by using this model-based approach, systems, spacecraft, or SoS can be designed in a smarter and optimized way. Users and designers can interact with the virtual model in an intuitive way, where the hardware and software architecture may vary but using the same methodology. The main advantages of the using the VR-based approach proposed combined with CE are:

- High traceability and almost real-time verification of the requirements;
- Ergonomic studies enhanced;
- Operational tasks and procedures verification;
- Great synergy and data exchange among all disciplines;
- Optimization oriented;
- Useful for training purposes (e.g. astronauts pre-assignment training, flight controllers training, etc.);
- Risk assessment and reduction;
- Cost and time saving;
- Possibility of real-time failures troubleshooting.

The introduction of the "digital mock-up/virtual prototype" gives the opportunity to access all the relevant data through VR and standard tools to

perform design review meetings and trade-off studies. Collective decision-making can be enhanced, especially if knowledge-based systems are considered for assisting the design and negotiation phases [156]. As described in section 3.1, the early decisions taken at the beginning of the project impact the most on the final result in terms of cost and time (development, production, and usage). The virtual prototypes can help to better address the design tasks: instead of using physical mock-ups, costly and almost never up-to-date hardware, tests can be performed using a digital replica, where the iterations for optimizing the final result are easier to implement. Moreover, the versatility achievable with distributed VR architecture, also considering telepresence operations, could lead to be independent by physical facilities, taking advantage of a cloud computing VE.

The proposed approach cannot only be adopted in the conceptual design phases, but its usage can be extended for production, operations, maintenance, service, and disposal (e.g. disassembling and recycling) phases to enforce collaboration, results sharing, and direct communications. If the virtual model becomes an effective "digital twin" of the final product to develop and mimics it alongside its real evolution, starting from the conceptual conceiving until the disposal phase, the TRL will be faster risen which results into shorter time-to-market. Industries, space agencies, and public entities can quicker satisfy the stakeholders involved, shrinking the programs duration, which is very useful for the space sector for not shelving the usually costly and long initiative as it happened in the past. The ongoing ESPRIT project CAVALCADE offers a first positive feedback on design, test, validate, and document a shared model in a distributed architecture, where engineers are geographically dispersed, which is typical of CE routine [84]. Those type of advancements bode well for the discussed VR application in the space mission design field.

A first tentative virtual shared environment has been created in the present research work and it has been integrated into a CDF architecture to firstly assess its feasibility. Among the several alternatives of CDF architectures and management software, the preferred solution adopted in this Ph.D. work is the ESA open-source ConCORDE-OCDT [336][25]. The high-level architecture to generate virtual scenes is somehow identical regardless of the VR

[25] The Open Concurrent Design Tool (OCDT) is a client / server software package developed under an ESA contract to enable efficient multi-disciplinary concurrent engineering of space systems in the early life cycle phases. The first implemented OCDT client is an easy-to-use add-in for Microsoft Excel® 2010 to perform simple analysis and simulation. This end-user tool is called Concurrent Concepts, Options, Requirements and Design Editor (ConCORDE).

software used. In particular, the user interface is handled using the widely-known spreadsheets manager, part of the Microsoft Office® suite, Excel® (2010 release) with an addon: this choice, operated by the ESA developer, facilitates a lot the operations to be performed thanks to the flexibility and the ease of use. The system engineers can monitor how the design is evolving and can easily validate the updates made by different experts by simply using a spreadsheet. Each cell represents an information that can be accessed by the design team: not all the data are available to everyone, but only the sensitive one for common calculations. Each expert can off-line use his/her own domain-specific tool for simulations. Only the relevant results can then be uploaded in the system for data sharing. The VR-based methodology proposed is trying to enhance how CDF sessions are currently done: instead of looking to mere numbers or to single software-specific output (e.g. CAD model to discuss spacecraft configuration), the creation of a virtual model will guarantee a collective understanding of the product criticalities through user interactions with it.

The virtual scene/model is autonomously generated and automatically updated using data inputs read from Microsoft Excel®: a macro is executed (pushing a button which recall a Visual Basic® script) that run the necessary processes for generating the virtual simulation. Numbers and text attribute are transformed into code lines to generate the VR simulations: those can recall information (e.g. spacecraft trajectory) and models (e.g. 3D CAD model of a planetary rover) that are opportunely stored into a knowledge-driven database. The final virtual result obtained can be visualized with immersive devices or with desktop-based applications.

Considering the Blender® solution, Python is used to generate and populate the virtual scene. When the Excel® macro is running, Blender® is opened in background, a Python script is then run which create the virtual scene. This Python-based script is able to open and query a database of models, which are stored with different file formats (all compatible with Blender®) and are used to render the virtual scene to visualize. The Blender®-based VR setup adopted is shown in Figure 5.57.

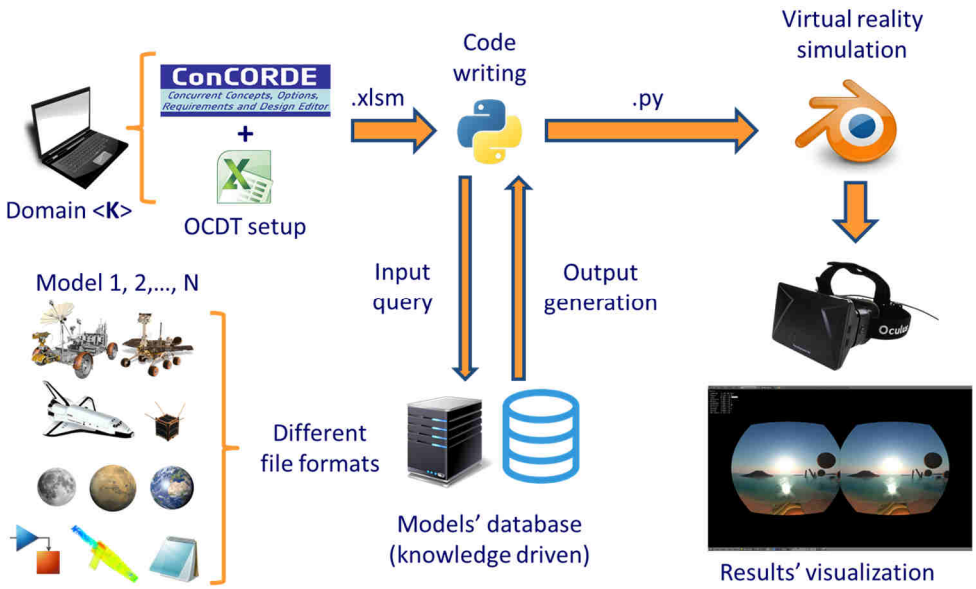

Figure 5.57 Blender® version of the autonomous virtual scene generation architecture

Considering the VERITAS solution, MATLAB® is used to generate and populate the virtual scene. When the Excel® macro is running, a MATLAB® script is opened: it contains all the instructions (code lines) to generate an XML file that is able to generate a virtual VERITAS scene. The XML instructions call a set of parameters to set up the VR simulation and all the necessary data and models, which are stored into knowledge-driven database (the same used also for Blender®). The Blender®-based VR setup adopted is shown in Figure 5.58.

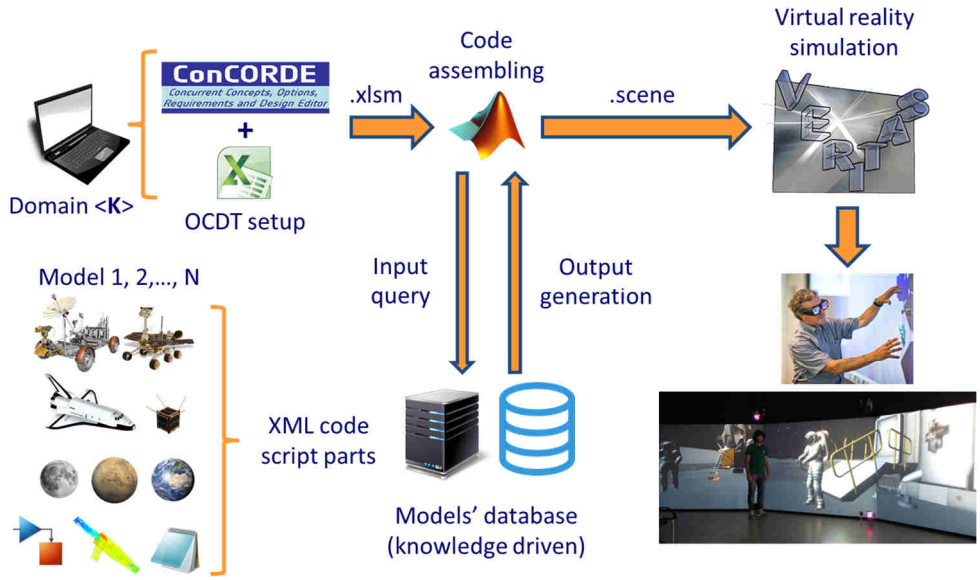

Figure 5.58 VERITAS version of the autonomous virtual scene generation architecture

A first comparison among the two solutions has been done using the NASA LRO mission as reference. A virtual scene has been rendered to simulate part of the mission. The LRO spacecraft model, retrieved from [334], has been incorporated in the VE. The celestial bodies (i.e. Earth and Moon) have been imported from the common database, whose relative positions and orientations are computed using ephemeris. A geocentric reference frame has been adopted, so also the LRO spacecraft orbit and attitude, calculated using AGI STK®, are referred to it. The final output is an interactive virtual scene: end-users can navigate into that, also visualizing (if enabled on request) relevant information like global time (e.g. GMT), trajectories, mission phase, etc.

The work flow to generate the virtual scene with both software solutions, using the CDF setup described, can be generically summarized as:

1. Set simulation time and time step of the scene;
2. Import CAD and material data of the spacecraft (LRO for this case study);
3. Import the celestial bodies model in the virtual scenario;
4. Import ephemeris data of celestial bodies;
5. Import orbital data from mission data;
6. Import attitude and position data of the spacecraft;
7. Set the position of the camera;
8. Set the light options for the virtual scene;
9. Render the virtual scene and eventually save movies, images, or other output data of interest.

No major differences exist between the two VR software, apart from graphical aspects. Blender used its BI render engine to create the VR simulation, while VERITAS used its internal one. A comparison of the LRO spacecraft flying on a lunar orbit is showed in Figure 5.59.

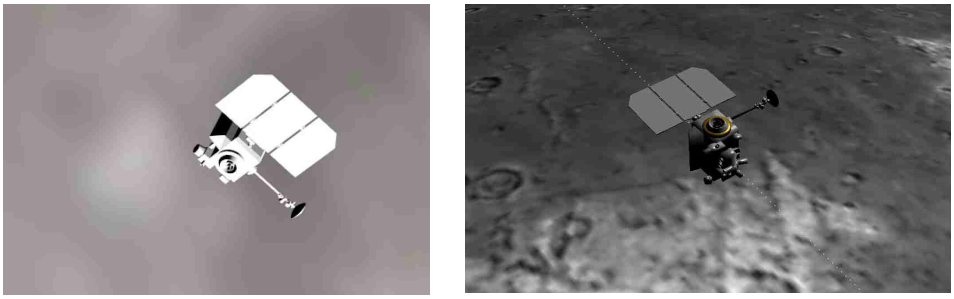

(a) (b)

Figure 5.59 Rendering of the LRO spacecraft flying on a lunar orbit using Blender® (a) and VERITAS (b)

Since VERITAS was the selected software for the simulations presented in chapter 5, its setup for the autonomous generation of virtual scenes has been used for a very first beta test. During the ESA Concurrent Engineering Challenge held between September 12th and 15th, 2017 [337], the design of a lunar remote sensing mission took advantage of the VR-CDF coupling. Specifically, for the first design iteration phases, the selection of the payload subsystems and their relative operative models (optics and sensors) was aided by the creation of a virtual scene. In fact, a simulation of the different illumination conditions of the lunar south pole spanning the entire mission timeframe

was rendered using VERITAS, where the mission data were derived by the OCDT database. Since the main mission requirements were the observation of the water/ice content and the radiation environment of the lunar south pole, and the creation of a database of high resolution images, visible cameras, neutron detector and radiation sensors were selected. The choice of visible-light instruments was possible only for the highly annual illumination rates of some areas of the lunar south pole, as simulated in the virtual scene. Moreover, the operative mode of the visible cameras was set accordingly to the seasonal light variations: during summer, longer sunlit periods are experienced by polar areas, thus the cameras were set on; during winter/autumn, the light/shadow alternance happens more frequently, thus the cameras were set off.

5.7 Results discussion

The virtual-based simulations and their results have been proven the effectiveness of including VR into the standard design tools. The data obtained from the virtual software used enabled the creation of a more complete and multidisciplinary simulation environment. The embedded 3D visualization properties and the intuitive immersion guaranteed by VEs can positively contribute to develop better and optimized products. Specifically, VERITAS showed great potentialities for assisting the trade-off analysis of the site selection strategy: this choice is typical of the early-design phases and VR has been successfully used to precisely calculate illumination rates for the Moon south pole region. Also Blender® was tested, but the inaccuracies observed and the longer computational time with respect to VERITAS led to discard it. The real-time shadows projection obtained with the VERITAS internal engine and the possibility to interactively navigate the virtual scene created are useful features to be used for space systems and missions design. The TAS-I internally developed software was able to simply manipulate different datasets with the same high-quality rendering and simulation fluidity. The simulations were run also to compare the results obtained from different datasets of two different missions (i.e. LRO and Kaguya) and the VERITAS handling capabilities in managing different models. Grid resolution, surface rendering, and computational cost were monitored: no major differences were noticed while running the virtual simulations. Via computing the same survey for the same lunar south pole region, i.e. the Shackleton crater surroundings, it was possible to assess how the two missions (and their on-board altimeters) mapped this area: even though the results are not the same (the LRO-LOLA

data used represents a smaller data subset of the Kaguya/SELENE one), the best illumination points and the global illumination maps computed showed consistency. As a future improvement, it is foreseen to increase the resolution (in terms of meters per pixel) adopted for the analyses to further increase the simulation precision: in particular, a join co-registered DEM of LOLA and Kaguya/SELENE will be used to better predict illuminations peaks [338].

The results obtained by coupling VR-based analyses and lumped parameters simulations are encouraging and confirm the successful integration of VR tools into the standard suite of design software. Normally, those kinds of preliminary studies are carried out with other software as AGI STK®: in fact, it is capable to run time-depended analyses for estimating the performances of solar panels, also including the possibility to import external terrain DEMs. Even if the integration with other standard tools (e.g. MATLAB®/Simulink®) may results simpler, it should be promoted however that the simulations created can only be visualized with a desktop-wise setup, thus lacking the immersivity that is intrinsically guaranteed by using VR-based tools. Moreover, the possibility to real-time modify the simulation scenario created is limited because off-line calculations are always necessary to compute the quantities to be plotted/displayed. Even if further improvements are still possible with respect with other traditional approaches, the final goal of the present research work has been reached. The virtual model of the photovoltaic plant created is able to accurately mimic its physical behaviour: the simulated features benefitted from including the results obtained by VERITAS in terms of replicating the environmental conditions of the Moon south pole. These promising first steps of using VR as a real design tool and not just as a nice graphical display are the proof that the methodology proposed in this research study is applicable for space mission design. The real-time rendering and the possibility for the user to directly interact with a VE offer a completely new and unexplored way to approach the design of future space missions and systems. As described in sections 5.6 and 6.2 visual attributes and the possibility to virtually interact with objects play a major role in speeding-up the negotiation phases and the decision-making process typical of CE: via testing the methodology described in section 3.4 with the present case study, the feasibility of using VEs since the early design stages has been demonstrated, paving the way for other research studies in this field.

The overall outcomes obtained were not only static numbers but contributed to create an overall description of the mission to design. In fact, the integration of virtual-based computations with a lumped parameters model led

to obtain a realistic model of the solar panel tailored for performances prediction. This first combination of different simulation environments showed its great potentialities not only as a simple proof of concept, but also as a funding paradigm to be adopted in the early design phases. However, computational difficulties still exist to eventually obtain a complete simulation of the entire SAPS, but the promising integration of VR-based data with at least one model (i.e. the solar panel) seems to confirm the usefulness of the proposed methodology. As presented in section 5.3.1, the image extraction and conversion process are still too slow (i.e. ~1 day) if compared to the simulation time required by complete SAPS model (i.e. tents of minutes for a 6 lunar day long simulation) and the resolution loss related to the image reduction process[26] is not ideal for a detailed analysis in more advanced project phases. Moreover, the complete SAPS model will be adjusted to incorporate the detailed solar panel model and the data obtained from VERITAS. Finally, validation procedures will be adopted to certify the entire model: test campaigns with real hardware have been already scheduled to validate each component of the SAPS indeed. In fact, a real SAPS will be used to partially power the EAC analogue facilities in the future.

The models aggregation to virtually replicate an example lunar (and Martian) base was positively tested as well as the user-immersive simulations. The freely camera movements and the fluid navigation with different prospective (external or first-person) are noteworthy features which create a major involvement and a total immersivity experience for the end-users. Even if a fully integration with the models used for the solar panel and the complete SAPS was not fully realised, the successful implementation of a first virtual lunar (and Martian) base bodes well for future research whose ultimate objective is to create a fully functional virtual replica of the base itself. The results obtained by coupling VR models and lumped parameters models are encouraging in this sense.

Ultimately, the tested integration into a CDF setup (as described in section 5.6) is a positive first step to improve the currently used tools: the virtual scenes created could be used to check the different solutions proposed into the early-design phases, to be then modified in the next iteration of the design loop. Specifically, the possibility to generate virtual scenes with real mission data (e.g. timeframe, celestial bodies, etc.), represents a first positive test even if very simple. The participants at the ESA competition, especially the

[26] The image rescaling process was adopted to limit the database size to be loaded before running the MATLAB®/Simulink® simulations of the solar panel described in section 5.3.2.

payload specialists/experts, recognised the importance of data visualization as one of the key aspects for taking optimal and balanced decisions. Being able to see in first person how the environment conditions of the area to be observed by the spacecraft change over time was fundamental for the decision-making process related to which sensors to mount and how to operate them. As described in section 6.2, an extensive test campaign is still needed to systematically collect the users' feedbacks and to investigate how the proposed setup can affect the design session, but a promising insight has been produced in the framework of this research.

Chapter 6

Conclusions

6.1 Summary of the research activities

An innovative methodology for space mission design using novel VR tools has been presented in this Ph.D. thesis. The final aim was to cast some lights on the creation of a VR-based flexible design environment to be used since the very early phases of the product life-cycle. The virtual model created is a computer-based representation of system under development: its aim is to actively and profitably support the decision-making process thanks to the intuitive representation and visualization of each proposed design solution. The immersive features and all the data relative to model, created into a shared VE, are easily accessible for every actor involved in the project. The results obtained from the different simulations presented in this research work belong to a common operative framework into which VR acts as integration medium. Even if a complete working virtual prototype has not been realised yet, all the necessary preliminary tests and preliminary assessments have been carried out with positive outcomes. These should be intended as precursor activities functional to realize a virtual model that is truly working replica of the real object to design, applying the methodology proposed.

The idea to couple VR tools with the standard software and procedures, typically used in the space missions and systems design domain, is an emerging trend, not only for space-based domains. The visual attributes of VR are extremely suited in several applications: sport, medicine, chemistry, manufacturing (cars, airplane, etc.), civil engineering, and, of course, entertainment

are the main examples that have been described in chapter 2. The cognitive processes such as learning and decision-making are enhanced by virtual technologies. Because of the natural tendency of being highly visual creatures, VR immersive simulations are perfect to assist human-in-the-loop computerized analysis. The wide variety of devices presents on the market underlines how this emerging technology is rapidly becoming established not only for amusement sector but also in real industrial and research entities.

The idea of this work was to evaluate how a VR-based methodology affect the engineering processes, ameliorating the current state-of-the-art of MBSE approaches and CE paradigms. Considering the actual situation and the future space exploration scenarios, new actors are joining the stakeholders' stage: private enterprises and national space agencies are initiating a new era of human and robotic exploration. Whether the target is the Moon or Mars, those international partners are starting to actively collaborate with commonly agreed plans, addressing the next exploration challenges. The resulting mission architectures and systems can be complex, with high-demanding scientific and technological objective, and even more complicated when coupled with the most complicated machine ever, i.e. the human being. Space engineers are called to address unprecedented technical challenges, also facing the demanding needs of cost effectiveness and environmental compatibility. The next generation of space systems should be conceived in this complicated framework thus a disruptive approach is required to overcome the limitations of the present design tools.

Taking advantage of the forward assets towards the exploration of the Moon in the upcoming decades, a permanent human surface outpost has been selected as a proof of concept to test the VR-based approach. In particular, the power system has been analysed in detail, integrating data obtained by VR simulations with a standard design tool, i.e. a lumped parameters model. The rendering of the illumination rates on both the lunar surface and the solar panel were obtained using the embedded graphical engine of the VR tools used. After benchmarking two different software solutions, one open-source and one proprietary *ad hoc* developed, only the proprietary one has been adopted for more precise simulations. The results obtained for the global terrain illumination analysis were validated using similar simulations from literature. Thanks to the accordance of results, in the virtual scene with the lunar south pole DEM and, using the same simulation setup, a solar panel was added to predict its performances variations with transient shadows. The output obtained by the real-time rendering of different lighting conditions

throughout the entire simulation timeframe were integrated with the solar panel model developed in a classical lumped parameters software environment. Since the solar panel are just one of the elements of the selected power system which should supply the human base, the entire SAPS was modelled in order to test the integration of all its components. Moreover, a first full virtual Moon outpost has been created: the great flexibility of the VR tool used in incorporating different models and the first-person interactive visualization, that may replicate future EVAs, were studied. The same preliminary assessment has been done also for a Martian outpost, addressing the next challenge of human deep-space exploration.

The results obtained show the potentiality of the methodology proposed where VR tools cannot only be used for visualization purposes but can provide real engineering data, opening the way to a new research branch for space engineering. Additionally, the coupling of VR with a typical CDF setup for the automatic creation of virtual scenes has been tested. A reduced case study has been selected for a first beta test of the simulation workflow produced in this research study. The users involved in this survey were positively impressed by the potentialities showed by the method proposed. In fact, the created VE enhanced direct communications and data exchange using a single common platform. The 3D/4D visualizations helped to directly highlight the important features of the mission to design at a single glance: trade-off studies, typical of the conceptual design phases, and design reviews are the areas which benefit the most from the VR introduction. Furthermore, the possibility to real-time interact with the virtual model in a natural way, thanks to the immersivity guaranteed by VR, can help to simplify cross-domain communications and to simplify the communication among different experts, thus obtaining more optimized and smarter solutions by saving both time and costs.

The possible extension in advanced design stages and the parallel development of the final product and its digital twin can help to improve sub-optimized project domains. The virtual prototype can be used for assessing production, operations, maintenance, service, and disposal (e.g. disassembling and recycling) aspects: the simulation of these attributes allows their in-depth analysis since the very early design phases, not overlooking them and not jeopardizing the entire design process with wrong early assumptions. Human factors, ergonomics, operations, and training can eventually be simulated. The computer-based virtual replica should aim to globally represents a system and its evolution throughout all its life-cycle, where also humans and human

interactions with it are included to better describe the overall project framework.

6.2 Future works

The results obtained by the work here presented are promising for the entire research domain of space missions design. Even if VR and VEs in general have been only introduced in the early design phases, as presented in this dissertation, other benefits can arise from their integration in all the product life-cycle stages. The final scope for these kinds of activities could be to obtain an accurate replica of the system to be design. For example, considering the human surface settlement here presented, a complete virtual version of the fully functional base can be envisioned: all the elements are digital twins of the real ones and are able to fully represent the functional and physical behaviours, thus enabling all the actors involved in the design phases to evaluate the final product obtained. The currently existing limitations of VR underlined in this thesis, can potentially be overcome in the near future, both with software and hardware improvements. The progresses obtained in generating more realistic virtual scenes can lead to create a complete multidisciplinary and VR-based platform where innovative concepts for optimizing procedures and operations can also be tested. The standard training procedures can be enriched by those kinds of powerful virtual tools, helping to smooth the familiarization with low gravity environments for both IVAs and EVAs.

The proposed solution of a shared VE, into which models and data are exchanged between all the experts that participate into the project, is promising but there is still room for further improving its reliability and for dovetailing the virtual world with the real one. A more detailed formalization of the proposed methodology and the adaptation to the industrial standards are other areas that could be perfected (e.g. using of web-based tools).

The intrinsic multidisciplinary nature of space systems should take into account more reliable and automatized technologies for negotiations, even if humans should not be excluded by the decision loop. In fact, for what concerns the integration of VR into CDFs, knowledge-based systems and artificial intelligence algorithms can be introduced to better assist the decision-making process and prevent the creation of non-fully-optimized products.

Specifically focusing on the selected VR software chosen, i.e. VERITAS, even if its great potentialities have been shown not only by the present work but also with other promising results, its maintenance (e.g. bug fixing) and updating (e.g. introduce new graphic libraries) is very time- and cost-

demanding. The own development of a powerful virtual engine is not a practical solution anymore for the current business model of TAS-I and the space industry in general. The current plan by TAS-I is to dismiss and replace VERITAS with the open-source graphical engine called Unreal Engine, reflecting what is happening in a world scale. Originally developed for videogames, this powerful tool can be *ad hoc* tailored for space applications, taking advantage of its great reconfigurability. The users' community auto-sustains it, partially eliminating maintenance and updates problems and costs, and positive contaminations from non-space-specific techniques can be exploited, enriching and possibly optimizing the final product. The heritage derived from VERITAS will be transferred and implemented in Unreal Engine. This fact will enable more advanced applications and higher fidelity levels. As an example, the quality of textures and the shadows rendering could have higher resolution. Therefore, a more powerful hardware is needed, also to increase the DEMs resolution. From the developing point of view, the creation and rendering of virtual scene, even the most complicated ones with a lot of animation, subscenes and/or many objects/models, will result simpler thanks to the visual intuitive GUI of Unreal Engine. VERITAS is in fact affected by the problem of literally coding every single virtual attribute, i.e. writing extensive XML scripts: this fact is really limiting to create very populated simulations. It will take some time for interfacing the visual scripting and the object-oriented language used by Unreal Engine with the setup presented in this research (i.e. coupling VR with lumped parameters models and with a CDF architecture), but the contents creation will have more design freedom and an overall better-quality rendering if compared to the VERITAS solution. The videogames produced with Unreal Engine are already the proof of this graphical engine potentialities from the technical point of view: photorealism and accurate mimic of the human behaviour for creating a total realistic immersion in the virtual world are the main strength points. In addition, the constant updates of Unreal Engine enable the compatibility with new technologies: new head-mounted 3D and AR visors, motion-capture systems, and haptic devices are just some of the novel hardware to use (e.g. the new HTC Vive Pro™).

Focusing more on the selected case study, it should be intended just as a proof of concept and not as an established and fixed mission scenario. One of the great advantages of the proposed methodology is the flexibility and reconfigurability. The mission architecture and the building blocks selected are plausible solutions for the upcoming exploration endeavours. The

incremental approach for supporting a permanent human surface outpost at the Moon south pole and eventually Martian journeys is in line with the vision of national space agencies. ISRU techniques shall be assessed in advance with some preparatory campaigns to further rely on them for consumables and propellant production. The unprecedented and unattempted task of profitably support the human presence on another celestial body and the establishment of a permanent base on a planetary surface represent the biggest challenges of the next generation of space missions, which could pave the way for the manned deep-space exploration. If some unexpected changes of plans or schedule will happen, the proposed mission scenario shall be adapted to the latest version of exploration strategy and technology roadmaps. More detailed budgets can be then calculated and more precise information about the final mission configuration (e.g. landing site, modules, subsystems configuration, etc.) can be estimated. However, the preliminary results obtained for a south pole lunar base have shown how the environmental conditions are really peculiar. The illumination conditions computed shall be accounted for conceiving the concept of operations: very long shadows and highly illuminated time periods could have a huge impact not only on the systems design, but also on the crew. EVAs planning, working hours and sleep time, staffed rotations, and physiological effects are only few of the aspects to consider in the human factors analysis.

Finally, also the lumped parameters model of the SAPS shall be updated and modified to reflect the real power loads of the components. As already planned by ESA-EAC, the SAPS model will be validated through an experimental test campaign. A specific fuel cell test rig has been developed in collaboration with Politecnico di Torino and other SAPS components will be tested using the analogues facilities currently under construction at EAC Cologne site.

An extension of the VR-based methodology throughout the entire product life-cycle is desirable to address all the different aspects of the project with a single common platform that is shared among the different users. As an example, the use of VERITAS for planetary terrain navigation seems to be appropriate for familiarization and navigation planning for EVAs and robotic operations. Despite the limitations listed in section 5.5, enhancing the training with VR can help to reduce the overall training time and so its cost. Concerning the Moon terrain visualization, assessing the lighting conditions is an important factor in navigation ability for both humans and robots. The introduction to the peculiar light conditions of the lunar south pole using a safe VE

can dramatically improve the familiarization phases and is the only method to accurately mimic the surface operations onto a distant celestial body. In fact, the lack of atmosphere alters the reflective properties and stark, monochromatic nature of the lunar surface. In a foreign terrain with no familiar landmarks, it is already extremely difficult for human to judge the sizes of objects, or distances to or between features on the surface. Understanding what sun angles and amounts of shadow are optimal for human processing of obstacles in the terrain is useful for future missions: planning human-controlled or teleoperated robotic explorers and developing training programs for astronauts or rover operators are the major areas of interest. VR systems can be used to assess visual processing ability under different lighting conditions: the test subject views the model (DEM of the selected lunar area of interest) in first person perspective and can actively interact with the virtual scene, which casts shadows based on the terrain morphology and light source. Measuring the performances of both the software and the subject (e.g. visually identifying obstacle presence or counting the number of craters and/or rocks) are the tasks to address with such analysis. To reduce motion sickness symptoms and to improve the immersivity, not only the software (graphical appearances) but also hardware can be upgraded (e.g. using head-mounted 3D visors).

As a final general comment on the work performed, it should be promoted that the results presented in this thesis lay the foundations for future researches in this field.

References

[1] R. L. Headcock, "The Voyager spacecraft," *Proceedings of the Institution of Mechanical Engineers*, vol. 194, no. 1, pp. 211–224, 1980.

[2] J. P. Grotzinger *et al.*, "Mars Science Laboratory mission and science investigation," *Space Science Reviews*, vol. 170, pp. 5–56, 2012.

[3] K. H. Glassmeier, H. Boehnhardt, D. Koschny, E. Kührt, and I. Richter, "The Rosetta mission: Flying towards the origin of the solar system," *Space Science Reviews*, vol. 128, pp. 1–21, 2007.

[4] D. L. Matson, L. J. Spilker, and J.-P. Lebreton, *The Cassini-Huygens Mission*. Springer, 2003.

[5] C. T. Russell, Ed., *New horizons*. Springer, 2009.

[6] S. K. Stephens, "The Juno mission to Jupiter: Lessons from cruise and plans for orbital operations and science return," in *IEEE Aerospace Conference Proceedings*, 2015.

[7] ISECG, "About ISECG," 2015. [Online]. Available: http://www.globalspaceexploration.org/wordpress/?page_id=50. [Accessed: 01-Sep-2017].

[8] ISECG, "The Global Exploration Roadmap," ESA, 2013.

[9] ISECG, "Scientific opportunities enabled by human exploration beyond Low Earth Orbit," ESA, 2016.

[10] ISECG, "Scientific opportunities enabled by human exploration beyond Low Earth Orbit - An ISECG science white paper," ESA, 2018.

[11] P. Messidoro, "From ISS to Human Space Exploration: TAS-I contribution and perspectives," *Memorie della Società Astronomica Italiana*, vol. 82, pp. 443–448, 2011.

[12] Near Earth LCC, "Supporting commercial space development Part 2: Support alternatives versus NASA commercialization priorities," 2010.

[13] K. Rainey, "Economic development of space," *NASA*, 2017. [Online]. Available: https://www.nasa.gov/mission_pages/station/research/benefits/economic_development. [Accessed: 19-Jun-2018].

[14] D. B. J. Bussey, J. C. Worms, J. Schlutz, and F. Spiero, "The ISECG science White Paper: a scientific perspective on the Global Exploration Roadmap," in *5th European Lunar Symposium (ELS)*, 2017.

[15] C. Richter, B. Braunstein, A. Winnard, M. Nasser, and T. Weber,

"Human biomechanical and cardiopulmonary responses to partial gravity - A systematic review," *Frontiers in Physiology*, vol. 8, 2017.

[16] Review of US Human Spaceflight Plans Committee Review, "Seeking a human spaceflight program worthy of a great nation," Washington, DC, (US), 2009.

[17] S. Cresto Aleina, N. Viola, R. Fusaro, and G. Saccoccia, "Effective methodology to derive strategic decisions from ESA exploration technology roadmaps," *Acta Astronautica*, vol. 126, pp. 316–324, 2016.

[18] S. Cresto Aleina, N. Viola, R. Fusaro, and G. Saccoccia, "Approach to technology prioritization in support of moon initiatives in the framework of ESA exploration technology roadmaps," *Acta Astronautica*, vol. 139, pp. 42–53, 2017.

[19] P. Messina, B. Bardini, D. Sacotte, and S. Di Pippo, "The Aurora Programme," *ESA Bulletin*, vol. 126, pp. 10–15, 2006.

[20] NASA, "Apollo program summary report," Huston, Texas (US), 1975.

[21] R. W. Orloff and D. M. Harland, *Apollo: the definitive sourcebook*. Germany: Springer, 2006.

[22] NASA, "Apollo 11 Mission report," Huston, Texas (US), 1969.

[23] D. E. Smith, M. T. Zuber, G. A. Neumann, and F. G. Lemoine, "Topography of the Moon from the Clementine lidar," *Journal of Geophysical Research: Planets*, vol. 102, no. E1, pp. 1591–1611, 1997.

[24] L. V. Starukhina and Y. G. Shkuratov, "The lunar poles: water ice or chemically trapped hydrogen?," *Icarus*, vol. 147, no. 2, pp. 585–587, 2000.

[25] B. H. Foing *et al.*, "SMART-1 mission to the moon: Status, first results and goals," *Advances in Space Research*, vol. 37, no. 1, pp. 6–13, 2006.

[26] P. O. Hayne *et al.*, "Evidence for exposed water ice in the Moon's south polar regions from Lunar Reconnaissance Orbiter ultraviolet albedo and temperature measurements," *Icarus*, vol. 255, pp. 58–69, 2015.

[27] S. Jin, S. Arivazhagan, and H. Araki, "New results and questions of lunar exploration from SELENE, Chang'E-1, Chandrayaan-1 and LRO-LCROSS," *Advances in Space Research*, vol. 52, no. 2, pp. 285–305, 2013.

[28] ILEWG, "International Lunar Exploration Working Group (ILEWG)," 2017. [Online]. Available: http://sci.esa.int/ilewg/. [Accessed: 01-Feb-2017].

[29] K. Schubert, P. Berthe, J. Grantier, K. Pietsch, P. Angelillo, and L. Price, "The Multi-Purpose Crew Vehicle European Service Module: a European contribution to human exploration," in *AIAA SPACE 2013 Conference and Exposition*, 2013.

[30] J. Crusan and R. Gatens, "Cislunar habitation and Environmental

Control and Life Support Systems," in *NASA Advisory Council*, 2017.
[31] J. Engle, T. Moseman, and M. Duggan, "A resilient cislunar spacecraft architecture to support key Mars enabling technologies and operation concepts," in *AIAA SPACE 2016*, 2016.
[32] M. Mammarella, C. A. Paissoni, N. Viola, A. Denaro, E. Gargioli, and F. Massobrio, "The Lunar Space Tug: A sustainable bridge between low Earth orbits and the Cislunar Habitat," *Acta Astronautica*, vol. 138, pp. 102–117, 2017.
[33] S. Cresto Aleina, N. Viola, F. Stesina, M. A. Viscio, and S. Ferraris, "Reusable space tug concept and mission," *Acta Astronautica*, vol. 128, pp. 21–32, 2016.
[34] J.-D. 'Jan' Wörner, "Moon Village: a vision for global cooperation and Space 4.0," *ESA*, 2016. [Online]. Available: http://blogs.esa.int/janwoerner/2016/11/23/moon- village/. [Accessed: 25-Feb-2017].
[35] D. Binns *et al.*, "Review and analysis of (European) building blocks for a future Moon Village," in *68th International Astronautical Congress (IAC)*, 2017.
[36] H. Lasi, P. Fettke, H. G. Kemper, T. Feld, and M. Hoffmann, "Industry 4.0," *Business and Information Systems Engineering*, vol. 6, no. 4, pp. 239–242, 2014.
[37] N. Jazdi, "Cyber physical systems in the context of Industry 4.0," *2014 IEEE Automation, Quality and Testing, Robotics*, pp. 2–4, 2014.
[38] A. Dujin, C. Geissler, and D. Horstkötter, "Industry 4.0 - The new industrial revolution How Europe will succeed," 2014.
[39] M. Brettel, N. Friederichsen, M. Keller, and M. Rosenberg, "How virtualization, decentralization and network building change the manufacturing landscape: an Industry 4.0 perspective," *International Journal of Information and Communication Engineering*, vol. 8, no. 1, pp. 37–44, 2014.
[40] J. Lee, H. A. Kao, and S. Yang, "Service innovation and smart analytics for Industry 4.0 and big data environment," *Procedia CIRP*, vol. 16, pp. 3–8, 2014.
[41] ESA, "What is Space 4.0?," 2016. [Online]. Available: http://www.esa.int/About_Us/Ministerial_Council_2016/What_is_space_4.0. [Accessed: 05-Oct-2017].
[42] ESA, "Space 4.0i," 2016. [Online]. Available: https://www.esa.int/About_Us/Ministerial_Council_2016/Space_4.0i. [Accessed: 05-Oct-2017].
[43] SpaceX, "Falcon 9," 2017. [Online]. Available: http://www.spacex.com/falcon9. [Accessed: 19-Aug-2017].
[44] Shackleton Energy Company, "Shackleton Energy Company website," 2013. [Online]. Available: http://www.shackletonenergy.com/. [Accessed: 10-Nov-2016].

[45] SpaceX, "BFR," 2017. [Online]. Available: http://www.spacex.com/mars.
[46] P. Ehrenfreund *et al.*, "Toward a global space exploration program: A stepping stone approach," *Advances in Space Research*, vol. 49, no. 1, pp. 2–48, 2012.
[47] R. Garner, "Lunar IceCube to take on big mission from small package," *NASA*, 2015. [Online]. Available: https://www.nasa.gov/feature/goddard/lunar-icecube-to-take-on-big-mission-from-small-package. [Accessed: 22-Jun-2018].
[48] Arizona State University, "LunaH-Map," *ASU*, 2016. [Online]. Available: http://lunahmap.asu.edu/. [Accessed: 22-Jun-2018].
[49] K. Northon, "NASA Space Launch System's first flight to send small sci-tech satellites into space," *NASA*, 2016. [Online]. Available: https://www.nasa.gov/press-release/nasa-space-launch-system-s-first-flight-to-send-small-sci-tech-satellites-into-space. [Accessed: 22-Jun-2018].
[50] J. Harbaugh, "International Partners provide science satellites for America's Space Launch System maiden flight," *NASA*, 2016. [Online]. Available: https://www.nasa.gov/exploration/systems/sls/international-partners-provide-cubesats-for-sls-maiden-flight. [Accessed: 22-Jun-2018].
[51] K. Matsumoto, T. Hashimoto, T. Hoshino, S. Tanaka, M. Otsuki, and J. I. Kawaguchi, "Japanese 1st Moon Lander SELENE-2 as SELENE follow-on," in *Joint Annual Meeting of ILEWG/LEAG/SRR*, 2008.
[52] T. Hashimoto, T. Hoshino, S. Tanaka, M. Otsuki, H. Otake, and H. Morimoto, "Japanese moon lander SELENE-2—Present status in 2009," *Acta Astronautica*, vol. 68, no. 7–8, pp. 1386–1391, 2011.
[53] T. Hashimoto *et al.*, "Study status of lunar polar exploration mission," in *16th Space Science Symposium*, 2016.
[54] J. D. Carpenter *et al.*, "Lunar exploration in ESA," in *Annual Meeting of the Lunar Exploration Analysis Group*, 2014.
[55] B. A. E. Lehner *et al.*, "Human Assisted Robotic Vehicle Studies - A conceptual end-to-end mission architecture," *Acta Astronautica*, vol. 140, pp. 380–387, 2017.
[56] D. E. Koelle and R. Janovsky, "Development and transportation costs of space launch systems," in *DGLR/CEAS European Air and Space Conference*, 2007.
[57] SpaceX, "SpaceX website," 2017. [Online]. Available: http://www.spacex.com/. [Accessed: 03-Sep-2017].
[58] C. G. Ferro, R. Grassi, C. Seclì, and P. Maggiore, "Additive manufacturing offers new opportunities in UAV research," *Procedia CIRP*, 2015.
[59] C. G. Ferro, S. Brischetto, R. Torre, and P. Maggiore, "Characterization of ABS specimens produced via the 3D printing

technology for drone structural components," *Curved and Layered Structures*, vol. 3, no. 1, pp. 172–188, 2016.

[60] S. Brischetto, A. Ciano, and C. G. Ferro, "A multipurpose modular drone with adjustable arms produced via the FDM additive manufacturing process," *Curved and Layered Structures*, vol. 3, no. 1, pp. 202–213, 2016.

[61] S. Brischetto, C. G. Ferro, P. Maggiore, and R. Torre, "Compression Tests of ABS Specimens for UAV Components Produced via the FDM Technique," *Technologies*, vol. 5, no. 2, p. 20, 2017.

[62] C. G. Ferro, A. E. M. Casini, and A. Mazza, "A novel design approach for space components: application to a multifunctional panel," in *68th International Astronautical Congress (IAC)*, 2017.

[63] C. Dordlofva, A. Lindwall, and P. Törlind, "Opportunities and challenges for additive manufacturing in space applications," in *12th Biennial Norddesign*, 2016.

[64] A. Lindwall, C. Dordlofva, and A. Öhrwall Rönnbäck, "Additive manufacturing and the product development process: insights from the space industry," in *21st International Conference on Engineering Design (ICED)*, 2017.

[65] S. Rawal, J. Brantley, and N. Karabudak, "Additive manufacturing of Ti-6Al-4V alloy components for spacecraft applications," in *6th International Conference on Recent Advances in Space Technologies (RAST)*, 2013.

[66] F. Mouriaux, "Motivation, opportunities and challanges of additive manufacturing for space application," in *RUAG Space*, 2015.

[67] M. Orme *et al.*, "A demonstration of additive manufacturing as an enabling technology for rapid satellite design and fabrication," in *International SAMPE Technical Conference*, 2017.

[68] S. Siarov, A. Cowley, M. Vera, M. Frateri, and J. Reguette, "Closed-loop 3D printing for the lunar village and future planetary exploration," in *10th IAA Symposium on the future of space exploration towards space village and beyond*, 2017.

[69] M. Müller, S. Gruber, M. D. Coen, R. Campbell, D. Kim, and B. Morrell, "Operational benefit and applicability of a 3D printer in future human Mars missions - results from analog testing," in *SpaceOps Conference*, 2018.

[70] Bigelow Aerospace, "BEAM," 2017. [Online]. Available: https://bigelowaerospace.com/pages/beam/. [Accessed: 10-Feb-2017].

[71] M. Garcia, "NASA extends expandable habitat's time on the International Space Station," *NASA*, 2017. [Online]. Available: https://www.nasa.gov/feature/nasa-extends-beam-s-time-on-the-international-space-station. [Accessed: 23-Jun-2018].

[72] M. A. Viscio, E. Gargioli, J. A. Hoffman, P. Maggiore, A. Messidoro, and N. Viola, "A methodology for innovative technologies roadmaps

assessment to support strategic decisions for future space exploration," *Acta Astronautica*, vol. 94, no. 2, pp. 813–833, 2014.
[73] J. Carpenter, B. Houdou, and B. Hufenbach, "Lunar exploration in the European exploration envelope programme," in *5th European Lunar Symposium (ELS)*, 2017.
[74] W. J. Larson and J. R. Wertz, Eds., *Space mission analysis and design*, 3rd ed. US: Microcosm Press, 1999.
[75] J. R. Wertz, D. F. Everett, and J. J. Puschell, Eds., *Space mission engineering: the new SMAD*. Microcosm Press, 2011.
[76] W. J. Larson and L. K. Pranke, Eds., *Human spaceflight: mission analysis and design*. McGraw-Hill, 1999.
[77] W. Ley, K. Wittmann, and W. Hallmann, Eds., *Handbook of space technology*. Wiley, 2009.
[78] G. Musgrave, A. Larsen, and T. Sgobba, Eds., *Safety design for space systems*. Elsevier, 2009.
[79] P. Fortescue, G. Swinerd, and J. Stark, Eds., *Spacecraft systems engineering*. John Wiley & Sons, 2011.
[80] M. A. Aguirre, *Introduction to space systems: design and synthesis*. Springer, 2013.
[81] M. A. Viscio, "Space exploration systems, strategies and solutions," Politecnico di Torino, 2014.
[82] G. E. Moore, "Cramming more components onto integrated circuits," *Electronics*, vol. 38, no. 8, 1965.
[83] J. Lee, B. Bagheri, and H. A. Kao, "A Cyber-Physical Systems architecture for Industry 4.0-based manufacturing systems," *Manufacturing Letters*, vol. 3, pp. 18–23, 2015.
[84] E. Gobbetti and R. Scateni, "Virtual Reality: Past , Present and Future," in *Virtual environments in clinical psychology and neuroscience: Methods and techniques in advanced patient-therapist interaction*, G. Riva, B. K. Wiederhold, and E. Molinari, Eds. Amsterdam: IOS Press, 1998, pp. 3–20.
[85] I. E. Sutherland, "The ultimate display," in *IFIPS Congress*, 1965.
[86] D. C. Smith, C. Irby, R. Kimball, and E. Harslem, "The star user interface: an overview," in *National Computer Conference*, 1982.
[87] S. R. Ellis, "Nature and origins of virtual environments: a bibliographical essay," *Computing Systems in Engineering*, vol. 2, no. 4, pp. 321–347, 1991.
[88] S. R. Ellis, "What are virtual environments?," *IEEE Computer Graphics and Applications*, vol. 14, no. 1, pp. 17–22, 1994.
[89] J. F. Balaguer and A. Mangili, "Virtual Environments," in *New trends in animation and visualization*, T. D. and N. Magnenat-Thalmann, Eds. Wiley, 1992.
[90] R. Chang, C. Ziemkiewicz, R. Pyzh, J. Kielman, and W. Ribarsky, "Learning-based evaluation of visual analytic systems," in *3rd*

Workshop: BEyond time and errors: novel evaLuation methods for Information Visualization (BELIV), 2010, pp. 29–34.

[91] K.-U. Doerr, H. Rademacher, S. Huesgen, and W. Kubbat, "Evaluation of a low-cost 3D sound system for immersive virtual reality training systems," *IEEE Transactions on Visualization and Computer Graphics*, vol. 13, no. 2, pp. 204–212, 2007.

[92] A. O. Frank, I. a. Twombly, T. J. Barth, and J. D. Smith, "Finite element methods for real-time haptic feedback of soft-tissue models in virtual reality simulators," in *IEEE Virtual Reality (VR)*, 2001.

[93] J. T. Reason and J. J. Brand, *Motion sickness*. London (UK): Academic press, 1975.

[94] D. A. Keim, F. Mansmann, J. Schneidewind, J. Thomas, and H. Ziegler, "Visual analytics: Scope and challenges," in *Visual data mining*, Springer, 2008, pp. 76–90.

[95] M. R. Endsley, R. Hoffman, D. Kaber, and E. Roth, "Cognitive engineering and decision making: An overview and future course," *Journal of Cognitive Engineering and Decision Making*, vol. 1, no. 1, pp. 1–21, 2007.

[96] F. L. Greitzer, C. F. Noonan, and L. Franklin, "Cognitive foundations for visual analytics," Pacific Northwest National Laboratory (PNNL), Richland, Washington (US), 2011.

[97] A. T. Bahill and A. M. Madni, *Tradeoff decisions in system design*. Springer, 2016.

[98] Y. N. Gong, "The simulation based on vitual reality technique," *Applied Mechanics and Materials*, vol. 644, pp. 6305–6308, 2014.

[99] J. M. Rosen, H. Soltanian, R. J. Redett, and D. R. Laub, "Evolution of virtual reality," *IEEE Engineering in Medicine and Biology Magazine*, vol. 15, no. 2, pp. 16–22, 1996.

[100] R. M. Satava and S. B. Jones, "Current and future applications of virtual reality for medicine," *Proceedings of the IEEE*, vol. 86, no. 3, pp. 484–489, 1998.

[101] S. Chan, F. Conti, K. Salisbury, and N. H. Blevins, "Virtual reality simulation in neurosurgery: technologies and evolution," *Neurosurgery*, vol. 72, no. SUPPL_1, pp. A154–A164, 2013.

[102] A. Gorini and G. Riva, "Virtual reality in anxiety disorders: the past and the future," *Expert Review of Neurotherapeutics*, vol. 8, no. 2, pp. 215–233, 2008.

[103] G. Saposnik, M. Levin, and Stroke Outcome Research Canada (SORCan) Working Group, "Virtual reality in stroke rehabilitation," *Stroke*, vol. 42, no. 5, pp. 1380–1386, 2011.

[104] K. Laver, S. George, S. Thomas, J. E. Deutsch, and M. Crotty, "Virtual reality for stroke rehabilitation," *Stroke*, vol. 43, no. 2, pp. e20–e21, 2012.

[105] R. T. Azuma, "A survey of augmented reality presence," *Teleoperators*

and Virtual Environments, vol. 6, no. 4, pp. 355–385, 1997.
[106] G. Riva, "Applications of virtual environments in medicine," *Methods of information in medicine*, vol. 42, no. 5, pp. 524–534, 2003.
[107] C. Schmandt, "Interactive three-dimensional computer space," in *SPIE Processing and Display of Three-Dimensional Data*, 1983, pp. 155–160.
[108] S. Tanner, "The use of virtual reality at Boeing's Huntsville laboratories," in *IEEE Virtual Reality Annual International Symposium*, 1993, pp. 14–19.
[109] R. B. Loftin and P. J. Kenney, "Training the Hubble space telescope flight team," *IEEE Computer Graphics and Applications*, vol. 15, no. 5, pp. 31–37, 1995.
[110] M. Wolff, D. Martinez Oliveira, A. Fortunato, A. Cowley, and A. Boyd, "Enhancement of the ESA mobile procedure viewer (mobiPV) beyond Low Eart Orbit," in *68th International Astronautical Congress (IAC)*, 2017.
[111] F. Nicolini, C. Scott, R. Seine, and M. Wolff, "3D Visual Training for operations on-board the International Space Station and beyond," in *67th International Astronautical Congress (IAC)*, 2016.
[112] NASA, "NASA RELEASE 15-139," 2015. [Online]. Available: https://www.nasa.gov/press- release/nasa-microsoft-collaborate-to-bring-science-fiction-to-science-fac. [Accessed: 27-Aug-2017].
[113] L. E. Hitchner and M. W. McGreevy, "Methods for user-based reduction of model complexity for virtual planetary exploration," in *SPIE 1913, Human Vision, Visual Processing, and Digital Display IV*, 1993, pp. 622–636.
[114] M. W. McGreevy, "Virtual reality and planetary exploration," in *Virtual reality: applications and explorations*, A. Wexelblat, Ed. Elsevier, 1993, pp. 163–197.
[115] J.-R. Kim, S.-Y. Lin, J.-W. Hong, Y.-H. Kim, and C.-K. Park, "Implementation of Martian virtual reality environment using very high-resolution stereo topographic data," *Computers & Geosciences*, vol. 44, pp. 184–195, 2012.
[116] L. Piovano, M. Brunello, L. Rocci, and V. Basso, "Representing planetary terrains into a virtual reality environment for space exploration," *Pattern Recognition and Image Analysis*, vol. 21, no. 3, pp. 549–552, 2011.
[117] G. Groemer *et al.*, "The AMADEE-15 Mars simulation," *Acta Astronautica*, vol. 129, pp. 277–290, 2016.
[118] Mars Planet, "MARS CITY PROJECT," 2017. [Online]. Available: http://www.mars-city.org/. [Accessed: 28-Aug-2017].
[119] J. Osterlund and B. Lawrence, "Virtual reality: Avatars in human spaceflight training," *Acta Astronautica*, vol. 71, pp. 139–150, 2012.
[120] M. Ferrino, E. Villata, V. Basso, and M. Cardano, "TAS-I Virtual

Reality tool for Columbus MSP/PEI stage analysis verification: case studies and lesson learned," *SAE Technical Paper*, vol. 2009-01-24, 2009.

[121] G. Fasano, D. Saia, and A. Piras, "Columbus stowage optimization by cast (cargo accommodation support tool)," *Acta Astronautica*, vol. 67, no. 3–4, pp. 489–495, 2010.

[122] M. Deshmukh, R. Wolff, P. M. Fischer, M. Flatken, and A. Gerndt, "Interactive 3D visualization to support Concurrent Engineering in the early space mission design phase," in *5th CEAS Air & Space Conference*, 2015.

[123] Y. Liu, M. Deshmukh, J. C. Wulkop, and P. M. Fischer, "Real-time immersive visualization for satellite configuration and version comparison," in *Simulation and EGSE for Space Programmes (SEPS)*, 2017.

[124] DLR, "Virtual Satellite," *DLR*, 2018. [Online]. Available: https://www.dlr.de/sc/en/desktopdefault.aspx/tabid-5135/8645_read-8374/. [Accessed: 03-Jul-2018].

[125] ESA, "Augumented Reality for AIT, AIV and operations," *ESA*, 2017. [Online]. Available: http://www.esa.int/Our_Activities/Space_Engineering_Technology/Shaping_the_Future/Augmented_Reality_for_AIT_AIV_and_Operations. [Accessed: 29-Jun-2018].

[126] K. Russell, "Lockheed Martin on cutting costs with Virtual Reality," *Via Satellite*, 2017. [Online]. Available: http://www.satellitetoday.com/innovation/2017/04/20/lockheed-martin-cutting-costs-virtual-reality/. [Accessed: 23-May-2017].

[127] J. Geng, Y. Li, R. Wang, Z. Wang, C. Lv, and D. Zhou, "A virtual maintenance-based approach for satellite assembling and troubleshooting assessment," *Acta Astronautica*, vol. 138, pp. 434–453, 2017.

[128] NASA, *NASA Systems Engineering Handbook*. Washington, DC, (US): NASA, 2007.

[129] INCOSE, *Systems Engineering Handbook*, 4th ed. Wiley, 2015.

[130] D. DeLaurentis, "Understanding transportation as a System-of-Systems design problem," in *43rd AIAA Aerospace Sciences Meeting and Exhibit*, 2005.

[131] IEEE Reliability Society, "Systems of Systems White Paper," 2015.

[132] S. D. Jolly and B. K. Muirhead, "System of systems engineering in space exploration," in *System of Systems Engineering: Innovations for the 21st Century*, M. Jamshidi, Ed. Wiley, 2009, pp. 317–347.

[133] NASA, "NPR 7120.5, NASA Space flight program and project management handbook," 2010.

[134] ESA, "ECSS-M-30A, Space Project Managment - Project Phasing and Planning," 1996.

[135] G. Ridolfi, “Space System Conceptual Design - Analysis methods for engineerign-team support,” Technische Universiteit Delft, 2013.
[136] J. W. Hedge, “Gaining insight into decision-making through a virtual world environment application,” Washington, DC, (US), 2011.
[137] A. J. Robotham and F. Shao, “The value of simulation and immersive virtual reality environments to design decision making in new product development,” in *EWG-DSS Workshop"Decision Support Systems & Operations Management Trends and Solutions in Industires"*, 2012.
[138] M. Roupé, “Development and implementations of Virtual Reality for decision-making in urban planning and building design,” Chalmers University of Technology, 2013.
[139] M. Strong, “Using Virtual Reality to assist decision making,” 2016. [Online]. Available: https://www.gaiaresorces.com.au/vr/. [Accessed: 20-Oct-2016].
[140] L. P. Berg and J. M. Vance, “An industry case study: investigating early design decision making in Virtual Reality,” *Journal of Computing and Information Science in Engineering*, vol. 17, pp. 01100-1-011001-7, 2016.
[141] INCOSE, “INCOSE Systems Engineering Vision 2020,” 2007.
[142] L. Delligatti, *SysML distilled: a brief guide to the Systems Modeling Language*. Pearson Education, 2013.
[143] S. Lilley, “Lost in translation,” *System Failure Case Studies*, vol. 3, no. 5, pp. 1–4, 2009.
[144] E. A. Euler, S. D. Jolly, and H. H. “Lad” Curtis, “The failures of the Mars Climate Orbiter and Mars Polar Lander: a perspective from the people involved,” in *24th Annual ASS guidance and control conference*, 2001.
[145] V. Schaus, D. Lüdtke, and A. Gerndt, “Advanced spacecraft systems design using model-based techniques,” in *2nd International Federated Satellite Systems (FSS) Workshop*, 2014.
[146] R. P. Smith, “The historical roots of Concurrent Engineering fundamentals,” *IEEE Transactions on Engineering Management*, vol. 44, no. 1, pp. 67–78, 1997.
[147] D. Belson, “Concurrent Engineering,” in *Handbook of Design, Manufacturing and Automation*, R. Dorf and A. Kusiak, Eds. Wiley, 1994.
[148] H. C. Zhang and D. Zhang, “Concurrent Engineering: an overview from manufacturing engineering perspectives,” *Concurrent Engineering: Reseach and Applications*, vol. 3, no. 3, pp. 221–236, 1995.
[149] T. T. Pullan, M. Bhasi, and G. Madhu, “Application of concurrent engineering in manufacturing industry,” *International Journal of Computer Integrated Manufacturing*, vol. 23, no. 5, pp. 425–440, 2010.

[150] M. I. Mohamad, "The application of concurrent engineering philosophy to the construction industry," Loughborough University, 1999.
[151] A. Abbas and I. A. Manarvi, "Concurrent Engineering applications and lessons learnt in oil refinery," in *Improving Complex Systems Today*, 2011, pp. 107–114.
[152] T. P. Tsai, H. C. Yang, and P. H. Liao, "The application of concurrent engineering in the installation of foam fire extinguishing piping system," *Procedia Engineering*, vol. 14, pp. 1920–1928, 2011.
[153] S. D. Wall, "Use of Concurrent Engineering in space mission design," in *2nd European Systems. Engineering Conference (EuSEC)*, 2000.
[154] M. Bandecchi, B. Melton, and F. Ongaro, "Concurrent engineering applied to space mission assessment and design," *Esa Bulletin*, vol. 99, pp. 34–40, 1999.
[155] M. Bandecchi, "Metodo ed Esperienza della CDF in ESTEC," in *Inaugurazione ASI Concurrent Engineering Facility*, 2013.
[156] L. Franchi, L. Feruglio, and S. Corpino, "Incorporation of knowledge based systems in Tradespace Exploration for space mission design," in *67th International Astronautical Congress (IAC)*, 2016.
[157] R. Findlay, A. Braukhane, D. Schubert, J. F. Pedersen, H. Müller, and O. Essmann, "Implementation of concurrent engineering to Phase B space system design," *CEAS Space Journal*, vol. 2, pp. 51–58, 2011.
[158] ESA, "Applying MBSE to a space mission," 2017. [Online]. Available: http://blogs.esa.int/cleanspace/2017/08/28/applying-mbse-to-a-space-mission/. [Accessed: 25-Oct-2017].
[159] L. Lindblad, M. Witzmann, S. Vanden Bussche, and H. K. Straße, "Systems Engineering from a web browser: turning MBSE into industrial reality," in *Systems Engineering and Concurrent Engineering for Space Applications (SECESA)*, 2016.
[160] H. Eisenmann, J. Miro, and H. P. de Koning, "MBSE for European Space-Systems Development," *Insight*, vol. 12, no. 4, pp. 47–53, 2009.
[161] B. Motamedian, "MBSE applicability Analysis," *International Journal of Scientific & Engineering Research*, vol. 4, no. 2, pp. 1–7, 2013.
[162] S. Vanden Bussche, M. Witzmann, and L. Lindblad, "The hardware development tool stack for future space exploration," in *68th International Astronautical Congress (IAC)*, 2017.
[163] B. Krassi *et al.*, "ManuVAR PLM model, methodology, architecture, and tools for manual work support throughout system lifecycle," 2010, pp. 694–704.
[164] B. Krassi, "ManuVAR," 2008.
[165] M. Ferrino, O. Secondo, A. Sabbagh, and E. Della Sala, "Advanced thermoplastic polymers and additive manufacturing applied to ISS Columbus toolbox: lessons learned and results," in *13th European*

Conference on Spacecraft Structures, Materials & Environmental Testing, 2014.

[166] M. Ferrino, B. Bekooy, D. Saia, E. Della Sala, A. Sabbagh, and E. Flesia, "Usability aspects for a new toolbox user needs based enabled by 3D additive manufacturing technologies for ISS Columbus module," in *65th International Astronautical Congress (IAC)*, 2014.

[167] M. Cardano, M. Ferrino, M. Costa, and P. Giorgi, "VR/AR tools to support on orbit crew operations and P/Ls maintenance in the ISS pressurized Columbus module," in *60th International Astronautical Congress (IAC)*, 2009.

[168] V. Basso, M. Pasquinelli, L. Rocci, C. Bar, and M. Marello, "Collaborative System Engineering usage at Thales Alenia Space Italia," in *2th International Systems & Concurrent Engineering for Space Applications conference (SECESA)*, 2010.

[169] V. Basso *et al.*, "TAS-I COSE Centre," in *Joint Virtual Reality Conference of euroVR and EGVE*, 2011, pp. 47–52.

[170] M. Pasquinelli, V. Basso, L. Rocci, M. Cencetti, C. Vizzi, and S. T. Chiadò, "Modelling and collaboration across organizations: Issues and a solution," *Concurrent Engineering*, 2017.

[171] B. Krassi, "Manual work support and integration with the PLM systems VTT Technical Research Centre of Finland," in *Workshop Virtual Design and Prototyping*, 2011.

[172] S. Aromaa, S.-P. Leino, S. Kiviranta, B. Krassi, and J. Viitaniemi, "Human-machine system design: the integrated use of human factors, virtual environments and product lifecycle management," *Tijdschrift voor Ergonomie*, vol. 37, no. 3, pp. 11–16, 2012.

[173] A. M. Soccini *et al.*, "Virtual Reality interface for multidisciplinary physical analysis of space vehicles," in *EuroVR*, 2014.

[174] C. Vizzi, "Virtual reality as a cross-domain language in collaborative environments," in *International Conference on Augmented and Virtual Reality (ARV)*, 2015, pp. 507–514.

[175] A. S. García *et al.*, "A collaborative workspace architecture for strengthening collaboration among space scientists," in *IEEE Aerospace Conference*, 2015.

[176] P. Eichler, R. Seine, E. Khanina, and A. Schön, "Astronaut training for the European ISS contributions Columbus module and ATV," *Acta Astronautica*, vol. 59, no. 12, pp. 1146–1152, 2006.

[177] M. Aguzzi, R. Bosca, and U. Müllerschkowski, "Astronaut training in view of the future: A Columbus payload instructor perspective," *Acta Astronautica*, vol. 66, no. 3–4, pp. 401–407, 2010.

[178] A. E. M. Casini, "Study and development of malfunction scenarios for EDR payload of ISS Columbus module for ESA training simulations," Politecnico di Torino, 2014.

[179] A. E. M. Casini, "Study and development of malfunction scenarios for

EDR payload of ISS Columbus module for ESA training simulations," in *11th AIAA-PEGASUS Student Conference*, 2014.
[180] A. Garro, "Modelling and simulation for system reliability analysis: the RAMSAS method," in *Conferenza INCOSE Italia su System Engineering (CIISE)*, 2016.
[181] B. Hufenbach *et al.*, "International mission to lunar vicinity and surface-near-term mission scenario of the Global Space Exploration Roadmap," in *66th International Astronautical Congress (IAC)*, 2014.
[182] R. Whitley *et al.*, "Global Exploration Roadmap derived concept for human exploration of the Moon," in *Global Space Exploration Conference (GLEX)*, 2017.
[183] LEAG, "The Lunar Exploration Roadmap," 2016.
[184] T. Hoppenbrouwers *et al.*, "Analogues for preparing robotic and human exploration on the Moon," in *SpaceOps Conference*, 2016.
[185] C. Circi, "Lunar base for Mars missions," *Journal of Guidance, Control, and Dynamics*, vol. 28, no. 2, pp. 372–373, 2005.
[186] B. Aldrin, S. Saikia, A. Aldrin, D. Minton, and J. Longuski, "Cycling Pathway to Occupy Mars Via Lunar Resources," in *67th International Astronautical Congress (IAC)*, 2016.
[187] D. Conte, M. Di Carlo, K. Ho, D. B. Spencer, and M. Vasile, "Earth-Mars transfers through Moon Distant Retrograde Orbits," *Acta Astronautica*, vol. 143, pp. 372–379, 2018.
[188] L. Levrino *et al.*, "Human life support in permanent lunar base architectures," in *65th International Astronautical Congress (IAC)*, 2014.
[189] H. G. Heinken, D. T. Vaniman, and B. M. French, Eds., *Lunar sourcebook: A user's guide to the Moon*. CUP Archive, 1991.
[190] G. L. Kulcinski, "Using lunar Helium-3 to generate nuclear power without the production of nuclear waste," in *20th International Space Development Conference*, 2001.
[191] V. Badescu, Ed., *Moon: Prospective energy and material resources*. Springer, 2012.
[192] A. Scalise Meynet, "Analityc study of filtration system with cyclone separator for space applications," Politecnico di Torino, 2010.
[193] A. E. M. Casini, "Cyclonic separators models analysis aimed to air filtration for space application," Politecnico di Torino, 2011.
[194] W. A. Ambrose, "The significance of lunar water ice and other mineral resources for rocket propellants and human settlement of the Moon," in *Energy resources for human settlement in the solar system and Earth's future in space*, W. A. Ambrose, J. F. I. Reilly, and D. C. Peters, Eds. 2013, pp. 7–31.
[195] J. H. Wickman, A. E. Oberth, and J. D. Mockenhaupt, "Lunar base spacecraft propulsion with lunar propellants," in *22nd Joint Propulsion Conference*, 1986.

[196] H. H. Koelle, “The influence of lunar propellant production on the cost-effectiveness of cislunar transportation systems,” in *2nd Conference on Lunar Bases and Space Activities of the 21st Century*, 1988, pp. 447–452.
[197] D. L. Linne and M. L. Meyer, “A compilation of lunar and Mars exploration strategies utilizing indigenous propellants,” 1992.
[198] A. C. Charania and D. DePasquale, “Economic analysis of a lunar In-Situ Resource Utilization (ISRU) propellant services market,” in *58th International Astronautical Congress (IAC)*, 2007.
[199] R. P. Mueller and W. Notordonato, “Development of a lunar consumables storage and distribution depot,” 2004.
[200] E. Hurlbert, M. Baine, and G. Grush, “An open exploration architecture using an L-1 space propellant depot,” in *SpaceOps 2010 Conference*, 2010.
[201] K. Ho, K. Gerhard, A. K. Nicholas, A. J. Buck, and J. Hoffman, “On-orbit depot architectures using contingency propellant,” *Acta Astronautica*, vol. 96, no. 1, pp. 217–226, 2014.
[202] J. W. Wilson, J. Miller, A. Konradi, and F. A. Cucinotta, “Shielding strategies for human space exploration,” Houston, Texas (US), 1997.
[203] I. Schneider, A. Daga, P. de Leon, and G. Harris, “Interim report for the human exploration of the Moon and Mars: Space radiation protection and mitigation strategies for a long term duration lunar base,” in *40th International Conference on Environmental Systems*, 2010.
[204] F. Formentin, “Protection system from the cosmic rays of a pressurized inhabited module for the lunar exploration,” Politecnico di Torino, 2008.
[205] B. Khoshnevis *et al.*, “Lunar contour crafting—a novel technique for ISRU-based habitat development,” in *43rd AIAA Aerospace Sciences Meeting and Exhibit*, 2005.
[206] LavaHive Team, “LavaHive,” 2016. [Online]. Available: http://www.lavahive.com/. [Accessed: 14-Jun-2016].
[207] C. Lobascio *et al.*, “New concepts evaluation of flexible water bags for space applications,” in *43rd International Conference on Environmental Systems (ICES)*, 2013.
[208] J. Parodi, “Development of a multifunctional bag prototype to increase the ECLSS of a pressurized space module,” Politecnico di Torino, 2013.
[209] A. I. Grigoriev, Y. E. Sinyak, N. M. Samsonov, L. S. Bobe, N. N. Protasov, and P. O. Andreychuk, “Regeneration of water at space stations,” *Acta Astronautica*, vol. 68, pp. 1567–1573, 2011.
[210] J. Haruyama *et al.*, “Possible lunar lava tube skylight observed by SELENE cameras,” *Geophysical Research Letters*, vol. 36, no. 21, pp. 1–5, 2009.

[211] F. Hörz, “Lava tubes - potential shelters for habitats,” in *Lunar bases and space activities of the 21st century*, W. W. Mendell, Ed. Huston, Texas (US): Lunar and Planetary Institute, 1985, pp. 405–412.
[212] C. R. Coombs and B. R. A. Y. Hawke, “A search for intact lava tubes on the Moon: Possible lunar base habitats,” in *2nd Conference on Lunar Bases and Space Activities of the 21st Century*, 1988, pp. 219–229.
[213] G. De Angelis, J. W. Wilson, M. S. Clowdsley, J. E. Nealy, D. H. Humes, and J. M. Clem, “Lunar lava tubes radiation safety analysis,” *Journal of Radiation Research*, vol. 43, no. Suppl., pp. S41–S45, 2002.
[214] J. Haruyama *et al.*, “Lunar holes and lava tubes as resources for lunar science and exploration,” in *Moon: Prospective energy and material resources*, V. Badescu, Ed. Springer, 2012, pp. 139–164.
[215] D. H. Needham and D. A. Kring, “Lunar volcanism produced a transient atmosphere around the ancient Moon,” *Earth and Planetary Science Letters*, vol. 478, pp. 175–178, 2017.
[216] A. Freundlich, A. Ignatiev, C. Horton, M. Duke, P. Curreri, and L. Sibille, “Manufacture of solar cells on the Moon,” in *IEEE Photovoltaic Specialists Conference*, 2005, pp. 794–797.
[217] L. Levrino, L. Colangelo, G. Gatto, J. A. Hoffman, N. Linty, and A. Tartaglia, “Lunar Relativistic Positioning System (LRPS) for human exploration,” in *Inventive Ideas for Micro/Nano-Satellites. The MIC3 Report*, R. Sandau, S. Nakasuka, R. Kawashima, and J. J. Sellers, Eds. IAA (International Academy of Astronautics), 2015, pp. 50–61.
[218] G. Gatto *et al.*, “Incremental architectures for a permanent human lunar outpost with focus on ISRU technologies,” in *65th International Astronautical Congress (IAC)*, 2014.
[219] R. W. Farquhar, D. W. Dunham, Y. Guo, and J. V. McAdams, “Utilization of libration points for human exploration in the Sun-Earth-Moon system and beyond,” *Acta Astronautica*, vol. 55, no. 3–9, pp. 687–700, 2004.
[220] J. Plescia, “Lunar precursor robotic program,” in *Lunar Reconnaissance Orbiter PSG Meeting*, 2006.
[221] W. K. Hofstetter, P. D. Wooster, and E. F. Crawley, “Analysis of human lunar outpost strategies and architectures,” in *AIAA SPACE 2007 Conference & Exposition*, 2007.
[222] W. K. Hofstetter, T. A. Sutherland, P. D. Wooster, and E. F. Crawley, “The intermediate outpost - An alternate concept for human lunar exploration,” in *AIAA SPACE 2007 Conference & Exposition*, 2007.
[223] D. Cooke, G. Yoder, S. Coleman, and S. Hensley, “Lunar architecture update,” in *3rd Space Exploration Conference*, 2008.
[224] G. B. Sanders, W. C. Carey, J.-C. Piedbœuf, and A. Lorenzoni, “Lunar In-Situ Resource Utilization in the ISECG human lunar exploration reference architecture,” in *61st International Astronautical Congress*

2010 (IAC), 2010.
[225] J. D. Carpenter, R. Fisackerly, D. De Rosa, and B. Houdou, "Scientific preparations for lunar exploration with the European Lunar Lander," *Planetary and Space Science*, vol. 74, pp. 208–223, 2012.
[226] M. a Rucker and S. Thompson, "Developing a habitat for long duration, deep space mission," in *Global Space Exploration Conference (GLEX)*, 2012.
[227] D. De Rosa *et al.*, "Characterisation of potential landing sites for the European Space Agency's Lunar Lander project," *Planetary and Space Science*, vol. 74, no. 1, pp. 224–246, 2012.
[228] J. E. Gruener, "Lunar outpost site selection: A review of the past 20 years," in *LEAG Workshop on Enabling Exploration: The Lunar Outpost and Beyond*, 2007.
[229] NASA, "A site selection strategy for a lunar outpost: science and operational parameters," Huston, Texas (US), 1990.
[230] NASA, "Developing a site selection strategy for a lunar outpost: science criteria for a site selection," Houston, Texas (US), 1990.
[231] R. L. Staehle, J. D. Burke, G. C. Snyder, R. Dowling, and P. D. Spudis, "Lunar base siting," in *Resources of near-Earth space.*, J. S. Lewis, M. S. Matthews, and M. L. Guerrieri, Eds. The University of Arizona Press, 1993, pp. 427–446.
[232] D. A. Paige *et al.*, "The Lunar Reconnaissance Orbiter Diviner Lunar Radiometer Experiment," *Space Science Reviews*, vol. 150, no. 1–4, pp. 125–160, 2010.
[233] D. A. Paige *et al.*, "Diviner lunar radiometer observations of cold traps in the Moon's south polar region," *Science*, vol. 330, pp. 479–483, 2010.
[234] M. C. Deans, S. Moorehead, B. Shamah, K. Shillcutt, and W. "Red" Whittaker, "A concept for robotic lunar south pole exploration," *Space 98*, pp. 333–339, 1998.
[235] J.-L. Margot, D. B. Campbell, R. F. Jurgens, and M. A. Slade, "Topography of the lunar poles from radar interferometry: A survey of cold trap locations," *Science*, vol. 284, no. 5420, pp. 1658–1660, 1999.
[236] R. N. Clark, "Detection of adsorbed water and hydroxyl on the moon," *Science*, vol. 326, no. 5952, pp. 562–564, 2009.
[237] D. B. J. Bussey, P. D. Spudis, and M. S. Robinson, "Illumination conditions at the lunar south pole," *Geophysical Research Letters*, vol. 26, no. 9, pp. 1187–1190, 1999.
[238] P. D. Spudis, B. Bussey, J. Plescia, J.-L. Joset, and S. Beauvivre, "Geology of Shackleton crater and the south pole of the Moon," *Geophysical Research Letters*, vol. 35, no. 14, pp. 1–5, 2008.
[239] M. Anand *et al.*, "A brief review of chemical and mineralogical resources on the Moon and likely initial in situ resource utilization (ISRU) applications," *Planetary and Space Science*, vol. 74, pp. 42–

48, 2012.
[240] J. R. Arnold, “Ice in the lunar polar regions,” *Journal of Geophysical Research: Solid Earth*, vol. 84, no. B10, pp. 5659–5668, 1979.
[241] R. S. Miller, D. J. Lawrence, and D. M. Hurley, “Identification of surface hydrogen enhancements within the Moon’s Shackleton crater,” *Icarus*, vol. 233, pp. 229–232, 2014.
[242] P. Tompkins and A. Stroupe, “Icebreaker: an Exploration of the Lunar South Pole,” in *14th Space Manufacturing Conference*, 1999.
[243] J. Haruyama *et al.*, “Lack of exposed ice inside lunar south pole Shackleton crater,” *Science*, vol. 332, no. 5903, pp. 938–939, 2008.
[244] A. Colaprete *et al.*, “Detection of water in the LCROSS ejecta plume,” *Science*, vol. 330, 2010.
[245] R. E. Milliken and S. Li, “Remote detection of widespread indigenous water in lunar pyroclastic deposits,” *Nature Geoscience*, vol. 10, no. 8, pp. 561–565, 2017.
[246] G. B. Sanders, W. E. Larson, J. W. Quinn, A. Colaprete, M. Picard, and D. Boucher, “RESOLVE for lunar polar ice/volatile characterization mission,” in *European Planetary Science Congress*, 2011.
[247] E. Detsis, O. Doule, and A. Ebrahimi, “Location selection and layout for LB10, a lunar base at the Lunar North Pole with a liquid mirror observatory,” *Acta Astronautica*, vol. 85, pp. 61–72, 2013.
[248] E. A. Fisher *et al.*, “Evidence for surface water ice in the lunar polar regions using reflectance measurements from the Lunar Orbiter Laser Altimeter and temperature measurements from the Diviner Lunar Radiometer Experiment,” *Icarus*, vol. 292, pp. 74–85, 2017.
[249] A. Cowley, A. Diekmann, S. Coene, V. Nash, and S. Cristoforetti, “Human lunar exploration at EAC - the LUNA analogue facility and the Spaceship EAC project,” in *68th International Astronautical Congress (IAC)*, 2017.
[250] D. A. Vakoch, Ed., *Psychology of space exploration*. Washington, DC, (US): NASA, 2011.
[251] T. Gushanas and B. Dunbar, “One-Year Mission,” *NASA*, 2017. [Online]. Available: https://www.nasa.gov/1ym. [Accessed: 15-Oct-2017].
[252] S. Bryant, “Lunar pole illumination and communications maps computed from Goldstone Solar System Radar elevation data,” 2009.
[253] K. Zacny *et al.*, “Robotic lunar geotechnical tool,” in *ASCE Earth and Space*, 2010, pp. 166–181.
[254] M. S. Anderson, M. K. Ewert, J. F. Keener, and S. A. Wagner, “NASA/TP-2015-218570, Life Support Baseline Values and Assumptions Document,” Huston, Texas (US), 2015.
[255] P. Eckart, *The lunar base handbook: an introduction to lunar base design, development, and operations*. McGraw-Hill, 2006.

[256] C. Dalton *et al.*, "Design of a lunar colony," 1972.
[257] NASA, *Lunar bases and space activities of the 21st century*. Huston, Texas, US: Lunar and Planetary Institute, 1985.
[258] E. Seedhouse, *Lunar outpost: The challenges of establishing a human settlement on the Moon*. Germany: Springer, 2009.
[259] H. Benaroya and L. Bernold, "Engineering of lunar bases," *Acta Astronautica*, vol. 62, no. 4–5, pp. 277–299, 2008.
[260] E. Seedhouse, *Bigelow Aerospace - Colonizing space one module at a time*. Springer, 2015.
[261] Astrium, "COL-RIBRE-MA-0045, Columbus Operational Manual," Bremen (Germany), 2006.
[262] D. A. Harrison, R. Ambrose, B. Bluethmann, and L. Junkin, "Next generation rover for lunar exploration," in *IEEE Aerospace Conference*, 2008.
[263] NASA, "FS-2011-08-045-JSC, Space Exploration Vehicle concept fact sheet," Huston, Texas (US), 2012.
[264] A. K. Hyder, R. L. Wiley, G. Halpert, D. J. Flood, and S. Sabripour, *Spacecraft power technologies*. Singapore (Singapore): Imperial College Press, 2000.
[265] L. Summerer, B. Gardini, and G. Gianfiglio, "ESA's approach to nuclear power sourced for space applications," in *International Congress on Advances in Nuclear Power Plants (ICAAP)*, 2007.
[266] K. Stephenson and T. Blancquaert, "Nuclear power technologies for deep space and planetary missions," in *8th European Space Power Conference (ESPC)*, 2008.
[267] O. Ulleberg, "Stand-alone power systems for the future: Optimal design, operation and control of solar-hydrogen energy sytems," Norvwegian University of Science and Technology, 1998.
[268] ESA, "European researchers invited to board 'Spaceship EAC,'" 2016. [Online]. Available: http://www.esa.int/About_Us/EAC/European_researchers_invited_to_board_Spaceship_EAC. [Accessed: 16-Mar-2016].
[269] ESA, "Spaceship EAC heading for the Moon," 2016. [Online]. Available: http://www.esa.int/spaceinvideos/Videos/2016/02/SpaceShip_EAC_heading_for_the_Moon. [Accessed: 16-Mar-2016].
[270] L. L. Kohout, "Cryogenic reactant storage for lunar base regenerative fuel cells," in *International Conference on Space Power*, 1989.
[271] E. B. Gietl, E. W. Gholdston, B. A. Manners, and R. A. Delventhal, "The electric power system of the International Space Station - a platform for power technology development," in *IEEE Aerospace Conference. Proceedings*, 2000, pp. 47–54.
[272] A. G. Jannette, J. S. Hojnicki, D. B. McKissock, J. Fincannon, T. W. Kerslake, and C. D. Rodriguez, "Validation of International Space

Station electrical performance model via on-orbit telemetry," in *37th Intersociety Energy Conversion Engineering Conference (IECEC)*, 2002, pp. 45–50.
[273] Boeing Company, "International Space Station Electric Power System (EPS)," 2009.
[274] ESA, "Margin philosophy for science assessment studies," Noordwijk (The Netherlands), 2014.
[275] Ballard, "FCvelocity HD family of products," 2016.
[276] E. Tazelaar, Y. Shen, P. A. Veenhuizen, T. Hofman, and P. P. J. van den Bosch, "Sizing stack and battery of a fuel cell hybrid distribution truck," *Oil & Gas Science and Technology – Revue d'IFP Energies nouvelles*, vol. 67, no. 4, pp. 563–573, 2012.
[277] B. V. Ratnakumar, M. C. Smart, L. D. Whitcanack, R. C. Ewell, and S. Surampudi, "Li-ion rechargeable batteries on Mars exploration rovers," in *2nd International Energry Conversion Engineering Conference*, 2004.
[278] M. C. Smart, B. V. Ratnakumar, L. D. Whitcanack, F. J. Puglia, S. Santee, and R. Gitzendanner, "Life verification of large capacity Yardney Li-ion cells and batteries in support of NASA missions," *International Journal of Energy Research*, vol. 34, no. 2, pp. 116–132, 2010.
[279] Tesla, "Tesla Powerpack," 2017. [Online]. Available: https://www.tesla.com/powerpack?redirect=no. [Accessed: 11-May-2017].
[280] M. Yamaguchi, "III-V compound multi-junction solar cells: Present and future," *Solar Energy Materials and Solar Cells*, vol. 75, pp. 261–269, 2003.
[281] Spectrolab, "XTJ Prime solar cell data sheet," 2016.
[282] G. Reitz, T. Berger, and D. Matthiae, "Radiation exposure in the moon environment," *Planetary and Space Science*, vol. 74, no. 1, pp. 78–83, 2012.
[283] ESA, "ECSS-E-ST-20-08C, Space engineering - Photovoltaic assemblies and," 2012.
[284] B. Vanoutryve *et al.*, "An analysis of illumination and communication conditions near the lunar south pole based on Kaguya data," in *7th International Planetary Probe Workshop (IPPW-7)*, 2010.
[285] A. A. Sickafoose, J. E. Colwell, M. Horányi, and S. Robertson, "Experimental levitation of dust grains in a plasma sheath," *Journal of Geophysical Research: Space Physics*, vol. 107, no. A11, 2002.
[286] T. J. Stubbs, R. R. Vondrak, and W. M. Farrell, "A dynamic fountain model for lunar dust," *Advances in Space Research*, vol. 37, no. 1, pp. 59–66, 2006.
[287] J. E. Colwell, S. Batiste, M. Horányi, S. Robertson, and S. Sture, "Lunar surface: Dust dynamics and regolith mechanics," *Reviews of*

Geophysics, vol. 45, no. 2, 2007.
[288] X. Wang, M. Horányi, and S. Robertson, "Experiments on dust transport in plasma to investigate the origin of the lunar horizon glow," *Journal of Geophysical Research: Space Physics*, vol. 114, no. A5, 2009.
[289] Blender Documentation Team, "Blender 2.75 Manual," 2017.
[290] Kent Trammell, "Blender Render VS Cycles," 2016. [Online]. Available: https://cgcookie.com/articles/big-idea-blender-render-vs-cycles. [Accessed: 12-Jun-2017].
[291] Mechdyne, "CAVE Virtual Reality," 2015. [Online]. Available: https://www.mechdyne.com/hardware.aspx?name=CAVE. [Accessed: 25-Mar-2016].
[292] L. Rocci and V. Basso, "VERITAS Software User Manual," Torino (Italy), 2016.
[293] E. Mazarico, G. A. Neumann, D. E. Smith, M. T. Zuber, and M. H. Torrence, "Illumination conditions of the lunar polar regions using LOLA topography," *Icarus*, vol. 211, no. 2, pp. 1066–1081, 2011.
[294] P. Gläser *et al.*, "Illumination conditions at the lunar south pole using high resolution Digital Terrain Models from LOLA," *Icarus*, vol. 243, pp. 78–90, 2014.
[295] G. D. Racca *et al.*, "SMART-1 mission description and development status," *Planetary and Space Science*, vol. 50, no. 14–15, pp. 1323–1337, 2002.
[296] H. Araki, S. Tazawa, H. Noda, T. Tsubokawa, N. Kawano, and S. Sasaki, "Observation of the lunar topography by the laser altimeter LALT on board Japanese lunar explorer SELENE," *Advances in Space Research*, vol. 42, no. 2, pp. 317–322, 2008.
[297] H. Araki *et al.*, "Lunar global shape and polar topography derived from Kaguya-LALT Laser Altimetry," *Science*, vol. 323, no. 5916, pp. 897–900, 2009.
[298] J. Haruyama *et al.*, "Data products of SELENE (Kaguya) Terrain Camera for future lunar missions," in *45th Lunar and Planetary Science Conference*, 2014.
[299] X. Ren *et al.*, "A method and results of color calibration for the Chang'e-3 terrain camera and panoramic camera," *Research in Astronomy and Astrophysics*, vol. 14, no. 12, pp. 1557–1566, 2014.
[300] P. Wessel and W. H. F. Smith, "Free software heps map and display data," *Eos, Transactions American Geophysical Union*, vol. 72, no. 41, pp. 441–446, 1991.
[301] JAXA, "Kaguya/SELENE data archive," 2012. [Online]. Available: http://darts.isas.jaxa.jp/planet/pdap/selene/index.html.en. [Accessed: 15-Apr-2016].
[302] NASA, "LRO-LOLA data archive," 2016. [Online]. Available: http://pds-geosciences.wustl.edu/missions/lro/lola.htm. [Accessed:

15-Apr-2016].
[303] D. E. Smith *et al.*, "The lunar orbiter laser altimeter investigation on the lunar reconnaissance orbiter mission," *Space Science Reviews*, vol. 150, pp. 209–241, 2010.
[304] M. A. Rosenburg *et al.*, "Global surface slopes and roughness of the Moon from the Lunar Orbiter Laser Altimeter," *Journal of Geophysical Research*, vol. 116, no. E2, pp. 1–11, 2011.
[305] ASU, "Lunar quickmap," *NASA*, 2017. [Online]. Available: https://quickmap.lroc.asu.edu/. [Accessed: 10-Aug-2018].
[306] E. J. Speyerer and M. S. Robinson, "Persistently illuminated regions at the lunar poles: Ideal sites for future exploration," *Icarus*, vol. 222, no. 1, pp. 122–136, 2013.
[307] H. Noda *et al.*, "Illumination conditions at the lunar polar regions by KAGUYA(SELENE) laser altimeter," *Geophysical Research Letters*, vol. 35, no. 24, pp. 2–6, 2008.
[308] D. B. J. Bussey *et al.*, "Illumination conditions of the south pole of the Moon derived using Kaguya topography," *Icarus*, vol. 208, no. 2, pp. 558–564, 2010.
[309] J. Fincannon, "Lunar south pole illumination: review, reassessment, and power system implications," in *5th International Energy Conversion Engineering Conference and Exhibit (IECEC)*, 2007.
[310] E. J. Speyerer, S. J. Lawrence, J. D. Stopar, P. Gläser, M. S. Robinson, and B. L. Jolliff, "Optimized traverse planning for future polar prospectors based on lunar topography," *Icarus*, vol. 273, pp. 337–345, 2016.
[311] P. Gläser, J. Oberst, G. A. Neumann, E. Mazarico, E. J. Speyerer, and M. S. Robinson, "Illumination conditions at the lunar poles: Implications for future exploration," *Planetary and Space Science*, pp. 1–9, 2017.
[312] W. M. Folkner, J. G. Williams, and D. H. Boggs, "The planetary and lunar ephemeris DE 421," 2009.
[313] K. Bauch, H. Hiesinger, and J. Helbert, "Estimation of lunar surface temperature: a numerical model," in *European Geosciences Union (EGU) General Assembly*, 2009.
[314] A. R. Vasavada, D. A. Paige, and S. E. Wood, "Near-surface temperatures on Mercury and the Moon and the stability of polar ice deposits," *Icarus*, vol. 141, no. 2, pp. 179–193, 1999.
[315] A. R. Vasavada *et al.*, "Lunar equatorial surface temperatures and regolith properties from the Diviner Lunar Radiometer Experiment," *Journal of Geophysical Research*, vol. 117, no. E12, pp. 1–12, 2012.
[316] J. P. Williams, D. A. Paige, B. T. Greenhagen, and E. Sefton-Nash, "The global surface temperatures of the Moon as measured by the Diviner Lunar Radiometer Experiment," *Icarus*, vol. 283, pp. 300–325, 2017.

[317] M. Killian and P. B. Hager, "Traverse planning on the lunar surface - Benefits from thermal modeling," in *45th International Conference on Environmental Systems (ICES)*, 2015.
[318] M. Killian, "Thermal simulation of a rover traverse at the lunar south pole," in *5th European Lunar Symposium (ELS)*, 2017.
[319] C. Qi and Z. Ming, "Photovoltaic module Simulink model for a stand-alone PV system," *Physics Procedia*, vol. 24, pp. 94–100, 2012.
[320] Krismadinata, N. A. Rahim, H. W. Ping, and J. Selvaraj, "Photovoltaic module modeling using Simulink/MATLAB," *Procedia Environmental Sciences*, vol. 17, pp. 537–546, 2013.
[321] H. Bellia, R. Youcef, and M. Fatima, "A detailed modeling of photovoltaic module using MATLAB," *NRIAG Journal of Astronomy and Geophysics*, vol. 3, no. 1, pp. 53–61, 2014.
[322] H. Rezk and E. S. Hasaneen, "A new MATLAB/Simulink model of triple-junction solar cell and MPPT based on artificial neural networks for photovoltaic energy systems," *Ain Shams Engineering Journal*, vol. 6, no. 3, pp. 873–881, 2015.
[323] X. H. Nguyen and M. P. Nguyen, "Mathematical modeling of photovoltaic cell/module/arrays with tags in MATLAB/Simulink," *Environmental Systems Research*, vol. 4, no. 24, 2015.
[324] N. Das, H. Wongsodihardjo, and S. Islam, "Modeling of multi-junction photovoltaic cell using MATLAB/Simulink to improve the conversion efficiency," *Renewable Energy*, vol. 74, pp. 917–924, 2015.
[325] A. B. Hussain, A. S. Abdalla, A. S. Mukhtar, M. Elamin, R. Alammari, and A. Iqbal, "Modelling and simulation of single- and triple-junction solar cells using MATLAB/Simulink," *International Journal of Ambient Energy*, vol. 38, no. 6, pp. 613–621, 2017.
[326] University of Colorado Boulder, "SORCE data," 2017. [Online]. Available: http://lasp.colorado.edu/home/sorce/data/. [Accessed: 07-May-2017].
[327] D. Rapp, *Use of extraterrestrial resources for human space missions to Moon or Mars*. Berlin, Germany: Springer, 2012.
[328] X. Li *et al.*, "Condition of solar radiation on the Moon," in *Moon: Prospective energy and material resources*, V. Badescu, Ed. Springer, 2012, pp. 347–365.
[329] E. Testa, "Multidisciplinary design and optimization of innovative electrical power systems for aerospace applications," Politecnico dit Torino, 2013.
[330] C. Y. Wang, "Fundamental models for fuel cell engineering," *Chemical Reviews*, vol. 104, no. 10, pp. 4727–4765, 2004.
[331] ZSW, "PEM FC Stack BZ 100-13," 2015.
[332] M. W. Fowler, R. F. Mann, J. C. Amphlett, B. A. Peppley, and P. R. Roberge, "Incorporation of voltage degradation into a generalised steady state electrochemical model for a PEM fuel cell," *Journal of*

Power Sources, vol. 106, pp. 274–283, 2002.
[333] D. Cooke, "Exploration strategy and architecture," in *2nd Space Exploration Conference*, 2006.
[334] NASA, "NASA 3D resources," 2016. [Online]. Available: http://nasa3d.arc.nasa.gov/. [Accessed: 15-May-2016].
[335] G. S. Parnell, P. J. Driscoll, and D. L. Henderson, Eds., *Decision making in systems engineering and management*, vol. 81. John Wiley & Sons, 2011.
[336] H. P. de Koning, S. Gerené, I. Ferreira, A. Pickering, F. Beyer, and J. Vennekens, "Open Concurrent Design Tool: ESA Community Open Source ready to go," in *6th International Systems & Concurrent Engineering for Space Applications conference (SECESA)*, 2014.
[337] E. Academy, "Students shoot for the Moon in ESA's Concurrent Engineering Challenge 2017," *ESA*, 2017. [Online]. Available: https://www.esa.int/Education/ESA_Academy/Students_shoot_for_the_Moon_in_ESA_s_Concurrent_Engineering_Challenge_2017. [Accessed: 16-Feb-2017].
[338] M. K. Barker, E. Mazarico, G. A. Neumann, M. T. Zuber, J. Haruyama, and D. E. Smith, "A new lunar digital elevation model from the Lunar Orbiter Laser Altimeter and SELENE Terrain Camera," *Icarus*, vol. 273, pp. 346–355, 2016.
[339] A. E. M. Casini *et al.*, "Analysis of a Moon outpost for Mars enabling technologies through a Virtual Reality environment," in *67th International Astronautical Congress (IAC)*, 2016.
[340] A. E. M. Casini, P. Maggiore, N. Viola, A. Cowley, V. Basso, and L. Rocci, "Virtual Reality in support of future lunar exploration: an illumination analysis case study," in *5th European Lunar Symposium (ELS)*, 2017.
[341] L. Franchi, A. E. M. Casini, D. Calvi, S. Corpino, P. Maggiore, and N. Viola, "Virtual Reality to assist the aerospace engineering decision making process: improving the Concurrent Design approach," in *68th International Astronautical Congress (IAC)*, 2017.
[342] A. E. M. Casini, A. Cowley, D. G. Mazzotta, P. Maggiore, and N. Viola, "A Virtual Reality approach for studying a future human lunar outpost: an integrated simulation case study of a Stand Alone Power system," in *68th International Astronautical Congress (IAC)*, 2017.
[343] A. E. M. Casini *et al.*, "Analysis of a Moon outpost for Mars enabling technologies through a Virtual Reality environment," *Acta Astronautica*, vol. 143, pp. 353–361, 2018.
[344] C. Careri, "Preliminary design and modelling of a photovoltaic plant for a crewed lunar outpost," Politecnico di Torino, 2017.
[345] F. Iannicelli and D. F. Luisi, "Modelling, simulation and experimentation of a regenerative energetic system for space applications," Politecnico di Torino, 2016.

[346] F. Iannicelli and D. F. Luisi, “Modelling, simulation and experimentation of a hydrogen-photovoltaic stand-alone power system for space applications,” in *13th AIAA-PEGASUS Student Conference*, 2016.

[347] E. Musk, “Making Life Multiplanetary,” *SpaceX*, 2017. [Online]. Available: https://www.youtube.com/watch?v=tdUX3ypDVwI. [Accessed: 10-Oct-2017].

Additional notes

Author's comments about auto-plagiarism

Part of the work described in chapters 2 and 3 has been previously published in [339–343].

Part of the work described in chapters 4 has been previously published in [339, 342–344].

Part of the work described in chapters 5 has been previously published in [339, 340, 342–346].